



Cultural diversity, population structure,  
and habitability during the eastern  
African Middle Stone Age

Thesis submitted in accordance with the requirements of the  
University of Liverpool for the degree of Doctor in Philosophy

by *Lucy Jasmine Timbrell*

*17th February 2023*



## Acknowledgements

The completion of this thesis would not have been possible without the guidance, assistance, and collaboration from many kind people. Firstly, I would like to thank my supervisors, Dr Matt Grove, Dr Kimberly Plomp and Dr Matthew Fitzjohn. Your advice has been fundamental to the completion of this work, and I am beyond grateful for your mentorship. I would also like to thank other staff at the University of Liverpool for their support throughout this project, specifically Chris Scott for his assistance with the inter-observer analysis and for facilitating access to teaching collections during the COVID-19 pandemic, Prof John Gowlett for his insights into eastern African Stone Age archaeology, Dr Rebecca Wragg-Sykes for her assistance translating the protocols into French for francophone collaborators and Prof Larry Barham for his general support throughout my time as a student of the University of Liverpool, among others.

I would also like to thank the numerous collaborators on this project. Firstly, I would like to thank Dr James Blinkhorn, whose enthusiasm for this work on the eastern African Middle Stone Age has been encouraging. Prof Andrea Manica and his team at the University of Cambridge have also been instrumental through facilitating access to the climatic simulations ahead of publication, as well as providing mentorship on my analyses of these data.

I would also like to thank Dr Emmanuel Ndiema, Dr Stephen Rucina, Christine Maroma, Simon Mboya and Sharon Manura from the National Museums of Kenya for their collaboration on this project in various capacities. Additionally, Dr Behailu Habte, Yosef Tefera, and Sahleselasie Melaku (National Museum of Ethiopia, Ethiopia), Benjamin Marais and Dr Wendy Black (Iziko Museums of South Africa, South Africa), Struan Henderson, Katherine Elmes, and Prof Curtis Marean (Mossel Bay Archaeology Project, South Africa), Mouna Qazzih and Prof Abdelouahed Ben-Ncer (Institut National des Sciences de l'Archéologie et du Patrimoine, Morocco), and Hélène Monod, Dr Stéphanie Bonilauri, and Dr Roland Nespoulet (Musée de l'Homme, France) were instrumental to this project. Without these collaborators, the continuation of this work through the COVID-19 pandemic would not have been possible and so I am extremely grateful for your support, open-mindedness, and guidance. I also thank my collaborators, Dr Paloma de la Peña and Dr Amy Way, for their ongoing cooperation with my research.

I would next like to acknowledge the site permit holders who allowed access to the archaeological material and provided additional contextual information and references about the sites studied.

Specifically, I would like to thank Dr David Pleurdeau and Dr Zelalem Assefa for facilitating access to and providing information about the Middle Stone Age collections at Porc-Epic and Goda Buticha, Dr John Shea for Omo Kibish, Prof Stanley Ambrose and Prof Charles Nelson for Prospect Farm, Dr Nick Blegen and Prof Christian Tryon for Kaputhurin Formation. I appreciate the opportunity to study these collections, especially in development of novel methods of data generation.

This thesis was generously supported by funding provided by The Lithic Studies Society (Jacobi Bursary Grantee, 2020), The Leakey Foundation (Movement, interaction, and structure: modelling population networks and cultural diversity in the African Middle Stone Age), The Wenner-Gren Foundation [grant number 10157] and the North-West Consortium Doctoral Training Partnership via Arts and Humanities Research Council [grant number AH/ R012792/1]. I would like to particularly thank the latter programme for also facilitating various training and professional development endeavours throughout my time as a doctoral student.

Finally, I would like to thank my family and friends for their emotional support throughout this process. In particular, I would like to thank Carys (my PhD sister) for keeping me sane, as well as Sophie, Bella, Rosa, Anna, Laura and many more for being there for me and making me smile. I truly appreciate my parents, Carolyn and Steve, and my siblings, Holly and Josh, as well as my grandparents for supporting me and for providing me with a safe haven. Final thanks go to Callum. Over the last few years, we have been through thick and thin, and I could not think of anyone better to have gone on this journey with.

# Table of Contents

|  |           |
|--|-----------|
| <b>CHAPTER 1. INTRODUCTION .....</b>   | <b>14</b> |
| 1.1. BRIEF BACKGROUND .....  | 14        |
| 1.2. AIMS AND OBJECTIVES.....  | 16        |
| 1.3. OUTLINE OF THESIS STRUCTURE .....   | 18        |
| <b>CHAPTER 2: THEORIES OF MODERN HUMAN EVOLUTION .....</b>   | <b>20</b> |
| 2.1. MULTIREGIONALISM .....  | 20        |
| 2.2. SIMPLE OUT OF AFRICA .....  | 23        |
| 2.3. COMPLEX OUT OF AFRICA .....   | 26        |
| 2.4. THE STRUCTURED AFRICAN METAPOPOPULATION MODEL.....  | 29        |
| 2.4.1. Evidence of structure in Late-Middle Pleistocene Africa .....   | 30        |
| 2.4.2. Environmental and ecological drivers of population structure .....  | 40        |
| 2.4.3. Summary of the theoretical implications of population structure .....   | 47        |
| 2.5. CONCLUSION .....  | 49        |
| <b>CHAPTER 3: EASTERN AFRICA AND THE MIDDLE STONE AGE .....</b>  | <b>50</b> |
| 3.1. GEOGRAPHY, GEOLOGY, HYDROLOGY, AND VOLCANISM .....  | 50        |
| 3.2. CLIMATE AND ENVIRONMENTS .....  | 52        |
| 3.3. RESEARCH HISTORY OF EASTERN AFRICAN STONE AGE ARCHAEOLOGY.....  | 54        |
| 3.4. WHAT IS THE MIDDLE STONE AGE? .....   | 56        |
| 3.4.1. Modern human behaviour and the Middle Stone Age .....   | 57        |
| 3.5. PREVIOUS RESEARCH ON THE EASTERN AFRICAN MIDDLE STONE AGE .....   | 60        |
| 3.5.1. Archaeological sites .....  | 60        |
| 3.5.2. Assemblage-level regional studies.....  | 63        |
| 3.6. CONCLUSION .....  | 66        |
| <b>CHAPTER 4: A SPATIOTEMPORALLY EXPLICIT PALEOENVIRONMENTAL FRAMEWORK FOR THE MIDDLE STONE AGE OF EASTERN AFRICA.....</b> | <b>67</b> |
| 4.1. INTRODUCTION .....  | 67        |
| 4.2. MATERIALS AND METHODS.....  | 70        |
| 4.2.1. Refining the climatic parameters .....  | 72        |
| 4.2.2. Cluster analyses .....  | 72        |
| 4.2.3. Biome classification .....  | 72        |
| 4.2.4. Phased climate suitability models .....   | 73        |
| 4.2.5. Mantel tests and multiple matrix regression .....   | 73        |
| 4.3. RESULTS.....  | 74        |
| 4.3.1. Middle and Late Pleistocene climates of MSA occupations .....   | 74        |
| 4.3.2. Classifying biomes and ecotones at MSA occupations.....   | 76        |
| 4.3.3. Characterising MSA environments throughout the Middle to Late Pleistocene .....                                     | 78        |
| 4.3.4. Phased habitability models.....   | 80        |
| 4.3.5. Exploring the relationship between climate and Middle Stone Age occupations .....                                   | 81        |
| 4.4. DISCUSSION.....   | 84        |
| 4.5. CONCLUSION .....  | 87        |
| <b>CHAPTER 5: MODELLING SUITABLE HABITATS FOR EASTERN AFRICAN MIDDLE STONE AGE POPULATIONS .....</b>                       | <b>89</b> |
| 5.1. INTRODUCTION .....  | 89        |
| 5.1.1. Species distribution modelling and ecological niche theory.....   | 90        |
| 5.1.2. Applying species distribution modelling to archaeological data.....   | 91        |
| 5.1.3. Additional factors than can condition habitability .....  | 92        |
| 5.2. MATERIALS.....  | 94        |

|   |            |
|---|------------|
| 5.3. METHODS .....  | 96         |
| 5.3.1. <i>Climate suitability</i> .....   | 96         |
| 5.3.2. <i>Topography and energetic cost of movement</i> .....   | 98         |
| 5.3.3. <i>Access to water</i> .....   | 98         |
| 5.3.4. <i>Aggregation of factors into a habitability index</i> .....  | 99         |
| 5.3.5. <i>Model validation</i> .....  | 100        |
| 5.4. RESULTS.....   | 103        |
| 5.4.1. <i>Habitability model</i> .....  | 104        |
| 5.4.2. <i>Model validation</i> .....  | 105        |
| 5.5. DISCUSSION.....  | 107        |
| 5.6. CONCLUSION .....   | 110        |
| <b>CHAPTER 6: A COLLABORATIVE MODEL FOR LITHIC SHAPE DIGITIZATION IN MUSEUM SETTINGS .....</b>                                      | <b>111</b> |
| 6.1. INTRODUCTION .....   | 111        |
| 6.2. BACKGROUND.....  | 113        |
| 6.2.1. <i>Lithic artefact digitization</i> .....  | 113        |
| 6.2.2. <i>Analyses of lithic shapes</i> .....   | 114        |
| 6.3. COLLABORATIVE DATA COLLECTION .....  | 115        |
| 6.3.1. <i>Photography protocols</i> .....   | 116        |
| 6.3.2. <i>Measurement protocols</i> .....   | 119        |
| 6.3.3. <i>Data recording, storage and sharing</i> .....   | 119        |
| 6.4. DISCUSSION.....  | 120        |
| 6.4.1. <i>'Helicopter research' in the museum context</i> .....   | 120        |
| 6.4.2. <i>Reducing the carbon footprint of museum research</i> .....  | 122        |
| 6.4.3. <i>Building resilience through collaborations with museums</i> .....   | 123        |
| 6.5. CONCLUSION .....   | 124        |
| <b>CHAPTER 7: TESTING INTER-OBSERVER ERROR UNDER A COLLABORATIVE RESEARCH FRAMEWORK FOR STUDYING LITHIC SHAPE VARIABILITY .....</b> | <b>126</b> |
| 7.1. INTRODUCTION .....   | 127        |
| 7.2. MATERIALS.....   | 130        |
| 7.3. METHODS .....  | 132        |
| 7.3.1. <i>Metric analyses</i> .....   | 134        |
| 7.3.2. <i>Two-dimensional geometric morphometric analysis</i> .....   | 135        |
| 7.4. RESULTS.....   | 137        |
| 7.4.1. <i>Linear metric analysis</i> .....  | 137        |
| 7.4.2. <i>Geometric morphometric analysis</i> .....   | 139        |
| 7.5. DISCUSSION.....  | 144        |
| 7.6. CONCLUSION .....   | 147        |
| <b>CHAPTER 8. EASTERN AFRICAN MIDDLE STONE AGE POINT SHAPE VARIABILITY .....</b>  | <b>149</b> |
| 8.1. INTRODUCTION .....   | 149        |
| 8.1.1. <i>Function of eastern African MSA points</i> .....  | 150        |
| 8.1.2. <i>Technology and typology of eastern African MSA points</i> .....   | 151        |
| 8.2. THEORETICAL EXPECTATIONS OF POPULATION STRUCTURE AND POINT VARIABILITY .....   | 153        |
| 8.2.1. <i>Hypotheses setting</i> .....  | 155        |
| 8.3. MATERIALS.....   | 157        |
| 8.3.1. <i>Background to the sites studied</i> .....   | 160        |
| 8.4. METHODS .....  | 163        |
| 8.5. RESULTS.....   | 165        |
| 8.5.1. <i>Relationship between shape and size</i> .....   | 166        |
| 8.5.2. <i>Raw materials</i> .....   | 166        |
| 8.5.3. <i>Inter-site shape variability</i> .....  | 168        |

|   |            |
|---|------------|
| 8.5.4. <i>Inter-assembly variability</i> .....  | 171        |
| 8.5.5. <i>Evaluation of point shape in relation to null models</i> .....  | 179        |
| 8.6. DISCUSSION.....  | 181        |
| 8.7. CONCLUSION .....   | 185        |
| <b>CHAPTER 9: INTEGRATING THE HABITABILITY MODEL WITH POINT SHAPE VARIABILITY.....</b>  | <b>186</b> |
| 9.1. INTRODUCTION .....   | 186        |
| 9.2. MATERIALS AND METHODS .....  | 188        |
| 9.3. RESULTS.....   | 190        |
| 9.4. DISCUSSION.....  | 194        |
| 9.5. CONCLUSION .....   | 197        |
| <b>CHAPTER 10: CONCLUDING REMARKS.....</b>  | <b>198</b> |
| 10.1. SUMMARY OF FINDINGS AND KEY RESULTS.....  | 198        |
| 10.2. SUMMARY OF CONTRIBUTIONS.....   | 202        |
| 10.2.1. <i>Point shape, demography and refugia</i> .....  | 204        |
| 10.2.2. <i>Collaborative and remote science</i> .....   | 206        |
| 10.3. LIMITATIONS OF RESEARCH AND FUTURE DIRECTIONS.....  | 208        |
| 10.3.1. <i>The question of resolution</i> .....   | 208        |
| 10.3.2. <i>Costs and benefits of inhabiting heterogenous landscapes</i> .....   | 210        |
| 10.4. FINAL THOUGHTS.....   | 211        |
| <b>REFERENCES .....</b>   | <b>212</b> |
| <b>APPENDICES .....</b>   | <b>239</b> |
| APPENDIX 1. SUPPLEMENTARY ONLINE MATERIALS FOR ‘A SPATIOTEMPORALLY EXPLICIT PALEOENVIRONMENTAL FRAMEWORK FOR THE MIDDLE STONE AGE OF EASTERN AFRICA’ (TIMBRELL ET AL., 2022; SCI REP).....                      | 239        |
| APPENDIX 2: SUPPLEMENTARY ONLINE MATERIALS FOR ‘TESTING INTER-OBSERVER ERROR UNDER A COLLABORATIVE RESEARCH FRAMEWORK FOR STUDYING LITHIC SHAPE VARIABILITY’ (TIMBRELL ET AL., 2022; ANTH. ARCHAEO. SCI.) ..... | 256        |
| APPENDIX 3: SUPPLEMENTARY MATERIALS FOR CHAPTER 8 – EASTERN AFRICAN MIDDLE STONE AGE POINT VARIABILITY .....  | 260        |
| APPENDIX 4: SUPPLEMENTARY MATERIALS FOR CHAPTER 9 – INTEGRATING THE HABITABILITY MODEL WITH POINT SHAPE VARIABILITY .....   | 263        |

## List of figures

|  |     |
|--|-----|
| <b>Figure 1.</b> Multiregionalism schematic diagram. Adapted from Stringer (2014). The arrows show the direction of gene flow. ....  | 22  |
| <b>Figure 2.</b> Composite of key inter-regional and regional climatic records, insolation, and temperature, precipitation and altitude parameters for dated eastern African Middle Stone Age occupations including (a) LR04 Benthic Stack $\delta^{18}\text{O}$ (Lisiecki and Raymo, 2005); (b) Lake Tana Ca/Ti ratio (Lamb et al., 2018); (c) Chew Bahir k-counts (Trauth et al., 2021); (d) Koora Basin diatom CA (Potts et al., 2020); (e) Magadi Pollen grass:aquatic ratio (Muirui et al., 2021); (f) Lake Malawi PC1 (Lyons et al., 2015); (g) Vostok $\delta\text{D}$ [‰ SMOW] (Jouzel et al., 2007); (h) mean Equatorial summer (Jun-Aug) insolation (W/m <sup>2</sup> ) (Laskar et al., 2004); mean (i) temperature (°C), (j) precipitation (mm), and (k) altitude (meters above sea level) within 50km radius of eastern African MSA assemblages, illustrated at the mid-age point for each occupation and symbolised according to its biome classification. Grey vertical bars indicate odd-numbered Marine Isotope Stages. Reprinted from Timbrell et al. (2022a). .... | 71  |
| <b>Figure 3.</b> Distribution of the eastern African Middle Stone Age occupations studied. This map was created in ArcGIS 10.5 using an SRTM (NASA).....   | 75  |
| <b>Figure 4.</b> Examples of xerophytic shrubland environments in modern eastern Africa, including typical species (sp.). A) <i>Acacia tortilis</i> B) <i>Commiphora</i> sp. C) <i>Acacia</i> sp. and <i>Duosperma eremophilum</i> . D) <i>Hyphaene compressa</i> , <i>Acacia</i> sp., <i>Salvadora persica</i> , <i>Cyperacea</i> and <i>L Lawsonia inermis</i> E) <i>Acacia</i> sp. and <i>Duosperma eremophilum</i> , F) <i>Acacia tortilis</i> (background: <i>Commiphora</i> sp. <i>Capparaceae</i> sp. <i>Tephrosia</i> sp. and <i>Indigofera spinosa</i> ). Photos taken by Dr Stephen Rucina. ...  | 77  |
| <b>Figure 5.</b> Hierarchical clustering of the occupations according to mean annual temperature and total annual precipitation. K means clustering identified ten clusters as the optimal division of the dendrogram, which have been highlighted here as well as the range of environmental conditions occupied by each cluster and the percentage of cells within 50km of that biome for all occupations within that cluster.....   | 79  |
| <b>Figure 6.</b> Mean annual temperature (top), total annual precipitation (middle) and combined (bottom) phased models of habitability, demonstrating the percentage of time intervals (1000 years per interval) that remain within the climatic range of the occupations dated to that Marine Isotope Stage (MIS). The palaeocoastline has been estimated based on the predicted mean sea-level for each MIS. ....   | 81  |
| <b>Figure 7.</b> Scatterplots of the Mantel test results (Table 6, Appendix 1: Supplementary Methods S3 Tables S1-2) between the pairwise distance matrix of toolkit composition (top) and raw material use (bottom) and the other distances matrices excluding the two binary variables, site type and method.....  | 83  |
| <b>Figure 8.</b> Ground-water refugia modelling in extreme dry (a) to extreme wet (c) climatic scenarios during a precessional cycle are modelled and the dispersal of hominins between hydro-refugia is predicted via agent-based modelling (black lines). Reprinted from Cuthbert et al. (2017).....   | 94  |
| <b>Figure 9.</b> A schematic flow chart summarising the habitability modelling process, including climate suitability, access to water and energetic cost of movement parameters.....  | 100 |
| <b>Figure 10.</b> Example time-slices extracted from the habitability model at every 50,000 years (kya), between 50-300 kya. Habitable cells fall closer to 1 whereas uninhabitable cells fall closer to 0.  | 104 |
| <b>Figure 11.</b> Histograms of (left) the climate suitability values at eastern African MSA sites, (middle) the median values and (right) the median absolute deviation values of the randomly permuted   |     |



samples. The median and median absolute deviation of the eastern African MSA is marked by a red dashed line. .... 106

**Figure 12.** Histograms of (left) the habitability values at eastern African MSA sites, (middle) the median values and (right) the median absolute deviation values of the randomly permuted samples. The median and median absolute deviation of the eastern African MSA sites is marked by a red dashed line..... 106

**Figure 13.** Cartoon of an example photography set-up, including a digital camera, a macro lens, a copy stand, photography lights, a spirit level, materials for holding the artefacts down, a small photography scale, and computer software for remote data capture..... 117

**Figure 14.** Example photos of lithic points from Omo Kibish, Ethiopia. All points are photographed with their dorsal surface facing the camera. Photos taken by Dr Behailu Habte, National Museum of Ethiopia..... 118

**Figure 15.** Image binarization process of a lithic point from Ifri n’Ammar, Morocco. Photo taken by Mouna Qazzih, Institut National des Sciences de l’Archéologie et du Patriome, Morocco. .... 119

**Figure 16.** The six 3D printed replica tools. Original lithics were knapped and scanned by CS in preparation for 3D printing. Example photos were taken by SH. Scale = 3cm. .... 131

**Figure 17.** Photographs from the 3D printing process. A) The 3D model of the tool is sent to the machine for printing. B) The resulting 3D prints once removed from the supports are cleaned using ethanol. 3D printing was carried out by LT and CS..... 132

**Figure 18.** A schematic of the Elliptic Fourier fitting process that generates the raw shape data for geometric morphometrics. Coefficients of sine and cosine terms (harmonics) are computed to reconstruct the x (blue) and y (red) coordinates from an arbitrary starting point moving along the outline. .... 136

**Figure 19.** Boxplots demonstrating the distribution of length, width, and thickness (mm) collected by multiple observers for each tool (1-6)..... 138

**Figure 20.** Principal component (PC) contributions along the first 3 axes of variance within the multiple observer outline data. .... 141

**Figure 21.** Scatterplots (top row) and boxplots (bottom row) of repeat capture scores along principal components (PC) 1-3, demonstrating the clustering within tools (1-6). PC1 represents 59.7% of the total variance, whilst PC2 and PC3 account for 33.4% and 3% respectively. .... 142

**Figure 22.** Scatterplots (top row) and boxplots (bottom row) of repeat capture scores along principal components (PC) 1-3, demonstrating the clustering within tools (symbols) and between data sets (colors). PC1 represents 60.4 % of the total variance, whilst PC2 and PC3 account for 33.5% and 3.3% respectively. .... 143

**Figure 23.** 3D visualisation of the null hypotheses in relation to how they explain archaeological diversity, adapted from Scerri (2013a). The arrows represent archaeological variability with the circles at the end of each arrow representing an assemblage conforming to a particular null model’s assumptions. Isolation by distance (H0a) represents diversity through space when controlling for time and environment (blue). Isolation by time (H0b) is marked by the yellow circle, variation only occurring through time. Isolation by environment (H0c) is marked by the red circle, with the environmental dimension the only influence over patterns of diversity. Cultural variation is likely explained by a combination of these factors, i.e., variation through timespace is represented by the green circle, and the correlation between space and environment means that assemblages that share the same environment and are close together are likely to be archaeologically similar (purple). .... 156

|  |     |
|--|-----|
| <b>Figure 24.</b> The chronological (left) and spatial (right) extent of the eastern African Middle Stone Age points studied in this analysis. ....  | 160 |
| <b>Figure 25.</b> Principal component (PC) contributions, highlighting the mean and standard deviation (SD) shape changes along PC1-6. ....  | 165 |
| <b>Figure 26.</b> Regressions of principal components (PC) 1-6 on centroid size, with 95% confidence intervals. ....   | 166 |
| <b>Figure 27.</b> Boxplots of point length, width, and thickness (mm) in relation to raw material. ....  | 167 |
| <b>Figure 28.</b> Principal components analysis (PCA) scatterplots (a-c) and boxplots (d) of principal component (PC) 1-3 (top) and PC 4-6 (bottom) against raw materials. ....  | 168 |
| <b>Figure 29.</b> Boxplots of point length, width, and thickness (mm) for each site. ....  | 169 |
| <b>Figure 30.</b> Principal components analysis (PCA) scatterplots (a-c) and boxplots (d) of principal component (PC) 1-3 (top) and PC 4-6 (bottom) for each site. ....  | 170 |
| <b>Figure 31.</b> Hierarchical cluster analysis demonstrating the structure of point shape variability between sites. The dendrogram has been split into six clusters (n = number of sites) which are highlighted by the red boxes. ....   | 172 |
| <b>Figure 32.</b> Boxplots of point length, width, and thickness (mm) for each assemblage. ....  | 174 |
| <b>Figure 33.</b> Boxplots of principal component (PC) scores along PC1-6 for each assemblage. ....  | 178 |
| <b>Figure 34.</b> Regressions of principal components (PC) 1, 3 and 5 against chronology, latitude, and precipitation according to which demonstrated independent relationships in the multiple matrix regression (see Table 22). 95% confidence intervals have been highlighted in grey. .... | 184 |
| <b>Figure 35.</b> Predicted dispersal corridors, calculated using least-cost pathways through the habitability index cost-surface corresponding to the mid-point between the chronological overlap of two assemblages. ....  | 193 |
| <b>Figure 36.</b> Spearman's correlation of the habitability index against principal component (PC)3 (left), PC6 (centre) and width (right). A regression line has been drawn with 95% confidence intervals. ....  | 195 |

## List of tables

|  |     |
|--|-----|
| <b>Table 1.</b> An overview of the published works included in this thesis.....  | 18  |
| <b>Table 2.</b> A summary of the theoretical assumptions of multiregionalism and Out of Africa. Adapted from Stringer and Andrews (1988).....  | 24  |
| <b>Table 3.</b> Cranial characteristics unique to modern <i>H. sapiens</i> , as established by Day and Stringer (1982) and Stringer, Hublin and Vandermeersch (1984). At least three of these are required for a specimen to be classified as <i>H. sapiens</i> . ....   | 26  |
| <b>Table 4.</b> Early <i>Homo sapiens</i> samples analysed by Gunz <i>et al.</i> (2009) and Mounier and Lahr (2019)...   | 32  |
| <b>Table 5.</b> A summary of the Milankovitch cycles. ....   | 42  |
| <b>Table 6.</b> Simple Mantel test results for the effects of precipitation and temperature on toolkit composition and raw material. Statistical significance highlighted at $p < 0.05$ (*) or $p < 0.01$ (**). The Benjamini-Hochberg procedure was used to adjust p values. ....   | 84  |
| <b>Table 7.</b> Multiple matrix regression results for toolkit composition and raw material. Descriptions of each variable can be found in Appendix 2: Supplementary Methods S2. Statistical significance highlighted at $p < 0.05$ (*) or $p < 0.01$ (**). ....   | 84  |
| <b>Table 8.</b> Date ranges for the 84 eastern African MSA occupations reported in Blinkhorn and Grove (2021). The occupations were anchored at their mid-age: the 1,000-year (kya) mid-point between the minimum and maximum age of the date range.....   | 101 |
| <b>Table 9.</b> Summary of the observers and the photography equipment used. This equipment was sourced locally; in most cases, the institutions already had access to the necessary apparatus, however in some cases it was rented and/or purchased and donated to the institution after the project, following guidelines provided by The Wenner Gren Foundation. .... | 133 |
| <b>Table 10.</b> Summary statistics reporting the mean (m) and standard deviation (sd) obtained for length, width and thickness, recorded by multiple observers versus a single observer for each tool (1-6). Standard deviation values have been rounded to 3 decimal places. ....  | 139 |
| <b>Table 11.</b> P-values from t-tests (difference in mean) and F-tests (difference in variance) comparing the metrics (length, width, and thickness) for each tool (1-6) measured by multiple observers versus a single observer. Statistical significance ( $p < 0.05$ ) is marked by an asterisk (*). All values have been rounded to 3 decimal places. ....          | 139 |
| <b>Table 12.</b> Coefficient of reliability (R) values for pair-wise combinations of observers using the first 3 PC scores. For observer abbreviations and associated assemblage numbers, see Table 1. All values have been rounded to 3 decimal places. ....  | 141 |
| <b>Table 13.</b> P-values from t-tests (difference in mean) and F-tests (difference in variance) comparing the principal component (PC) scores of the repeats of each tool (1-6) captured by multiple observers versus a single observer. Statistical significance ( $p < 0.05$ ) is marked by an asterisk (*). All values have been rounded to 3 decimal places. ....   | 143 |
| <b>Table 14.</b> Summary statistics reporting mean (m) and standard deviation (sd) of principal component (PC) scores of the repeats of each tool (1-6), captured by multiple observers versus a single observer. All values have been rounded to 3 decimal places. ....   | 144 |
| <b>Table 15.</b> A summary of the eastern African Middle Stone Age point sample studied in this thesis, accessed via remote data collection. Samples without information regarding assemblage attribution and/or are surface finds are left unassigned are removed from analyses beyond the site-level.....  | 158 |

|  |     |
|--|-----|
| <b>Table 16.</b> Summary statistics for point length, width, and thickness (mm) for each raw material, highlighting the sample size (n), mean (m) and standard deviation (sd) .....  | 167 |
| <b>Table 17.</b> Summary statistics for point length, width, and thickness (mm) for each site, highlighting the sample size (n), mean (m) and standard deviation (sd) .....  | 169 |
| <b>Table 18.</b> P-values from Tukey Honestly Significant Difference analyses for length, width, and thickness as well as principal component (PC)1, 3 and 6. Statistical significance is highlighted at $p < 0.05$ (*) and at $p < 0.01$ (**). All values have been rounded to 3 decimal places.....  | 171 |
| <b>Table 19.</b> Summary statistics for point length, width, and thickness (mm) for each assemblage, highlighting the sample size (n), mean (m) and standard deviation (sd) .....  | 172 |
| <b>Table 20.</b> P-values from Tukey Honestly Significant Difference analyses for length, width, and thickness, as well as principal component (PC)1, 3 and 6 and centroid size (CS) for each pair of assemblages. Statistical significance is highlighted at $p < 0.05$ (*) and at $p < 0.01$ (**). All values have been rounded to 2 decimal places. ....  | 174 |
| <b>Table 21.</b> Principal component (PC) scores for the mean (m) shapes of each assemblage. Standard deviation (sd) is also reported demonstrating the variability of each assemblage in each dimension. All values have been rounded to 2 decimal places.....  | 179 |
| <b>Table 22.</b> Multiple matrix regression standardised test statistics and adjusted $R^2$ for principal components (PC) 1-6, as well as an overall model incorporating all 6 PCs. Variance explained by each PC is given as well as the percentage of shape data explained by each PC is given as well as the percentage of shape data explained by the overall model (%), calculated by multiplying the percentage variance of each PC with the models $R^2$ value. Those relationships that are significant at $p \leq 0.05$ are shaded grey. ....   | 180 |
| <b>Table 23.</b> Multiple matrix regression standardised test statistics and adjusted $R^2$ for length, width, and thickness in addition to the other variables, as well as an overall model incorporating all three dimensions (form). Those relationships that are significant at $p \leq 0.05$ are shaded grey. ....  | 180 |
| <b>Table 24.</b> Summary of the overlapping assemblages studied in this analysis, with a justification of which time slice was chosen for the model. ....  | 189 |
| <b>Table 25.</b> Habitability index values of each assemblage alongside the standard deviations of length, width and thickness (mm) for that assemblage. ....  | 190 |
| <b>Table 26.</b> Multiple matrix regression standardised test statistics, including the habitability index rather than the raw climatic variables, and adjusted $R^2$ for principal components (PC) 1-6, as well as an overall model incorporating all 6 PCs. Variance explained by each PC is given as well as the percentage of shape data explained by each PC is given as well as the percentage of shape data explained by the overall model (%), calculated by multiplying the percentage variance of each PC with the models $R^2$ value. Those relationships that are significant at $p \leq 0.05$ are shaded grey. .... | 191 |
| <b>Table 27.</b> Multiple matrix regression standardised test statistics and adjusted $R^2$ for length, width, and thickness in addition to the other variables including the habitability index, as well as an overall model incorporating all three dimensions (form). Those relationships that are significant at $p \leq 0.05$ are shaded grey. ....   | 192 |
| <b>Table 28.</b> Scaled distance matrix highlighting the degree of point shape variation (as captured by principal components 1-6) between assemblages. ....   | 196 |

## Abstract

Although it was originally thought that our own species, *Homo sapiens*, evolved from a single population in Africa, patterns of diversity in fossil, archaeological, and genetic data now suggest a much more structured and reticulate process in response to varying environmental conditions through time. This thesis provides an investigation of environmentally driven population dynamics during the Middle Stone Age in a case study region of eastern Africa. A variety of complementary quantitative methods are applied to identify the impacts of habitat fluctuation on cultural diversity during this key period when our species first emerges in the record. Specifically, complex shape analyses of Middle Stone Age points, an (albeit imperfect) archaeological proxy for group identity, are used to test the predictions of group interaction from a climatically driven model of habitation that maps how conditions conducive to early human habitation fluctuated through time and space. This model delineates the changing areas of potential human occupation across Africa and the potential corridors between them, which are correlated with patterns of similarity and difference in the archaeological data. To collect the archaeological data during the COVID-19 pandemic, a scientifically robust collaborative data collection framework was developed to facilitate remote access to African museum collections, involving an equitable and cooperative approach to data generation.

The results indicate that eastern African Middle Stone Age populations occupied diverse landscapes, with precipitation and access to water vital for determining site locations and corridors between them, as well as having significant influences over cultural diversity at both the assemblage and artefact-level. Almost half of the variance in point shape is found to be explained by spatial, temporal, and environmental autocorrelation, potentially suggesting stable cultural transmission throughout the region, though a large proportion of unexplained variance can be linked to stylistic variability between individual assemblages. The suitability of the environment that a population is situated within appears to condition point shape diversity to an extent, with interesting patterns of variance between assemblages observed considering the speculative dispersal routes between sites. Overall, complex modelling approaches, such as the one taken in this thesis, are needed to explain the ever-richer African record, will help develop new anthropological and archaeological theory and methods for understanding past population structure, and will advance our knowledge of the effects of climate change on human evolution.

# Chapter 1. Introduction

## 1.1. Brief background

Understanding links between climate change and human behaviour will likely be vital for our species' continued survival. The African Middle Stone Age (MSA), occurring from around ~300-50 thousand years ago (kya), is an ideal laboratory for testing evolutionary hypotheses about human-environment responses, as during this period modern humans emerged against a backdrop of dramatic climatic fluctuations. Early theories of human evolution typically envisaged an eastern African source for *Homo sapiens* (*H. sapiens*; Stringer and Andrews, 1988), yet patterns of diversity within the Late-Middle Pleistocene archaeological record no longer show strong support for simplistic models (Scerri *et al.*, 2014; 2018, Scerri, Chikhi and Thomas, 2019). Now, it is considered much more likely that the migratory patterns of early human populations, the route and extent of which were governed by varying environmental conditions through time and across space, led to complex interaction networks of early human groups, potentially leading to the evolution of 'modern human behaviour', defined by some as increases in technological and cultural complexity associated with symbolism, more sophisticated hunting technology and long distance trade, among other behaviours (Powell, Shennan and Thomas, 2009; Scerri, Chikhi and Thomas, 2019).

Recently, Scerri *et al.* (2018) in a seminal review summarised new developments in this area of research, such as the discovery and re-dating of the Jebel Irhoud fossils in Morocco (Hublin *et al.*, 2017). These authors concluded that the mosaic-like appearance of anatomical and behavioural traits associated with *H. sapiens* during the MSA implies a structured pattern of evolution across Africa prior to extra-continental dispersals. Unlike previous theories, this novel framework implicates the whole African continent in a complex evolutionary process, including regions that have been historically understudied like West and Central Africa as well as those more commonly associated with the evolution of *H. sapiens*, like eastern and South Africa. Early *H. sapiens* is hypothesised to have comprised sets of interconnected regional subpopulations forming a metapopulation that was distinct from other *Homo* metapopulation sets, such as the Neanderthals and Denisovans (Scerri, Chikhi and Thomas, 2019). Scerri *et al.* (2018)'s structured African metapopulation (SAM) model has been gaining momentum in recent years, with archaeological, fossil, genetic and paleoenvironmental evidence seeming to increasingly align in support of structured, pan-African evolution of *H. sapiens* (Scerri and Will, 2023).

One of the major hypotheses of Scerri *et al.*'s (2018) SAM model is that the population structure of the earliest *H. sapiens* was likely driven, at least in part, by the fluctuating environmental conditions experienced during the Late-Middle Pleistocene. Climatic perturbation and its effects on the availability and distribution of suitable habitats is hypothesised to have caused the periodic coalescence and fragmentation of the *H. sapiens* metapopulation. Subpopulations are suggested to have been interconnected by intermittent migration, periodically reshuffling genetic and cultural traits through the isolation and mixing of previously distinct populations. This fluctuating pattern of episodic interaction and seclusion has been argued to explain the non-linear appearance of autapomorphic *H. sapiens* traits in the fossil record (Gunz *et al.*, 2009; Hublin *et al.*, 2017), as well as patterns of genetic diversity in living and ancient African populations (Harding and McVean, 2004; Tishkoff *et al.*, 2009; Lipson *et al.*, 2022) and aspects of cultural diversity in MSA assemblages (Scerri *et al.*, 2014, 2018; Blinkhorn and Grove, 2018, 2021), such as the appearance and disappearance of regional MSA variants (Wurz, 2002; Jacobs *et al.*, 2008; Iovita, 2011; Mackay, Stewart and Chase, 2014; Scerri *et al.*, 2014; d'Errico *et al.*, 2017).

Distinctive point typologies first appear during the African MSA, and usually form part of the criteria of its various defined lithic industries. Points are considered to be a highly variable 'taxon' and thus is a technological category that likely subsumes tools with multiple functions (Douze *et al.*, 2020).

Nonetheless, the emergence of pointed flake technology across Africa at a broadly similar time at the onset of the MSA represents a shift towards a shared technological concept that seemed to have had some behavioural significance for hominin evolution (Maier *et al.*, 2023). Much of the typological variation of points is considered to be an indication of group boundaries and interaction patterns, as is seen in the ethnographic hunter-gatherer exchange system 'hxaro' where retouched projectiles of specific designs are exchanged between interacting individuals (Yellen, 1977; Wiessner, 1982, 1983, 1985; Nicholas and Kramer, 2001). Points are routinely cited to be the single artefact category most reflective of inter-populations contact and regional traditions during the MSA (McBrearty and Brooks, 2000; Wilkins, 2010; Scerri, 2013a; Scerri and Will, 2023), thus their variable typology has the potential to act as an informative proxy for testing hypotheses of the SAM model.

This thesis will provide a quantitative investigation of the environmental hypotheses of the SAM model as described in Scerri *et al.* (2018). This will involve investigating MSA point shape diversity in relation to habitat variation across a case study region of eastern Africa. Arguably, some of the most compelling evidence supporting the SAM model currently derives from the mosaic appearance of 'modern' traits in the fossil record, yet it is the MSA archaeological record that has the most potential as a testing ground of its evolutionary implications due to the more abundant sample and better representation of variation

across the region. Eastern Africa has been selected due to its rich MSA archaeological record; additionally, it does not have widely applied cultural industries that divides its MSA record as seen in other regions (Scerri *et al.*, 2017a; Wurz, 2013). Thus, the archaeological record of this region is variable yet relatively free from historical assumptions about the underlying spatiotemporal structure of cultural variation at a regional level. Eventually investigations should be extended to include other areas and indeed the whole of the African continent, following the hypotheses of the SAM model.

## 1.2. Aims and objectives

The overarching aim of this thesis is to provide a quantitative assessment of the SAM model as proposed by Scerri *et al.* (2018) within the context of the eastern African MSA. The specific hypothesis to be tested is that the fluctuating availability and distribution of hominin-suitable habitats were fundamental for driving inter-group interaction dynamics within and between regions. This aim will be achieved via the following objectives:

- I. I will first characterise the palaeoenvironments inhabited by eastern African populations during the MSA using novel climatic simulations.
- II. I will then produce a comprehensive habitability model incorporating various geographic factors that could condition suitability, such as climate, topographic complexity, and the availability of water, into a single index.
- III. I will collect shape data, specifically that for metric and geometric morphometric analysis, from lithic points at multiple eastern African MSA sites, acting as a proxy for cultural groups.
- IV. Finally, I will integrate the archaeological data with the habitability model to understand how eastern African population networks may have been influenced by fluctuating conditions.

To reconstruct the environments inhabited by eastern African MSA populations, I will produce a high-resolution and spatiotemporally explicit paleoenvironmental framework for the region. To realise this aim, the following objectives will be achieved:

- I. I will extract time-specific climate data from eastern African archaeological site locations to produce a characterisation of MSA palaeoenvironments at a regional level.
- II. I will next use ethnographic data to predict areas across the landscape that were climatically suitable for hunter-gatherers throughout the Late-Middle Pleistocene.



- III. I will calculate the distance to water sources and the energetic cost of movement across heterogenous landscapes for integration with the climate suitability model to produce a single index of habitability.
- IV. Lastly, I will test how well the habitability model predicts MSA site locations using a permutation approach.

To identify population structure in the archaeological data, null models of spatial, temporal, and environmental autocorrelation will be used (Shennan, 2020), as deviations from such models likely are indicative of culturally structured patterns of variability. I will apply this body of theory from genetics, referred to as isolation by distance, time, and environment, to the eastern African MSA record to test the SAM model (Scerri *et al.*, 2018). This will be achieved by:

- I. Utilising archaeological data that is potentially indicative of inter-group social dynamics: the typology of MSA points. Point designs are routinely used in archaeology as proxies for group identity (Shott, 2020), including in the MSA (Wilkins, 2010; McBrearty and Brooks, 2000; Iovita, 2011; Archer *et al.*, 2015, 2016).
- II. Ensuring point samples are sufficiently isolated through space, time, and environments to effectively test the assumptions of the null models.
- III. Applying bespoke statistical methods to identify and factor out autocorrelation in the shape data as well as Geographic Information Systems (GIS) approaches to understand the spatial implications of habitat suitability on MSA point shape diversity.

This thesis was carried out during the COVID-19 pandemic, a time when travelling to museum collections for access to archaeological samples was untenable. Therefore, another unforeseen aim of this thesis was to develop and validate a remote method of collaboration with multiple museums that can enable comparatively robust analyses to those carried out by a single observer. Although only the data from two museums is reported here (National Museums of Kenya and National Museum of Ethiopia), this sub-project was initiated with a total of six museum partners from Africa and Europe to extend the scope of the project far beyond this thesis. The objectives to realise this aim are:

- I. To build connections with local researchers at National Museums of Kenya, National Museum of Ethiopia, Iziko Museums of South Africa, Mossel Bay Archaeological Project, Institut des Sciences de l'Archéologie et du Patrimoine and Musée de l'Homme.
- II. To secure funding to support the local collaborators for the duration of the project.

- III. To work with collaborators to develop data collection protocols and subsequently build a database of samples.
- IV. To develop a bespoke inter-observer error test to establish the extent of variability between datasets to ensure accurate results.

### 1.3. Outline of thesis structure

This thesis is organised into ten chapters, of which three represent published works (see Table 1 for an overview). The chapters can be grouped into five key components:

- I. Theoretical and literature background to the research (Chapters 1-3)
- II. Paleoenvironmental analysis (Chapters 4-5)
- III. Collaborative data collection (Chapters 6-7)
- IV. MSA point analysis (Chapters 8)
- V. Comprehensive analysis of population structure (Chapters 9-10)

**Table 1.** An overview of the published works included in this thesis.

| Title   | Chapter | Full Reference  |
|---|---------|---|
| A spatiotemporally explicit palaeoenvironmental framework for the Middle Stone Age of eastern Africa        | 4       | Timbrell, L., Grove, M., Manica, A., Rucina, S. and Blinkhorn, J. (2022a). A spatiotemporally explicit palaeoenvironmental framework for the Middle Stone Age of eastern Africa. <i>Scientific Reports</i> . 12, 3689<br><a href="https://doi.org/10.1038/s41598-022-07742-y">https://doi.org/10.1038/s41598-022-07742-y</a>  |
| A collaborative model for lithic shape digitization in museum settings                                      | 6       | Timbrell, L. (2022). A collaborative model for lithic shape digitization in museum settings. <i>Lithic Technology</i> .<br><a href="https://doi.org/10.1080/01977261.2022.2092299">https://doi.org/10.1080/01977261.2022.2092299</a>  |
| Testing inter-observer error under a collaborative research framework for studying lithic shape variability | 7       | Timbrell, L., Scott, C., Habte, B., Tefera, Y., Monod, H., Qazzih, M., Marais, B., Black, W., Maroma, C., Ndiema, E., Henderson, S., Elmes, K., Plomp, K and Grove, M. (2022b). Testing inter-observer error under a collaborative research framework for studying lithic shape variability. <i>Archaeological and Anthropological Sciences</i> 14, 209.<br><a href="https://doi.org/10.1007/s12520-022-01676-2">https://doi.org/10.1007/s12520-022-01676-2</a> |

Chapter 1 introduces the thesis, including the rationale behind the study and the overall aims and objectives of the research. This section is followed by Chapter 2, which provides the theoretical

framework within which this thesis sits, as well as historical ideas about modern human evolution. Multiple lines of evidence are addressed, and the theoretical implications of the SAM model are introduced. Then, Chapter 3 provides the literature background to the study region and period, the eastern Africa MSA, including an overview of research history of African Stone Age archaeology.

Chapter 4 is the first analysis chapter of the thesis. It presents a spatiotemporally explicit palaeoenvironmental framework for the eastern African Middle Stone Age, including analyses testing the relationships between climate and technology. Chapter 5 builds upon the methodology introduced in Chapter 4 and reports a comprehensive habitability model for the Late-Middle Pleistocene that is independently validated against the eastern African MSA record.

Chapter 6 presents the collaborative research framework that was developed to collect the raw shape data for the MSA point research. Chapter 7 tests the validity of this framework using a bespoke error analysis involving the production of 3D printed replica assemblages.

Chapter 8 reports a geometric morphometric study of eastern African MSA point variability, which applies null models of isolation by distance, time, and environment against which population structure can be tested.

Chapter 9 integrates the geometric morphometric data within the habitability model presented in Chapter 5 to assess the implications of habitat variability on point shape diversity. This is done using a combination of correlational methods and least-cost path approaches. Finally, Chapter 10 provides a summary of the results and some concluding comments, including the limitations and future directions of the research.

## Chapter 2: Theories of modern human evolution

Human evolution, particularly the emergence of ‘modern’ humans (used loosely here to refer to *H. sapiens*), has a long history of research. Models claiming to accurately represent the evolution of *H. sapiens* have historically fallen into two main categories – ‘multiregionalism’ and ‘Out of Africa’. Whilst multiregionalism was initially popular among the research community, Out of Africa has garnered almost ubiquitous support in recent years, causing near-universal rejection of multiregionalism theory as originally proposed by Wolpoff, Wu and Thorne (1984). However, although a recent African origin of *H. sapiens* is largely coherent with the available data, it alone cannot explain the global diversity of both early and living human populations. More complex models are thus required. A recent variant of the Out of Africa framework, the structured African metapopulation (SAM) model, sometimes referred to as ‘African multiregionalism’, provides a new framework for understanding the evolution of *H. sapiens* in Africa prior to dispersal (Scerri *et al.*, 2018; Scerri, Chikhi and Thomas, 2019). The SAM model has growing support in the literature because of its apparent correspondence with various forms of data, and forms the theoretical basis of this thesis. This chapter presents historical theories about the evolution of *H. sapiens* before outlining the fossil, archaeological, genetic, and climatic evidence in favour of the SAM model.

### 2.1. Multiregionalism

Multiregional evolution was the first comprehensive model devised to explain modern human evolution. It argued that the origins of *H. sapiens* and their ensuing regional diversity was the result of continuity from archaic Middle Pleistocene species to contemporaneous populations across the Old World (Wolpoff, Wu and Thorne, 1984; Wolpoff, 1989; Thorne and Wolpoff, 1992). This framework was initially inspired by work by Weidenreich (1938, 1946) and Coon (1962), who noted that the regionally polytypic cranial morphology of *Homo erectus* (*H. erectus*) fossils appeared similar to that of living *H. sapiens* populations in the same area. This led to the hypothesis that *H. erectus* evolved into *H. sapiens* in a series of evolutionary grades, with universal aspects of morphological change, such as the reduction of the supraorbital torus, transpiring across the Old World at region-specific rates, time of initiation, and evolutionary trajectories (Wolpoff, 1986). Such processes were hypothesised to have been affected by differences in the gene-pools of the source populations and the adaptive mechanisms, such as selection and genetic drift, acting to shape diversity. A limited amount of gene flow between regions was proposed to have constrained regional diversification and inhibited speciation (Wolpoff, 1989), whilst directional

gene flow from the centre of the region to the peripheries maintained regional-specific evolutionary trajectories (Frayer *et al.*, 1993).

Multiregionalists tend to stress a lack of speciation within later hominin evolution (Wolpoff, Wu and Thorne, 1984; Wolpoff, 1986; Wolpoff *et al.*, 1994), revisiting ideas from ‘the single species hypothesis’ (Brace, 1969). This suggests that, like all other mammals, hominins occupy a specific ecological niche as a result of their distinctive cultural abilities and thus it would be impossible for more than one species to have co-existed within the same geographical area over an extended period of time (Brace, 1969). It has been contended that the fossil record also currently lacks a well-defined boundary between *H. erectus* and *H. sapiens*, with Wolpoff *et al.* (1994) arguing that clear diagnostic features allowing for operational definitions of ‘anatomical modernity’ are absent in the literature. Wolpoff *et al.* (1994) maintain that *H. erectus* is polytypic with geographical variants showing regional continuity with those seen in similarly polytypic *H. sapiens*. Therefore, the current morphological criteria for ‘anatomical modernity’ are deemed inadequate by these authors for describing variation in modern populations (see further discussion in Chapter 2.2) as a distinct spatiotemporal taxonomic boundary cannot be defined, thus a merging of taxa into a single evolutionary species is argued to be necessary, though really this is more a reflection of our inability to interpret the hominin record.

Growing evidence for archaic admixture in the genomes of living human genomes confirms that the ancestors of modern *H. sapiens* populations interbred with archaic species of hominins (Kaifu, 2017; Browning *et al.*, 2018; Durvasula and Sankararaman, 2020). This evidence for assimilation supports the multiregionalists appeal for a single species framework through challenging the core assumption of the biological species concept of reproductive isolation (Mayr, 1942), though recently this has been concluded to be a ‘biologically misplaced expectation’ (Meneganzin and Bernardi, 2023). Additionally, it is not yet clear how widespread and significant hybridisation events were, as the prevalence of archaic genes in contemporary *H. sapiens* is relatively low. Around 2% of an average Eurasian genome derives from Neanderthal admixture, and 4-6% of Melanesian genomes was introgressed from Denisovans (Browning *et al.*, 2013; Fu *et al.*, 2014; Skov *et al.*, 2020). Whether this low percentage represents the infrequency of hybridisation events or their lack of viability remains to be identified (Stringer, 2014), though some work suggests the latter may be more probable (Sankararaman *et al.*, 2014). Nonetheless, the multiregionalism framework, by definition, assumes a high rate of successful interbreeding to sustain spatiotemporal regional continuity and lack of speciation. Therefore, this growing body of ancient DNA (aDNA) research is yet to offer substantial support for a multiregional framework for human evolution.

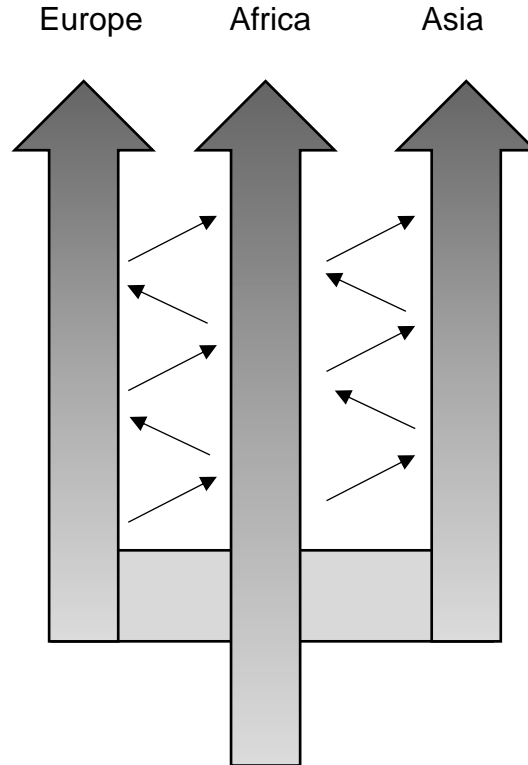


**Figure 1.** Multiregionalism schematic diagram. Adapted from Stringer (2014). The arrows show the direction of gene flow.

Hominin fossil evidence is generally used in arguments in favour of the multiregionalism hypothesis, particularly from southeast Asia where notable and distinctive similarities have been observed between past and present populations, such as the late *H. erectus* Ngandong population in Java and near-contemporary Aboriginal Australians (Thorne, 1984). Many classify the Ngandong as ‘transitional’ between *H. erectus* and *H. sapiens* as their enlarged cranial capacity is characteristically modern yet other aspects of their cranial morphology are more archaic (Wolpoff *et al.*, 1994). However, recent dating would suggest the Javanese *H. erectus* population at 117-108 kya was extinct before the appearance of *H. sapiens* in the area much later (Rizal *et al.*, 2020). In addition, further morphometric analyses have found a number of unique autapomorphies in the Ngandong morphology, such as the lengthening of the midcranial base, implying that this group did not significantly contribute to the lineage that led to *H. sapiens* (Kaifu *et al.*, 2008). Therefore, whether the morphological link made by Wolpoff *et al.* (1994) between Aboriginal Australian and Ngandong crania is due to an ancestral connection is unlikely. Recent morphometric analyses on Late-Middle Pleistocene hominin remains from Hualongdong in China controversially have been argued to show support for regional continuity, reporting consistencies in

skeletal and dental features between the archaic and modern morphologies in that area. (Wu *et al.*, 2019). However, without aDNA, a direct ancestral connection remains spurious due to the lack of further examples of regional consistencies over extended periods of time.

Multiregionalism, whilst earning only limited support in the recent literature (e.g. Wu *et al.*, 2019), is almost universally dismissed by the contemporary academic community, who largely deem it an inadequate model for characterising modern human evolution. Demonstrating regional continuity between archaic and living populations, with extensive networks allowing gene flow through space and time to inhibit speciation, remains a huge challenge given the available evidence, especially as extensive data in various forms now point to Africa as the single point of origin. Multiregionalism as a hypothesis for modern human origins should no-doubt be dismissed in favour of the Out of Africa model, yet such notions of regional continuity have been invoked in discussions of the SAM model (Klein, 2019; Scerri, Chikhi and Thomas, 2019), thus warranting its presentation and discussion in this thesis.

## 2.2. Simple Out of Africa

Whilst multiregionalism predicts a pattern of variation involving temporal and regional consistency, the Out of Africa model instead relies on the process of population replacement to explain hominin diversity outside of Africa: the single point of origin for *H. sapiens* (see Table 2 for a summary). Out of Africa assumes a recent African common ancestor for all *H. sapiens* populations, with dispersals within and beyond the continent allowing for the establishment of modern regional diversity. Out of Africa is supported by the consistent observation that genetic (Harpending and Rogers, 2000; Prugnolle, Manica and Balloux, 2005; Ramachandran *et al.*, 2005), linguistic (Atkinson, 2011) and cranial (Manica *et al.*, 2007; von Cramon-Taubadel and Lycett, 2008; Betti *et al.*, 2009) diversity decreases with increasing distance from Africa. This pattern is often referred to as a serial founder effect due to the iterative loss of variation as a result of bottlenecks causing decreased diversity in each successive founding population (Ramachandran *et al.*, 2005). A recent African origin is also supported by the lack of transitional fossils occurring outside of the continent (Stringer and Buck, 2014) and the earliest appearance of *H. sapiens* in the record occurring in Africa (White *et al.*, 2003; Hublin *et al.*, 2017; Vidal *et al.*, 2022). In its simplest form, the Out of Africa model suggests that *H. sapiens* evolved within a single population in a single region of Africa, and then expanded throughout Africa and into the Old World; the model allows for a small amount of archaic admixture (DeGiorgio, Jakobsson and Rosenberg, 2009) but mainly suggests that this process contributed heavily to the eventual extinction of other archaic hominin groups.

**Table 2.** A summary of the theoretical assumptions of multiregionalism and Out of Africa. Adapted from Stringer and Andrews (1988).

| Feature   | Multiregionalism   | Out of Africa   |
|---|--|---|
| Regional patterns of human evolution                          | Continuity from Middle Pleistocene <i>Homo</i> to present  | Continuity only from Late Pleistocene <i>H. sapiens</i> to present  |
|   | Morphological differences between regions are high, with the greatest between each peripheral area           | Morphological differences between regions are relatively low, with the greatest between African and non-African populations   |
|   | Within-group variation is the greatest in populations occupying the geographic centre of the human range     | Within-group variation is the greatest in African populations   |
| Regional consistencies and the emergence of <i>H. sapiens</i> | Transitional fossils are present across Old World  | Transitional fossils are restricted to Africa, with population replacement occurring outside of Africa  |
|   | Modern regional characters of high antiquity are present at the peripheries                                  | Modern regional characters of low antiquity are present at the peripheries (except within Africa)   |
|   | No consistent chronological pattern of the appearance of ' <i>H. sapiens</i> ' characteristics between areas | Phased establishment of the ' <i>H. sapiens</i> ' suite of characters: <ol style="list-style-type: none"> <li>1. Africa</li> <li>2. Southwest Asia</li> <li>3. Other areas</li> </ol> |
| Selection and behaviour                                       | Selection factors are varied and widespread, with local behavioural continuity                               | Selection factors are specific and localised in Africa, with behavioural discontinuity expected outside Africa  |

Early genetic studies noted that variation in living *H. sapiens* populations is comparably low in relation to that between closely related primate taxa. Latter (1980) found that only 10% of human protein polymorphisms were related to inter-regional differences, compared to the 84% linked to differences within regions and 6% due to 'nationality'. This ratio of diversity was mirrored in mitochondrial DNA (mtDNA) studies; however, whilst all human populations share this overall lack of diversity when compared to other species, it was revealed that sub-Saharan African populations possess much greater



within-population diversity than other global groups (Cann, Stoneking and Wilson, 1987; Stoneking and Cann, 1989). The authors deduced from this that there must be a greater antiquity of genetic lineages within these African populations and therefore modern humans must have originated in Africa (Cann, Stoneking and Wilson, 1987). Rogers and Jorde (1995) challenged this finding, proposing that these patterns of diversity in mtDNA are actually reflective of the fact that Africa held a larger effective population size during this period. Nonetheless, Harpending *et al.* (1993) concluded that even when taking group size into account, a signal of the Out of Africa event can be identified. The development of whole-genome and next generation sequencing technologies has also provided valuable resources for studying the Out of Africa dispersal (e.g., Reich *et al.*, 2001; Marth *et al.*, 2004; Plagnol and Wall, 2006). For example, the 1000 Genomes Project confirmed that Africans have a higher number of single nucleotide polymorphisms compared to populations outside of Africa (Genomes Project *et al.*, 2015). Additionally, regressions explaining 76-78% of global genetic variation have strongly showed that diversity linearly decreases from Africa, with an expansion originating in Africa the most likely explanation of the observed data (Ramachandran *et al.*, 2005).

Additional advances in revolutionary chronometric dating methods, such as electron spin resonance (ESR) and thermoluminescence (TL), have since confirmed that Africa possesses the earliest examples of *H. sapiens* in the archaeological record (Day, 1969; White *et al.*, 2003; Hublin *et al.*, 2017; Vidal *et al.*, 2022). The first proposed appearances of *H. sapiens* fossils were initially noted at eastern African sites, such as those discovered in Ethiopia at Omo Kibish, originally dated to  $195 \pm 5$  kya (McDougall, Brown and Fleagle, 2005) but redated to  $233 \pm 22$  kya (Vidal *et al.*, 2022), and Herto, dated to between 160-154 kya (White *et al.*, 2003). Three adult individuals were recovered from Omo Kibish in 1967 (known as Omo I, II and III) and were believed to be of similar age (Day, 1969). However, they show marked differences in cranial morphology; Omo I is considered to be more ‘modern’, with the presence of a chin, modern dentition and a rounded occipital bone, whereas the Omo II was originally likened to more ‘archaic’ African hominins, like the Kabwe ‘Broken Hill’ cranium (Day, 1969), believed to belong to *Homo heidelbergensis* (*H. heidelbergensis*).

Distinguishing between the ‘modern’ morphology of *H. sapiens* and their archaic ancestors is, however, somewhat difficult. This is due to the absence of a ubiquitous definition of ‘anatomical modernity’ as well as the high degree of morphological variability observed during the Middle Pleistocene. Most scholars use the criteria established by Day and Stringer (1982) and Stringer, Hublin and Vandermeersch (1984), which provides a list of cranial characteristics considered autapomorphic of *H. sapiens* in comparison to other Late-Middle Pleistocene hominins (Table 3). At least three of the defining features are required for

a fossil to be classified as *H. sapiens* under this framework. However, for some, the suite of cranial traits is not broad enough, with many contemporary *H. sapiens* crania falling outside of the established parameters (Wolpoff, 1986; Mirazón Lahr, 1996). For example, Wolpoff (1986) found that 43% of Tasmanian crania did not meet the Day and Stringer (1982) definition, and Mirazón Lahr (1996) reported that the mean frontal angle for Fuegian/Patagonian crania fell outside the given range for *H. sapiens*. Some researchers had claimed that the inadequacy of the trait-list is a result of an Euro/African bias in the definition of *H. sapiens* (Wolpoff, 1986) though Mirazón Lahr (1996) disagrees, as inadequacies were found to be spread among different populations, including those from Europe. To rectify this inadequacy, Schwartz and Tattersall (2003) use a narrower version of nine cranial characteristics (although many are similar to those described in Table 2) to differentiate between modern and archaic hominin species, suggesting that many fossils considered *H. sapiens* have been wrongly classified (Schwartz and Tattersall, 2003). Regardless, the inadequacies of previous trait-based approaches, and the inconsistencies between them, speaks to the highly variable and non-sequential nature of human morphological evolution, making drawing distinctions between species based on current evidence a difficult and perhaps even futile exercise.

**Table 3.** Cranial characteristics unique to modern *H. sapiens*, as established by Day and Stringer (1982) and Stringer, Hublin and Vandermeersch (1984). At least three of these are required for a specimen to be classified as *H. sapiens*.

|  |
|--|
| A relatively short and high cranial vault; basion-bregma height/glebella-occipital length >0.70; vertex radius/glebella-occipital length >0.64 |
| A high frontal bone; frontal angle <134°   |
| A long and curved parietal bone which bends in the mid-sagittal plane; parietal angle <138°  |
| A long and high parietal arch which narrows inferiorly; asterion-bregma length/biasterionic breadth >1.19                                      |
| A long and narrow occipital bone which is not particularly projecting; occipital angle >113°   |
| Small dentition, especially the anterior teeth   |
| A weak supraorbital torus which is divided into medial and lateral sections  |
| True external occipital protuberance   |
| Canine fossa   |
| Well-developed mental eminence   |

### 2.3. Complex Out of Africa

Despite the Out of Africa model providing a more parsimonious framework for understanding modern human evolution, Mirazón Lahr and Foley (1994) pointed out that a hypothesis invoking a single African population giving rise to all modern populations both inside and outside of Africa lacks specificity about the evolutionary processes generating spatiotemporal patterns of diversity. These authors therefore

devised the 'Multiple Dispersals Model'. This model still implicates Africa as the single origin of *H. sapiens* but that multiple dispersals out of the continent took place to eventually colonise the Old World (Mirazón Lahr and Foley, 1994). This complex Out of Africa scenario suggests that dispersal events during the Late Pleistocene happened frequently and acted as the primary mechanism by which the modern human population initially diversified (Mirazón Lahr and Foley, 1994; Mirazón Lahr, 1996). Variations in the ancestral morphology of successful dispersing populations would have influenced patterns of global variability, followed by local adaptation and inter- and intra-regional migration (Mirazón Lahr, 1996; Mirazón Lahr and Foley, 1994). A microevolutionary perspective is therefore adopted, with 'evolutionary geography' playing a central role in shaping the selective forces that affect the diversification of regional populations in terms of the local pressures on survival, range and demography (Mirazón Lahr and Foley, 1998).

Whilst many agree that the Complex Out of Africa scenario theoretically explains the diversity observed outside of Africa during the Late Pleistocene, the number and routes of dispersals out of the continent are contested. Originally, Mirazón Lahr and Foley (1994) argued that the main expansion of modern humans occurred around 45 kya, with an earlier expansion of genetically, behaviourally, and morphologically differentiated groups around 100-50 kya, likely originating from eastern Africa with dispersal towards the Indian subcontinent. This could explain why some of the earliest evidence of modern human occupation occurs in Australia at ~60-50 kya (Roberts, Jones and Smith, 1990; Clarkson *et al.*, 2017), many thousands of years before the widespread occupation of Europe. This first dispersal was suggested to have involved a rapid migration via a coastal route through southeast Asia, supported by the retention of a genetic signal from this initial dispersal in 'relict' populations, such as Australians, Melanesians and Papuans (Ghirotto, Penso-Dolfen and Barbujani, 2011; Rasmussen *et al.*, 2011; Reyes-Centeno *et al.*, 2014). Such populations are proposed to retain plesiomorphic traits, as a consequence of their relative isolation from subsequent migrations, inhabiting geographical refugia and/or by developing specific niches, in addition to having small population sizes (Reyes-Centeno *et al.*, 2015). Early extra-African dispersals were hypothesised to have occurred from the Horn of Africa during the transition between Marine Isotope Stage (MIS) 5 and 6, crossing the Bab el Mandeb during a period of low sea level and increased rainfall, with occupation of eastern Arabia by the last interglacial as demonstrated by archaeological site Jebel Faya (Armitage *et al.*, 2011). Using least-cost analyses, Field and Mirazón Lahr (2005) assessed the southern route out of Africa and found that dispersals would have initially occurred rapidly due to the presence of coastlines and rivers producing a 'funnelling effect', but as populations expanded into the South Asia interior and along the Sunda Shelf, movement would have slowed due to the density of tropical forests. Genetic studies also support this southern dispersal route; for example,

Soares *et al.* (2012) and Fernandes *et al.* (2012) concluded that individuals assigned to mtDNA haplogroup L3 likely migrated out of the continent via the Bab el Mandeb strait. Groucutt *et al.* (2015a) challenged their conclusions, demonstrating that L3 could have originated either inside or outside of Africa if gene flow occurred between the ancestors of Africans and non-Africans following their initial divergence. This contests the assumption of previous mtDNA studies that L3 represents a remnant eastern African haplogroup (Quintana-Murci *et al.*, 1999) and that human evolution is likely much more reticulated than the “tree-like” structure traditionally adopted (Scerri, Chikhi and Thomas, 2019).

Contrastingly, a proposed northern route out of Africa suggests that movement of modern humans occurred through Egypt and the Sinai Peninsula into the Levant. Evidence for *H. sapiens* occupation of Greece at ~210 kya is suggested from Apidima Cave (Harvati *et al.*, 2019), yet only a small fragment of the cranium was recovered and it is highly distorted, making it difficult to draw strong conclusions about taxonomy. The northern route is supported by the discovery and dating of the Levantine Skhul and Qafzeh fossils, antedating to 120 kya and 100-90 kya respectively. (Stringer *et al.*, 1989; McDermott *et al.*, 1993). It is believed that these fossils represent some of the first populations to move out of Africa, although many consider them to have been failed dispersals (Oppenheimer, 2003). This is because there is a considerable gap in the fossil record of the area following these finds, with the next human remains not appearing until 55 kya (Hershkovitz *et al.*, 2015), apart from a single phalanx from Al Wusta in Saudi Arabia at around 85 kya (Groucutt *et al.*, 2018). Additionally, regional climatic records suggest that humans would not have survived the onset of glacial conditions at 90 kya (Pope and Terrell, 2008). However, Groucutt *et al.* (2015b) identified similarities between eastern African lithic technologies from MIS 8 onwards and Middle Palaeolithic assemblages as far east as India by MIS 5, suggesting that these early periods were likely critical for human dispersals from northeast Africa to the Levant. Genetic studies have also shown support for the northern route; Pagani *et al.* (2015) found that modern non-African haplotypes were more similar to those of Egyptians than to those of Ethiopians.

The multiple dispersals model offers a much more nuanced explanation for how modern human diversity evolved from a single point of origin: Africa. However, the model fails to adequately address the archaeological and fossil diversity *within* Africa during the key period when *H. sapiens* traits first appear in the fossil record. Mirazón Lahr and Foley (1998) suggest that one relatively large ancestral population of all *H. sapiens* would have existed, which developed unique adaptations to warrant its survival over other ‘near-modern’ populations. This is hypothesised to have led to expansions both within and beyond the initial area of endemism, which was proposed to be northeastern sub-Saharan Africa. However, this does not account for the fact that some of the earliest fossils, classified as *H. sapiens* or belonging to the

*H. sapiens* lineage, appear in diverse areas of the continent at broadly the same time (Grün, 2016; Hublin *et al.*, 2017; Vidal *et al.*, 2022).

## 2.4. The structured African metapopulation model

Whilst multiple lines of evidence point to Africa as being the clear point of origin of *H. sapiens*, it is becoming increasingly clear that the whole continent should be the centre of focus when trying to understand modern human origins. As previously described, for many years it was believed that all contemporary humans originated from a panmictic population in a distinct region of the continent, suggested to have been eastern Africa (Mirazon Lahr and Foley, 1998). Yet increasingly data seem to indicate that early *H. sapiens* were highly diverse and lived across the continent (Gunz *et al.*, 2009; Scerri *et al.*, 2014; Skoglund *et al.*, 2017), likely comprising transient sets of interconnected regional subpopulations that formed a continental metapopulation. This process is captured by the SAM model (Scerri *et al.*, 2018; Scerri, Chikhi and Thomas, 2019), which provides the flexibility necessary to adequately explain patterns in the current data, emphasising structure within evolutionary lineages due to changing configurations of fission, fusion, gene flow and local extinction (Mirazón Lahr and Foley, 1998; Scerri, Chikhi and Thomas, 2019).

For the sake of convenience, this pan-African origins scenario has previously been dubbed a form of ‘African multiregionalism’ (Scerri *et al.*, 2018) yet, unlike traditional multiregionalism as described in Chapter 2.1, the SAM model does not imply a rigid regional structure and continuity through time, as (mis)interpreted by Klein (2019) in his critique. Instead, an oscillating evolutionary process, facilitating periodic connection and isolation of subpopulations and causing a reshuffling of gene and culture constellations, would have led to the eventual fixation of certain traits of modernity within the species (Klein, 2019; Scerri, Chikhi and Thomas, 2019). The SAM model may also involve hybridisation between the *H. sapiens* metapopulation and that of more divergent hominins surviving in distinct populations across Africa (Wall, Lohmueller and Plagnol, 2009; Hammer *et al.*, 2011; Mendez *et al.*, 2013; Durvasula and Sankararaman, 2020). For example, *Homo naledi* (*H. naledi*), found in the Rising Star Cave system in South Africa, dates to a broadly similar time and is described as having primarily primitive, though some modern, anatomical features, as well as complex culture like mortuary behaviour and the manipulation of fire (Berger *et al.*, 2015; Dirks *et al.*, 2017), though the evidence is contested, and some not yet peer reviewed. It is somewhat unlikely that interbreeding between *H. naledi* and *H. sapiens* would have produced viable offspring, though it is not beyond the realms of possibility. Regardless, the

appearance of a morphologically ‘primitive’ hominins relatively late in the record attests to the complex evolutionary landscape during the Middle Pleistocene,

#### 2.4.1. Evidence of structure in Late-Middle Pleistocene Africa

Early manifestations of *H. sapiens* automorphisms appear in the fossil record at around 300 kya (Hublin *et al.*, 2017). However, we do not see a linear progression towards contemporary human morphology; instead putative early *H. sapiens* fossils exhibit great morphological diversity (Gunz *et al.*, 2009) and geographical range (Blinkhorn *et al.*, 2022). In combination with archaeological and genetic evidence, these data are consistent with the SAM model, suggesting that our species originated and diversified within structured populations, living across Africa and connected by sporadic gene flow (Mirazón Lahr and Foley, 1998; Pearson, 2008; Gunz *et al.*, 2009; Scerri *et al.*, 2014, 2018; Skoglund *et al.*, 2017; Klein, 2019; Scerri, Chikhi and Thomas, 2019). Critically, networks of subpopulations were likely driven and maintained by fluctuations in ecological boundaries (Basell, 2008; Blome *et al.*, 2012; Mackay, Stewart and Chase, 2014; Uren *et al.*, 2016), implying a previously underacknowledged complexity in *H. sapiens* African origins.

##### 2.4.1.1. Morphological diversity in the *Homo sapiens* clade

Whilst the exact constellation of the morphological features characterising *H. sapiens* still lacks consensus, the earliest manifestations of ‘anatomical modernity’ emerge during the Late-Middle Pleistocene in Africa (Stringer, 2016). As previously discussed, contemporary human crania are usually characterised by a list of features that make them distinguishable from archaic species (see Table 3). However, these automorphisms have been found to emerge in a mosaic-like fashion in the fossil record, with each early example appearing to have a different combination of ‘modern’ and ‘archaic’ traits. For example, fossils from Jebel Irhoud in northern Africa are commonly cited as some of the earliest members of the *H. sapiens* lineage at ~315 kya (Hublin *et al.*, 2017; Richter *et al.*, 2017); however, the Irhoud crania possess both ‘modern’ and ‘primitive’ characteristics. Irhoud 1 and the reconstruction of Irhoud 10 possess a derived facial, mandibular and dental morphology, falling within the range of contemporary modern humans (Harvati, Hublin and Gunz, 2010; Hublin *et al.*, 2017). Some of the ‘modern’ craniofacial characteristics of the Irhoud fossils ubiquitously include a short and retracted facial skeleton, although they vary in their degree of brow ridge protrusion (Harvati, Hublin and Gunz, 2010), which has been attributed to sexual dimorphism (Hublin *et al.*, 2017). Despite the presence of certain modern features, the Irhoud crania retain an elongated brain case shape (Bruner and Pearson, 2013;

Hublin *et al.*, 2017). This specific combination of both derived and archaic features has led to the hypothesis that the facial skeleton evolved first with other aspects of modernity, such as the brain case, appearing later within the *H. sapiens* lineage (Hublin *et al.*, 2017), a pattern similarly seen in Neanderthal evolution (Arsuaga *et al.*, 2014).

The morphological diversity of the Omo Kibish fossils also suggests a high degree of population structure. These remains were key to the original diagnosis of *H. sapiens* morphology as, until the discovery of the Jebel Irhoud fossils, they were believed to represent the earliest dated *H. sapiens* fossils (Aubert *et al.*, 2012). Omo I was found partially *in situ* whereas Omo II was a surface find from over 2.5km away (Day and Stringer, 1982); due to the lack of context for Omo II, both crania have been assumed to be of the same age as a result of uranium-series dating of Omo I (Aubert *et al.*, 2012; Vidal *et al.*, 2022). Yet, despite the fossils having a similar datum, they exhibit a high degree of morphological variation (Stringer and Buck, 2014). Differences between the fossils include neurocranial globularity and occipital morphology (Day and Stringer, 1982). Variation at Omo Kibish has thus been suggested to represent the co-existence of morphologically distinct populations within Ethiopia, with evolution progressing independently in different populations as a result of morphological structure at the population level (Stringer, 2002). Omo II is classified by Bräuer (2012) as ‘late archaic’ *H. sapiens*, whilst Omo I and III are described as having ‘reached anatomical modernity’, reinforcing the argument that morphological evolution did not have a linear trajectory and rather occurred in a mosaic-like fashion.

Elsewhere in eastern Africa, there are other fossil examples exhibiting diverse constellations of both ‘modern’ and ‘archaic’ characteristics, such as the recent discovery of a child skeleton at Panga Ya Saidi, coastal Kenya (Martinon-Torres *et al.*, 2021). Additionally, the cranium discovered at Herto, dated to ~160 kya (Clark *et al.*, 2003), was assigned the sub-species label *Homo sapiens idaltu* and proposed to represent an intermediary population between archaic and anatomically modern humans (White *et al.*, 2003). In contrast to the Irhoud fossils, the Herto remains possess a relatively globular braincase with a robust occipital and large facial skeleton (White *et al.*, 2003). The Eliye Springs crania (KNM-ES 1169327), dated to 270-300 kya based on the morphology of the nearby Guomde fossil (Bräuer and Leakey, 1986), exhibits another different combination of cranial characteristics, sharing affinities to Omo II and Florisbad in some features (e.g., cranial vault shape), whereas in other features (e.g., cranial capacity) it appears more similar to the LH18 fossil. LH18, dated to 200-300 kya, was discovered at Laetoli in Tanzania and has been deemed (tentatively) as early *H. sapiens* by some (Day, Leakey and Magori, 1980), and *H. helmei* by others (Mirazón Lahr, 1996; Mirazón Lahr and Foley, 1998). However, perhaps it would seem more productive to view some of these fossils as part of the diversity exhibited by

the earliest members of a *H. sapiens* clade, rather than assigning species/subspecies labels to single fossils without knowing the extent of variability within these populations.

Numerous analytical studies have concluded that cranial shape diversity within Late-Middle Pleistocene fossils is indicative of the existence of deep population structure (Gunz *et al.*, 2009; Harvati *et al.*, 2011; Mounier and Lahr, 2019). Gunz *et al.* (2009) used three-dimensional (3D) geometric morphometrics to compare the variation of Late-Middle Pleistocene crania with other groups of *Homo* and contemporary modern humans. The Late-Middle Pleistocene group were found to be the most variable and showed more similarities to recent geographically dispersed human populations than other archaic groups. High variability was concluded to indicate the presence of structure during this time period (Gunz *et al.*, 2009). However, the sample of early *H. sapiens* available in this study lacked good chronological and spatial coverage of the fossil record and Gunz *et al.* (2009) only analysed the morphology of the neurocranium, thus offering limited insight into the patterns of cranial shape variability. Mounier and Lahr (2019) in similar analyses included a wider range of fossils than Gunz *et al.* (2009) and measured the full cranium of each specimen (Table 4). Nonetheless, similar conclusions were reached about Late-Middle Pleistocene population structure. Mounier and Lahr (2019) also used phylogenetic modelling in conjunction with 3D geometric morphometrics to predict the morphology of the last common ancestor (LCA) of all modern humans, which was then compared to the sample of Late-Middle Pleistocene fossils. It is worth noting that many relevant specimens had to be omitted from this section of the analysis due to poor preservation. Their results supported a complex scenario for the evolution of anatomical modernity and suggested that various morphological lineages existed within Africa. Mounier and Lahr (2019) concluded that the Irhoud crania likely represents an extraneous lineage that did not contribute to living *H. sapiens* and that the LCA likely originated in South Africa (with some contributions from eastern African populations), as the predicted LCA morphology shared the most similarities with the Florisbad cranium, dated to around 259 kya (Grün, 2016).

**Table 4.** Early *Homo sapiens* samples analysed by Gunz *et al.* (2009) and Mounier and Lahr (2019).

| Gunz <i>et al.</i> (2009) | Mounier and Lahr (2019)      |
|---------------------------|------------------------------|
| Irhoud 1                  | Irhoud 1                     |
| Irhoud 2                  | Omo II                       |
| LH18 (Ngaloba)            | LH18 (Ngaloba)               |
| Omo II                    | Florisbad                    |
| Qafzeh 6                  | KNM-ES 11693 (Eliye Springs) |
| Qafzeh 9                  | Qafzeh 6                     |
| Skhul 5                   | Qafzeh 9                     |
|                           | Skhul 5                      |



The full suite of cranial features characteristic of contemporary humans (as defined by Day and Stringer 1982) does not seem to occur in the record until around 100-40 kya (Neubauer, Hublin and Gunz, 2018). However, a selection of fossils from the Late Pleistocene and Early Holocene highlight both the retention of ‘archaic’ traits and the maintenance of extensive morphological diversity until relatively recently. Using geometric morphometrics, the Iwo Eleru cranium from Nigeria, dating to ~11 kya, was found to fall outside the range of contemporary human variation, possessing an intermediary neurocranial shape between that of archaic hominins and contemporary humans (Harvati *et al.*, 2011). This highlights the issue of the underrepresentation of western Africa in models of modern human evolution, as well as the non-linear evolution of our species, with late surviving ‘archaic’ features occurring in distinct pockets around the continent, as also seen at Rising Star Cave (Berger *et al.*, 2015; Dirks *et al.*, 2017). The Iwo Eleru fossil was also found to share more similarities to Late Pleistocene African crania and the Levantine Skhul and Qafzeh fossils than with contemporary samples (Harvati *et al.*, 2011).

As well as the Apidima 1 crania at > 270 ka (Harvati *et al.*, 2019), though this is controversial, and a maxilla discovered in Misilya Cave (Hershkovitz *et al.*, 2018), fossils discovered at Skhul and Qafzeh represent some of the earliest modern humans outside of Africa, dated to ~90 and ~120 kya (Stringer *et al.*, 1989; McDermott *et al.*, 1993). The near complete Skhul 5, Qafzeh 6 and Qafzeh 9 are relatively large and robust when compared to contemporary *H. sapiens* populations; however, many aspects of their morphology, such as the posterior vault, falls within the modern human range (Harvati, Hublin and Gunz, 2010). Morphometric comparison of the Lukeyna Hill cranium found substantial differences from that of recent African populations and Holocene specimens, particularly in the neurocranium, indicating that elements of modern human morphology are not present in the current lineage (Tryon *et al.*, 2015). Other Late Pleistocene African fossils from Nazlet Kater 2 (~38 kya) in Egypt, Hofmeyr in South Africa dated to around 50-30 kya (Ribot, Ghalem and Crevecoeur, 2023), and Pestera cu Oase (~40 kya) in Romania possess a facial morphology that is more archaic than that of contemporary samples, whilst their neurocranium has an anatomically ‘modern’ shape (Crevecoeur *et al.*, 2009). When comparing the variation of these specimens and other Pleistocene samples against recent populations, Crevecoeur *et al.* (2009) found greater diversity in the Late Pleistocene, complementing genetic evidence indicating that the variation present in living humans is only a small subset of the variation found in past *H. sapiens* groups (Weaver and Roseman, 2008).

#### 2.4.1.2. *The Pan-African cultural patchwork and Middle Stone Age industries*

The emergence of *H. sapiens* is being increasingly linked to the development of the African Middle Stone Age (MSA). Whilst it is not impossible that other species, like *H. naledi* and *H. heidelbergensis*, are also associated with this cultural stage, only *H. sapiens* fossils have yet to be found in association with MSA assemblages. The MSA can be seen as a phase of technological reconfiguration that involved the abandonment of large handheld cutting tools (hand-axes), characteristic of the Early Stone Age (ESA), and an increased emphasis on hafting and flaked tools from prepared cores, alongside a suite of other behavioural shifts, such as long-distance trade and symbolic behaviour (McBrearty and Brooks, 2000; Scerri et al., 2018). These developments seem to have arisen across Africa at a broadly similar time of ~300 kya from the following sites: Jebel Irhoud in Morocco (Hublin et al., 2017), Olorgesailie in Kenya (Brooks et al., 2018), Kalambo Falls in Zambia (Barham et al., 2015) and Florisbad in South Africa (Grun, 2016). In West Africa, the appearance of the MSA occurs later, with the earliest occurrence dated to ~121 kya at Ravin Blanc I in Senegal (Douze et al., 2021), though most MSA sites appear after MIS 4 and 3. Whilst there appears to be a broad continental-wide technological shift from the ESA to the MSA, MSA artefacts exhibiting high levels of inter-regional variability. This variation is often used to group assemblages into ‘industries’ that share similar technological characteristics and inventories of artefact categories (Clark, 1982; Shea, 2020).

The regionalisation of cultural traditions is argued to first emerge during the African MSA (Clark, 1982; Barham, 2001; Phillipson, 2005). For example, the Lumpemban is a Central African variant of the early MSA considered to represent Late-Middle Pleistocene adaptations to rainforest and woodland environments, including heavy-duty axes, bifacial worked lanceolate points, backed flakes and blades, picks and segments (Taylor, 2016, 2022). This industry has been discovered as far south as Namibia, and as far east as the Lake Victoria region, with some of the earliest examples discovered at Twin Rivers in Zambia at ~230 kya (Barham, 2000), and Mumba Rock Shelter in Tanzania at ~130 kya (Glignani et al., 2012). The Sangoan industry is deemed to exhibit features of both the ESA and MSA, preserving large picks, core-axes, core-scrapers, and other relatively large “heavy-duty” core-tools (Shea, 2020; Douze et al., 2021). Originally, the Sangoan was also believed to represent a Central African forest adaptation, yet recently Sangoan-like tools have been suggested from sites across Africa, including in open habitats, both questioning the association between the industry and forest ecosystems and implying it may have a much wider geographic distribution than initially assumed (Taylor, 2022). However, few occurrences have been securely dated, so it is difficult to ascertain the behavioural significance of the Sangoan, though Taylor (2022) suggests that it could be better understood as a variant of the Acheulean rather than as an MSA industry.

The Aterian, defined as the presence of tanged technologies, is found widely distributed across northern Africa, from Morocco to the Western Desert of Egypt and as far south as the Sahel. Due to insights from use-wear and experimental work, the tang is hypothesised to represent a hafting modification (Rots and Tomasso, 2018), developed from an existing pool of knowledge deriving from sub-Saharan populations that moved northwards during a period of increased precipitation (Osborne *et al.*, 2008; Richter *et al.*, 2010; Drake *et al.*, 2011; Drake, Breeze and Parker, 2013; Scerri, 2013a). The Nubian complex is another example of a northern African regional MSA variant, which is found primarily along the Nile Valley, and can be recognised by being produced almost exclusively by Levallois-based strategies (Rots, Van Peer and Vermeersch, 2011). Nubian points have been discovered both across northern Africa and as far as the Arabian peninsula, implying that early human expansions out of Africa may have originated from these northeastern populations (Rose *et al.*, 2011; Crassard and Hilbert, 2013). Notably, Hallinan and Shaw (2020) also report Nubian-like points in South Africa, specifically within arid settings comparable to Late Pleistocene North Africa, indicating that convergent evolution and adaptation may also play a role in shaping patterns of technological variability throughout the MSA. The Lower Nile Valley Complex is a geographically restricted industry from Upper Egypt and Nubia, and has been deemed contemporaneous to the Nubian Complex (Vermeersch, 2002; Rots, Van Peer and Vermeersch, 2011).

Southern Africa saw a comparable emergence of distinctive MSA industries during the Late-Middle Pleistocene, namely the Still Bay (SB), Howiesons Poort (HP) industries, which appear to be both chronologically and regionally specific (McBrearty and Brooks, 2000). The SB has been proposed to be limited to the southern Cape coast of South Africa (Goodwin and van Riet Lowe, 1929) whilst the HP is found more widely distributed, at sites in the Cape region, such as Klasies River (Wurz, 2002), to Apollo 11 on the border between Namibia and South Africa (Vogelsang *et al.*, 2010), from Cave of Hearths in the Transvaal (McNabb *et al.*, 2009) to Border Cave on the border between Zululand and Swaziland (Butzer, Beaumont and Vogel, 1978; Backwell *et al.*, 2018). The SB is defined based on the presence of elongated bifoliate ‘willow leaf’ points, though several point designs are actually present in SB assemblages (Way and Hiscock, 2021). Shallow invasive retouching is used to make these SB points, which were typically manufactured using good quality, fine-grained raw material with few inclusions (Soriano *et al.*, 2015). One of the most famous examples of the SB is found at Blombos Cave, where over 50% of the retouched tools are bifacial points (Henshilwood *et al.*, 2002; Villa *et al.*, 2009). The HP, on the other hand, tends to be characterised by small, well-retouched unifacial and bifacial foliate points alongside backed geometrics as complex solutions for hafting (Way *et al.*, 2022), though these artefact types are found in both preceding and posterior assemblages (Tribolo *et al.*, 2013). The Pietersburg industry is typically found in Gauteng and currently is dated based on Bushman Rock Shelter to MIS 5

(Porraz *et al.*, 2018), whereas the Bambata industry is found in Zimbabwe, Namibia and Botswana and is dated using TL and amino acid racemization to 70-80 kya at Gi in Botswana (Brooks and Yellen, 1977; Brooks *et al.*, 1990). The Pietersburg industry is characterised by unifacial (though sometimes bifacial) elongated points on blades with peripheral trimming, whilst the Bambata industry is typified by both bifacial and unifacial short, broad foliate and triangular points.

The usefulness of dividing the MSA record into stone tool industries has seen recent renewed attention. For example, eastern African archaeologists tend to assign MSA assemblages younger than 100 kya to a variety of local Named Stone Tool Industries (NASTIES; Shea, 2014), though few appear at more than one site located over 50 km apart (Shea, 2020). Blinkhorn and Grove (2018) found that these later MSA assemblages in eastern Africa vary widely with little obvious geographic or chronological patterning. Wilkins (2020), taking examples from the southern African record, agrees that discrete NASTIES fail to account for patterns of variability between coeval lithic assemblages. Shea (2020) thus calls for a rehaul in stone tool systematics, suggesting that rather than rejecting widely used nomenclatures, a region-specific approach to addressing problematic areas of lithic categorisation should be adopted. Timbrell (2020a) provides a critical review of Shea's (2020) Eastern African Stone Tool (EAST) Typology, highlighting the potential of this unbiased system for categorising eastern African lithic technology. Overall, while stone tool industries could end up being redundant units of analysis, they reflect the fact that a high amount of diversity exists within the MSA cultural stage, with regional traits fluctuating in their spatial and temporal distribution.

MSA stone tool industries are suggested to evidence the emergence of regional subpopulations (Clark, 1982). Studies focussing on structure within regions have thus far proved fruitful for explaining patterns of variability in the MSA archaeological record. For example, whilst there is clearly variation throughout the eastern African MSA (see Chapter 3 for a full discussion of studies related to the eastern African MSA), there appears to be underlying continuity in material cultural (Groucutt *et al.*, 2015b) and some MSA assemblages in the region do not carry an obvious signal of regionalisation (Thompson *et al.*, 2018). In northern Africa, Scerri *et al.* (2014), using a spatiotemporally explicit paleoenvironmental model incorporating palaeohydrological networks, found that the distribution of different biomes and the availability of fresh water drove population budding between ~130 and 75 kya (Drake *et al.*, 2011). A high degree of structure is inferred through the complex patterns of similarity and difference between north African assemblages, forming technological clusters that articulate with what is known about the paleoecology of the region but do not reflect those that are implied by the terms 'Aterian' and 'Nubian' (Scerri *et al.*, 2014). Similarly, Scerri (2013a,b) found that diversity within Aterian assemblages appears

to be driven by factors other than that of tanged tools; for example, basally thinned points show variation at a finer scale than the term ‘Aterian’ implies. This suggests that tang shape may not be particularly informative about patterns of variability between sites, despite the research focus on its morphology (e.g. Iovita, 2011). Scerri *et al.* (2014) reported that similarity between technological groups decreases with distance, except when connected by palaeohydrological corridors, implying that successful occupations across habitable parts of the desert landscapes (i.e., areas with fresh water) were facilitated by shared technological solutions that were adapted to similar ecological situations. Differences between northwest coastal groups and other more eastern sites, such as Haa Fteah, have been explained as resulting from the restricted movement of populations between the two regions, separated by a hyper-arid zone (Scerri *et al.*, 2014). North African group dynamics was therefore likely to have been shaped by ecological factors, such the availability of fresh water, due to their importance for survival in harsh arid environments.

Patterning within southern African MSA archaeology also demonstrates the existence of a number of technologically distinct populations (Wurz, 2013; Wadley, 2015; d’Errico *et al.*, 2017). Wurz (2013), in an overview of the archaeology of the region, indicated that, instead of a linear increase in complexity across the MSA, technological change was non-directional through time or space, driving a mosaic-like evolution of ‘behavioural modernity’ throughout the region. Wurz (2013) noted that diversity in behavioural innovation in south Africa is best represented through a number of relatively short-lived technological trajectories of the HP and SB industries. It is thought that similarities in bifacial and unifacial point forms observed among spatiotemporally disparate SB and HP sites reflect intergroup interactions (Villa *et al.*, 2009; Mackay, Stewart and Chase, 2014), as these complex shared behaviours may reflect the geographic spread of behaviourally distinct populations across the region, mapping their networks of contact (Jacobs *et al.*, 2008). That said, further analyses by Archer *et al.* (2016) argued that the discontinuous nature of formal variation among SB bifacial points is actually indicative of convergent evolution to shared ecological conditions, as opposed to deriving from group contact. This hypothesis is also supported by Ziegler *et al.* (2013) who argue that the sporadic emergence of the SB and HP is associated with cool temperatures and humid conditions in southeast South Africa. Modelling by d’Errico *et al.* (2017) suggested that the SB was a coastal adaptation, exploiting a narrow niche during mild conditions, whereas HP populations had a much broader niche, incorporating more arid and high-altitude environments, and thus developed a cohesive adaptive system with flexible technologies. Yet Jacobs *et al.* (2008) found the timing of MSA industries was not correlated with - or observed under - any particular climatic regime, though it is likely that using NASTIES as units of analysis is unlikely to resolve conflicting results between technological and environmental change in the southern African MSA (Wilkins, 2020). Mackay, Stewart and Chase (2014) in an analysis of the Late Pleistocene archaeology of

southern Africa suggest that, rather than the SB and HP being the result of adaptation to specific environmental conditions, environmental change actually drove coalescence and fragmentation, influencing the patterns of variability in this region. Demography and ecology remain popular explanations for the appearance (and disappearance) of certain technological characters in the South African MSA (Wurz, 2002; Jacobs *et al.*, 2008; Mackay, Stewart and Chase, 2014; Wadley, 2015; d'Errico *et al.*, 2017), and indeed the MSA as a whole (Scerri and Will, 2023).

In western Africa, the MSA persists into the Holocene, as seen at Ndiayène Pendao, Laminia and Saxomununya in Senegal (Scerri, 2017b; Scerri *et al.*, 2017, 2021). Moreover, dating at Tiémassas, coastal western Africa, indicates that MSA technologies were continually used throughout the Pleistocene, despite them being replaced by around MIS 3 elsewhere in Africa (Niang, Blinkhorn and Ndiaye, 2018; Niang *et al.*, 2020). Douze *et al.* (2021) also note that technological concepts from the Sangoan industry are found relatively late in western Africa. Paralleling the fossil record of the region (Harvati *et al.*, 2011), this independent trajectory of the western African archaeological record suggests that it may have formed a discrete evolutionary realm in the forest ecotone, centred between the extreme aridity of northern Africa and the grasslands and savannahs in southern and eastern Africa (Mercader, 2002), with a remote river basin network. Tiémass is located in a broadly similar to ecological context to that of Kenyan site of Panga ya Saidi - occupying a coastal location at close proximity to mangroves in ecotonal grassland/woodland settings (Roberts *et al.*, 2020; Faulkner *et al.*, 2021). Yet, despite these parallels, considerable cultural dynamism is apparent at Panga Ya Saidi (Shipton *et al.*, 2018), when compared to the consistency of technology at Tiémassas (Niang *et al.*, 2020), though coastal occupations in southern Africa are also linked to patterns of enduring occupation and population migration (Will *et al.*, 2016). Overall, the MSA of West Africa demonstrates remarkable diversity during MIS 4 and 3 (Scerri *et al.*, 2017; Niang *et al.*, 2020; Douze *et al.*, 2021), with West Africa appearing slightly chronologically offset compared with other African regions, supporting the local development of cultural trajectories across Africa (Scerri and Will, 2023).

#### 2.4.1.3. *Population structure in modern and ancient African DNA*

The genetic origin of *H. sapiens* is widely discussed in the literature, and it is generally accepted that Africa is the source area for humanity due to the high levels of genetic diversity of African populations (Stringer and Andrews, 1988; Deshpande *et al.*, 2009; Tishkoff *et al.*, 2009). Initial evidence from uniparental genetic studies, i.e. mtDNA and Y-chromosome, pointed towards sub-Saharan Africa as the singular origin of *H. sapiens* (Cann, Stoneking and Wilson, 1987; Seielstad *et al.*, 1999), which was

suggested to be eastern Africa due to the historic abundance of fossil and archaeological evidence (Seielstad *et al.*, 1999). However, more recently evidence has suggested that southern Africa may have accommodated the source populations that gave rise to modern humans. The Khoisan have been found to have the greatest genetic diversity among contemporary human populations and represent one of the most deeply divergent genetic branches within the *H. sapiens* clade at 150-300 kya (Tishkoff *et al.*, 2009; Schlebusch *et al.*, 2012; Mallick *et al.*, 2016). Many have interpreted this as support for a single southern African origin model for *H. sapiens*, especially considering that there is evidence for a south to north decrease in genetic diversity within Africa (Henn *et al.*, 2011). Chan *et al.* (2019) also suggested that *H. sapiens* originated in southern Africa based on data from 198 modern mtDNA samples, though this paper has been heavily criticised methodologically, theoretically, and ethically (Ackermann *et al.*, 2019; Schlebusch *et al.*, 2021). Moreover, divergence estimates are difficult to corroborate between studies as the variation in approximations produced may actually reflect differences between methodologies, model assumptions and data samples, rather than necessarily being anthropologically meaningful (Scerri *et al.*, 2018). In addition, recent movements within Africa have likely obscured signatures of early demographic processes in the human lineage; these may include the migration of Bantu-speaking populations from West Africa around 2-1.5 kya (Tishkoff *et al.*, 2009; Patin *et al.*, 2017) or the ‘backwards’ migrations from Europe and Southwest Asia into Africa (Pagani *et al.*, 2012; Pickrell *et al.*, 2014; van de Loosdrecht *et al.*, 2018). Therefore, attempting to pin-point the exact genetic origin of *H. sapiens* may be a futile exercise, especially as it was unlikely to be a clean, easily discernible divergence from archaic species (Scerri, Chikhi and Thomas, 2019).

The structure of modern genetic diversity was largely shaped by past demographic events (Scerri, Chikhi and Thomas, 2019). However, many models can be used to explain the effects of these processes on diversity in modern genomic data, and therefore equifinality is a major issue when trying to infer information about the past from modern populations. Models are, in essence, abstractions and simplifications about true population histories and therefore differences between models can become problematic when reconstructing past population structure (Scerri *et al.*, 2018). For example, many genetic studies have identified genes within African populations that have coalescence times on the order of 1 million years, which have previously been interpreted as the result of admixture with archaic species (Hammer *et al.*, 2011; Xu *et al.*, 2017). Yet, the distribution of coalescence times, even in a single human population, do often include very early values at ~1 million years ago, and therefore such conclusions based on the extreme tail of these distributions should be treated with caution as this may result in model misspecification (Scerri *et al.*, 2018). Instead, several authors have argued that deep coalescence times in modern populations support the hypothesis that *H. sapiens* evolved from a human lineage in Africa with

deep structure (Eriksson and Manica, 2012; Chikhi *et al.*, 2018). For example, the demographic model produced by Eriksson and Manica (2012) using modern human and Neanderthal genetic samples suggested that ignoring spatial population structure can cause models to underestimate the geographic diversity expected in the absence of hybridisation with archaic species.

Ancient DNA (aDNA) evidence also indicates the presence of prehistoric population structure. Studies on Holocene samples have revealed complex interaction and dispersal patterns within Africa; for example, Skoglund *et al.* (2017) assembled genome-wide data from 16 prehistoric sub-Saharan African individuals and found evidence for a geographic cline of structured populations from Ethiopia to South Africa, with deeper structure in western Africa, mirroring archaeological and fossil evidence. The authors concluded that the deepest diversifications of African populations were complex, likely involving continuous gene flow among geographically disparate groups. Recent analyses of three Late Pleistocene and three early-middle Holocene fossils by Lipson *et al.* (2022) highlight the existence of highly divergent source populations, including deeply diverged eastern and southern source and a central-African-related source, persistent population structure throughout the Late Pleistocene, and the development of long-distance networks from 80-20 kya. van de Loosdrecht *et al.* (2018) retrieved Late Pleistocene (~15 kya) aDNA from seven individuals at Grotte des Pigeons in Morocco and found evidence to suggest that there was a Late Pleistocene connection between north Africa and the Near East, which could suggest that the ancestral population of this group, perhaps linked to the Natufian culture, may have been widespread across northern areas of Africa.

Together, evidence from studies on both modern and ancient genomes demonstrates that patterns of human genomic diversity are most accurately explained by reticulate models involving fluctuating population structure over long periods (Chikhi *et al.*, 2018; Scerri *et al.*, 2018; Scerri, Chikhi and Thomas, 2019). Mirazón Lahr and Foley (1998) and Ambrose (1998) suggest that the ancestral populations to modern humans would have gone through a speciation bottleneck thus arguing for a single recent African origin, yet Harding and McVean (2004) argue that there is no evidence to support a major reduction and recovery in ancestral population size, with the current evidence for population structure in archaeological and fossil evidence supporting that patterns of genetic diversity should be interpreted as the existence of sub-divided populations prior to African dispersals.

#### 2.4.2. Environmental and ecological drivers of population structure



Climatic conditions in the Late-Middle Pleistocene provide the backdrop to modern human evolution. Importantly, African paleoclimates varied asynchronously across time and space, and induced heterogenous shifts in biome distribution across the continent (Blome *et al.*, 2012). Phylogenetic patterns in numerous mammalian species across a variety of trophic levels suggest that these fluctuations in climatic conditions were a major driver of faunal population structure and speciation (Pitra *et al.*, 2002; Moodley and Harley, 2005; Linder *et al.*, 2012; Bertola *et al.*, 2016), with ecological refugia playing an important role in the generation of structure within African fauna (Levinsky *et al.*, 2013). Human subsistence behaviour has been found to correlate significantly with climatic variables (Kelly, 1993; Binford, 2001; Kuhn and Stiner, 2001) and the diversification of the MSA is commonly cited to be a consequence of shifts in resource distribution and availability in response to environmental fluctuations (Ambrose and Lorenz, 1990; Marean *et al.*, 2007; Ziegler *et al.*, 2013). Whilst strict environmental determination likely cannot account for the full range of causal mechanisms influencing human behavioural change, paleoenvironmental variability and its direct effect on Africa flora and fauna during the Late-Middle Pleistocene, likely shaped the biological diversity, distribution and behaviour of early *H. sapiens* (Scerri *et al.*, 2018; Scerri, Chikhi and Thomas, 2019).

#### 2.4.2.1. Climatic change

The Africa continent is immense and highly diverse, supporting a range of biome-types due to its variable climatic and altitudinal gradients, from deserts and savannahs to tropical rainforests and woodlands (Blome *et al.*, 2012). Glacial (cold and dry) and interglacial (warm and wet) cycles, often referred to as Marine Isotope Stages (MIS), are regulated by the Milankovitch cycles (see Table 5 for summary). For example, tropical insolation, defined as the amount of solar energy reaching the surface of the earth (Hays, Imbrie and Shackleton, 1976), is primarily governed by eccentricity-modulated precession whilst obliquity has more of an effect at higher (absolute) latitudes (Imbrie and Imbrie, 1980). As such, cyclically fluctuating temperature and precipitation regulates the net primary productivity (energy stored as biomass in the ecosystem) and carrying capacity (maximum population size of a species that a biome can sustain) of a given area at a given time (Whittaker, 1975). Interglacials are generally periods of greater productivity, as higher temperatures lead to the melting of ice caps and the resulting higher levels of 'free water' circulates as precipitation. The Milankovitch cycles also have a strong effect on seasonality, an important consideration for Late-Middle Pleistocene population dynamics. Obliquity influences seasonality at higher latitudes whereas precession drives the seasonal cycles at lower latitudes, though this is modulated by eccentricity which has a highly irregular amplitude. Net effects of precession

(~23,000 years) and eccentricity (~100,000 years) at low latitudes means that Africa tends to show strong variation in seasonality.

**Table 5.** A summary of the Milankovitch cycles.

| Orbital cycle | Length         | Causal mechanism                          | Effect on climatic change   |
|---------------|----------------|---|---|
| Precession    | ~23,000 years  | Direction of the earth's axis of rotation | More extreme seasonal variation in one hemisphere and less extreme in the other |
| Obliquity     | ~41,000 years  | Angle of the earth's axial tilt           | Amplitude of the seasons  |
| Eccentricity  | ~100,000 years | Shape of the earth's orbit around the sun | Length of seasons, global annual insolation                                     |

Blome *et al.* (2012) synthesised palaeoclimatic records from 150-30 kya to compare with a database of 64 radiometrically-dated paleoanthropological sites and proposed that, at the continental scale, both population and climate change was asynchronous, occurring under different regimes of climate forcing that created sporadic opportunities for migration into adjacent regions. For example, precipitation was highly variable throughout the Late-Middle Pleistocene because, although mediated by the orbital cycles, the African continent is also strongly affected by the position of the winter Westerlies at both its northern and southern tips, driven by changes in Atlantic Ocean circulation. Other areas experience monsoonal rainfall associated with the intertropical convergence zone (ITCZ), the strength and positioning of which is driven by variation in precession-modulated insolation (Blome *et al.*, 2012). Past movements of the ITCZ northwards elicited periods of extreme aridity in contemporary areas of tropical Africa, whereas the Sahara contracted and fluvial networks of rivers and lakes expanded across previously arid areas of northern Africa (Drake *et al.*, 2011; Drake, Breeze and Parker, 2013; Scerri *et al.*, 2014). Such shifts were mirrored in the Arabian Peninsula, allowing movement of African fauna (and also the hominin populations that hunted them) into these areas during periods of increased precipitation (Groucutt *et al.*, 2015a). Whether the two rainfall systems ever migrated far enough to merge and form a truly 'green' Sahara is unclear, though it is believed that fresh-water corridors through the desert would have been sufficient to permit migration of fauna within the arid zone (Drake *et al.*, 2011; Scerri *et al.*, 2014; Drake and Breeze, 2016). This is supported by the presence of mammalian remains, such as giant buffalo (*Pelorovis antiquus*) in the Maghreb between 92-129 kya, corresponding with the widespread occurrence of the Aterian (Drake and Breeze, 2016).

Precipitation regimes across Late Pleistocene Africa were also influenced by El Niño Southern Ocean oscillation (ENSO) variability, a manifestation of the Walker Circulation, which were driven by changes

in eccentricity (Kaboth-Bahr *et al.*, 2021). Palaeo-ENSO drive changes in the east-west moisture gradient, with La Niña-like conditions causing eastern Africa to experience drier conditions than western Africa, and El Niño-like conditions leading to a reversal (Kaboth-Bahr *et al.*, 2021). These low-latitude insolation-driven oscillations likely caused forest fragmentation in eastern and western African during dry phases, increasing ecotonal regions that were likely preferred habitats for hominins (Basell, 2008). Smaller changes in patterns of rainfall have been found by others to affect the distribution of savannah and forest biomes in west Africa (deMenocal, 2004; Miller and Gosling, 2014).

Overall, climatic variables have been found to be a major determinant of vegetation change and biome distribution, with strong impacts on the structure and composition of faunal species (Whittaker, 1975). This is because, for a habitat to be suitable, it must fall within both the temperature and precipitation range that a species can tolerate and provide appropriate flora and/or fauna for subsistence. Whittaker (1975) demonstrated that small fluctuations in temperature and precipitation values, especially at boundaries between habitat types, have the potential to dramatically affect the primary productivity of an area due to the influence of temperature over the yield of fauna and flora in an environment. This consequently influences the ability of an area to support *H. sapiens*; for example, Kelly (1995) found that hunter gatherers inhabiting areas of low temperature are required to relocate their foraging bases more often than those in higher temperatures to compensate for the fact that primary resource density is lower. Deeply stratified sites such as Blombos Cave (Jacobs *et al.*, 2013), Pinnacle Point (Brown *et al.*, 2012; Smith *et al.*, 2018) and Klasies River Mouth (Wurz *et al.*, 2018) yield archaeological evidence that suggest that areas of southwestern South Africa were abandoned during a period of unusually dry conditions around 50-40 kya (Quick *et al.*, 2016), highlighting that, like other mammals, humans adapted to changing conditions and shifted their geographic distribution accordingly. This is reflected in the population structure of contemporary KhoeSan groups, which corresponds with geographical barriers and the ecology of the Kalahari Basin (Uren *et al.*, 2016).

#### 2.4.2.2. *Mammalian evolutionary ecology*

All mammalian species are habitat-specific, though species vary in their tolerance to habitat change (Vrba, 1992), and therefore climate shifts have a dramatic effect on species distributions over the landscape. Species respond to changing climatic conditions in a number of ways (Vrba, 1992, 1993). Firstly, a species can persist and undergo no net change. Alternatively, species can endure climatic change by either passively shifting their distribution without vicariance or extinction or fragmenting their distribution (vicariance) causing intra-specific variation without speciation whilst maintaining habitat-

fidelity. Alternatively, species can undergo fragmentation to the limit and go extinct, or alternatively fragmentation can lead to speciation. Allopatry, defined as the geographic separation of populations of a single species, can facilitate species vicariance and encourages the accumulation of variation, population divergence and speciation through genetic drift and adaptation (Mayr, 2001).

Research into the evolutionary history of African fauna indicates that species distributions were transient as whole ecosystems were frequently required to fragment and coalesce in the face of climatic change (Vrba, 1992, 1993). For example, Linder *et al.* (2012) used cluster analysis techniques to analyse data from birds, mammals, amphibians and snakes and found seven statistically defined and robust biogeographical regions within sub-Saharan African fauna; Congolian, Zambezian, Southern African, Sudanian, Somalian, Ethiopian and Saharan. East Africa, the West African coast and the transitional zone between the Congolian, Sudanian and Zambezian region were unassigned whilst the Cape area of South Africa, Afromontane areas and the coastal region of East Africa were not well defined regions, but were characterised by high neighbourhood heterogeneity, rapid turnover of species and high levels of narrow endemism (Linder *et al.*, 2012). Bertola *et al.* (2016), using phylogeographic data, reported that there were three main lion clades in sub-Saharan Africa - West/Central, East, and South - a phenomenon also reported in different taxonomic groups occupying other trophic levels (Moodley and Harley, 2005), including modern humans (Gonder *et al.*, 2007; Tishkoff *et al.*, 2009). Pleistocene refugia and river networks played an important role in structuring central African gorilla populations, with Mantel tests revealing that genetic diversity correlated with the distance required to circumnavigate intervening rivers, as well as isolation by distance (Anthony *et al.*, 2007), a pattern also observed in the north African MSA (Scerri *et al.*, 2014). Together these results are highly indicative that spatially varied environmental conditions were a major evolutionary driver of patterns of genetic diversity in various African animal species.

The Turnover Pulse hypothesis and the Variability Selection hypothesis have been developed to understand the relationship between environment and the evolution of African species in the archaeological record. Vrba (1992, 1993) proposed the Turnover Pulse hypothesis to explain the focussed bursts ('pulses') of extinction, speciation, and migration in bovids that largely coincide with climatic fluctuations, with dramatic rapid increases in diversity and abundance of arid-adapted ungulates correlating with cool, dry phases. However, it has recently been found that periods of aridity encouraged continuous and gradual evolution of Pleistocene mammals (Bibi and Kiessling, 2015). In a faunal analysis of the Omo sequence in Ethiopia, Bobe, Behrensmeyer and Chapman (2002) also found that, rather than distinct turnover at the species level, shifts in population hierarchies were driven by climatic forces

towards the end of the Pliocene, with different species dominating during different periods due to environmental change. This attests to the complex nature of environment-fauna interactions in Africa, with ecosystem structure changing through space and time as opposed to distinct species turnover.

In the Variability Selection hypothesis, Potts (1998) suggests that increased climatic variation would drive selection in favour of more versatile ('generalist') species. Initially taking evidence from the shift from highly specialised taxa at Olororgesailie at ~1 million years ago, the Variability Selection hypothesis was proposed to explain the onset of hominin adaptations that enhanced versatility in times of strong environmental variability (Potts and Faith, 2015). Several studies have supported the hypothesis that increased climatic variability is a driving force of hominin dispersal and speciation events (Grove, 2011, 2015; Potts and Faith, 2015; Stewart *et al.*, 2019). The Variability Selection hypothesis proposes that African hominins were able to occupy increasingly diverse habitats in response to the onset of dramatic paleoclimatic variability throughout the Late-Middle Pleistocene, and that more versatile adaptations allowed persistence in the face of such variation. Therefore, whilst habitat tracking and retiring to ecological refugia (see Chapter 2.4.2.3) may have been an effective solution to avoid extinction in the short-term, the adaptation of versatility would have buffered against the impacts of climate variability over the long-term. Gradually, this would have released the constraints on environmental tolerance to allow humans to expand their climatic niche (and become 'generalists'), leading to the eventual occupation of all environments of the world. Humans have evolved unique technological and cultural adaptations that enable them to modify their environment, changing the conditions for selection and even effecting global climate change through anthropogenic warming (Odling-Smee, Laland and Feldman, 2003; Iovita *et al.*, 2021).

#### 2.4.2.3. *Refugia*

Refugia can be defined as central areas in a species geographic distribution where populations have survived for the entire interglacial-glacial cycle, representing the maximum contraction of a species geographical range (Stewart *et al.*, 2010; Keppel *et al.*, 2012; Stewart and Stringer, 2012; Blinkhorn *et al.*, 2022). Specific adaptations of each species and their environmental tolerances contribute to the location, size and timing of refugia of a species, and they tend to exhibit the greatest level of genetic diversity within a species as well as higher levels of endemism (species unique to a defined geographic location) than surrounding areas (Stewart *et al.*, 2010). Expansion and contraction of a species range contributes to patterns of variability in an organism; for example, populations in refugia tend to diverge from other refugial groups during periods of habitat contraction as a result of genetic drift and adaptation to specific

ecological conditions within each refugial area (Stewart and Stringer, 2012). Vicariance between isolated populations is therefore intensified as a result of ecological variation between refugial zones (Hewitt, 2000; Stewart, 2009). Favourable conditions may then allow these differentiated populations to come back into contact, whereby they may merge again and become less differentiated (Stewart and Stringer, 2012).

Studies have found that there are a number of ecological refugia for faunal species within the African continent. For example, Levinsky *et al.* (2013) modelled habitat suitability for mammals and birds during the Last Glacial Maximum and suggested that there are five refugia in sub-Saharan Africa: Upper Guinea, Cameroon Highlands, Congo Basin, Ethiopian Highlands, Angola-Namibia, and East/Southern Africa. Potential refugia were identified as those areas with the greatest species richness, as they showed a higher overlap in climatically-suitable ranges than was expected based on the random models (Levinsky *et al.*, 2013). A number of these refugial zones map onto genetic clades in modern species; for example, the five refugia are represented by five clades of sub-Saharan lions (Bertola *et al.*, 2016). Giraffes, zebras and sable antelopes show evidence for the existence of a refugia in Angola-Namibia (Pitra *et al.*, 2002; Moodley and Harley, 2005; Bock *et al.*, 2014) whereas genetic diversity in kob, impala and greater kudu implies that East Africa was an area of ecological refugia (Nersting and Arctander, 2001). Overall, it is clear that ecological refugia were important for structuring past and present African biodiversity.

Early humans, like other mammalian species, also likely tracked their habitat during periods of climatic deterioration and retreated into refugial areas (Mirazón Lahr and Foley, 1998; Basell, 2008; Stewart and Stringer, 2012). In recent work, Blinkhorn *et al.* (2022) found that between 27.5% and 66.3% of the African continent may have acted as a refugia for humans throughout the Late Pleistocene. Ambrose (1998a) hypothesised that Africa itself was refugial following the eruption of Toba in MIS 4 which may have caused a volcanic winter. Despite the flaws in his specific hypothesis (see Oppenheimer, 2002), Ambrose (1998a) also proposed that forest refugia, for example in far-west Africa, central-west Africa, the montane peripheries of the Congo basin, Ethiopian highlands and parts of South Africa, were particularly important for the persistence of hominin groups during periods of climatic stability, which has been supported by other works (Brandt, 1986; Basell, 2008). Basell (2008) found that volcanic eruptions likely played a role in generating instability in eastern African refugia, which could have influenced dispersal within and/or out of Africa. This author also draws attention to the availability of fresh water which would have been equally or more important for hominins during the MSA than in earlier periods. Therefore, it is likely that push (i.e., volcanism and tectonics) and pull (climatic change) factors both stimulated *H. sapiens* migratory activity into and away from refugia. Refugial areas have also

been suggested for other hominin species; for example, it is believed that terminal Neanderthal populations retracted to southern areas, such as Iberia, the Balkans and the Levant (Finlayson *et al.*, 2006; Higham *et al.*, 2006; Belmaker and Hovers, 2011), at the onset of Heinrich events H4 (~39 kya) and H5 (~48 kya) which caused periods of extreme cold (Müller *et al.*, 2011). Dalén *et al.* (2007) found that populations of the Arctic Fox become extinct rather than tracking their favoured habitat into refugial areas; this could suggest that populations in refugia descend from ancestors already in place during expansion phases, and therefore extra-refugial populations may contribute little to the long term evolution of that species (Stewart *et al.*, 2010). More work is needed to understand the fate of groups occupying areas outside of refugia, especially in the context of human evolution, and the potential impact this has on biocultural evolution.

#### 2.4.3. Summary of the theoretical implications of population structure

Unlike the simple Out of Africa model, the SAM model rejects a single African origin of *H. sapiens* in favour of a framework that assumes a dynamic process of interaction and isolation between structured subpopulations with Africa, challenging the view that our species was endemic to a single region or habitat (Scerri, Chikhi and Thomas, 2019). Ecological change is proposed to have been a key driver of genetic, morphological, and cultural variation during this period, as what is known of Late-Middle Pleistocene environmental conditions is largely consistent with and helps explain the available biological and cultural data, thus invoking notions of ‘evolutionary geography’ as originally coined by Mirazón Lahr and Foley (1998).

Structure offers theoretical flexibility to describe and explain morphological patterns of human evolution. For example, models including structure better account for the mosaic evolution of derived morphological features diagnostic of *H. sapiens*, such as a globular braincase, gracile facial morphology and a prominent chin (Stringer, 2016). These features appear at various times across Africa; however, they are only found together at around 100-40 kya (Neubauer, Gunz and Hublin, 2009). Constellations of ‘archaic’ and ‘modern’ traits can be observed in crania dating as late as ~ 11 kya in Nigeria, and are expressed to some extent in certain contemporary populations (Wolpoff, 1986; Mirazón Lahr, 1996), refuting ideas of a simple linear morphological trajectory towards ‘modernity’. The SAM model hypothesises that modern features evolved separately in distinct regional subpopulations and fluctuating gene flow facilitated their asynchronous spread across the continent (Scerri *et al.*, 2018; Scerri, Chikhi and Thomas, 2019). Evolution would have proceeded independently in different regions and/or groups, especially if some populations were semi-isolated by distance or ecological barriers at certain points in time (Scerri *et al.*,

2018). This is exemplified by recent work at Iwo Eleru, which characterises the region as a persistent forest ‘island’, perhaps contributing to the unique morphological features of the *H. sapiens* fossil discovered there (Cerasoni *et al.*, 2023). Structure can therefore explain the lack of the sequential emergence of ‘modern’ features in the fossil record and goes further to suggest that the dichotomy between ‘modern’ and ‘primitive’ traits is reductive and underrepresents the complexity of population dynamics during the Late-Middle Pleistocene. Moreover, the recent dating of other archaic hominins like *H. naledi* (Dirks *et al.*, 2017) and *H. heidelbergensis* (Grün *et al.*, 2020) suggests that various hominin species would have coexisted with *H. sapiens*, making archaic interbreeding events within Africa probable. This may have contributed to the high levels of morphological diversity observed in the Late-Middle Pleistocene record. Evoking structure in models of human evolution negates the use of subspecies labels, such as *H. helmei* (Foley and Mirazón Lahr, 1997), through the understanding that high levels diversity reflects deep but fluid population structure within a continental metapopulation rather than the presence of definable subspecies.

The SAM model may also explain both the widespread features of MSA material culture and the fluctuating presence of region-specific technologies by drawing theory from genetic models. The existence of multiple periodically interacting subpopulations across the continent would have permitted the divergence of some, but not all, cultural and genetic variants within the metapopulation (Harding and McVean, 2004). The SAM model has thus been suggested to be the only means of jointly explaining genetic and archaeological data that often produce contradictory results (Scerri, Chikhi and Thomas, 2019). For example, as described by Scerri *et al.* (2018), it has been shown that larger populations maintain both more cultural complexity and greater genetic variability (Powell, Shennan and Thomas, 2009). At the local level, structuration leads to a decrease in cultural complexity and genetic diversity whereas, at the metapopulation level, it leads to more genetic diversity due to its effect on connectivity and lower cultural complexity (Henrich *et al.*, 2016). This may be why there is a fluctuating appearance of seemingly ‘sophisticated’ behaviours throughout the MSA rather than cumulative adoption of innovations towards ‘behavioural modernity’, with this technological phase persisting with little consistent change over hundreds of thousands of years (Scerri and Will, 2023).

Tree-like evolutionary models have been typically used in genetic studies to infer population divergence times between hominin species, however these have since been found to be insufficient as they neglect and simplify population structure, even when a degree of gene flow is predicted between branches (Scerri *et al.*, 2018; Scerri, Chikhi and Thomas, 2019). Population structure should be fundamentally fluid in nature, transient through time and space, and therefore models that rely on a rigid structure through space,



such as that assumed under ‘African multiregionalism’ as (mis)interpreted by Klein (2019), are limited in their representation of real-life population dynamics (Chikhi *et al.*, 2018). Evidence for admixture with Neanderthals and Denisovans highlights that simple tree-like models cannot accurately represent the complexity of modern human evolution (Mirazón Lahr and Foley, 1998; Eriksson and Manica, 2012). More reticulate models that allow for varying levels of gene flow between evolutionary trajectories and the merging and/or splitting of branches are now required (Chikhi *et al.*, 2018; Scerri, Chikhi and Thomas, 2019). As described by Harding and McVean (2004), metapopulations consist of fluid sub-populations connected by intermittent migration and subject to fluctuation in size, sometimes resulting in extinction. Structure would have periodically reshuffled subpopulations, isolating and then mixing previously distinct populations, which would have increased the probability of producing novel gene combinations. Klein (2019) suggests that natural selection would have favoured the spread of advantageous gene constellations and cultural feedback would have accelerated its eventual fixation in the ancestral lineage that led to fully modern *H. sapiens*. Increasing genetic evidence for early population structure in *H. sapiens* suggests that our species had a varied and dispersed ancestry (Lipson *et al.*, 2022), involving differential patterns of extinction, recolonisation and admixture between regions.

## 2.5. Conclusion

The SAM model provides a satisfactory explanation of the currently available fossil, archaeological and genetic data across Late-Middle Pleistocene Africa. Nonetheless, the association between demographic and paleoenvironmental change requires quantitative exploration at a regional level to establish the effects that habitat stability and distribution have over population connectivity and cultural diversity. Although the archaeological evidence for population structure is perhaps most discernible in regions with highly defined patterns of spatiotemporal diversity, such as northern and southern Africa with their supposedly distinctive MSA variants, the literature suggests that eastern African MSA provides the most useful laboratory for developing methods and theory about the underlying effects of populations interaction as it is relatively less constrained by historical frameworks regarding perceived MSA cultural boundaries and divisions. Indeed Will *et al.* (2019) concluded from the “Comparative Analysis of Middle Stone Age Artefacts in Africa (CoMSAfrica)” workshop in 2018, that until the analysis of the MSA lithics is standardised, continental-scale comparisons (which will be necessary to fully test the SAM model) will suffer from divergent research traditions, definitions, and units of analysis. I suggest that taking a data-led approach, as is done in this thesis, is a step in the right direction to achieve these goals.

## Chapter 3: Eastern Africa and the Middle Stone Age

Whilst the SAM model argues that the African origins of *H. sapiens* was continental rather than specific to any region of Africa, eastern Africa maintains a key position in debates surrounding the evolution of modern behaviour and anatomy. Extensive research in the region has revealed a rich behavioural record, particularly at MSA sites (Clark, 1988; Basell, 2008; Tryon and Faith, 2013; Blinkhorn and Grove, 2018, 2021), providing an important laboratory to test hypotheses about the evolution of our species. The fossil record of the region has yielded some of the earliest examples deemed to be *H. sapiens* (McDougall, Brown and Fleagle, 2005; Vidal *et al.*, 2022) and has historically been considered to be the centre of endemism for our species. Eastern Africa is defined here as the modern-day countries of Tanzania, Kenya, Uganda, Ethiopia, Somalia, Djibouti and Eritrea, as suggested by Tryon and Faith (2013). This definition, based on modern political boundaries, is rooted primarily in convenience but also provides a useful geographic unit in that most of the sites that fall within these countries share a common environmental context in the present-day, occurring either within or near the boundaries of the Somali-Masai centre of regional endemism, as originally defined by White (1983).

### 3.1. Geography, geology, hydrology, and volcanism

Eastern Africa has a diverse and unique geography, hydrology, geology, and environment. It lies at the conjunction of the Arabian, Nubian and Somalian tectonic plates (Schlüter, 1997), movements of which have created its distinctive volcanic landscapes and rift valleys. Due to its central position within the African continent, the region is well connected, acting as a corridor for movements of flora and fauna between Saharan Africa, southwest Asia and sub-Saharan Africa. Almost all of the major mammalian dispersals within Africa or between Africa and Eurasia have left a trace in the eastern African fossil record (Werdelin and Sanders, 2010) and it appears that no major technological innovation bypassed the region as hominin populations spread from the continent into Eurasia and vice versa (Shea, 2020).

Eastern Africa has a north-south running coastline and lakes and rivers that flow through the region in all fundamental directions. The Eastern African Rift System (EARS) runs 4,500 km from southwest Asia to southeastern Africa, preserving several major water bodies, including Lake Turkana, Lake Victoria, Lake Tanganyika, and Lake Malawi, draining to the north by the Nile River, to the west by the headwaters of the Congo River, and to the south by the Zambezi River. These hydrological features of eastern Africa have important evolutionary implications. For example, the distribution of animal populations across the

landscape has been suggested to have been influenced by the cyclical expansion and contraction of the major lakes that divided and reconnected populations, leading to high rates of speciation and instances where ‘parent’ and ‘daughter’ species live in the same areas (Trauth *et al.*, 2010). Similarly, Lake Turkana today acts as a natural barrier for modern human populations, isolating hunter-gatherers to the west and east and periodically connecting Nilotic people in the adjacent hot and dry Suguta Valley during periods of increased precipitation (Lewis, 2009). Lake Victoria sits on the junction between central African rainforests and savanna habitats to the east, forming an important boundary for large mammal populations (Tryon *et al.*, 2016). Modelling by Beyer *et al.* (2019) found that dispersal beyond eastern Africa and into Arabia would have been impossible without the presence of the Nile, stressing the importance of water availability for survival and mobility in and beyond the region.

Volcanism and the EARS have created a unique and evolutionarily significant suite of topographic conditions (Trauth *et al.*, 2007). Volcanism has raised the Ethiopian Plateau and EARS high above those adjacent areas of Africa of similar latitude (King and Bailey, 2006; Bailey, Reynolds and King, 2011). Cyclonic storms tracking eastward across equatorial Africa irrigate the Plateau and the westward-facing slopes of the EARS, whereas eastward facing slopes receive precipitate from monsoons travelling up the coastline of the Indian Ocean (Trauth, Larrasoña and Mudelsee, 2009). The EARS itself remains relatively dry due to rain shadow effects, though freshwater is abundant throughout the landscape via river networks and lakes (Cuthbert *et al.*, 2017). High topographic relief in eastern Africa insulates ecosystems from abrupt, orbitally forced changes in temperature and precipitation patterns, though not completely as the area still experiences drought and periods of low water availability (Cowling *et al.*, 2007; Blome *et al.*, 2012). Whilst in northern and equatorial Africa, vegetation zones move north-southwards, in eastern Africa vegetation zones shift altitudinally, forcing fauna to respond by moving along local elevation gradients (Ambrose and Sikes, 1991). The EARS has thus been proposed to have sheltered the hominins living there from the prolonged and severe megadroughts that afflicted hominins elsewhere. Ambrose (2001) hypothesised that hominins in eastern Africa would have shifted their settlement patterns in response to climatic change among the chain of Rift Valley lakes and rivers draining the Ethiopia and Kenya-Uganda highlands. Additionally, the topography of the EARS is complex at a multitude of geographical levels, ranging from extremely localised to larger regional scales, providing a mosaic of diverse resources (King and Bailey, 2006). Different ecotones are preserved in eastern Africa as a result of the high topographic relief of the EARS and Ethiopian Plateau, bringing forest, woodland and grassland communities closer together than they would normally occur in less topographically complex landscapes (Foley, 1995). Living in or near different ‘ecotones’, defined as the

boundary between different biome types, has been proposed to have allowed humans and other ‘generalists’ to exploit a variety of food sources throughout the Late-Middle Pleistocene (Basell, 2008).

### 3.2. Climate and environments

Climate change in eastern Africa has been studied extensively. This is because the lakes and basins in the EARS are excellent preservers of paleoenvironmental proxies and therefore record diachronic climatic change exceptionally well. For example, the long sequences at the Ologasaille basin, southern Kenya, have revealed rich Acheulean layers associated with relatively stable environmental conditions, though with some Acheulean strata in the upper Ologasaille Fm around 800 kya associated with dynamic environments (Owens *et al.*, 2018; Potts *et al.*, 2018). Alternatively, the MSA phases at the site have been linked to highly dynamic and fluctuating arid-moist climate variability (Owens *et al.*, 2018; Potts *et al.*, 2018, 2020). Faunal, phytolith and isotopic data indicate that the MSA occupations of Ologasaille occurred in a predominantly grassland environment near to a reliable water source that also maintained woodland vegetation. Leaf waxes from Lake Malawi reveal an amelioration of conditions after the Middle Pleistocene, with warmer, wetter conditions than seen previously, especially during inter-glacial periods (Johnson *et al.*, 2016). Interestingly, lake levels at Lake Malawi decreased multiple times between 600 kya and 100 kya, whereas lakes in the Kenyan rift expanded (Ivory *et al.*, 2018; Trauth *et al.*, 2007). Numerous vegetation shifts from tropical forests to desert-semi arid bushlands are reported at Lake Malawi, with large-scale landscape transitions occurring across the basin due to the effects of drought on the availability of nutrients in the soil (Brown, 2011; Ivory *et al.*, 2018). The Lake Malawi record indicates a megadrought during periods when eastern Africa experienced wetter conditions (Johnson *et al.*, 2016), as documented at Lake Chew Bahir during late MIS 5 and MIS 6 (Foerster *et al.*, 2022), highlighting the asynchrony of climate change even within a relatively small area. Together, this likely has major implications for structuring early human habitats and dispersal patterns through time and space.

In a synthesis of regional climatic variability, Blome *et al.* (2012) proposed that eastern Africa experienced increased precipitation from ~145 kya to 120 kya, ~110 kya to 95 kya, ~80 kya to 65 kya and ~50 kya to 55 kya. These periodic wet phases relate to a complex change in the influences of the north-east and south-west monsoon regimes. The authors also noted the presence of a regional megadrought in the tropical region (from Lake Bosumtwi in Ghana and Lake Challa to the Kalahari Desert) from ~115 kya to 90 kya, with a gradual trend towards humidity from 90-35 kya (Blome *et al.*, 2012). Pollen-based reconstructions at Lake Bosumtwi indicate oscillations between forested biomes during La Niña-like conditions and open savanna coinciding with El Niño-like conditions (Miller and Gosling, 2014), yet the

reverse is true at Lake Magadi in eastern Africa (Owen *et al.*, 2018), highlighting the asynchrony of low latitude climatic change (Kaboth-Bahr *et al.*, 2021). Blome *et al.* (2012) propose that populations in tropical and eastern Africa show a relatively muted response to climatic change due to the relative stability in site densities through time, though Blinkhorn and Grove (2018) in an extended analysis of eastern African MSA sites conversely found fluctuating levels of occupation across interglacial-glacial cycles. Smaller-scale palaeo-ENSO variability likely caused the fragmentation of forest in eastern and western Africa during dry phases, increasing the area of resource-rich ecotones that were key refugia for hominins and encouraging population growth (Kaboth-Bahr *et al.*, 2021). Therefore, the influence of climate on hominin demography is complex and may not be reconcilable with inter-glacial/glacial cycles.

Periods of increased aridity may have been offset in eastern Africa by the steep gradients in altitudinal relief and rainfall that allowed movements upwards to cooler and wetter altitudes, as well as the expansion of forest populations when the canopy was more open and fragmented (Ambrose, 1998a; Basell, 2008; Blome *et al.*, 2012). Evidence from Fincha Habera, located in the Bale Mountains in Ethiopia, suggests this high-altitude region saw recurrent occupation from 47 kya to 31 kya, coinciding with a phase of glaciation and extreme cold temperatures (Groos *et al.*, 2021). Ossendorf *et al.* (2019) argue that mountains would have provided humid refugia during periods when the lowland were arid. As well as high-altitude regions, eastern Africa also saw occupation of tropical coastal regions. Panga ya Saidi, coastal Kenya, yields multiple proxies indicating its position at a tropical forest-grassland ecotone. Terrestrial molluscs, which require humid shady conditions, the presence of open and bush/forest adapted mammalian species and woody, grass, and palm phytoliths from the immediate environment surrounding the site all indicate the ecotonicity of the site (Shipton *et al.*, 2018; Roberts *et al.*, 2020; Faulkner *et al.*, 2021). Sedimentological and magnetic susceptibility data indicates a shift towards drier conditions around ~78 kya to 73 kya, corresponding with isotope data which suggests an increase in C4 plants found in grasslands in the diets of fauna being exploited at the site (Shipton *et al.*, 2018). Throughout MIS 4 to MIS 1, the palaeoecological datasets from Panga Ya Saidi are in correspondence with those from Lakes Challa and Malawi that suggest a period of low amplitude environmental changes (Moernaut *et al.*, 2010).

Basell (2008), in a synthesis of chronometrically dated MSA assemblages across eastern Africa, found that the placement of MSA sites was limited to ecotonal settings where access to wooded ecologies was available. Lake margins and highland areas were proposed to have offered habitat stability during periods of aridity as well as coastal areas. Basell (2008) suggested that wooded environments would have protected hominins from increasing heat and lakes would have acted as oases, whilst increasing areas of savanna may have created temporary barriers between populations. Yet, grasslands provide a range of

resources both above and below the ground (Vincent, 1985), and are populated by large herds of ungulates (Fritz and Duncan, 1994), making them ideal hunting grounds as they are today for the Hadza (Marlowe, 2010), therefore savannah likely comprised a key component of MSA habitats. Volcanism, tectonics, and climate change were also proposed by Basell (2008) to affect the habitability of the region. For example, aridity during MIS 6 likely caused the reduction, isolation, and disconnection of populations across the landscape. Improving climatic conditions during MIS 5 are hypothesised to have facilitated the movement of populations out of lake margins and highland refugia and into new environments, eliciting new behavioural adaptations. This corresponds with evidence from Chew Bahir where the development of humid conditions coincides with the earliest *H. sapiens* fossils in the region (Schaebitz *et al.*, 2021). More suitable habitats were proposed by Basell (2008) to have been a ‘pull’ factor for population expansion beyond refugia zones, with volcanic and tectonic evidence acting as a ‘push’ factor, both stimulating migrations within and potential out of eastern Africa.

### 3.3. Research history of eastern African Stone Age archaeology

The stone tool record of eastern Africa has an extensive research history. As Shea (2020) notes, this history can be organised into three phases: the Exploratory period (1940s and earlier), a Culture-History Period (1940s-1970s), and a Processual Period (1970s and later). Others have argued for a five-phase history (Trigger, 1989; Barham and Mitchell, 2008), paralleled by Shea's (2020) more recent framework. Briefly, the Exploratory period can be defined as a phase when archaeologists used lithic artefact-types as markers of particular periods and industries, similarly to how palaeontologists use index fossils (*fossiles directeurs*), often attributing named stone tool industries (‘NASTIES’) to a specific ancient human population (or ‘race’, using the terminology of the day). Wayland's (1929) pluvial framework, arguing that glacial periods in northern latitudes coincided with periods of increased rainfall and higher lake levels in equatorial Africa, dominated research agendas until the development of radiometric dating and sophisticated modes of paleoclimatic reconstruction rendered it obsolete. Africa's ‘Three Age System’ was born in the Exploratory period (Goodwin and van Riet Lowe, 1929) as a result of the desire of African archaeologists to develop indigenous terminology free from the assumptions about associations with the European record (Haddon, 1905), driven by political and empirical observations.

The Culture-History period can be seen to have been initiated by the first Pan-African Congress of Prehistory and Quaternary Studies in 1947, which facilitated efforts to correlate both geological and cultural stratigraphy across wider regions. The first, and until relatively recently the only, regional synthesis of the evidence from eastern Africa was published during this period by Cole (1954). This phase

of prehistoric research in eastern Africa saw archaeologists devote more time to identifying regional variation within age-stages, expressed through the growing numbers of NASTIES whose names hinted at connections to other regions, such as Europe and southern Africa. Whilst lithic *fossiles directeurs* were still important in the Culture-History Period, archaeologists also began defining and comparing artefact types in terms of measurements and relating industries in terms of relative frequencies. There was also an explosion of fieldwork in eastern Africa during this period, promoting the development of new dating techniques and taphonomic science (Behrensmeier and Hill, 1980). The Burg-Wartenstein Conference in 1965 marks the end of the Culture-History Period (Kleindienst, 1967). As Kleindienst (2006) reflects, the participants of the conference attempted to bring some order to the ‘lithic systematics anarchy’, to use a phrase from Shea (2020), that had developed; however, whilst they had generally accepted the proposal to sink some terminology (particularly those named after European industries), it did not lead to a ceased use of universal age-stages, such as the Earlier, Middle and Later Stone Age. This is because they remained useful as broad developmental phases even though they lacked precision about population-level or time-specific dynamics. Despite these early efforts, there continues to be a lack of standardized artefact typologies and inconsistent procedures for developing names for new industries (Parkington, 1993; Kleindienst, 2006). The Processual period that followed differs from the Culture-Historical period in that culture is viewed as a dynamic and changing adaptive system rather than a fixed set of attributes that defined hominins living at specific times and places. Processual archaeologists interpreted lithic and other evidence using models and hypotheses from systems theory and behavioural ecology, rather than from ethnography and history as in the Culture-Historical period and organic evolution as in the Exploratory period (though this broad intellectual trend is an oversimplification, with exceptions like Binford [1978] continuing to draw analogues and data from hunter-gatherer ethnography).

The ‘Three Age’ system is still widely used to describe the archaeology of the Late-Middle Pleistocene in Africa. However, terms like ‘the Middle Stone Age’ have been extensively criticised for failing to capture the diversity found in the African record at this time, through artificially homogenising material within chronological or technological blocks (Parkington, 1993; Kleindienst, 2006; Barham and Mitchell, 2008; Shea, 2020). For example, Kleindienst (2006) highlights that it is currently unclear what level of similarity is required for inclusion in the Middle Stone Age. Some prefer to use Clark’s (1969) five mode system, with Barham and Mitchell (2008) stressing the advantage of this is that when applying one ‘Mode’ to a given assemblage, it doesn’t imply that other techniques were not also used. Shea (2020) recently produced a novel mode-based classification system for the stone tools of Eastern Africa (the EAST typology), a nested hierarchical framework employing a combination of letters and numbers to avoid labelling ambiguous assemblages uniquely as, for example, Middle Stone Age or Mode 3 (see

Timbrell [2020a] for a critical review). Whilst each eastern African assemblage will need to be individually redescribed in order for the system to realise its full potential as a standardised system, which is not a small or easy feat, such work could be revolutionary for eastern African archaeology, especially if combined with rigorous quantitative analysis such as Grove and Blinkhorn (2020). These authors applied neural networks to examine the changing constellations of technologies between assemblages classified as MSA and LSA. The trained network classified over 94% of the assemblages and identified 7 key technologies that significantly distinguish between MSA and LSA assemblages. Interestingly, they identified no single technology acting alone as a *fossile directeur* of either the LSA or MSA, emphasising that constellations of co-occurring technologies increase the chances of an assemblage being classified as MSA or LSA and that there is more technological continuity than change between MIS 2 and MIS 5. When removing the 7 technologies that do distinguish the classes, the models misclassify less than 5% of assemblages, demonstrating that it is possible to still establish signatures of MSA and LSA without these key defining tool types. Thus, these analyses suggest that the current usage of the ‘Three Age’ system, at least in terms of the MSA and LSA lithic record, reflects a real division in the data, supporting the ongoing use of the ‘MSA’ as a unit of analysis in this thesis. That said, the analyses by Grove and Blinkhorn (2020, 2021) do not consider the full archaeological record; Tryon (2019) proposes a more comprehensive approach including symbolic artefacts, though most of these similarly cannot be considered as *fossiles directeurs* of either the MSA or LSA.

### 3.4. What is the Middle Stone Age?

As proposed by Tryon (2019), the MSA is better understood as a suite of particular technologies rather than a specific time period. MSA assemblages tend to differ from those found in the ESA in a number of ways. For example, large cutting tools (LCT) characteristic of the ESA, such as cleavers and hand-axes, remain somewhat prominent in the MSA; however, they change in size over time, with large LCTs appearing mainly in contexts >100 kya and smaller LCTs persisting occasionally at later MSA sites (McBrearty and Brooks, 2000; Tryon and Faith, 2013; Shea, 2020). Compared to the LSA, backed and truncated pieces are present but less common in MSA toolkits and tend to be larger than the microliths preserved in the LSA (Tryon and Faith, 2013, 2016; Tryon, 2019; Shea, 2020). There is a general decline in artefact size between the MSA and LSA. Diagnostic features of assemblages assigned to the MSA include the use of varied Levallois methods as well as prismatic blade core reduction whereby a series of blades are detached (Clark, 1988; McBrearty and Brooks, 2000; Tryon, 2019; Shea, 2020). Blades are defined as relatively long flakes with parallel lateral edges and dorsal flakes scars aligned parallel the flake’s long axis (Shea, 2020). The MSA is also marked by a shift in focus to a diverse retouched toolkit



and the proliferation of point technologies (Clark, 1988; McBrearty and Brooks, 2000). Core-axes (elongated tools featuring a convex retouched edge at one end), foliate points (extensively, bifacially and invasively retouched pieces) and flake-points (triangular flakes with convergent distal retouch) are common in MSA toolkits in eastern Africa (Shea, 2020). Foliate and flake points have been found to grade into each other, and also with smaller LCTs (Shea, 2020). Some MSA toolkits preserve grindstones, tabular rocks and other stones with flat-abraded surfaces but little or no other evidence of shaping (Shea, 2020), with grindstones becoming increasingly common over time (Mehlman, 1989).

Quantitative analyses have largely corroborated the previously qualitative definition of MSA assemblages. For example, Blinkhorn and Grove (2018) explored the presence and absence of artefact types in MSA assemblages from eastern Africa and identified Levallois and blade technologies, discoid cores, retouched points, scrapers and denticulates as key components of MSA assemblages. Grove and Blinkhorn (2020, 2021) confirmed that, when compared to the LSA in the region, eastern African MSA assemblages can be defined by the appearance of core tools, Levallois flakes, point technology and scrapers, whereas backed pieces, bipolar technology and blade technology defined the LSA.

### 3.4.1. Modern human behaviour and the Middle Stone Age

As well as the stone tool evidence, the MSA is also characterised by a suite of behavioural changes (Tryon and Faith, 2013), often suggested to represent the emergence ‘modern human behaviour’ (McBrearty and Brooks, 2000). One of these behaviours is the use of ochre, evidence for which commonly occurs with the presence of grindstones, suggesting a functional association (Tryon and Faith, 2013). Ochre has many potential uses, such as a pigment (Barham, Pinto and Andrews, 2000), for symbolic activities and body decoration (Dapschauskas *et al.*, 2022) or the tanning of hides (Rifkin, 2011), and/or as a mosquito repellent (Rifkin, 2015), a hafting adhesive (Wadley, 2005), and a sunblock (Rifkin *et al.*, 2015). Whilst pigment use is the behaviour most commonly associated with the emergence of ‘modernity’, all are indicative of a higher order cognition than seen previously in the hominin record. Dapschauskas *et al.* (2022) defined three phases of increasing ochre use during the MSA referred to as initial, emergent, and habitual. The initial use of ochre occurred from 500 to 330 kya and occurs at 7% of sites across Africa during this time frame. Some examples include Kathu Pan 1, Wonderwerk Cave and Canteen Kopje in South Africa where pigment use dates to at least 500 kya (Watts, Chazan and Wilkins, 2016). In eastern Africa, McBrearty and Brooks (2000) note the widespread presence of hematite, the main ingredient of ochre, at GnJh-15 in Kaputhurin Formation in Kenya, dated to ~284-500 kya, although here they are too friable to preserve traces of grinding. During the preceding emergent phase, from 300 to

160 kya, ochre use becomes increasingly visible in the record and coincides with clear cultural changes associated with the MSA. For example, Twin Rivers in Zambia preserves over 400 pieces of ochre dated to 230 kya (Barham and Smart, 1996; Barham, 1998, 2000). Hypothesised grinding tools with ochre residues have been discovered at Sai Island 8-B-11 in Sudan (van Peer, Rots and Vroomans, 2004), the only MSA site where yellow ochre dominates. Finally, from 160-40 kya, ochre used is believed to have become habitual, and therefore was a regular part of the social life of hominins across Africa. Ochre is present at 31% of sites with lithics during this period, many of which are in eastern Africa, though the highest concentrations are reported at southern African sites. 4500 ochre pieces have been discovered at Porc-Epic in Ethiopia (Rosso, Marti and d'Errico, 2016), whilst grindstones and ochre have been found at Aduma, also Ethiopia (Yellen *et al.*, 2005), the Mumba and Nasera rock shelters in Tanzania (Mehlman, 1989), and at Panga ya Saidi in Kenya (Shipton *et al.*, 2018; d'Errico *et al.*, 2020). Habitual ochre use is thought to mark a shift in increasing ritual activity as *H. sapiens* evolved and demographically expanded across Africa and into Eurasia (Dapschauskas *et al.*, 2022).

A shift in foraging behaviour and dietary preference is also noted in the eastern African MSA. This is investigated through analysing the location of archaeological sites and faunal data. For example, the location of Porc-Epic and Nasera suggests that they were selected for their vantage over game pathways (Mehlman, 1989; Tryon and Faith, 2013), whilst the natural features of GvJm46 at Lukenya Hill and Rusinga Island in Kenya, like low topography and proximity to streams and springs, would have made them useful in the acquisition of game (Marean, 1992a; Tryon *et al.*, 2010). Coastal environments were also exploited by Pleistocene populations in eastern Africa as seen at Panga ya Saidi (Shipton *et al.*, 2018) and the MSA artefacts found in a coastal reef in Eritrea dating to ~125 kya (Walter *et al.*, 2000). Faunal assemblages found at GvJm46 at Lukenya Hill, Porc-Epic, and Rusinga Island suggest that eastern African populations exploited large mammals during the Late Pleistocene, including large and small ungulates (Assefa, 2006; Tryon *et al.*, 2010; Tryon and Faith, 2013), and carried animal carcasses to caves for further processing and consumption (Tryon and Faith, 2013). Long-distance transport of meat to central places has been argued to distinguish MSA foraging strategies from those documented in the ESA in eastern Africa, such as at Olduvai Gorge (Faith, Domínguez-Rodrigo and Gordon, 2009).

Territorial range and the expansion of physical and social landscapes familiar to hominin groups is also believed to have developed during the MSA. Raw material sourcing provides an estimate of the scale of movement across the landscape, and this is especially true for the Rift Valley, which has been geochemically characterised (e.g. Merrick, Brown and Nash, 1994). In the ESA, site-to-source distances were found to be around <60 km whereas in the MSA this increases to, and often exceeds, 300 km. For

example, obsidian cores, flakes and finished tools were transported 139 km to Porc-Epic; such a dramatic increase suggests that stone artefacts were transported through the landscape by highly mobile foragers and/or transferred via group exchange (Tryon and Faith, 2013). Beyond 305 km from the source, obsidian frequency declines and only finished tools and flakes are discovered, proposedly reflecting the shift in raw material procurement strategies to the provisioning of individuals rather than places (Kuhn, 2004), or the exchange of finished pieces rather than cores among groups. Different patterns are found from sites at a similar distance from the nearest source with and outside of the Rift Valley; obsidian is rarer at sites, and is limited to tools and flakes, in the Lake Victoria region (Songhor and Muguruk) as opposed to sites in the Rift Valley. This suggests that movement was likely driven by the heterogenous topography within the region, as it may have been difficult to move across the steep and densely vegetated margins of the Rift Valley as opposed to across the open valley floor, as also seen in the raw material procurement patterns in Europe (Féblot-Augustins, 1993).

Symbolic behaviour, such as elaborate mortuary practises and personal ornamentation is also seen to emerge during the MSA. At the Bouri Formation, Ethiopia, the Herto crania shows evidence of peri or post-mortem treatment with cut and polish marks dating to 154-167 kya (Clark *et al.*, 2003; White *et al.*, 2003). At the Acheulean site of Bodo in Ethiopia, there is evidence for the defleshing of a hominin skull at ~500 kya (White, 1986), indicating a significant time depth for such behaviours in the region. Beads, one of the earliest direct pieces of evidence for personal ornamentation, have been found throughout the eastern African MSA. Modified gastropod opercular associated with MSA artefacts were directly dated to between ~33-43 kya at Porc-Epic (Assefa, Lam and Mienis, 2008). Ostrich eggshell (OES) beads have been discovered from Bed V and Lower Bed III at Mumba Rockshelter, dated to 30-60 kya (Glignic *et al.*, 2012), although whether these are associated to MSA or LSA industries has been contested (Mehlman, 1989; Eren, Diez-Martin and Dominguez-Rodrigo, 2013). Direct dates from OES beads from other MSA/LSA strata at Mumba confirm personal ornamentation in the region at ~29-33 kya (Conard, 2004). At Enkapune ya Munto, OES beads from MSA/LSA strata date to ~40 kya (Ambrose, 1998b). Large numbers of OES and marine shell beads are also reported from Panga ya Saidi, although almost all of the specimens come from the later layers (25-14 kya) (Shipton *et al.*, 2018; d'Errico *et al.*, 2020). OES beads from Panga Ya Saidi show clear differences in production, style and heat-induced colouring as well as size through the sequence (d'Errico *et al.*, 2020), as is also observed from Kisese II (Tryon *et al.*, 2018). This could suggest a number of possible scenarios: 1) different groups were carrying different variants of the ornaments as they occupied the site or 2) one group had access to the customs of different groups through trade networks, or 3) that one resident group employed different traditions of OES bead technology (d'Errico *et al.*, 2020). Recent analyses by Miller and Yang (2022) found that OES bead

manufacture probably emerged in eastern Africa and spread southward to southern Africa around 50–33 kya via inter-regional population interaction. These authors note that, from patterns of dissimilarity between the style of OES beads from the regions, social networks between eastern and southern Africa appear to break down around the same time as the southward shift of the ITCZ, which would have caused periodic flooding of the Zambezi River catchment which connects the two regions. This strongly supports Scerri's *et al.* (2018) SAM model as it highlights the role of climatic fluctuations in shaping human social networks.

### 3.5. Previous research on the eastern African Middle Stone Age

Eastern Africa preserves a rich MSA record as a consequence of the erosional regime of the EARS, revealing geographical strata of appropriate age. For this reason, there has been a historical focus on the eastern African MSA, with many archaeological sites discovered and subsequently analysed via qualitative and, increasingly more recently, quantitative methods.

#### 3.5.1. Archaeological sites

The eastern African MSA encompasses a period that spans the Late-Middle Pleistocene. Following Tryon and Faith (2013) and McBrearty and Tryon (2006), the MSA record itself can be split into “early” and “late” phases, based broadly on radiometric dating with the Early MSA referring to sites predating the Last Interglacial (~120 kya) and the Late MSA to those within or after the Last Interglacial. Early and Late MSA assemblages show many similarities and overlap in multivariate space, although Tryon and Faith (2013) highlight that some Late MSA assemblages appear more distinctive as they yield substantially more beads, backed pieces, bipolar cores, blades, grindstones, and anvils, much like the LSA.

##### 3.5.1.1. Early MSA

The earliest appearance of MSA artefacts in eastern Africa appears around ~320 kya to 305 kya at Olorgesailie in Kenya (Deino *et al.*, 2018). Olorgesailie documents stone technology, fauna, and environmental conditions from ESA to the MSA, with MSA layers being distinctive from the ESA due to an hiatus in the record from 499 kya and 320 kya (Brooks *et al.*, 2018; Deino *et al.*, 2018; Potts *et al.*, 2018). Raw material sourcing of 688 obsidian MSA artefacts from Olorgesailie revealed that around 78%

of the samples were attributed to sources located from 25-50 km in five directions from the sites, with a small number of artefacts made from raw material deriving from more distant sources (Brooks *et al.*, 2018). The occurrence of multiple distant sources suggests the formation of networks of exchange or procurement over a substantial area, perhaps an adaptation to mitigate the risk associated with unpredictable environments as observed in ethnographic hunter-gatherers (Yellen and Harpending, 1972) and suggested by modelling work (Whallon, 2006; Grove, 2018). Raw material source diversity and distance was also found to increase in younger deposits with the distinct artefact levels representing multiple reoccupations, indicating repeated visits to focal points in the landscape (Brooks *et al.*, 2018).

The Kaputhurin Formation, also in Kenya, yields early examples of MSA assemblages predating ~285 kya. Sites within the Formation show no clear unidirectional succession from the Acheulean to the MSA, as hand axes are found in higher strata than those containing points, despite the former being associated with the ESA and the latter being associated with the MSA (Tryon and McBrearty, 2006). The archaeological record from Kaputhurin Formation therefore suggests that the ESA and MSA in eastern Africa could have overlapped both in space and time, and thus cannot be defined based on chronology alone. The ESA and MSA industries, like the Sangoan, were defined at Kaputhurin Formation by the presence of single *fossiles directeurs* (i.e. handaxes for the ESA, points for the MSA and picks for the Sangoan), calling into question the utility of using only a few diagnostic tools to assign industrial classifications, especially when they comprise only a small portion of the total assemblage. More recent work in the Kaputhurin Formation by Blegen, Jicha and McBrearty (2018) has extended the MSA archaeological record of the area forward to ~100 kya.

Sites at Gademotta, located in the central Ethiopian Rift, similarly represent some of the earliest MSA occupations in eastern Africa, dating from 280-100 kya (Sahle *et al.*, 2014). Analyses by Douze and Delagnes (2016) of the three main sites at Gademotta, two of which mark the transition between the ESA and LSA and the more recent corresponding to the climatic amelioration of MIS 5, indicate two diachronic changes in convergent tool production: specifically 1) the development of Levallois core reduction methods for the production of point technologies, and 2) the shift from unifacial and bifacial shaping of convergent tools to localised slight retouch of predetermined points. As such, the earlier MSA assemblages at Gademotta were argued to still be embedded within a ESA-concept of tool production whereas the later industries demonstrate the emergence of a new constellation of cultural behaviours indicative of a fully MSA tradition (Douze and Delagnes, 2016). These technological changes may have been accompanied by shifts in the social structures and subsistence strategies of MSA-making groups over time in eastern Africa.

### 3.5.1.2. Late MSA

Panga ya Saidi in coastal Kenya documents a 78 thousand year archaeological record, notably revealing a later phase of the MSA transitioning to the LSA (Shipton *et al.*, 2018; d'Errico *et al.*, 2020). Interestingly, older MSA technological traits such as Levallois cores exist alongside LSA innovations at Panga ya Saidi, such as the backed artefacts and blades (Shipton *et al.*, 2018). Iron-rich fragments from MSA layers suggest that red pigment was transported and perhaps processed at the site between 76 kya to 67 kya, although the first definitive use of ochre appears at 48.5 kya (d'Errico *et al.*, 2020). There is some evidence to suggest that puka shells were worn as personal ornaments by MSA populations as early as 67 kya, though there is more concrete evidence for this behaviour between 33 kya and 25 kya, potentially around the same time as OES beads are first found (d'Errico *et al.*, 2020). If the stratigraphic distribution of these bead types is confirmed by future work at Panga ya Saidi, this would indicate that beads were in use in coastal regions of eastern Africa before inland areas (d'Errico *et al.*, 2020). Palaeoecological evidence suggests that Panga ya Saidi was consistently part of the forest-grassland ecotone for the past ~67 thousand years, accompanying evidence for increasing occupation intensity thanks to the mosaic habitats in the region (Shipton *et al.*, 2018).

MSA occupations at Prospect Farm in the Central Rift, Kenya, have been tentatively proposed to date to between 45.7-120 kya (Van Baelen *et al.*, 2019). Van Baelen *et al.* (2019) have suggested that the archaeological sequence includes at least seven MSA occupation phases, with lithic artefacts from phase I and III demonstrating an early presence of bifacially retouched points in eastern Africa, if current dating is confirmed to be accurate by future work. MSA levels at Prospect Farm yield a high density of artefacts, indicating that foraging groups likely repeatedly reoccupied the area over many thousands of years, possibly for the harvesting of obsidian sources on the slopes of Mount Eburru for use and exchange (Van Baelen *et al.*, 2019). Obsidian sourcing has shown that groups in the area were moving around and perhaps beyond the Nakuru-Naivasha basin to either bring in a limited amount of exotic obsidian or obtaining it via exchange networks (Van Baelen *et al.*, 2019). The MSA/LSA transition occurs at Prospect Farm between ~53.5 kya and 46.7 kya, though MSA artefacts were still manufactured until ~40 kya to 35 kya. Elsewhere in the Central Rift, Enkapune ya Munto possesses layers that similarly mark the MSA/LSA transition at ~46 kya (Ambrose, 1998b). Attribute analysis by Leplongeon (2016) found that there is a major shift in technology from the MSA to the LSA at Enkapune ya Munto, marked by the appearance of blade-based assemblages.

In Tanzania, Mumba rock shelter contains one of the richest continuous sequences from the MSA to the Iron Age in eastern Africa. Transitional assemblages between the MSA and LSA have been discovered at Mumba, yielding LSA-like geometric microliths and knives, OES beads, and MSA-like stone points, dating to between ~49.4 kya and 40 kya (Gliganic *et al.*, 2012). Moreover, archaic *H. sapiens* fossils have been discovered at nearby Lake Eyasi (Domínguez-Rodrigo *et al.*, 2008). To the north of Lake Eyasi, Nasera also documents the MSA-LSA transition, marking a gradual shift from Levallois and bipolar reduction strategies, the replacement of points by backed microliths and the decrease in artefact size (Tryon and Faith, 2016). Obsidian is rare at the site but is acquired from sources approximately 250 km away (Tryon and Faith, 2016). Tryon and Faith (2016) used lithic and faunal data to propose that there was decreased residential mobility from the MSA-LSA at Nasera, with increased population density and corresponding technological changes, with dispersals out of the region potentially marking a complementary response to larger population sizes.

In Ethiopia, the MSA finds at Aduma in the Middle Awash Valley likely date to ~80-100 kya. Yellen *et al.* (2005) propose that the Aduma archaeology represents a regional variant characterised by distinctive point, scraper, and core types, notably their small 'microlithic' size which becomes more emphasised through time. Analysis of faunal evidence from Aduma in association with hominin remains, which meet the morphological definition of *H. sapiens*, indicate how these early members of our species were using multiple habitats with a strong reliance on riverine resources (Yellen *et al.*, 2005). Porc-Epic cave, whose MSA layers date to ~40 kya, is located between the Afar Depression and the Somali Plateau. At Porc-Epic, a large amount of ochre and ochre processing tools were discovered in an area devoted to the activity (Rosso, Martí and d'Errico, 2016). Perforated opercula shells have been also discovered dating from 33 kya to 43 kya, with evidence of polishing suggesting that they were used as beads (Assefa, Lam and Mienis, 2008). At nearby Goda Buticha, late MSA technological characteristics appear with LSA components well into the mid-Holocene, which is unseen elsewhere in the Horn of Africa (Tribolo *et al.*, 2017). There is a hiatus (from ~25 kya to 7.5 kya) in the sequence at Goda Buticha coinciding with the arid conditions of MIS 2, yet the MSA characteristics post-date this gap in occupation. This has been suggested to represent the reintroduction of cultural traits or convergence resulting from regional-scale population movements from refugial areas, rather than the localised persistence in technological traditions (Tribolo *et al.*, 2017).

### 3.5.2. Assemblage-level regional studies

The structure of diversity in the eastern African MSA has received a considerable amount of focus at the assemblage level. Early work by Clark (1988) noted the marked variability within the region, with no cultural feature appearing ubiquitously across assemblages. Clark (1988) proposed that the eastern African MSA was distinctive but also diverse, especially in the form of points. This author noted that sites with long sequences, such as Gademotta, Mumba, Nasera and Porc-Epic, show no specific trends through time, such as a consistent shift from large to small artefacts. When comparing assemblages across the region, he noted that sites in the Lake Victoria Basin, eastern Sudan, and the coastal zone each have their own distinct variant of heavy-duty tools which distinguishes them from other MSA assemblages, proposed to be reflective of local style as well as strategic and technological innovations. He suggested that assemblage variability was driven by the diverse topological environments and climatic conditions of the region, as well as raw material availability, an assertion which has proved robust since increased chronological resolution has improved our understanding of eastern African population dynamics (Basell, 2008; Blinkhorn and Grove, 2018, 2021).

Using correspondence analysis, Tryon and Faith (2013) considered the presence/absence of key artefacts and also noted a distinction between MIS 5-3 assemblages and those dated earlier. They found that early and late MSA assemblages overlapped in multivariate space, however a distinctive subset of late MSA assemblages exist, including those <75 kya from Mumba, Nasera, Porc-Epic, Mochena Borago and undated assemblages from Mtongwe. These assemblages yield more beads, ochre, backed pieces, bipolar cores, blades, grindstones, and anvils, and some have suggested that these assemblages are therefore transitional between the MSA and the LSA (e.g., Marks and Conard, 2008). Tryon and Faith (2013) also found evidence that there is a weak but significant relationship between geographic distance and assemblage similarity. This suggests that geography and its isolating effect on distant populations had at least some effect on the observed patterning, though Blinkhorn and Grove (2018) point out that this may be due to habitat differences across eastern Africa, rather than isolation by distance.

Blinkhorn and Grove (2018) used a combination of dissimilarity matrices and hierarchical clustering and discovered that, during humid periods, MSA behaviours persisted but were significantly augmented with new combinations of stone tool types. This underlying continuity in the eastern African MSA was also noted by Groucutt *et al.* (2015b), who proposed that the shifting frequencies of tool types across eastern Africa may reflect demographic factors, such as occasional contact with groups from other regions (Scerri *et al.*, 2018). Blinkhorn and Grove (2018) proposed a tripartite split of the MSA record, whereby variation in tool types present was higher in MIS 5 assemblages than those preceding and succeeding them, corresponding to an increase in environmental variability (Blinkhorn and Grove, 2018). Seven clusters of



assemblages were noted using agglomerative clustering methods and eight with divisive; importantly, no single tool types appear in only a single cluster though some tool types were more prevalent than others. Multiple assemblages from single sites were found to often cluster together under one method, whereas a more limited number of sites have multiple assemblages that cluster together consistently under both methods (Koimilot [Kaphurin Formation], Koobi Fora, Naisiusiu, Nasera, Olorgesailie, Porc-Epic and Prospect Farm). The largest cluster of assemblages based on toolkit diversity appears widely distributed across eastern Africa, with a similar lack of spatial structuring occurring within most of the smaller clusters. This may be due to the mosaic nature of environments in the eastern African MSA, with sites far apart demonstrating similar habitats (i.e., Kenyan and Ethiopian Rift) as well as different environments appearing close together. Sites falling within the Kenyan Rift Valley were found to possess the most heterogenous habitat in terms of both altitude and both modelled and modern climatic conditions. Broad latitudinal banding of habitats is noted in the sites from the Turkana basin and the Ethiopian rift, with the Turkana basin presenting a low-altitude hot and arid environment, separating the mountainous and humid Ethiopian rift. Coastal Kenyan sites were found to repeatedly fall within more humid environmental clusters, diverging from sites in the Kenya Rift under some conditions despite their comparable latitude. Panga Ya Saidi, Mtongwe and Nyara River all fall within heavily forested regions today, with persistent humidity in past conditions perhaps perpetuating the distinction between the majority of eastern African MSA site habitats. Despite these differences, the continued use of some constellations and some environmental contexts spanning the MSA suggests enduring behavioural adaptations which are augmented with new combinations of stone tools and the colonisation of different landscapes during MIS 5.

To further test the effects of distance, time and environments on the variability in the eastern African MSA, Blinkhorn and Grove (2021) used matrix correlation statistics and found that toolkit diversity correlates most strongly with raw material use and vice versa, a relationship that was found to be largely independent of other factors examined. This may suggest that the means to produce a diverse tool kit may have been mediated through the availability and selection of diverse raw materials. Raw material choice correlates independently with geography, supporting Tryon and Faith's (2013) suggestion that isolation by distance plays a role in explaining diversity in the MSA records of eastern Africa. Partial Mantel tests show that the relationship between both raw material and toolkit diversity and environmental variables is reduced when controlling for toolkit diversity and raw material respectively. Blinkhorn and Grove (2021) suggest that this reflects modulation of assemblage and raw material use by physical landscapes and ecological contexts, but this is expressed as flexibility rather than a strict requirement for certain tools in certain environments. Chronology correlates more strongly with raw material than with toolkit diversity,

and whilst no strong trends occur, a shift in emphasis occurs from earlier assemblages that use more basalt to later assemblages which contain more quartz, with both found in MIS 5. An extracorrelated variable combining time and space exhibits a stronger correlation with behavioural distance that is independent of other spatial variables under consideration, which could indicate cultural inheritance playing a role in adaptation and innovation. Site type (differentiating between open air and cave/rock shelters) independently correlates more with toolkit diversity than with raw material use, perhaps reflecting the alternate size of artefact and raw material inventories used. Terrain roughness was found to play a key, independent role in structuring variability in both raw material choice and toolkit diversity, highlighting the importance of considering the impacts of mobility on the archaeological record. Differences in altitude and environmental conditions show significant correlations with toolkit diversity and raw material use, though raw material and altitude show a weaker relationship. Temperature rather than precipitation shows the strongest correlations with patterns of assemblage composition and raw material use, though this correlation was variable when using either Last Glacial Maximum (LGM), Last Interglacial (LIG), and modern datasets and was not found to be independent in multiple matrix regressions, suggesting spatial autocorrelation may be playing a role in explaining variability in the two climatic variables (Blinkhorn and Grove, 2021).

### 3.6. Conclusion

The eastern African MSA record provides a fruitful case study for testing links between environmental and cultural diversity of early *H. sapiens*. Thanks to an extensive research history, the region boasts a rich archaeological record within varied palaeoecological settings, with the MSA acting as a relatively well-defined cultural stage that is a useful analytical unit at the chronological scale relevant to the emergence of *H. sapiens*. As Kleindienst (2006) suggests, rather than taking a ‘top-down’ approach as is often done when analyses are limited to within pre-defined industrial stages, this thesis adopts a data-led, inductive approach to defining cultural traditions; as a region, eastern African MSA is the arguably the most suitable case study for this line of enquiry. Moreover, previous research has found links between MSA diversity and environmental variables, particularly climatic and topographic factors, implicating a potential correlation between fluctuating habitats, cultural variation and demography that requires investigation within a sophisticated and highly refined framework that moves beyond interglacial/glacial stages to explore the evolutionary hypotheses of the SAM model.

## Chapter 4: A spatiotemporally explicit paleoenvironmental framework for the Middle Stone Age of eastern Africa

This chapter was published in Scientific Reports on the 7<sup>th</sup> of March 2022 under a Gold Open Access agreement (Timbrell *et al.*, 2022a). It was co-authored by me (lead author), Matt Grove (University of Liverpool), Andrea Manica (University of Cambridge), Stephen Rucina (National Museums of Kenya) and James Blinkhorn (Max Planck Institute of Geoanthropology, Royal Holloway University). Please note that some formatting to the structure and referencing style has been carried out to maintain consistency with the rest of the thesis, however the overall content remains unedited.

### Abstract:

Eastern Africa has played a prominent role in debates about human evolution and dispersal due to the presence of rich archaeological, palaeoanthropological, and palaeoenvironmental records. However, substantial disconnects occur between the spatial and temporal resolutions of these data that complicate their integration. Here, we apply high-resolution climatic simulations of two key parameters, mean annual temperature and precipitation, and a biome model, to produce a highly refined characterisation of the environments inhabited during the eastern African Middle Stone Age. Occupations are typically found in sub-humid climates and landscapes dominated by or including tropical xerophytic shrubland. Marked expansions from these core landscapes include movement into hotter, low-altitude landscapes in Marine Isotope Stage 5 and cooler, high-altitude landscapes in Marine Isotope Stage 3, with the recurrent inhabitation of ecotones between open and forested habitats. Through our use of high-resolution climate models, we demonstrate a significant independent relationship between past precipitation and patterns of Middle Stone Age stone tool production modes overlooked by previous studies. Engagement with these models not only enables spatiotemporally explicit examination of climatic variability across Middle Stone Age occupations in eastern Africa but enables clearer characterisation of the habitats early human populations were adapted to, and how they changed through time.

### 4.1. Introduction

Fossil, archaeological, and environmental records, together with the geographic placement of the region, suggest that eastern Africa played a prominent role in the evolution and dispersal of our species, *Homo sapiens* (Shea, 2020). The mosaic morphology of recently discovered Mtoto fossils at Panga Ya Saidi

demonstrates that eastern Africa sustained great diversity amongst Middle Stone Age (MSA) populations into the Late Pleistocene (Martinón-Torres *et al.*, 2021), supporting a pan-African origin for *H. sapiens* rather than a single centre of endemism (Scerri *et al.*, 2018, Scerri, Chikhi and Thomas, 2019). Across the continent, the MSA is becoming increasingly associated with the emergence of our species due to the near-simultaneous appearance of cultural innovations diagnostic of the MSA and hominin fossils possessing ‘modern’ features autapomorphic to *H. sapiens* (Porat *et al.*, 2010; Hublin *et al.*, 2017; Grün, 2006; Brooks *et al.*, 2018). The MSA archaeology record in eastern Africa is particularly rich compared to other regions, largely because of an extensive research history combining extensive use of chronometric dating and controlled excavation as well as its ideal conditions for preservation. This makes it an essential testing ground for hypotheses regarding modern human behavioural evolution (Clark, 1988, Basell, 2008; Tryon and Faith, 2013; Blinkhorn and Grove, 2018; 2021), especially in relation to palaeoclimatic change (Potts, 1998; Trauth *et al.*, 2007, 2010; Grove *et al.*, 2015).

Historically, there have been relatively scarce terrestrial climate records from eastern Africa, particularly in contrast to the richness of the archaeological record (Blome *et al.*, 2012). Over the past decade, recently assembled lacustrine records now provide evidence for climatic changes in several major basins spanning the region. The near-continuous core record from Lake Tana demonstrates increased climatic fluctuation towards the end of the penultimate glacial period, followed by abrupt change to stable humid conditions during Marine Isotope Stage (MIS) 5e-c (Lamb *et al.*, 2018). The Lake Tana record, from which Ca/Ti elemental ratios are used as a proxy for effective moisture, has been used to assess Out of Africa dispersal chronologies (Grove *et al.*, 2015). However, the lack of stratigraphically secure archaeological records proximate to the core site limits the potential to make strong links between dispersals and climate change. Elsewhere, at Olorgesailie high-resolution core data is associated with Acheulean and MSA deposits just 24km away from the drill site, allowing for the identification of a period of increased variability coinciding with the origin of the MSA (Potts *et al.*, 2020; Lupien *et al.*, 2021). This is supported by the pollen records at nearby Lake Magadi where the general trend of increased aridification for this period is also reported (Owen *et al.*, 2018). Late Pleistocene records from the Chew Bahir basin similarly demonstrate a series of wet-dry transitions of varying amplitude and duration through K counts (Schaebitz *et al.*, 2021), with the early modern human fossil site Omo Kibish lying close to (but not within) the basin. This record therefore could potentially offer a climatic context for MSA occupations of the site, considering that highly favourable humid conditions are reported at 200-125 kya (Schaebitz *et al.*, 2021) which broadly corresponds to the new date of the Omo fossils of  $212 \pm 16$  kya (Vidal *et al.*, 2022). Despite this improvement in resolution, paleoclimatic patterns and the records

used to generate them are diverse and rooted in a small number of lake basins (Fig. 2), complicating their use with the widely distributed MSA records in the region.

Archaeological studies of the eastern African MSA have noted a link between the distribution of sites, behavioural diversity, and environmental condition (Clark, 1988, Basell, 2008; Tryon and Faith, 2013; Blinkhorn and Grove, 2018, 2021). Basell (2008) made a key contribution by integrating modelled ecological data with a landmark synthesis of MSA assemblages. This highlighted the placement of MSA site locations near to but not necessarily within wooded ecologies, stressing the importance of ecotonal settings for enduring habitability in the region. Tryon and Faith (2013) made important advances in the quantitative assessment of eastern African MSA lithic assemblage composition, though they lacked the means to make similar developments in the characterisation of MSA environments, acknowledging the mismatched geographies and scales of archaeological and environmental records (Blome *et al.*, 2012). Blinkhorn and Grove (2018, 2021) in a suite of quantitative analyses, brought together ecology and archaeology using an expanded dataset of MSA lithic artefact typology alongside modern environmental datasets and models for the Last Glacial Maximum (LGM) and Last Interglacial (MIS 5e). Their results stressed the influence of environmental settings over the spatiotemporal distribution of MSA sites, with pulsed patterns of occupation intensity occurring during interglacial stages (Blinkhorn and Grove, 2018). Significant relationships between raw material and stone tool types and geographic and environmental variables were reported (Blinkhorn and Grove, 2021), with the strongest relationships with topographic ‘roughness’, emulating earlier hypotheses by King and Bailey (2006). These results validate the emphasis placed by earlier studies on ecology and the physical landscape (Clark, 1988); however, it remains to be tested whether Blinkhorn and Grove’s (2018, 2021) use of arid and humid models as representations of the extremes of variability observed within an interglacial-glacial cycle effectively characterise change throughout the MSA.

As such, our understanding of Middle to Late Pleistocene diachronic change has been greatly improved by high-resolution climatic records, whilst a series of regional syntheses of MSA assemblages has encouraged considerations of the ecological implications of prehistoric climate change (Basell, 2008), the quantitative assessment of MSA archaeology (Tryon and Faith, 2013), and their integration (Blinkhorn and Grove, 2018, 2021). However, as also stressed in a recent review by Patalano *et al.* (2021), lake cores offer very limited insights into spatial patterns of climate change due to the inability to extrapolate across the wider landscape, the difficulty of translating relative wet and dry proxies into tangible climatic or ecological parameters, the non-linear relationship between different proxies and the phenomena they represent and the lack of directly associated, stratigraphically secure archaeological assemblages.

Conversely, studies that rely on simplistic arid-humid simulated datasets (Basell, 2008; Blinkhorn and Grove, 2018, 2021) or use modern biogeographic zones to represent Pleistocene environments (Tryon and Faith, 2013) lack chronological precision, and assume uniformity across successive glacial / interglacial cycles. Here we overcome such limitations to provide a sophisticated examination of the distribution and diversity of eastern African MSA occupations through time and space within the context of Middle to Late Pleistocene climate change. We integrate novel high-resolution climate and biome simulations (Krapp *et al.*, 2021) with a database of chronometrically dated eastern African MSA stone tool assemblages (Blinkhorn and Grove, 2021) to refine the characterisation of MSA environments, map their extent across the landscape, and produce a climatic envelope for eastern African MSA occupations.

## 4.2. Materials and methods

We employed here simulated climate and biome reconstructions for the past 800 kya (Krapp *et al.*, 2021). Mean annual temperature (bio01), total annual precipitation (bio12) and biome (biomeoutput04) were extracted from the model for 1000-year time slices and stored in a raster stack using the ‘raster’ R package (Hijmans *et al.*, 2021). We then selected the time slices corresponding to the mid-age of each assemblage (the mid-point between the minimum and maximum date range of the occupation), rounded to the nearest 1000 years to match the resolution of the climate data (see Appendix 1: Supplementary Table S1). Each time slice was cropped according to the predicted sea level for that period, using global sea-level change data (Spratt and Lisiecki, 2016) and a bathymetry model (GEBCO, 2020; see Appendix 1: Supplementary Methods S1).

We integrated the climate model with an archaeological dataset reported in Blinkhorn and Grove (2021) which comprises presence/absence data of 16 tool types and 8 raw material types for eastern African MSA assemblages, as well as other typological characteristics, such as site type and method of excavation (see Appendix 1: Supplementary Methods S2 for further description).

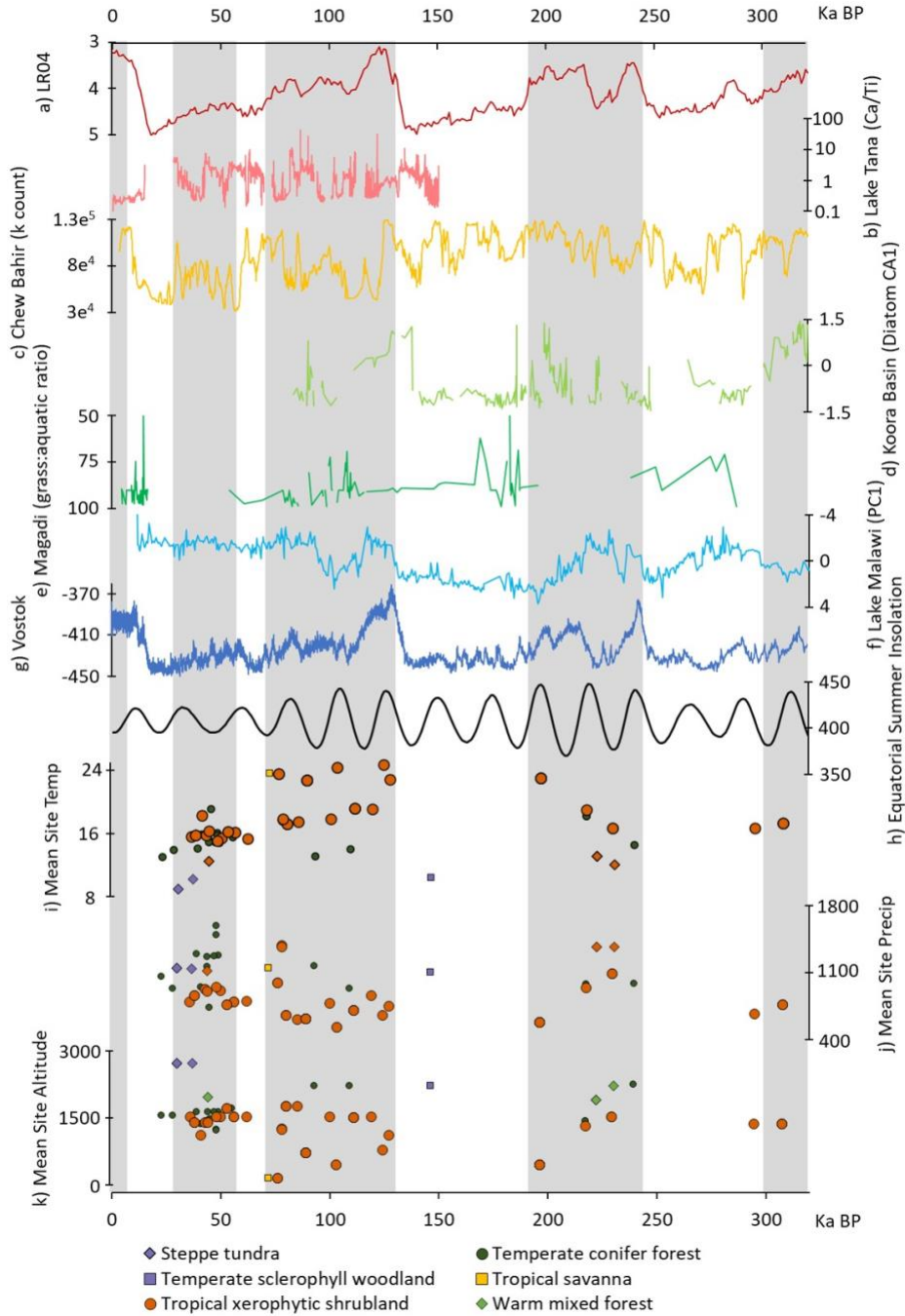


**Figure 2.** Composite of key inter-regional and regional climatic records, insolation, and temperature, precipitation and altitude parameters for dated eastern African Middle Stone Age occupations including (a) LR04 Benthic Stack  $\delta^{18}\text{O}$  (Lisiecki and Raymo, 2005); (b) Lake Tana Ca/Ti ratio (Lamb *et al.*, 2018); (c) Chew Bahir k-counts (Trauth *et al.*, 2021); (d) Koora Basin diatom CA (Potts *et al.*, 2020); (e) Magadi Pollen grass:aquatic ratio (Muirui *et al.*, 2021); (f) Lake Malawi PC1 (Lyons *et al.*, 2015); (g) Vostok  $\delta\text{D}$  [‰ SMOW] (Jouzel *et al.*, 2007); (h) mean Equatorial summer (Jun-Aug) insolation ( $\text{W}/\text{m}^2$ ) (Laskar *et al.*, 2004); mean (i) temperature ( $^{\circ}\text{C}$ ), (j) precipitation (mm), and (k) altitude (meters above sea level) within 50km radius of eastern African MSA assemblages, illustrated at the mid-age point for each occupation and symbolised according to its biome classification. Grey vertical bars indicate odd-numbered Marine Isotope Stages.

Reprinted from Timbrell *et al.* (2022a).

#### 4.2.1. Refining the climatic parameters

We extracted temperature and precipitation values (Krapp *et al.*, 2021) in 50 km radius buffers around the coordinates of each occupation from its mid-age time slice, representing the home range sizes of hunter-gatherer populations (Binford, 2001) and regional patterns of local raw material procurement (Ambrose, 2012; Faith *et al.*, 2015; Blegen, 2017; Brooks *et al.*, 2018). In order to better characterise patterns of landscape variability across this range, we downsampled model datasets from 30' to 2.5' by resampling the data using bilinear interpolation, following examination of alternate methods (see Appendix 1: Supplementary Methods S3). We calculated the mean and standard deviation of the values across the 50km buffer for each occupation.

#### 4.2.2. Cluster analyses

Dissimilarity matrices for the temperature and precipitation data were calculated using the Euclidean distance. Hierarchical clustering of the dissimilarity matrices was then employed to examine grouping of occupations according to temperature and precipitation combined in equal combinations to characterise environments, following Blinkhorn and Grove (2018). Cluster analysis iteratively merges cases into a group using a measure of closeness (i.e., the opposite of dissimilarity). We applied the average silhouette method, which uses k-means clustering to automatically determine the optimal number of clusters from the data. The average silhouette method evaluates the quality of clustering by determining how well each occupation lies within its cluster, producing a measure of how similar an occupation is to its own cluster relative to other clusters. We created a dendrogram of the occupations, which was cut according to the k-means output ( $k = 10$ ) to define our clusters.

#### 4.2.3. Biome classification

To classify the biomes occupied by each occupation, we used the modelled biome dataset (Krapp *et al.*, 2021). To increase the resolution of the data to 2.5', we resampled the raster layers using the nearest neighbour method, which is most suitable for categorical data. We extracted the biome type for each assemblage location at its mid-age and then recorded the number of cells (each representative of 4.63 km) assigned to each biome within a 50 km radius around each occupation. To evaluate whether the proportion of biomes inhabited by MSA populations was significantly different to the proportion of biomes available across the landscape, we used 2-sample proportion tests. We also used a chi-square test



to investigate whether biome proportions changed through time to test whether changes in habitat are due to preference shifts throughout the MSA or a reflection of the underlying ecologies available.

#### 4.2.4. Phased climate suitability models

We used the temperature and precipitation values from within a 50km of each occupation to produce phased models of ‘habitability’. To do this, we subsetted the occupations according to MIS, and produced a series of climatic ranges based on the inhabited temperature and precipitation values during that period. We then calculated the percentage of time slices within each MIS that fall within the climatic range of occupations dated to that period. This produced phased models mapping the areas of the landscape that would have been comparable to those inhabited during that MIS, indicating the degree of habitat stability over time.

#### 4.2.5. Mantel tests and multiple matrix regression

To explore the relationships between toolkit diversity, raw material choice and environments, we used simple Mantel tests and multiple matrix regression, the null hypothesis for which assumes that there is no correlation between two distance matrices (e.g., toolkit composition and temperature), factoring in the impact of additional variables (e.g., raw material) for multiple matrix regressions. Positive correlation in dissimilarity between two distance matrices, like toolkit composition and temperature, would suggest that occupations experiencing similar temperatures share more similar constellations of tool types, whereas a negative correlation would suggest that as dissimilarity increases in one variable, it decreases in another.

As described in Blinkhorn and Grove (2021), the additional distance matrices used as variables that may explain variation in MSA toolkits for multiple matrix regression are site type, method of excavation, simple age (mid-age), cost path (a measure of physical distance), altitude within 50 km and roughness within 50km (calculated as amount of energy needed to move across the logistical landscape). A description of how each distance measure was calculated can be found in Appendix 1: Supplementary Methods S2, following Blinkhorn and Grove (2021). Simple Mantel tests were conducted using the ‘vegan’ R package (Okasen *et al.*, 2020), employing 999 permutations to obtain p-values. The Benjamini-Hochberg procedure was used to adjust p values. Multiple matrix regression was performed with 999 permutations using the ‘phytools’ package in R (Revell, 2012).

Additional binary logistic regressions using penalized maximum likelihood were conducted to determine the effects of significant predictors on individual technologies using the ‘brglm’ R package (Kosmidis, 2007; see Appendix 1: Supplementary Methods S4). Unlike our initial correlation statistics that use a single distance measure to represent archaeological diversity, binary logistic regression is based on the presences and absences of certain technologies, with each regression controlled for the effects of all other variables, except cost path which is only available as a distance matrix and thus inappropriate for logistic regression analysis. Appendix 1: Supplementary Methods S4 Table S1 demonstrates the positive and negative significant effects of independent variables on each tool type.

### 4.3. Results

#### 4.3.1. Middle and Late Pleistocene climates of MSA occupations

We first examined MSA occupations ( $n = 84$ , Fig. 3) spanning the Middle to Late Pleistocene using simulated climate data. We extracted mean annual temperature (bio01) and total annual precipitation (bio12) values from the climate model (Krapp *et al.*, 2021) within a 50km radii, centred on the occupation’s mid-age date range rounded to the nearest 1000-year (kyr) time slice, to characterise environments across the wider logistical landscape (following Blinkhorn and Grove, 2018, 2021). The climatic conditions for each occupation can be found in Appendix 1: Supplementary Table S1 and are illustrated in Figure 2.

We found that average temperatures at eastern African MSA occupations varied between 9°C and 25°C, with 59 occupations falling within the 68% confidence interval of 14-23°C. The warmest environments occupied were found in coastal regions, such as Abdur along the Red Sea coast of modern-day Eritrea (25°C) and Panga Ya Saidi situated on the Kenyan coast (24°C), as well as in the Lower Omo Valley of southwestern Ethiopia (24-23°C). These hot environments were inhabited during MIS 5 and MIS 7. On the other hand, the coldest environments inhabited were at high altitude, at Fincha Habera in the Bale Mountains of southern Ethiopia (9-10°C) and at Kenyan Rift Valley occupations of Marmonet Drift (10-14°C) and Enkapune ya Muto (13°C), most of which date to MIS 3. Average precipitation levels experienced by Middle to Late Pleistocene MSA populations in eastern Africa ranged between 396mm and 1593mm, with 59 occupations falling within the 68% confidence interval of 620-1150mm, corresponding to the precipitation bracket of sub-humid landscapes. The wettest habitats were located on islands within and along the shore of Lake Victoria at Rusinga Nyamtia (1593mm) and Karungu (1374-1499mm) in MIS 3 and 5, as well as within the Ethiopian Rift Valley at Gademotta (1368mm), the

Ethiopian Highlands at Mochena Borago (1270-1297mm), and the Kenyan Rift Valley at Marmonet Drift (1173-1368mm) in MIS 3, 5 and 7. On the other hand, the driest occupations occurred at Laas Geel in Somaliland during MIS 3 (396mm) as well as within the Lower Omo Valley (534-582mm) during MIS 5 and 7.

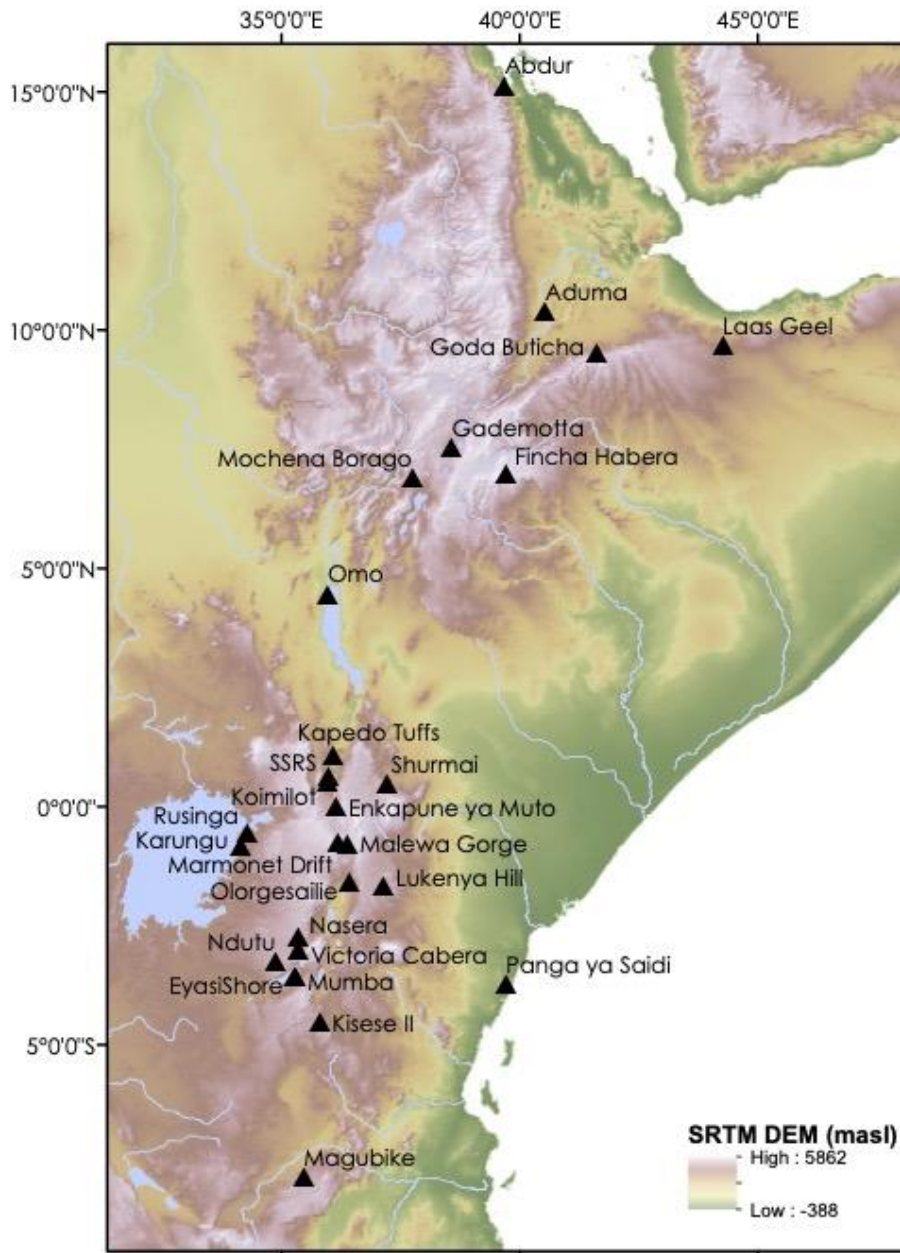


**Figure 3.** Distribution of the eastern African Middle Stone Age occupations studied. This map was created in ArcGIS 10.5 using an SRTM (NASA).

#### 4.3.2. Classifying biomes and ecotones at MSA occupations

We then used the modelled biome dataset (biome4output) (Krapp *et al.*, 2021) to classify the local ecology of each MSA occupation within a 50km radius. We found that 38% of the occupations ( $n = 32$ ) had access to only tropical xerophytic shrubland within their logistical landscape (see Fig. 4. for modern examples of this biome), and a further 42% with this biome among others within a 50km radius ( $n = 35$ ). Tropical xerophytic shrubland was persistently occupied throughout the Middle to Late Pleistocene (Fig. 1), and whilst it was the most prevalent biome type available, representing 61.9% of the biomes present during occupational phases across the region (Appendix 1: Supplementary Fig. S1 and Table S2), eastern African MSA adaptive systems were likely specialised for engagement with tropical xerophytic shrubland, and its modulation may therefore have influenced patterns of Middle to Late Pleistocene human distribution. Nonetheless, the proportion of occupations with access to tropical xerophytic shrubland was significantly higher using a 2-sample proportion test than the proportion of the biome available across the region throughout MSA occupational phases ( $Z$ -value = 3.38,  $p$ -value = 0.0007; Appendix 1: Supplementary Table S3), suggesting preferential occupation of tropical xerophytic shrubland and emphasising it as an important ecosystem for MSA populations.

In total, 57% of the occupations had a logistical landscape falling on the boundary between multiple biomes ( $n = 48$ ; Appendix 1: Supplementary Table S1). The majority of these ecotonal sites are situated between 'open' and 'closed' biome types, supporting the assertion of Basell (2008) that access to wooded ecologies was vital for MSA populations. Forest biomes made up relatively low proportions of the available environments available throughout the Middle to Late Pleistocene; however, importantly, we found the proportions of forest biomes occupied by MSA occupations to be significantly higher than would be expected based on the prevalence of these biomes, especially in MIS 3 and MIS 7 (see Appendix 1: Supplementary Fig. S1 and Tables S2-3), supporting the contention that MSA hominins preferred the rarer habitats which were near to woods and forests. The most common ecotone occupied during the eastern African MSA was that between tropical xerophytic shrubland and temperate conifer forest, which is seen as far north as Goda Buticha in southeastern Ethiopia, and as far south as Mumba in Tanzania. However, the region to the east of Lake Victoria shows the most intense occupation of this ecotone, the boundary of which fluctuates through time and space (Appendix 1: Supplementary Table S1).

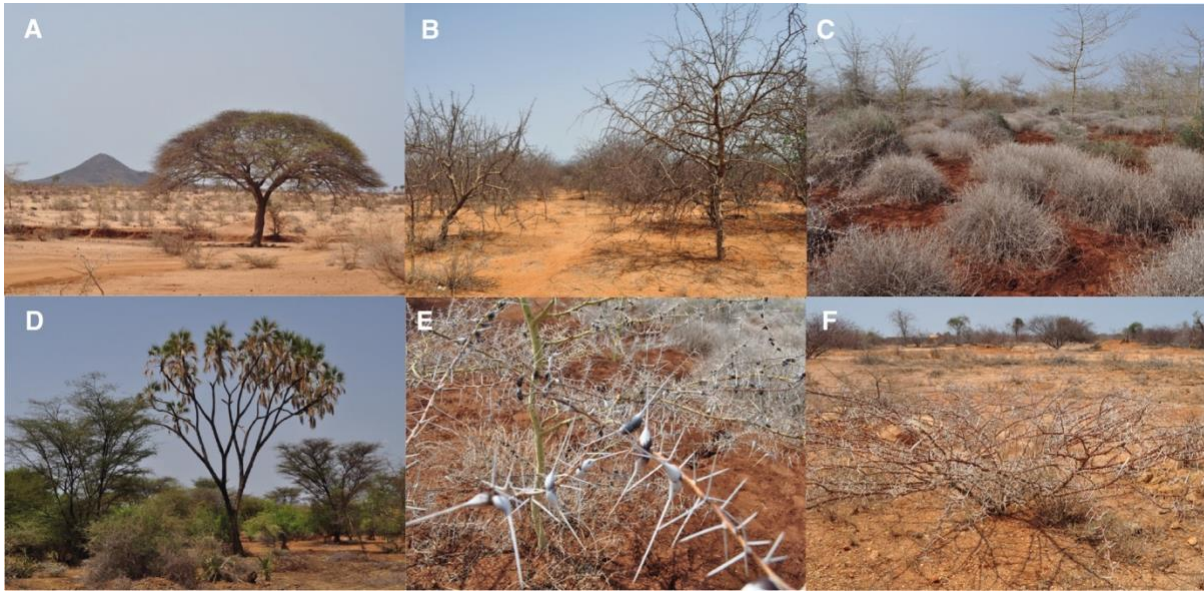


**Figure 4.** Examples of xerophytic shrubland environments in modern eastern Africa, including typical species (sp.). A) *Acacia tortilis* B) *Commiphora* sp. C) *Acacia* sp. and *Duosperma eremophilum*. D) *Hyphaene compressa*, *Acacia* sp., *Salvadora persica*, *Cyperaceae* and *L Lawsonia inermis* E) *Acacia* sp. and *Duosperma eremophilum*, F) *Acacia tortilis* (background: *Commiphora* sp. *Capparaceae* sp. *Tephrosia* sp. and *Indigofera spinosa*). Photos taken by Dr Stephen Rucina.

We found that MIS 7 saw the preferential occupation of closed ecotones between temperate conifer forest and warm mixed forest, as well as tropical xerophytic shrubland and associated ecotones which are generally occupied throughout the period. MIS 5 saw a slight increase in habitat diversity, though expansions primarily involved the tracking of tropical xerophytic shrubland environments (as shown by all occupations in MIS 5 having access to this biome within 50km) with exposure to new ecotones occurring at the peripheries. This can be seen at occupations distributed widely across the region; for example, certain occupations at Omo would have involved engagement with deserts alongside tropical xerophytic shrubland, whereas some MSA populations at Panga Ya Saidi had access to tropical deciduous forest and tropical savannah environments within their logistical landscape. MIS 3 saw the greatest variety in the ecologies occupied, where expansions can be seen into new and previously uninhabited environments, such as steppe tundra and warm mixed forest, with a distinct emphasis on temperate conifer forest rather than tropical xerophytic shrubland. Importantly, a chi-square test revealed that the relative proportions of biomes in the region do not differ significantly between the Marine Isotope Stages ( $\chi^2 = 9.07$ , p-value = 0.99), strongly suggesting that variation in the environments occupied through time reflects a shift in preference as opposed to fluctuation in the underlying ecology (see Appendix 1 Supplementary Tables S2-3).

### 4.3.3. Characterising MSA environments throughout the Middle to Late Pleistocene

We used cluster analyses to group the occupations based on their climatic values to assess patterns in habitat choice. To do this, we scaled and combined the temperature and precipitation data and employed an automated clustering algorithm (the average silhouette method) to ascertain the optimal number (k) of clusters in the data. The algorithm found ten clusters to represent the best division of the data (Fig. 5, Appendix 1: Supplementary Fig. S2).

Most of the occupations (n = 45) fall within warm to temperate sub-humid clusters (2,4,5 and 7) with a broad temperature range of 13-19°C and a precipitation range of 613-1297mm. These clusters are dominated by tropical xerophytic shrubland and temperate conifer forest environments and their ecotones. We found that only two clusters (8,9) did not include occupations with access to tropical xerophytic shrubland, indicating that this biome was present across a large portion of the MSA climatic range, except at the coldest extreme. We found that the coldest cluster, cluster 9 (temperature range 9-10°C), was the most ecotonal, with all occupations situated at high altitude where populations would have had access to steppe tundra, temperate conifer forest, temperate sclerophyll woodland and warm mixed forest, the complex topography allowing diverse biomes to appear closer together than is usually possible (Foley, 1995). Extremely humid occupations from around Lake Victoria (Karungu and Rusinga Nyamita) formed cluster 10 (1374-1593mm precipitation). These occupations have moderate temperatures (16-18°C) and occupy an ecotone between tropical xerophytic shrubland and temperate conifer forest. Panga Ya Saidi and Laas Geel form their own respective clusters (3 and 6) due to their distinctively hot temperatures; however, at Panga Ya Saidi, this is coupled with moist sub-humid conditions and a diverse tropical environment (24°C, 996-1153mm), whereas Laas Geel possesses the lowest annual precipitation of all the occupations (18°C, 396mm), making its hot-dry environment unique for the eastern African MSA. However, the occupation at Laas Geel falls within the tropical xerophytic shrubland biome, with access to some open conifer woodland within 50km, suggesting that whilst occupying a climatic extreme, this distinct habitat represents an extension of the types of environments that eastern African MSA populations were already well-adapted to.

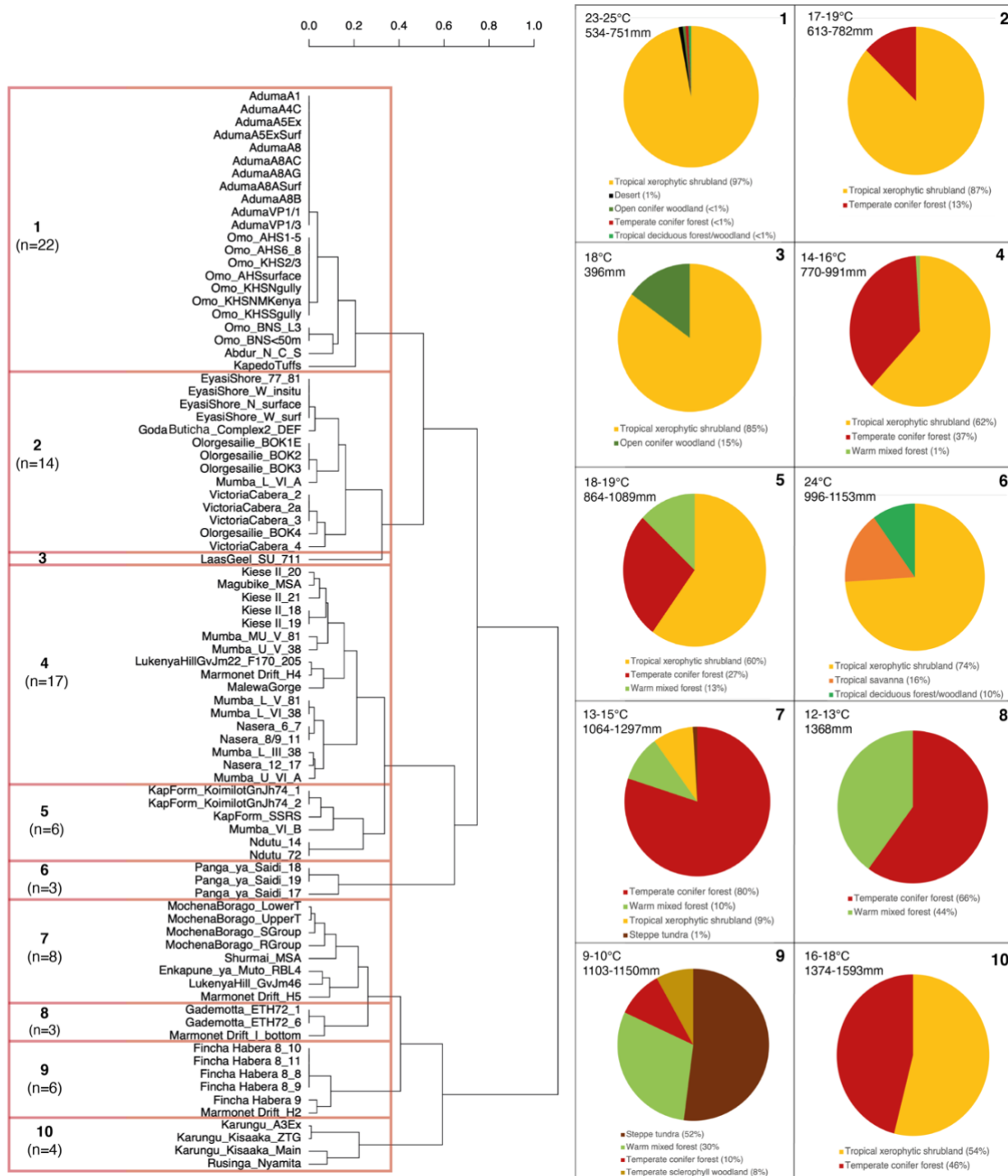


**Figure 5.** Hierarchical clustering of the occupations according to mean annual temperature and total annual precipitation. K means clustering identified ten clusters as the optimal division of the dendrogram, which have been highlighted here as well as the range of environmental conditions occupied by each cluster and the percentage of cells within 50km of that biome for all occupations within that cluster.

#### 4.3.4. Phased habitability models

We used the precipitation and temperature data from the occupations as the parameters to produce phased ‘habitability’ models for the more abundantly populated interglacial phases of the MSA, demonstrating the extent of the landscape that experienced comparable climatic settings to occupations dated within that period. The climatic range produced by each phased subset was projected throughout every 1000-year time interval for that MIS, and then the percentage of ‘habitable’ cells (i.e., cells that remain within that climatic range) was calculated to identify areas that were persistently habitable, as well as the geographic range and temporal scope of impersistent habitable landscapes.

Figure 6 demonstrates the temperature, precipitation, and combined habitability models for each phase. MIS 9 shows the most limited habitable zone out of the interglacial phases, however the lower number of occupations available to construct the distribution likely has impacted the construction of the models. MIS 7 marks a period of expansion, with the region surrounding Lake Victoria and the Eastern Rift Valley Lakes and the Ethiopian Highlands showing the most persistent habitability across the region. For temperature, large areas of the Horn and modern-day Sudan show less persistent habitability (*ca.* 40-50% cells falling within the temperature range of 12-23°C seen at MIS 7 occupations), with pockets of unsuitability along the coast of the Baab el Mandeb and the border between modern-day Ethiopian and Somalia. However, arid zones of the southern Sahara are completely uninhabitable in terms of precipitation (0% of cells fall within the precipitation range of 582-1368mm at MIS 7 occupations), as is the tip of the Horn. Precipitation is thus the limiting factor when considering habitability for MIS 7, as the area deemed habitable in terms of precipitation is more geographically restricted than that derived from temperature. MIS 5 sees the largest increase in habitable area for temperature, with all cells showing temperature values within the MIS 5 occupation range of 13-25°C for at least 60% of the period. Precipitation habitability, that we considered here to be ranging between 554-1385mm, is however more fragmented, with pockets of uninhabitability forming around the northeast edge of Lake Victoria, in the region to the south of Lake Tana, and within modern-day Tanzania. Like MIS 7, this means that habitability is limited by precipitation in MIS 5. However, the habitability models for MIS 3 demonstrates the opposite pattern. Temperature habitability, defined as between 9-19°C by the sites dating to MIS 3, shows the most restricted distribution of all the models, with habitable areas concentrated to the areas around Lake Victoria and the Ethiopian highlands, which are linked towards the southeast of Lake Turkana. Yet, MIS 3 shows the most persistent and widely distributed zone of habitability for precipitation, where much of eastern Africa, except towards the Sahara and the very tip of the Horn of Africa, remains persistently within the range of precipitation values experienced by MIS3 occupations



(396-1593mm). Overall, these models propose that interglacial MSA occupations, especially in MIS 5, may have been much more spatially diverse than presently known, however we note that these distributions are based purely on climatic data and ignore the potential effects of volcanic eruptions and subsequent ashfalls that have also been argued to have conditioned habitability in this region (Basell, 2008).

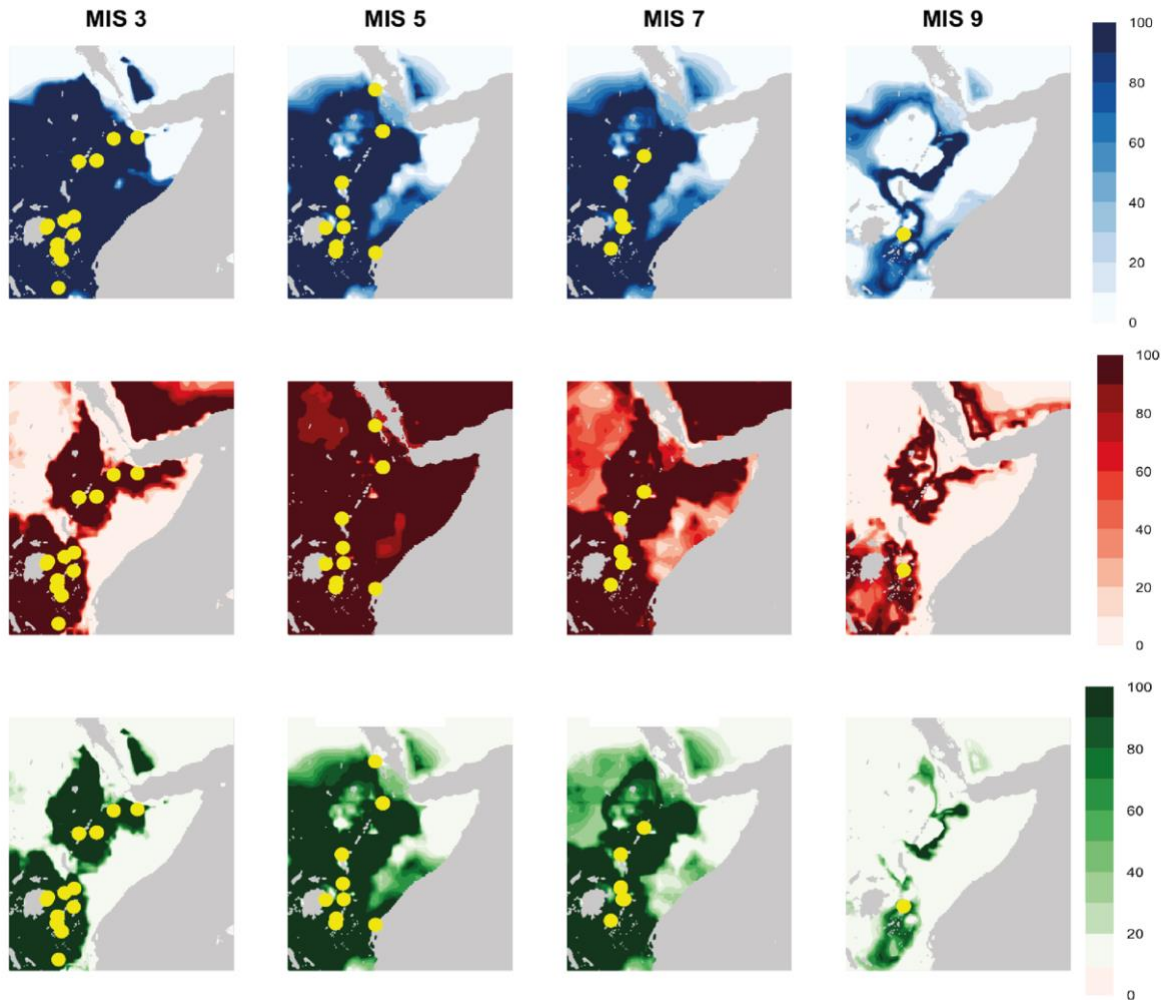


**Figure 6.** Mean annual temperature (top), total annual precipitation (middle) and combined (bottom) phased models of habitability, demonstrating the percentage of time intervals (1000 years per interval) that remain within the climatic range of the occupations dated to that Marine Isotope Stage (MIS). The palaeocoastline has been estimated based on the predicted mean sea-level for each MIS.

#### 4.3.5. Exploring the relationship between climate and Middle Stone Age occupations

We then examined the extent to which patterns of variability in stone tool assemblage composition and raw material use correlated with environmental conditions within a 50km radius at the mid-age of

occupation of each assemblage, as well as a suite of other variables recorded by Blinkhorn and Grove (2021; Appendix 1: Supplementary Methods S2 for details). Figure 7 demonstrates the relationships between these variables and toolkit composition and raw material use, revealed using simple Mantel tests (Table 6 and Appendix 1: Supplementary Methods S3 Tables S1-2). We found that MSA assemblage composition was correlated with differences in both mean annual temperature (adj.  $p = 0.001$ ; Table 6) and total annual precipitation (adj.  $p = 0.003$ ; Table 6), and raw material use also shows statistically significant relationships with both mean annual temperature (adj.  $p = 0.001$ ; Table 6) and total annual precipitation (adj.  $p = 0.003$ ; Table 6). With the use of Pleistocene climate models at high temporal resolutions, these results refine the findings of Blinkhorn and Grove (2021), which relied on comparisons of the climatic extremes of the LGM and LIG.

We next employed multiple matrix regressions to resolve independent, significant correlations between differences in either stone tool assemblage composition or raw material use, and differences across the different variables. Table 7 demonstrates that four variables exhibit independent significant effects on toolkit composition ( $F = 68.0$ , multiple  $R^2 = 0.15$ ,  $p = 0.001$ ) - raw material use, roughness, site type and precipitation. In the multiple matrix regression for raw material (Table 7), five variables were found to have independent effects ( $F = 54.8$ , multiple  $R^2 = 0.12$ ,  $p = 0.001$ ) – toolkit composition, cost path, roughness and simple age, with precipitation being very close to significant. In each instance, these results complement earlier findings, but the use of highly resolved climate models illustrates the independent and significant relationship between MSA behaviour and precipitation that was not evident from previous analyses that were reliant on models for climatic extremes (Blinkhorn and Grove, 2021). This highlights the benefit of using highly chronologically resolved model data to more accurately characterise the climatic parameters of MSA occupations in eastern Africa and to reveal the relationship between environmental and behavioural variability.

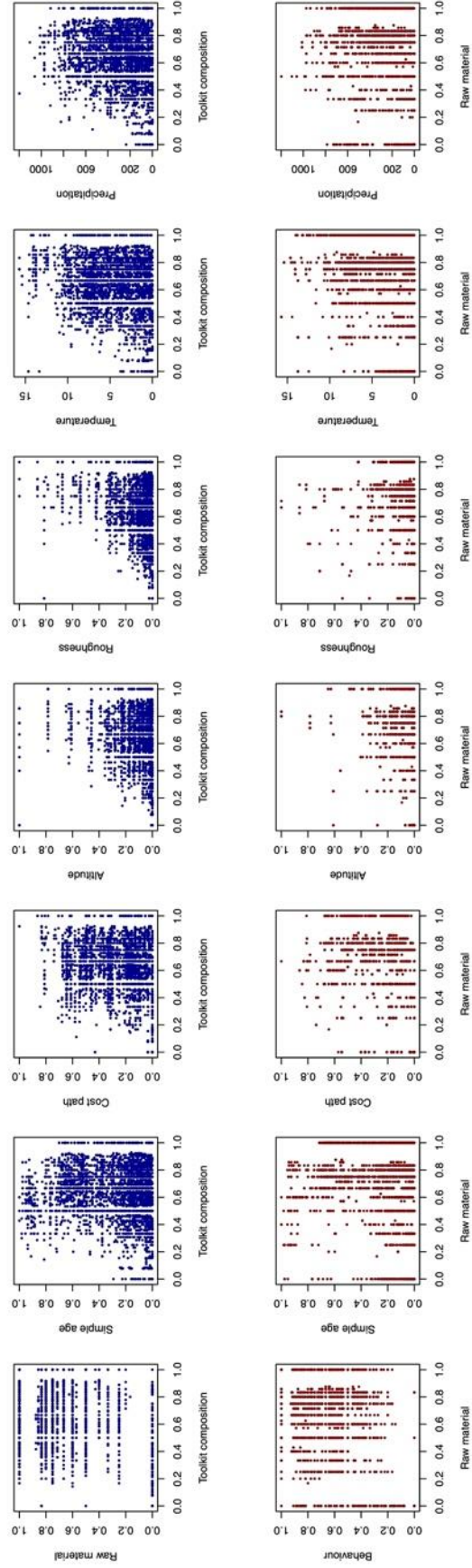


**Figure 7.** Scatterplots of the Mantel test results (Table 6, Appendix 1: Supplementary Methods S3 Tables S1-2) between the pairwise distance matrix of toolkit composition (top) and raw material use (bottom) and the other distances matrices excluding the two binary variables, site type and method.

**Table 6.** Simple Mantel test results for the effects of precipitation and temperature on toolkit composition and raw material. Statistical significance highlighted at  $p < 0.05$  (\*) or  $p < 0.01$  (\*\*). The Benjamini-Hochberg procedure was used to adjust p values.

|               | Toolkit composition |         |         | Raw material |         |         |
|---------------|---------------------|---------|---------|--------------|---------|---------|
|               | coefficient         | p       | adj. p  | coefficient  | p       | adj. p  |
| Precipitation | 0.1972              | 0.001** | 0.003** | 0.1587       | 0.001** | 0.003** |
| Temperature   | 0.2144              | 0.001** | 0.003** | 0.1532       | 0.001** | 0.001** |

**Table 7.** Multiple matrix regression results for toolkit composition and raw material. Descriptions of each variable can be found in Appendix 1: Supplementary Methods S2. Statistical significance highlighted at  $p < 0.05$  (\*) or  $p < 0.01$  (\*\*).

|                     | Toolkit composition |         | Raw material |         |
|---------------------|---------------------|---------|--------------|---------|
|                     | coefficient         | p       | coefficient  | p       |
| Toolkit composition | NA                  | NA      | 0.3119       | 0.001** |
| Raw material        | 0.1483              | 0.001** | NA           | NA      |
| Method              | 0.009               | 0.698   | 0.0351       | 0.192   |
| Site type           | 0.0328              | 0.018*  | -0.0061      | 0.7     |
| Simple Age          | 0.0184              | 0.668   | 0.149        | 0.007** |
| Cost path           | 0.0172              | 0.669   | 0.1991       | 0.001** |
| Altitude            | -0.09               | 0.473   | 0.2206       | 0.106   |
| Roughness           | 0.2645              | 0.004** | -0.2286      | 0.017*  |
| Temperature         | 0.0673              | 0.298   | -0.0108      | 0.896   |
| Precipitation       | 0.111               | 0.015*  | 0.1124       | 0.053   |

#### 4.4. Discussion

Using high-resolution modelled climatic data, we have conducted more sophisticated analyses of the environments inhabited by MSA-making populations than was previously possible, bridging former disconnects between archaeological and climatic records within a spatiotemporally explicit framework. Figure 1 highlights the challenge of generalising from proxy core records which we have overcome through the parameterisation of temperature and precipitation with simulated models, revealing interpretable patterns in terms of MSA environments. Our analyses have extended previous work applying models of the LGM and LIG to represent climatic extremes (Blinkhorn and Grove, 2018, 2021) and importantly have revealed the climatic bracket of eastern African MSA occupations to around 9-25°C mean annual temperature and 396-1593mm total annual precipitation. MSA occupations are more prevalent during interglacial phases (MIS 3, 5, and 7) and we found that populations during these periods

inhabited more diverse and widely distributed environments. Most occupations are located within or with access to tropical xerophytic shrubland, and usually are found within proximity to at least one forest or woodland biome, even though these environments only make up a small proportion of those available throughout the Middle to Late Pleistocene. Using spatiotemporally explicit models we also established that precipitation levels experienced by MSA populations had an impact on both behavioural variability and the use of raw materials, which we explore further here using penalised logistic regression.

Our results highlight spatial and diachronic trends in the environments inhabited by eastern African MSA populations, which are demonstrated by Figure 2, 5 and Appendix 1: Supplementary Table S1. MIS 9 and 8 saw occupations that were typical for the eastern African MSA in terms of temperature, precipitation, altitude, and biomes inhabited. During MIS 7, there was a dramatic increase in the environments occupied, spanning much of the climatic range of the later interglacial phases with emphasis on forest/woodland ecotones and tropical xerophytic shrubland. MIS 6 saw the occupation of a cold, high-altitude environment; however, the phase is only represented by a single occupation, Marmonet Drift H2, with a large date range so we do not place too much emphasis on its mid-age climatic placement. MIS 5 was marked by another phase of expansion, though with limited presence in woodland habitats and typically warmer, drier and low altitude occupations. MIS 5 has been proposed to represent a transitional point within the MSA stone tool record, due to the augmentation of MSA toolkits with new combinations of stone tools and the colonisation of different landscapes into the Late Pleistocene (Basell, 2008; Tryon and Faith, 2013; Blinkhorn and Grove, 2018). Engagement with these new environments likely occurred at the edge of the logistical landscape, with many eastern African MSA occupations falling on ecotonal boundaries between tropical xerophytic shrubland and previously unoccupied biome types. An example of this is found with the youngest MSA occupation at Panga Ya Saidi, which is placed at a unique tropical ecotone (d'Errico *et al.*, 2020). MSA occupation of Panga Ya Saidi at the end of MIS 5 is rapidly followed by cultural change, with the appearance of the Later Stone Age here occurring earlier than anywhere else in the region (d'Errico *et al.*, 2020). New constellations of tools within MIS 5 toolkits suggest corresponding changes in behaviour previously unseen in the MSA (Blinkhorn and Grove, 2018), which perhaps may have been key for these expansions beyond tropical xerophytic shrubland. Together, this suggests that certain MSA toolkits may have led to adaptation, as opposed to adaptations being a pre-requisite for expansion, with transient ecotonal habitats requiring the adoption of a range of survival strategies and potentially mediating interaction between different groups across different environmental contexts (Shipton *et al.*, 2018; d'Errico *et al.*, 2020; Martinon-Torres, *et al.*, 2021). Occupations dated to MIS 4 show a climatic range close to that of MIS 3, where we see a push into higher precipitation woodland habitats with a limited change in temperature and altitude. Habitability modelling for MIS 3

suggests that temperature, rather than precipitation as seen during earlier interglacial periods, constrained expansions into new landscapes, with populations occupying cooler landscapes than seen previously during the MSA, specifically within mountainous settings. There is some discussion about whether MIS 3 can be considered a true interglacial due to its erratic nature (Clement and Peterson, 2008) however, it does include some very warm (albeit short-lived) periods, and thus mountain ranges may have offered refuges when lower-altitude landscapes were especially arid (Ossendorf *et al.*, 2019). Moreover, unpredictable climates have been found to favour the evolution of ‘generalist’ strategies and behavioural plasticity (Grove *et al.*, 2022), perhaps explaining why there appears to be a notable extension of the precipitation regime inhabited during MIS 3, with the occupation of both extreme dry and wet environments.

Eastern African MSA occupations are primarily located within tropical xerophytic shrubland, characterised by arid-adapted species such as that from the *Acacia* and *Commiphora* genera. Whilst it is the most abundant biome across modern eastern Africa as well as the Middle to Late Pleistocene (see Appendix 1: Supplementary Fig. S1 and Tables S2-3), the intense occupation of tropical xerophytic shrubland and its associated ecotones suggests that eastern African MSA adaptive strategies were centred around engaging with subsistence resources associated with this biome. Our results also confirm the importance of access to wooded ecotones for sustaining MSA populations (Basell, 2008), with the most common ecotone occurring between temperate conifer forest and tropical xerophytic shrubland, distributed widely across the region though most concentrated towards the eastern edge of Lake Victoria and the associated region. Today, Lake Victoria sits on the junction between central African rainforests and savanna habitats to the east, forming an important boundary for large mammal (Tryon *et al.*, 2016) and human (Lewis, 2009) populations. Our phased models (Fig. 6) propose that the region to the east of Lake Victoria, including the Eastern African Rift Valley, would have seen sustained and persistent occupation throughout the Middle to Late Pleistocene in the face of climatic fluctuation, implicating it as a potential refugium for hominins in eastern Africa. The availability of freshwater provided by surrounding rivers and springs (Cuthbert *et al.*, 2017) and the complex topography of the Rift Valley (King and Bailey, 2006; Ambrose, 2001) may also have helped buffer against the strongest effects of climate change in the area (Blome *et al.*, 2012). Occupying refugia likely required minimal cultural adaptation to environmental change, which could explain why assemblages from within the Lake Victoria basin show distinct differences from the general eastern African MSA (Tryon, 2019). Moreover, Lake Victoria, which is relatively young but estimated to exist by 500-400 kya (Williams, 2019), is the source of the White Nile, and therefore its refugial position could also have interesting implications for dispersals from the region out of the continent (Beyer *et al.*, 2021). Together, this highlights the potential role of

refugia in structuring MSA cultural and biological diversity (Scerri *et al.*, 2018, Scerri, Chikhi and Thomas, 2019), laying the critical foundations for later human evolution, with microhabitat variability in refugial zones likely being a key component in creating resource-rich landscapes (Patalano *et al.*, 2021; Blinkhorn *et al.*, 2022).

Beyond simply characterising MSA environments and ecologies, our use of matrix correlations presents an important means to examine the extent to which climatic features influenced behaviour, here characterised by stone tool assemblage composition. Our multiple matrix regression results demonstrate that precipitation has a significant, independent effect on toolkit composition; further examination of the presences and absences of individual technologies via binary logistic regression shows statistically significant decreases in the probability of backed microliths, borers, centripetal technology, platform cores, and scrapers occurring in assemblages as precipitation levels increase, after controlling for all other variables in the analysis (see Appendix 1: Supplementary Methods S4). Some of these tool types have been found to be significant indicators of either Later Stone Age (backed pieces) or MSA (scrapers) toolkits (Grove and Blinkhorn, 2020, 2021), perhaps linking changes in precipitation to the development of the LSA. Roughness also has a significant impact on toolkit composition, with further analyses demonstrating that the probability of backed microliths and points, both components of projectile technology associated with hunting of grassland species in flatter landscapes (Brooks *et al.*, 2006) as well as Levallois blades and flakes decreases as the energetic demands of the environment increase. Further analysis of the site type variable demonstrates that it has significant effects on the probability of backed microliths, bipolar technology, and Levallois flakes appearing in assemblages, with all these technologies occurring more frequently in cave or rock shelter sites. Finally, there are numerous independent effects of the use of particular raw materials on the presence of individual technologies in the assemblages, as summarised in Appendix 1: Supplementary Methods S4 Table S1. Whilst precipitation has a close to significant effect on raw material use, independent explanations of variability are presented by cost path, roughness, simple age and toolkit composition. This constellation of geographic variables suggests a complex combination of spatial autocorrelation, likely grounded in the uneven availability of raw materials across eastern Africa as well as their accessibility in different landscape settings, such as mountains. Overall, these results demonstrate a complex interaction between the environment and MSA behaviour, with the energetic requirements of the physical landscape and local precipitation regimes likely requiring different constellations of tools from the MSA toolkit.

#### 4.5. Conclusion

The MSA record of eastern Africa is fundamental for the exploration of ideas surrounding the role of climate change and the environment in recent human evolution and dispersals within and beyond the continent. Our application of high-resolution paleoenvironmental reconstructions has enabled a previously impossible characterisation of the ecosystems inhabited by early human populations at this scale, with existing site-based paleoenvironmental reconstructions being very useful but difficult to integrate and translate into a comprehensive framework for the region. Whilst the application of high-resolution climatic simulations to archaeological data is inherently limited by the uncertainty surrounding radiometric dates – indeed, future work should focus on developing methods that address the effects of dating error on conclusions derived from climatic models (see Will *et al.*, 2021) – our results are important for demonstrating the environmental conditions inhabited throughout the eastern African MSA, with levels of diversity far beyond that typically assumed by classic habitat-specific hypotheses for human evolution (Dart, 1925, 1953; Rayner, Moon and Masters, 1993; Washburn, 1960). By establishing the role of shifting environmental conditions and ecological boundaries on the distribution and variability of dated MSA assemblages, our work also helps illuminate some of the processes that shaped behavioural diversity during this key period, such as that MSA toolkits likely facilitated expansions into diverse environments, adding further complexity to within-region migration than environment tracking (Mirazón Lahr and Foley, 1998). Understanding this complex interaction between population dynamics, dispersals, cultural evolution and the environment is also key to moving beyond simplistic single-origin models in favour of more complex reticulate models for recent human evolution (Scerri *et al.*, 2018, Scerri, Chikhi and Thomas, 2019).



# Chapter 5: Modelling suitable habitats for eastern African Middle Stone Age populations

## 5.1. Introduction

Eastern Africa has a distinctive geography, hydrology, geology, and environment compared to the rest of the African continent. Particularly, the Eastern African Rift Valley System (EARS), and the lakes and rivers it preserves, provide a unique landscape in which hominins likely thrived (Trauth et al., 2010; Maslin et al., 2014). These traits, together with its rich Stone Age archaeological and fossil record, means it has important evolutionary implications for the evolution of early modern human behaviour and morphology, as well as for intra and extra-African dispersals (King and Bailey, 2006; Basell, 2008; Trauth et al., 2010; Cuthbert et al., 2017; Blinkhorn and Grove, 2018, 2021; Timbrell et al., 2022). Additionally, some of the earliest *H. sapiens* fossils are found in the region (McDougall, Brown and Fleagle, 2005; Vidal *et al.*, 2022), as well as some of the first examples of Middle Stone Age (MSA) archaeology (Potts *et al.*, 2020), believed to represent a major shift in behaviour corresponding broadly with the emergence of the *H. sapiens* lineage (Scerri and Will, 2023).

Chapter 4 revealed that ecological conditions at eastern African MSA sites were varied through time and space, yet one cannot assume that all areas of the region were equally desirable, suitable, or accessible for human habitation. Basic habitability models were constructed in the previous chapter, though these were focussed around interglacial/glacial cycles, which may not be the most informative for mapping changes in the extent of hominin-suitable habitats. Moreover, various studies have concentrated on understanding which factors condition the spatiotemporal distribution of Late and Middle Pleistocene archaeological sites (King and Bailey, 2006; Basell, 2008; Trauth *et al.*, 2010; Cuthbert *et al.*, 2017; Blinkhorn and Grove, 2018, 2021; Timbrell *et al.*, 2022); however, these have tended to focus on the individual aspects of the physical environment rather than incorporating these into a comprehensive model of habitation. Basell (2008) provides the most comprehensive investigation into the different factors influencing eastern African MSA site locations, though novel data and methods present ways to build upon this contribution. Here I utilise species distribution modelling (SDM) in conjunction with Geographic Information Systems (GIS) approaches to model and predict the extent of suitable landscapes across eastern Africa during the Late-Middle Pleistocene. The model is then independently validated with the eastern African MSA archaeological record.

### 5.1.1. Species distribution modelling and ecological niche theory

Species distribution models (SDM) are popular tools within ecology to quantify and predict the relationship between biodiversity and the environment, often referred to as a species ecological niche. As input data, SDM requires species' presences (i.e., the location of where an individual/population is living at a given point in time) as the dependent variable and geographic layers of environmental predictors (such as climate, net primary productivity etc.) as the independent variables. Data from the predictor variables is then extracted from the site presences and can be used in a variety of statistical and/or machine learning algorithms to predict the relationship between a species distribution and an environmental space that consists of various abiotic and biotic factors that can influence habitability (Holt, 2009). Once this relationship is established, estimations of the species geographic range can be made throughout space and time by projecting the model via interpolation (limiting mapping to the sampling area and period) or extrapolation (extending mapping beyond the sampling area and or period). It is worth noting that, within the literature, SDM can stand for both 'species distribution modelling' and 'species distribution model'; the former refers to the process and the latter refers to the output, and I refer to both as SDM in this thesis.

More than 50 years ago, Hutchinson (1957) in a seminal essay distinguished between the 'fundamental niche' and the 'realised niche'; the former represents all the abiotic environmental conditions where the species can survive indefinitely, whereas the latter is the subset of the former where the species can survive despite the presence of competitors. In these original conceptions, Hutchinson (1957) suggested that if an area has conditions that fall within a species niche, a population should persist and experience growth, whereas if conditions fall outside of the niche, it faces extinction without migration (Vrba, 1992). Since then, further work has nuanced ecological niche theory; for example, facilitation (positive interspecific interactions; Bruno, Stachowicz and Bertness, 2003) and dispersal capacity (Soberon, 2007) have been suggested to play important roles in determining whether a species is indeed present in all areas identified as potential suitable habitats. Yet recent syntheses have concluded that contemporary ecological theory and methodology cannot be reconciled with Hutchinsonian niche concepts (McInerney and Etienne, 2012). This is because it is unclear whether the estimated species-environment relationship produced by an SDM approximates the fundamental niche, the realised niche, or the occupied niche (i.e., the geographic area that is actually occupied by the species), and if indeed these distinctions are useful in the context of SDM, which are methodologically varied (Araujo and Guisan, 2006; McInerney and Etienne, 2012). Araujo and Guisan (2006) propose that a clearer distinction is needed between niche models based

on environmental factors only, which yield predictions of potential habitats, and models based on niche and spatially explicit factors combined, which project potential geographic distributions of species.

### 5.1.2. Applying species distribution modelling to archaeological data

Even though until relatively recently the methodology had only seen limited application within archaeological and anthropological sciences, there are a number of features of SDM that make them suitable for studying prehistoric animal-environment interactions. Firstly, SDM can be performed using sparse observation data, so long as there is an adequate sample size. Moreover, many SDM methods rely on ‘presence-only’ data – they do not necessarily require input regarding where a species is absent. Because archaeological data is often opportunistic and exhibits spatial sampling biases due to variation in taphonomic preservation and research intensity, the absence of data does not necessarily equate to the absence of humans. Many of these presence-only methods, such as MaxENT and Random Forests, use background data or pseudo-absence data instead of the true absences used by methods like generalised linear models. These presence-only methods randomly sample background or pseudo-absences from the study area (Phillips and Dudik, 2008; Gomes *et al.*, 2018), however Phillips *et al.* (2009) note that when spatial biases occur, the difference between the randomly sampled background and the biased occurrence data can lead to inaccurate models and thus requires careful consideration in prehistoric contexts. Moreover, envelope-based presence-only SDM methods, such as BIOCLIM (Nix, 1986; Booth *et al.*, 2014) which map the species range across multiple dimensions, often treat habitability as a binary classification, thus oversimplifying ecological reality as environmental suitability can vary even within an environmental envelope. Thus, whilst archaeological research can benefit from SDM, careful consideration is required as to the limitations of individual methodologies.

Previous studies have successfully used SDM methods in a variety of archaeological contexts. For example, both human (Burke *et al.*, 2017) and faunal (Banks *et al.*, 2008) distributions have been modelled for the LGM to determine whether the climatic niche changed over time. Burke *et al.*, (2017) use an iterative series of random forests to identify the climatic variables that predict site presences and mapped the resulting models across Western Europe during the LGM. These were then subsequently applied by Wren and Burke (2019) in the production of an agent-based model of human mobility and interaction. However, Frankin *et al.* (2015) draw attention to the fact that distribution models used for hindcasting should always be checked against independent evidence when possible, such as with archaeological or phylogenetic data not used in the initial model fitting. A good example of this is Blinkhorn *et al.* (2022), who produced a SDM to map Late Pleistocene African precipitation refugia using

ethnographic data. The models, which mapped both ‘broad’ and ‘narrow’ refugia using 95% and 68% confidence intervals respectively, were then independently validated with the eastern African MSA and LSA archaeological records; 79% of sites were located within the narrow refugia and a further 18% were located beyond the narrow refugia but within the range of the broad refugia, suggesting that modern hunter-gatherers were a useful analogue in this context.

Blinkhorn *et al.*'s (2022) Late Pleistocene refugia models, whilst demonstrating a good coherence with site presences, determined habitability through a binary system – habitable or uninhabitable. This approach was also taken in the production of models by Beyer *et al.* (2021) who also used precipitation thresholds from ethnographic data to predict potential routes out of Africa. In Chapter 4, basic habitability models were constructed for each MIS using mean annual temperature and precipitation at eastern African MSA sites. Binary models were produced based on the climatic envelope of eastern African MSA occupations, but the models were not validated against independent evidence and the spatial distribution of the input data was heavily skewed towards the regions of eastern Africa that have seen intensive research history, i.e., the Central EARS, which perhaps unsurprisingly remains habitable throughout the Late-Middle Pleistocene. A methodology that can be independently validated using archaeological data and is not based on spatially biased input data, like Blinkhorn *et al.* (2022), but which also produces contours of suitability rather than a simple threshold method would add nuance to these previous Late-Middle Pleistocene models.

### 5.1.3. Additional factors that can condition habitability

Although the climate system is a key parameter in modifying local habitats and resource distributions, a range of other geographic variables contribute to making an area suitable for habitation, and thus can be used to predict the geographic extent of a species (Araujo and Guisan, 2006). Water, for example, is a fundamental resource for survival for all animals, and therefore access to water sources is considered important for mediating how humans interacted with the landscape (Potts, 1998, 2012). Recent ground water refugia modelling has suggested that even in the most extreme dry phases, movement within specific regions of the EARS, such as around Lake Turkana, would have been possible, but limited to between spring networks and along major rivers (Cuthbert *et al.*, 2017; Fig. 8a). Interestingly, under climatic conditions comparable to today (Fig. 8b), mobility was found to occur transverse to the rift axis rather than along it, in contrast to other work (Trauth *et al.*, 2010; Strait and Wood, 1999). Under the wettest scenario (Fig. 8c), dispersal potential was found to be widespread, suggesting potential occupation of much of the landscape. Overall, Cuthbert *et al.* (2017) argue that persistent ground-water would have

buffered against climatic flux in eastern Africa, enabling occupation of regions otherwise too dry based solely on precipitation.

High-altitude landscapes have also been highlighted as potentially important habitats during periods of climatic stress, as these areas tend to be cooler than lower elevations, with increased levels of humidity, such as that seen at MSA sites Fincha Habera and Mochena Borago in the Ethiopia Rift (Ossendorf *et al.*, 2019; Brandt *et al.*, 2017) and Melikane Rocksele in the Lesotho Highlands (Pazan, Dewar and Stewart, 2022). Moreover, topographic complexity, also known as ‘roughness’, in the EARS provides localised conditions optimised for human survival (King and Bailey, 2006; Bailey, Reynold and King, 2011). King and Bailey (2006) argued that the distinctive tectonics of the EARS provided prehistoric populations with a unique geological environment, offering a wide range and abundance of food resources within relatively limited areas, abundant and easily accessible water supplies, and protection from predators. In Chapter 4, I found that the composition of MSA toolkits in eastern Africa were strongly influenced by roughness of the environment, mirroring the initial results of Blinkhorn and Grove (2018, 2021) and suggesting that the occupation of topographically complex landscapes requires a different suite of cultural behaviours than flatter habitats. However, some models of prehistoric landscape-use and mobility, in contrast, assume that regions of variable topography are energetically expensive, with higher relief regions likely being avoided in favour of landscapes bearing fewer and less dramatic slopes (e.g., Gravel-Miguel *et al.* 2021). In response to this conflict, Bailey, Reynold and King (2011) argue that roughness and slope are not necessarily referring to the same aspect of the geomorphology of the landscape, with rough terrain referring to smaller-scale features as opposed to the larger scale slopes that are typically captured in the digital elevation models used in cost-movement analyses. Following Blinkhorn and Grove (2018, 2021), roughness has been coded as the cost of movement over slopes of varying steepness in this thesis. However, whilst small-scale features of the terrain likely correlate with variation in relief, as shown by the relationship between high tectonic activity in the EARS and greater roughness (Bailey, Reynold and King, 2011), further consideration about the effects of topography on early human mobility and settlement patterns may be required in future work (see Chapter 10.3.2).

Overall, producing a model that only considers the climatic impact on MSA site distributions, as seen in Chapter 4, is likely limited to predicting the distribution of potential habitats whereas the inclusion of properties of the physical environment enables the prediction of the geographic distribution of a species (Arajou and Guisan, 2016). This is particularly likely to be the case in an area with complex topography and hydrology, such as the EARS. Additionally, the habitability models in Chapter 4 are still focussed on understanding the changes in suitability between MIS, yet these cycles are not the most dominant driver

of climatic change at lower latitudes, with palaeo-ENSO oscillations of different cyclicity having more fine-grained influence over pan-African climate processes, such as the availability and distribution of vegetation and fauna in eastern Africa (Kaboth-Bahr et al., 2021). Therefore, the development of a habitability model at higher chronological resolution than MIS and incorporating additional geographic variables would be more informative about how MSA populations would have occupied and moved around the landscape, and go far beyond previous models, which only consider glacial/interglacial cycles.

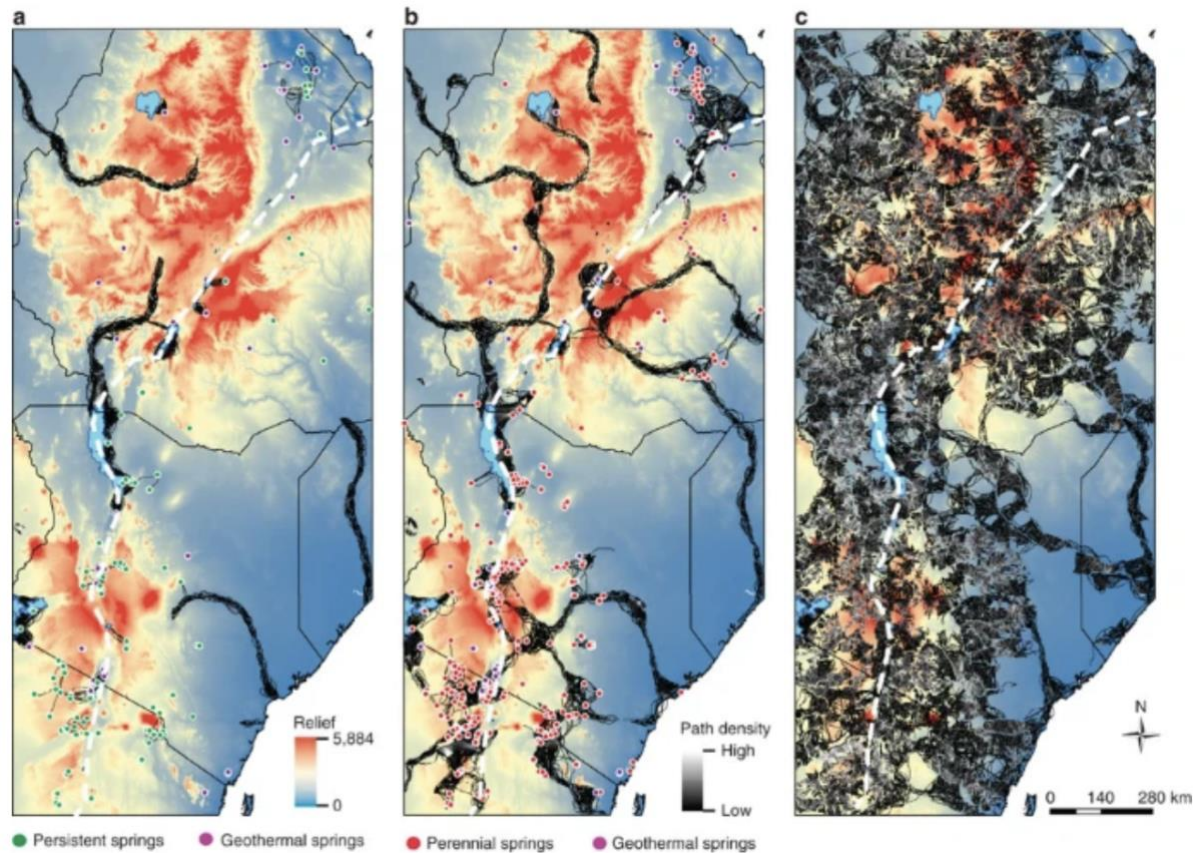


**Figure 8.** Ground-water refugia modelling in extreme dry (a) to extreme wet (c) climatic scenarios during a precessional cycle are modelled and the dispersal of hominins between hydro-refugia is predicted via agent-based modelling (black lines). Reprinted from Cuthbert *et al.* (2017).

## 5.2. Materials

To produce a comprehensive habitability model for the Late-Middle Pleistocene, I used the following parameters to assess how appropriate an area is for human occupation: climate suitability, sea level, cost of movement across uneven slopes, and proximity to water.

Following Blinkhorn *et al.* (2022) and Beyer *et al.* (2021), I used the Binford (2001) ethnographic dataset as the input data of species occurrences for the SDM. This dataset demonstrates that hunter-gatherer mobility patterns are influenced by environmental variables (Binford, 2001); however, to constrain the selection so that it is more likely to be representative of the mobility patterns of Late Pleistocene hunter-gatherers, I only used data for the hunter-gatherer groups that are fully mobile ( $n = 175$ ). To produce the climate suitability maps, I applied the climate emulator of Krapp *et al.* (2021), described in Chapter 4, extracting mean annual temperature (bio01) and precipitation (bio12). The data for predicting sea-level is similarly detailed in Chapter 4 – a sea-level change stack (Spratt and Lisiecki, 2016) and a global bathymetry model at 15 arc-second intervals (GEBCO, 2020). The bathymetry model was also used to calculate the cost of movement over complex topography. For water availability, I used the extent of modern major rivers, perennial streams, and large water bodies (Natural Earth, 2020) in ArcGIS Pro (Esri Inc., 2020), as Cuthbert *et al.* (2017)'s agent-based modelling of ground-water refugia suggests that hominin movement primarily occurred along the major rivers and between perennial spring networks, though this varied between models (Fig. 8).

Whilst the climate data is time specific, with reconstructions for every 1,000-year intervals, modern topographic and hydrological datasets were used in the model as static parameters. Using modern conditions to represent those of the Pleistocene is not without its limitations; however, it can be justified given the following considerations. Firstly, modelling tectonic change in the region is particularly difficult, but it is reasonable to assume that the cost of movement across the landscape has not changed dramatically even if the underlying topography may have changed slightly (i.e., if the Rift Valley has risen by 2mm it is still going to be a relatively higher cost than flatter areas). Bailey, Reynolds and King (2011) indicate that the more active areas of the EARS have changed through time, but overall, the EARS is unusually dormant by global standards in terms of volcanic activity.

Like topography, modelling water features over time remains challenging; however, the distribution of water networks is predominantly mediated by the roughness of the landscape. Given that tectonic and volcanic activity has been limited in eastern Africa since the Pleistocene, the geographic positioning of major regional rivers has remained fairly stable throughout climatic cycles (Joordens *et al.*, 2011). The extent of larger water bodies, such as lakes, has varied through time, as shown by Trauth *et al.* (2010), however the difficulty of predicting evaporation rates makes incorporating this parameter into the model impractical at this stage. Modern major rivers, perennial streams and large lakes, following Figure 8b by Cuthbert *et al.* (2017), act as an effective mid-point between the arid-humid extremes of a precessional cycle. Present conditions in the EARS have been found to be broadly analogous to relatively dry (though

not extreme) periods throughout the Pleistocene (Döll and Fiedler, 2008), therefore the use of the modern distribution of surface water could even be considered a conservative estimate of the availability of water. However, one limitation of the use of modern water bodies is that many lakes and streams, particularly in the eastern section of the EARS, are alkaline and/or saline, with only 8 out of 34 bearing fresh water (Cuthbert *et al.*, 2017). However, some of these currently non-potable lakes, such as Lake Turkana, support fresh-water fish populations, and often freshwater springs can be found within the immediate lake catchment (Cuthbert *et al.*, 2016), supporting their inclusion in the model as habitable zones.

### 5.3. Methods

#### 5.3.1. Climate suitability

Following Beyer *et al.* (2021) and Blinkhorn *et al.* (2022), I applied the Binford (2001) dataset using the ‘binford’ R package (Marwick *et al.*, 2016). I implemented a distribution-based contouring approach using a non-parametric probability density function which provides much more detail regarding the relative suitability of an area for human habitation. Unlike Beyer *et al.* (2021) and Blinkhorn *et al.* (2022) who employed precipitation thresholds, I also included mean annual temperature due to the combined impact on the primary productivity of an ecosystem and the biome-type experienced on the ground (e.g., Whittaker, 1975). Although precipitation, and not temperature, was found to have a significant impact on MSA material cultural in Chapter 4, modelling studies have shown that both precipitation and temperature variables can influence aspects of hunter-gatherer behaviour more relevant to dispersal and habitation, such as mobility (Kelly, 1993; Grove, 2009). The inclusion of temperature in the modelling therefore marks a step beyond current models of habitability that have applied the novel climate emulator (e.g., Beyer *et al.*, 2021; Blinkhorn *et al.*, 2022).

I used kernel density estimation (KDE) to produce a smooth curve of the distribution of temperature (‘cmat’) and precipitation (‘bio12’) values inhabited by fully mobile hunter-gatherers, extracted using the ‘binford’ R package (Marwick *et al.*, 2016). The values were used to predict the probability of each raster cell of falling within the sample range. The probability density function was calculated using the ‘kdensity’ R package (Moss and Tveten, 2020) under the assumption that whilst it cannot be too wet, it can be too hot. This means that values above a threshold precipitation value (calculated as 333mm from the kernel fits using the ‘findpeaks’ function in the ‘pracma’ R package [Borchers, 2022]) are deemed habitable regardless of how far above the threshold they are. Archaeological evidence from Lupemban and Sangoan assemblages, proposed to represent Pleistocene tropical rainforest adaptations (Taylor,



2022), show that occupation of extreme humid zones occurred in Africa during the Late-Middle Pleistocene, despite historical ideas that such environments lack suitable resources to sustain foraging populations (Mercader, 2002). Tropical forest occupation during the Late Pleistocene is also supported by recent modelling studies within Central Africa (Padilla-Iglesias *et al.*, 2021). The threshold value from the kernel density fits corresponds almost exactly to the lower precipitation bracket for eastern African MSA occupations calculated in Chapter 4 (around 336mm), supporting it as key for marking the environments that can sustain early human populations. Whilst it is also true that, at the other end of the spectrum, extremely arid environments were occupied during the Late-Middle Pleistocene, as demonstrated by Aterian populations inhabiting northern Africa (Scerri, 2013a,b), expansions into such areas were modulated by the amelioration of climatic conditions and the availability of freshwater (Drake *et al.*, 2011; Scerri *et al.*, 2014), both of which are accounted for later in the modelling.

KDE uses the equation:

$$f_{presence}(x) = \frac{1}{n} \sum_{i=1}^n \frac{1}{h_x} K\left(\frac{x - x_i}{h_x}\right) \quad [5.1]$$

where  $f_{presence}(x)$  represents the estimated probability density function of species presence with respect to the environmental factor  $x$ ,  $x_i$  is the value of  $x$  at presence location  $i$ , and  $n$  is the total number of presences (following Zhang *et al.*, 2018).  $K$  is the kernel density function, within which a Gaussian kernel was adopted (Silverman, 1986):

$$K\left(\frac{x - x_i}{h_x}\right) = \frac{1}{\sqrt{2\pi}} e^{-\frac{(x-x_i)^2}{2h_x^2}} \quad [5.2]$$

$h_x$  is the bandwidth, which is a smoothing parameter for  $x$  (the environmental factors). The bandwidth is directly equivalent to the standard deviation of the normal distribution, so the higher the bandwidth, the more smoothing is applied. I used the optimal bandwidth automatically selected in the function, which minimises noise which capturing variability.

When compared to other methods, KDE imposes no assumptions about the nature of the species-environment relationships as it is a non-parametric method. In addition, SDMs produced using KDE have been found to produce a prediction accuracy comparable to MaxENT, whilst providing clear ecological interpretations as it is model free (Zhang *et al.*, 2018). Unlike MaxENT, which utilises background samples, KDE is a true presence-only method that is more reliable when using spatially biased input data.

KDE has the added advantage that variability in climate suitability can be mapped using contours as it is distribution-based rather than reliant on a binary classification. Habitability (calculated as the multiplied precipitation and temperature probability values) was scaled to be between 0 and 1 (with 1 as the most suitable and 0 as the most unsuitable) and mapped at 0.1 increments across space and time throughout the Late-Middle Pleistocene using the climate emulator of Krapp *et al.* (2021).

### 5.3.2. Topography and energetic cost of movement

Using the cropped raster bathymetry layers created in Chapter 4 to model sea-level change, I calculated the energy required to transverse complex topography. Although topographic roughness at small-scales can provide a wide range of resources, extremely steep environments are energetically expensive habitats for foragers to travel across, and therefore were likely circumnavigated in favour of more flat routes. I used the formula presented by Minetti *et al.* (2002) to produce a series of rasters representing the energy consumption (in joules) required for traversing different slopes ( $x$ ) encountered at every 1km. This equation measures the cost of walking ( $cw$ ).

$$cw = (280.5x^5 - 58.7x^4 - 76.8x^3 + 51.9x^2 + 19.6x + 2.5) \quad [5.3]$$

The equation calculates the minimum cost of walking 1km at a slope of -10% (downhill), with increases in cost at both more negative and more positive gradients. For each time slice, a cost of movement raster layer was produced, which were cropped using the predicted sea-level and projected to the same spatial extent as the climate suitability maps.

### 5.3.3. Access to water

Access to water was next considered in the model. Geographic data on the modern distribution of major rivers, perennial streams and large rivers were accessed from Natural Earth (2020) and uploaded in ArcGIS (Esri Inc., 2020). Costed buffers were calculated around the hydrological network based on the time taken to travel to the water source. Similar to Gravel-Miguel *et al.* (2021), who created an agent-based model of habitability during the ESA and MSA, I applied the assumption that, humans require water daily, and therefore a 12-hour round-trip (6 hours there and 6 hours back) would represent the maximum amount of travel time available for accessing water. This is presuming that travel would only be undertaken during day-light hours. Costs in the buffers were therefore weighted based on the amount of time ( $t$ ) taken to travel to the water source, using the reciprocal of Tobler's Hiking Function (Tobler,

1993), an equation that accounts for the anisotropic and non-linear nature of the cost of movement over heterogeneous landscapes (slope,  $x$ ).

$$t = 1/(6e^{-3.5|x+0.05|})$$

[5.4]

Buffers were calculated so that they increase in cost for each hour taken to travel to a water source, with a cost of 1 at 6 hours or more away from a river and lake, and a cost of 0 at the water source (0 hours).

#### 5.3.4. Aggregation of factors into a habitability index

I aggregated the climate suitability maps, energetic cost of movement maps and water buffers to create a comprehensive and spatiotemporally explicit habitability index of Late-Middle Pleistocene eastern Africa (Fig. 9). Proximity to water networks and bodies is intimately linked to climate suitability in that both play a vital role in providing drinking water and access to food resources, as water attracts fauna and local climates provide the necessary growing conditions for flora. Therefore, to merge the climate suitability raster layers with the water buffer raster to create a single ecological index, I scaled the water buffer raster to between 0 and 1 (with 1 being furthest away from water and 0 being closest to water) and then took the lowest value of the climate suitability rasters and the water buffer raster for each time slice. This assumes that a) an area would be inhabitable if a water source was nearby, no matter the surrounding climatic conditions (Cuthbert *et al.*, 2017), and b) that areas of the landscape would have been inhabitable despite not being close to water sources when exhibiting optimal precipitation and temperature values, as this would imply the presence of an ecosystem with precipitation levels sufficient for sustaining occupation (Basell, 2008). This calculation considers that different parameters likely became important under different circumstances. For example, during particularly arid periods, access to water becomes more salient than when experiencing more favourable conditions (following Cuthbert *et al.*, 2017). Topography was then incorporated into the model by scaling the cost of movement rasters to between 0 and 1 (with 0 being very steep areas and 1 being very flat areas), ensuring that extreme topography is unfavourable when compared to flatter landscapes. The cost of movement rasters were then combined equally with the ecological rasters to produce the final comprehensive habitability model. A summary of the modelling process is captured in Figure 9.

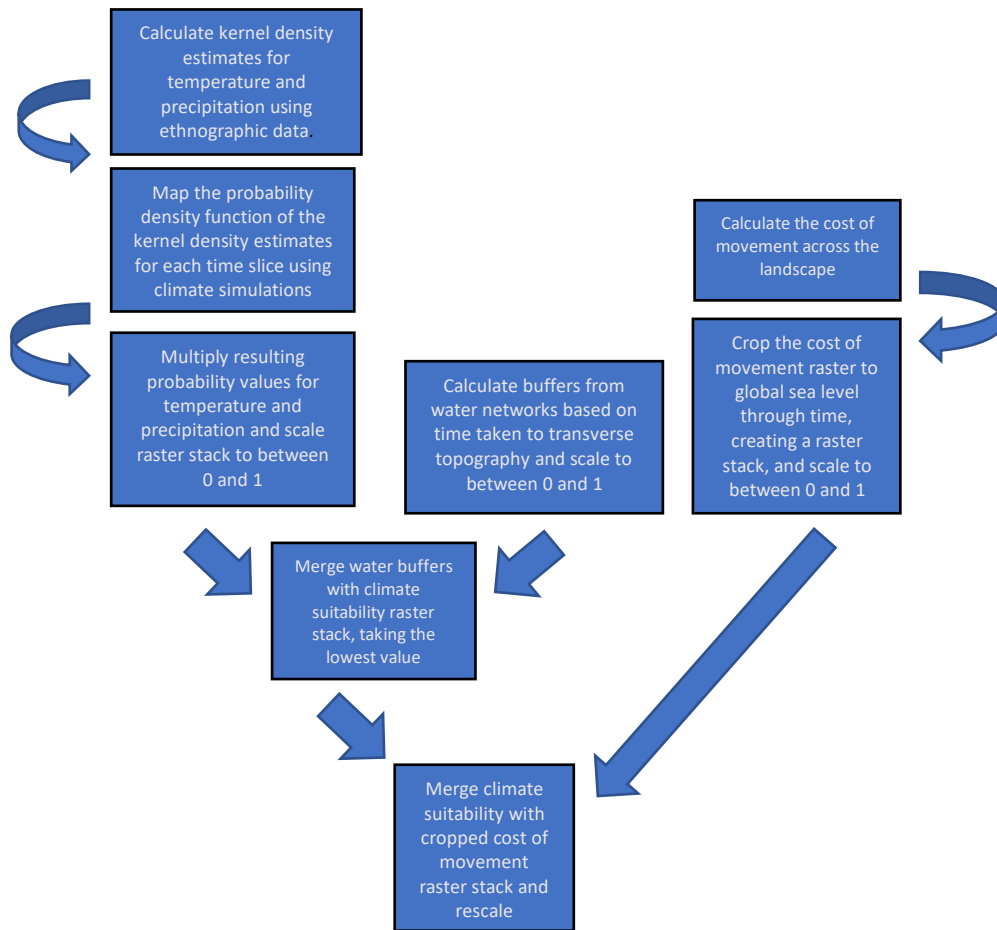


**Figure 9.** A schematic flow chart summarising the habitability modelling process, including climate suitability, access to water and energetic cost of movement parameters.

### 5.3.5. Model validation

To test the model with independent data, I used the eastern African MSA record (Blinkhorn and Grove, 2021), following Blinkhorn *et al.* (2022). Table 8 reports the mid-ages and dating error of each occupation ( $n = 84$ ). Model validation was performed in two steps: 1) testing of the climate-based SDM and 2) testing of the comprehensive habitability model. For each test, I extracted the model values at the sites in the dataset at the mid-age timeslice (Blinkhorn and Grove, 2018, 2021) and then compared them to random samples of habitability values from the model, performing 1000 permutations of the 84 dated occupations. I then compared the distributions of the random samples with the habitability values inhabited by Middle to Late Pleistocene populations. If the habitability model is better at explaining site

distribution than random, then it is expected that the central tendency will be higher than all of the permuted samples. Moreover, because the background distributions are all randomly generated, it is hypothesised that their dispersion should also be greater than that of the MSA sites.

**Table 8.** Date ranges for the 84 eastern African MSA occupations reported in Blinkhorn and Grove (2021). The occupations were anchored at their mid-age: the 1,000-year (kya) mid-point between the minimum and maximum age of the date range.

| Assemblage                 | Minimum age (kya) | Maximum age (kya) | Mid-age (kya) |
|----------------------------|-------------------|-------------------|---------------|
| Goda Buticha_Complex2_DEF  | 22                | 70                | 46            |
| Mumba_L_III_38             | 33                | 40                | 37            |
| Mumba_L_V_81               | 52                | 61                | 57            |
| Mumba_L_VI_38              | 52                | 61                | 57            |
| Mumba_L_VI_A               | 86                | 115               | 101           |
| Mumba_MU_V_81              | 47                | 55                | 51            |
| Mumba_U_V_38               | 44                | 53                | 49            |
| Mumba_U_VI_A               | 57                | 69                | 63            |
| Mumba_VI_B                 | 86                | 153               | 120           |
| Panga_ya_Saidi_17          | 65                | 80                | 73            |
| Panga_ya_Saidi_18          | 67                | 86                | 77            |
| Panga_ya_Saidi_19          | 67                | 86                | 77            |
| Enkapune_ya_Muto_RBL4      | 43                | 45                | 45            |
| Fincha Habera 8_10         | 27                | 34                | 31            |
| Fincha Habera 8_11         | 27                | 34                | 31            |
| Fincha Habera 8_8          | 27                | 34                | 31            |
| Fincha Habera 8_9          | 27                | 34                | 31            |
| Fincha Habera 9            | 33                | 42                | 38            |
| Kiese II_18                | 38                | 39                | 39            |
| Kiese II_19                | 31                | 46                | 39            |
| Kiese II_20                | 42                | 45                | 44            |
| Kiese II_21                | 43                | 46                | 45            |
| LaasGeel_SU_711            | 40                | 42                | 42            |
| LukenyaHillGvJm22_F170_205 | 25                | 32                | 29            |
| Magubike_MSA               | 35                | 48                | 42            |

|                          |     |     |     |
|--------------------------|-----|-----|-----|
| MochenaBorago_LowerT     | 49  | 50  | 50  |
| MochenaBorago_RGroup     | 36  | 43  | 40  |
| MochenaBorago_SGroup     | 43  | 46  | 45  |
| MochenaBorago_UpperT     | 45  | 49  | 48  |
| Nasera_12_17             | 53  | 58  | 56  |
| Nasera_6_7               | 50  | 58  | 54  |
| Nasera_8/9_11            | 50  | 58  | 54  |
| Shurmai_MSA              | 39  | 50  | 45  |
| Abdur_N_C_S              | 118 | 132 | 125 |
| AdumaA1                  | 80  | 100 | 90  |
| AdumaA4C                 | 80  | 100 | 90  |
| AdumaA5Ex                | 80  | 100 | 90  |
| AdumaA5ExSurf            | 80  | 100 | 90  |
| AdumaA8                  | 80  | 100 | 90  |
| AdumaA8AC                | 80  | 100 | 90  |
| AdumaA8AG                | 80  | 100 | 90  |
| AdumaA8ASurf             | 80  | 100 | 90  |
| AdumaA8B                 | 80  | 100 | 90  |
| EyasiShore_77_81         | 91  | 132 | 112 |
| EyasiShore_W_insitu      | 91  | 132 | 112 |
| Gademotta_ETH72_1        | 172 | 274 | 223 |
| Gademotta_ETH72_6        | 172 | 274 | 223 |
| KapForm_KoimilotGnJh74_1 | 198 | 237 | 218 |
| KapForm_KoimilotGnJh74_2 | 198 | 237 | 218 |
| KapForm_SSRS             | 198 | 237 | 218 |
| Karungu_A3Ex             | 42  | 115 | 79  |
| LukenyaHill_GvJm46       | 21  | 27  | 24  |
| Marmonet Drift_H2        | 89  | 205 | 147 |
| Marmonet Drift_H4        | 90  | 130 | 110 |
| Marmonet Drift_H5        | 90  | 98  | 94  |
| Marmonet Drift_I_bottom  | 205 | 257 | 231 |
| Ologesailie_BOK1E        | 295 | 320 | 308 |
| Ologesailie_BOK2         | 295 | 320 | 308 |

|                      |     |     |     |
|----------------------|-----|-----|-----|
| Olorgesailie_BOK3    | 295 | 320 | 308 |
| Olorgesailie_BOK4    | 288 | 301 | 295 |
| Omo_AHS1-5           | 193 | 201 | 197 |
| Omo_AHS6_8           | 193 | 201 | 197 |
| Omo_BNS_L3           | 96  | 111 | 104 |
| Omo_KHS2/3           | 193 | 201 | 197 |
| VictoriaCabera_2     | 70  | 91  | 81  |
| VictoriaCabera_2a    | 70  | 91  | 81  |
| VictoriaCabera_3     | 70  | 91  | 81  |
| VictoriaCabera_4     | 79  | 91  | 86  |
| AdumaVP1/1           | 80  | 100 | 90  |
| AdumaVP1/3           | 80  | 100 | 90  |
| EyasiShore_N_surface | 91  | 132 | 112 |
| EyasiShore_W_surf    | 91  | 132 | 112 |
| KapedoTuffs          | 120 | 135 | 128 |
| Karungu_Kisaaka_Main | 42  | 56  | 49  |
| Karungu_Kisaaka_ZTG  | 42  | 115 | 79  |
| MalewaGorge          | 240 | 240 | 240 |
| Ndutu_14             | 220 | 240 | 230 |
| Ndutu_72             | 220 | 240 | 230 |
| Omo_AHSsurface       | 193 | 201 | 197 |
| Omo_BNS<50m          | 96  | 111 | 104 |
| Omo_KHSNgully        | 193 | 201 | 197 |
| Omo_KHSNMKenya       | 193 | 201 | 197 |
| Omo_KHSSgully        | 193 | 201 | 197 |
| Rusinga_Nyamita      | 42  | 56  | 49  |

#### 5.4. Results

An animation of the final habitability model can be found at:

<https://docs.google.com/document/d/1sQB79NJwb1tdGvQtx53wQ4YCO67k-px/edit?usp=sharing&oid=103900458115874885604&rtpof=true&sd=true>

### 5.4.1. Habitability model

The resulting habitability model (Fig. 10) highlights the regions that would have been most suitable for human habitation (1) and the areas least suitable for human habitation (0). Throughout the model, the areas in immediate proximity to eastern Africa's extensive water network is the most favourable, though this is a static component of the model. This means that the general Kenyan Eastern African Rift Valley region remains habitable throughout the period due to the spatial distribution of perennial rivers and lakes.

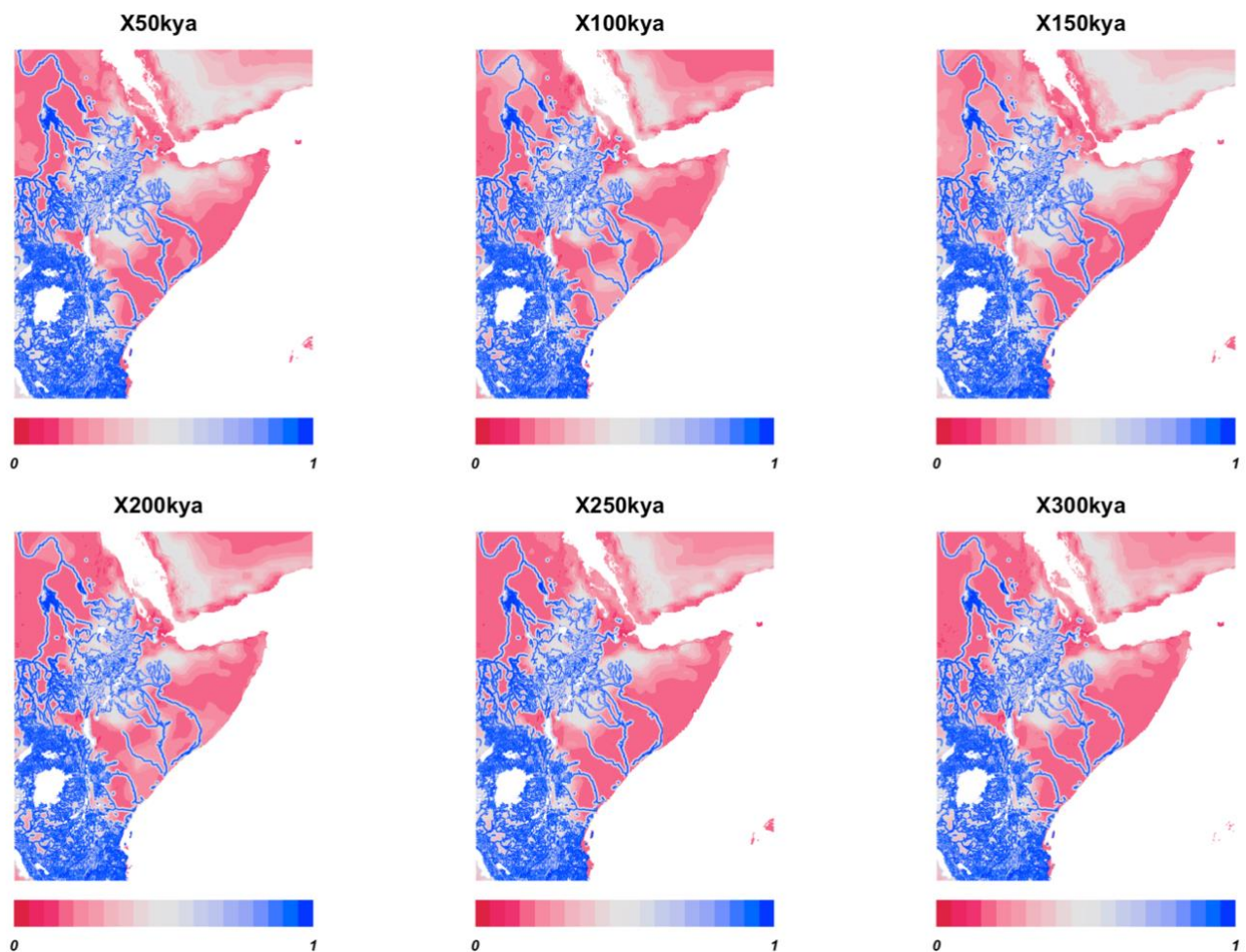


**Figure 10.** Example time-slices extracted from the habitability model at every 50,000 years (kya), between 50-300 kya. Habitable cells fall closer to 1 whereas uninhabitable cells fall closer to 0.



Climate suitability appears to be relatively stable across the Ethiopian Highlands, with the habitable zone often extending into the Horn of Africa, though most predominantly at 150 kya. During this time, there is also a dramatic extension of the suitable area into the interior of the Arabian Peninsula and a lowering of the sea level. However, at 100 kya, the climatically suitable region in Arabia becomes restricted to that along the coast, and sea level rises considerably. In eastern Africa at 100 kya, the habitable region becomes more fragmented, with pockets of more climatically suitable areas away from river networks becoming more disjointed than in other periods. The coast of Kenya and the Sahara remains largely uninhabitable throughout the Late-Middle Pleistocene apart from in areas that are close to river networks.

Around 115-120 kya, the model predicts large pockets of high climate suitability within the region where the White Nile and Blue Nile splits at Khartoum in southern Sudan. Also, between 115-130 kya, there are large highly climatically suitable regions just along the Somali coast between the Jubba, Tana and Shebelle rivers. At around 240-245 kya, smaller pockets of very high climatic suitability form, predominately on the Bab Al Mandeb Strait coastline, around the Somali coast rivers and in the northern most area of the region surrounding the Nile. The region around and to the south of Lake Victoria appears to be the centre of habitability in eastern Africa, primarily due to the dense networks of rivers and consistently high levels of precipitation.

#### 5.4.2. Model validation

I first tested whether the climate suitability maps predict eastern African MSA occupations site locations. The climate suitability values are not normally distributed (Fig. 11) therefore the median and median absolute deviation were used as measures of central tendency and dispersion. The median climate suitability value at eastern African MSA sites (0.46) was higher at eastern African MSA sites than all of the random permutations (Fig. 11). Nonetheless, the median habitability of MSA sites is somewhat low at 0.46, and the distribution of the habitability values (Fig. 11) suggests that there is considerable variability in the climate suitability experience by eastern African MSA populations, with some sites having very low values (lowest = 0.1). Median absolute deviation scores for 839 of the 1000 random samples were found to be greater than that for eastern African MSA occupations, suggesting that even though there is variance in the suitability of the climates experienced, it still tends to be lower than that generated at random.

Given these results, I then tested whether the comprehensive habitability model (climate suitability, access to water and topography) was more reflective of where eastern African MSA occupations are

found than just climate suitability. The median habitability value at eastern African MSA sites (0.90) was considerably higher than all the random permutations (Fig. 12). Moreover, all the random samples had a higher median absolute deviation than the eastern African MSA sites (0.06; Fig. 12). Nonetheless, Figure 12 demonstrates that, although the habitability values are higher than when only climate is considered (Fig. 12), there are several occupations ( $n = 10$ ) that have a relatively low habitability score (i.e., below 0.5). Nonetheless, the fact that the median habitability score doubles when access to water and topography are included as parameters in the model, the median absolute deviation is lower than the random permutations and the number of sites with low habitability decreases significantly compared to the climate-only SDM suggests that this model performs well in terms of adequately describing the types of environments that were most suitable for habitation.

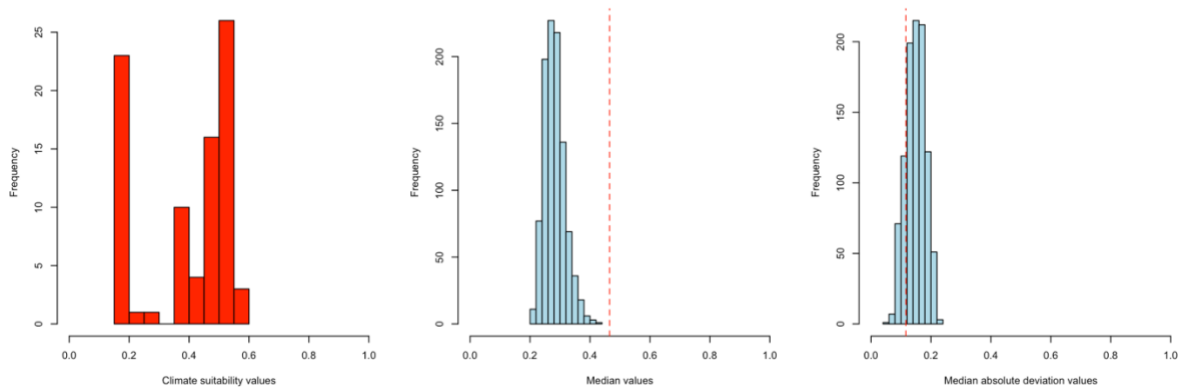


**Figure 11.** Histograms of (left) the climate suitability values at eastern African MSA sites, (middle) the median values and (right) the median absolute deviation values of the randomly permuted samples. The median and median absolute deviation of the eastern African MSA is marked by a red dashed line.

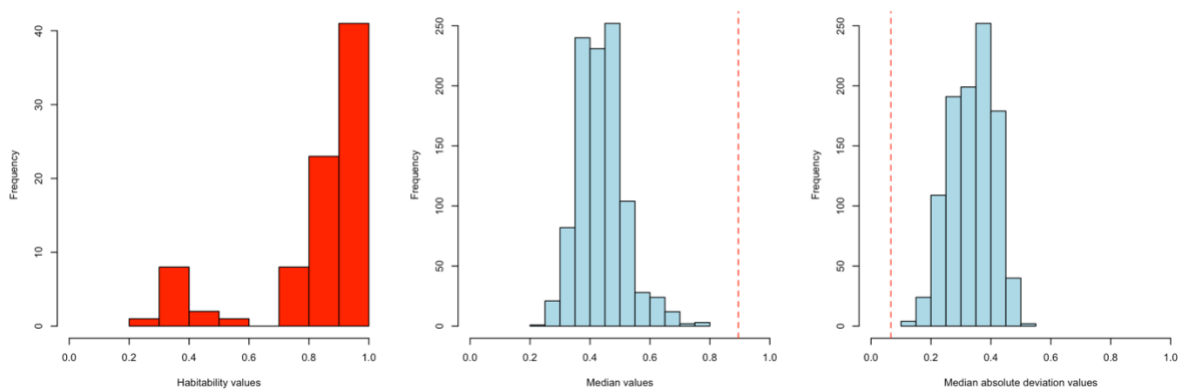


**Figure 12.** Histograms of (left) the habitability values at eastern African MSA sites, (middle) the median values and (right) the median absolute deviation values of the randomly permuted samples. The median and median absolute deviation of the eastern African MSA sites is marked by a red dashed line

## 5.5. Discussion

An archaeologically validated model of habitability was produced, predicting suitable areas across the landscape throughout the eastern African MSA. As in Chapter 4, the region surrounding and to the south of Lake Victoria represents the most consistent habitable zone due to the density of water networks and increased levels of precipitation. Tryon (2019) noted that the archaeological record of Lake Victoria preserved extinct taxa not seen elsewhere in the region, suggesting it as an area of endemism among large-bodied mammals. Indeed, this refugial zone may have had profound implications for hominin demography in the region, potentially acting as a ‘source’ for intra-regional migrations during the eastern African MSA (following the demographic model proposed for the European Middle Palaeolithic by Dennell, Martinon-Torres and Bermudez de Castro [2011]). As highlighted by Scerri and Will (2023), patterns of cultural evolution in the MSA were likely affected by spatially specific and historically contingent ecological, biological, and demographic contexts across Africa; within a refugial region with potential for stable occupation, information transmission between groups may serve as attractors to reach similar adaptive peaks, resulting in homogeneous signals of cultural evolution across the area (Wright, 1982). As suggested in the previous chapter, occupying these consistently habitable areas may not require further adaptation to climatic fluctuations, with extra-refugial populations more likely to develop adaptive technological solutions to different environmental conditions.

Whilst the model was found to be an accurate predictor of MSA site locations, an important observation is that there are also areas of high climate suitability that currently do not yield dated MSA archaeological sites. For example, the region on the border between Kenya and Somalia fluctuates between extremely uninhabitable and very inhabitable. Terminal Pleistocene LSA sites, Buur Hakaba and Rifle Range Site, are found within this region and demonstrate a shifting pattern of occupation intensity, with periods of low resource predictability and abundance as seen during the droughts and famine of today, as well as ephemeral occupation during brief intervals of climatic amelioration (Jones, Brandt and Marshall, 2017). These sites could thus provide a window into how marginal landscapes were occupied during earlier periods. Another region that demonstrates fluctuations in climate suitability is the Sudanese region of the Nile Valley. Interestingly, the Singa cranium – dated to earlier than 133 kya, during what is proposed to be a period of unsuitability – was discovered along the Blue Nile near Khartoum (McDermott *et al.*, 1996). The Singa cranium demonstrates a distinct pathological condition, suggesting that the individual suffered from a blood disorder or anaemia (Spoor, 1998). Whether this can be linked to dietary stress (e.g., from inconsistent consumption of meat), due to climatic deterioration in the region is currently

unclear, though requires consideration in light of this model. Overall, this habitability model has the potential to focus the search for archaeological sites in eastern Africa beyond the well-documented regions, as well as to help refine the probable chronology of occupations with large dating errors through indicating when landscapes were the most suitable for human populations at specific locations.

Climate suitability is found to be relatively low for eastern African MSA sites (0.46). This may reflect the imperfect representation of regional archaeological populations by global ethnographic hunter-gatherers. Nonetheless, the ethnographic sample from Africa alone doesn't provide a sufficient sample size for a valid analysis. Most MSA occupations have been found to occur very close to modern water sources, hence why the mean habitability score increases dramatically when this parameter is included in the model. Nonetheless, modelling the importance of different types of rivers could require further investigation; for example, larger rivers could have acted as a barrier to movement as they are often surrounded by dense canopy forest, and some large water bodies serve as malarial swamps that people may have avoided. Cuthbert *et al.* (2017) found that movement was likely facilitated along perennial streams and rivers in eastern Africa during periods of extreme climatic deterioration, suggesting a potential preference for smaller, fast-moving rivers. Adding such complexity into the model offers an avenue for future research. Increased mobility during times of increased water availability has been argued to be linked to the occupation of wider range of conditions, with an increased focus on ecotones (Basell, 2008). This result was analysed in Chapter 4, where more favourable interglacial phases are associated with higher site numbers and a wider range of environments occupied. Elsewhere in Africa, there is an emphasis placed on water availability for early human survival. In northern Africa, Scerri *et al.* (2014) found that MSA populations were likely structured along water networks during periods of aridity, with similarities between toolkits decreasing with distance (i.e., isolation by distance; Shennan, 2020) except when connected by palaeohydrological corridors. In southern Africa, Ga-Mohana Hill in the southern Kalahari demonstrates distinct Late Pleistocene occupations that have dates which broadly coincide with tufa episodes, acting as evidence for streams, waterfalls and shallow pools in the past (von der Meden *et al.*, 2022). Interestingly, these authors found that by the LGM, water availability alone did not constrain human occupation, which could reflect the point whereby new social and technological adaptations helped hunter-gatherers buffer against the most arid conditions.

Although the model is better at predicting site presences than random, there are some sites that retain low habitability values that need exploring. Potts *et al.* (2018, 2020) found that the ecology of early MSA site Olorgesailie demonstrates high levels of temporal variability, characterised by resource unpredictability and risk with frequent recurrence of short dry intervals. The mid point of the Olorgesailie occupations at

301 kya and 320 kya coincide broadly with the presence of palaeosols, indicating periods of lake desiccation and extreme dryness (Potts *et al.*, 2020). This therefore could highlight a limitation of the framework in Chapter 4, which utilises the mid-age point to anchor the occupations within the model (see Table 8), and the robusticity of dating error and its effect over results of statistical tests will be explored in Chapter 9. The site of Laas Geel in Somaliland was found in Chapter 4 to occupy a uniquely hot and dry environment, a marginal environment and thus explaining its low habitability score here. Whilst this site was found to represent a climatic extreme, the biome analysis in Chapter 4 indicates that the occupation of this area was likely the result of tracking the preferred tropical xerophytic shrubland landscape. Moreover, elsewhere in Africa, additional sites have been found with evidence of an arid climate, such as at the North African site of Uan Tabu between ~60-90 kya (Cremaschi, Di Lernia and Garcea, 1998), leading to the question of whether certain MSA populations may have distinct cultural adaptations for surviving in these landscapes. The MSA site at Abdur, located on the Red Sea Coast of Eritrea, also has a low habitability score; Beyin (2016) suggested that early humans would have settled close to the coast during periods of climatic stress due to surface water availability, therefore, despite the surrounding climate being deemed unsuitable for habitation, the coastal location of this site would likely have buffered against these effects. Mochena Borago, southwestern Ethiopia Rift, Goda Buticha, southeastern Ethiopian Highlands, and Enkapune Ya Muto, Central Rift Valley, are all located at the peak or embedded within steep slopes (Marean, 1992b; Brandt *et al.*, 2017; Tribolo *et al.*, 2017). These sites therefore have a high cost of movement associated with accessing them, which has been coded into the model. This highlights a limitation of the model in that, whilst steep environments are energetically expensive to transverse, they also tend to act as cooler humid refuge when lower lying areas are hot and dry, offering both shelter and a diverse range of resources compressed within a relatively small region, potentially explaining the locations of these sites. Future research should focus on understanding under what circumstances the benefits of mountainous areas outweighs the cost of movement to transverse them.

Overall, SDM and GIS approaches in combination with rigorous quantitative archaeological analyses have huge potential in human evolution research. Such work enables a better understanding of how early humans interacted with the environment and can illuminate how past behavioural changes may have led to the eventual expansion of the hominin niche. Studying technological variability within different types of habitats, as well as ecological refugia, will be critical for exploring how populations successfully adapted and expanded into unfamiliar landscapes, plus the relative contributions of different African regions and habitats to recent human evolution.

## 5.6. Conclusion

Basic habitability models produced in Chapter 4 highlighted the potentially widespread occupation of eastern Africa throughout the Late-Middle Pleistocene. However, these lacked specificity through the binary characterisation of habitability and could not be independently validated against the MSA archaeological record. This chapter builds upon this work to develop a predictive model of past human habitation in relation to multiple geographic and environmental variables. The model was considerably better than random at predicting site presences, with the availability of water and cost of movement dramatically improving the performance of the model. This suggests that the overall suitability of the landscape for habitation, rather than just that provided by climatic conditions, influences the location of MSA sites. Nonetheless, the suitability scores of eastern African MSA sites are varied, with some occupations (primarily in the Central EARS and around Lake Victoria) occurring in areas of stability whilst other potentially occur in marginal landscapes. Understanding the cultural implications of living in such areas requires exploration in further analyses and will be addressed in later chapters.

## Chapter 6: A collaborative model for lithic shape digitization in museum settings

This chapter was published in *Lithic Technology* on the 11<sup>th</sup> of July 2022 (Timbrell, 2022). It is a sole author publication and published under a Gold Open Access agreement.

Abstract:

The COVID-19 pandemic halted scientific research across the world, revealing the vulnerabilities of modern field-based disciplines to disruption. To ensure resilience in the face of future emergencies, archaeological practice needs to be more sustainable with meaningful international collaboration at the forefront. This article presents a collaborative data collection model for capturing lithic morphologies using digital photography and physical measurements taken *in-situ* by international collaborators. Photography and measuring protocols for standardising the data capture are outlined here, and guidelines are provided for data curation, storage and sharing. Adopting collaborative research strategies can have long-term advantages for the field beyond the COVID-19 pandemic, by encouraging knowledge-sharing between international collaborators, decreasing emissions associated with archaeological research, and improving accessibility for those who are not able to travel for access to international samples. This article proposes that archaeology can use the COVID-19 pandemic as a catalyst for change through encouraging deeper collaborations and the development of remote equitable models of science as a complement to in-person research visits.

### 6.1. Introduction

In January 2020, the World Health Organisation declared the SARS-CoV-2 virus that causes COVID-19 to be a global threat to public health. Containment measures intended to reduce the spread of the virus, such as restrictions on travel and social interaction, have since been implemented across the world, and have (perhaps permanently) changed day-to-day life as we once knew it. Field-based sciences have felt these knock-on effects, and major disruptions to research activities slowed the usual rate of progression across multiple disciplines. Postponement and/or cancellation of excavations, overseas research trips and in-person conferences, funding cuts to research, recruitment and training, job insecurity and losses, the livelihoods of global communities within which research is conducted and the increased vulnerability of

cultural heritage to looting have all been affected within archaeological sciences (Douglass, 2020; Ogundiran, 2020).

Globally, we are still a considerable distance from ‘pre-pandemic’ normality, if indeed it is ever returning. Despite many restrictions on day-to-day life easing, the pandemic is still ongoing in spatiotemporally fragmented outbreaks that will continue until vaccination is widespread, and likely even so after (Forni *et al.*, 2021). Strategies that have dealt with the pandemic’s immediate challenges, such as virtual meetings, postponement of fieldwork and funding extensions, whilst useful in the short-term, assume that cheap, fast, and unrestricted travel and in-person interactions will return (Scerri *et al.*, 2020). However, the COVID-19 pandemic has revealed the vulnerability of modern archaeological practice to global catastrophes, in addition to the inequitable power dynamics in the Global South which creates a research environment where foreign principal investigators (PI) control how, when, and where archaeological research will be done, and the extent to which local communities and scholars are involved and are recognised for their role in generating archaeological data (Chirikure, 2015). To be able to cope with future emergencies, such as climate change, conflict and other pandemics, archaeology needs a shift towards more sustainable and resilient research practices through increasing collaboration with in-country researchers, especially across the Global North-South divide (Douglass, 2020; Scerri *et al.*, 2020).

Many scholars, within archaeology (Douglass, 2020; Ogundiran, 2020; Scerri *et al.*, 2020) and field-based sciences more broadly (e.g., Krause *et al.*, 2021), have suggested that the COVID-19 pandemic poses a unique opportunity to make some vital revolutions to scientific practice. This comprises the development of remote models of archaeological research, including within museum and laboratory contexts. For a sustainable future, this article argues that data collection does not necessarily have to lie in individual researchers visiting artefact collections, but rather it requires a dramatic increase in collaboration and museum-driven data collection and curation. Such collaborative research models have the potential to encourage the re-articulation of modern research frameworks through fostering dual-project development and the sharing of responsibilities among international collaborators. As a field, we have acknowledged the deep-rooted issues within archaeological research, such as its colonial history, large carbon footprint and inaccessibility, yet we have struggled to develop effective and actionable solutions to combat them (though see Douglass, 2020; Sahle, 2021; Nordling, 2021), particularly in museum settings. Collaborative projects may be more appropriate than a series of in-person research visits in certain scenarios, such as when samples are relatively small but globally disparate, researchers are unable to travel extensively due to limitations imposed by disability, child-care, pandemics, and conflict, and/or concerns about the carbon-footprint of large-scale projects are raised.



This article presents research protocols for standardising the digitisation of lithics using photography and physical measurements, which facilitates research under a remote collaborative model with multiple collaborators. The data generated can enable a variety of analyses, such as qualitative descriptions, linear metrics, and geometric morphometrics, in addition to being used for digital museum archives and display purposes. Whilst developed for a project focussing on African Middle Stone Age points, these protocols can be adapted for other lithic tool types from different periods, and the collaborative data collection model more widely applied to museum and collection-based work.

## 6.2. Background

### 6.2.1. Lithic artefact digitization

Digital imaging technology, such as photography, laser scanning and photogrammetry, have transformed the way that archaeologists describe and analyse the shape of artefacts. The most widespread, cheapest, and efficient of these methods is digital photography, as cameras are easy to source and use by novices yet are high-resolution devices. As well as capturing the dimensions and properties of artefacts, digital photography is used in many other aspects of archaeological research, such as structure from motion 3D photogrammetry (Timbrell and Plomp 2019, Magani *et al.*, 2020; Bennet, 2021), aerial photography (Bescoby, 2006; Davis and Douglass, 2020; Musson, Rog and Stefano, 2013; Fowler, 2018), multispectral imaging (Howell, 2018; Picollo *et al.*, 2020), image enhancement such as decorrelation stretch (Kersten and Lindstaedt, 2012; Domingo *et al.*, 2013, 2015) and reflectance transformation imaging (Earl *et al.*, 2011; Newman, 2013; Miles *et al.*, 2014).

Lithic photography needs to take into account the many different material properties of stone as a raw material. Cerasoni (2021) recently presented protocols for photographing lithics and highlight that surface colour, patination, roughness and opacity amongst other factors require consideration. For example, vitreous raw materials, like obsidian, reflect light, whilst quartz can be moderately-highly translucent, thus transmitting light. These properties present challenges for photography as lights need to be positioned to minimise reflection and/or increase contrast whilst also highlighting the features of interest, such as through the avoidance of dark shadows for identifying artefact outlines.

Whilst Cerasoni (2021) provides excellent basic guidelines, lithic photography for capturing morphological shape, through metric measurements and two-dimensional (2D) geometric morphometrics, has further requirements for image standardisation (Loy and Slice, 2010). For example, geometric morphometrics can be highly sensitive to both intra and inter-observer error, which can be introduced at various stages of the workflow and lead to imprecision (Menendez, 2017; Evin, Bonhomme and Claude, 2020). One major concern for digitizing lithic shape from photographs is image distortion, which can arise through parallax when the specimen is too close to or not directly centred beneath the camera. Mullin and Taylor (2002) found that whilst parallactic error does have a negative effect on geometric morphometric analyses, when the camera set-up is standardised, and calibrated variation is small and constant enough for accurate results. Image standardisation across a collaborative project requires further attention, as there are more opportunities for error, such as through multiple operators using different equipment.

Aspects of lithic shape, such as the length of width of the platform or the thickness of the flake, can be captured from photographs, when a scale is included within an image, and by using digital callipers. Like with digital photography, clearly defining the dimensions being measured is vital for ensuring that the data collected is standardised (Lyman and VanPool, 2009). For example, in a metric analysis of mammalian teeth, Simpson, Roe and Lewontin (1960) found that 'length' had been determined using at least six different definitions, suggesting that the dimension has not been measured consistently between researchers. When pooling morphological data from multiple sources, clear protocols are thus integral to ensure that both photographs and measurements are captured reliably between collaborators.

### 6.2.2. Analyses of lithic shapes

Morphologies of lithics have traditionally been examined through qualitative descriptions (Inizan *et al.*, 1999), typological assessment, (Bordes, 1961) and/or linear measurements and metric analyses (Roe, 1964; McNabb, 2017). Metric data have been used to inform archaeologists on a variety of trends, such as functional differences (Shott, 1997) and tracing social interactions (de la Peña, 2015; Scerri *et al.*, 2016). With advancements in biological morphometrics and computing, geometric morphometrics are now also routinely applied in the analysis of lithics to understand evolutionary questions such as processes of artefact manufacture, phylogenetic relations between archaeological units, and cultural transmission through space, time and in relation to environments (Lycett, 2009; Cardillo, 2010; Shott and Trail, 2010; Serwatka and Riede, 2016).

Geometric morphometrics can be divided into methods that use landmarks, homologous points on the artefacts in two- or three-dimensional space (Cardillo, 2010; Buchanan and Collard, 2010; Petrik *et al.*, 2018; Buchanan, Collard and O'Brien, 2020), and those that use geometric descriptions of whole homologous outlines or surfaces, (Iovita, 2009, 2011; Ivaonovaité *et al.*, 2020; Mesfin *et al.*, 2020; Wang and Marwick, 2020), often through analysis of surface or outline harmonics and eigenshapes (Mitteroecker, 2021). Landmark-based approaches distil the morphological information captured to allow for the examination of questions specific to shape without random noise, however, their application to artefacts is often more challenging than biological structures due to the difficulty and potential subjectivity of identifying homologous landmarks (Okumura and Araujo, 2018). Outline-based geometric morphometrics have been argued to offer a 'homology-free' and information-rich alternative for quantifying shapes (Matzig *et al.*, 2021) and, whilst this is an oversimplification as the theoretical underpinnings of outline methods still rely on the assumptions of homology (Klingenberg, 2008) and semilandmark approaches can be just as detailed (Gunz and Mitteroecker, 2013), this makes them an appealing approach for investigating lithic variation when the information of interest is represented by the outline shape.

### 6.3. Collaborative data collection

The protocols were initially developed for an ongoing project aimed at exploring the diversity of African Middle Stone Age (MSA) lithic points. This project involves an equitable collaboration with personnel affiliated with the National Museums of Kenya, the National Museum of Ethiopia, Iziko Museums of South Africa, Mossel Bay Archaeological Project, Musée de l'Homme and Institut National des Sciences de l'Archéologie et du Patrimoine (see Acknowledgements for full list of collaborators).

When undertaking a collaborative research project with a museum or laboratory, it is advised that funding should be sought to support local collaborators, be it for training, equipment or aiding with travel or subsistence during the project. The customary application process should be completed, with permissions from site permit holders sought where necessary. Additionally, if a collaborative project is being initiated due to a global public health crisis or conflict, safety procedures should be put in place to ensure that collaborators are not at increased risk when carrying out the project. Each collaborator should follow the advice of their local governments and institutions and the project should only proceed during periods when the collections are deemed safe to open. When appropriate, containment measures, such as wearing of face masks, washing hands regularly, and maintaining a physical distance should be enforced and regular testing and vaccination, wherever possible, should be advised.

An integral part of any collaborative model is that everyone involved should take an active role in each stage of the research project. Many types of lithic analyses require that data collection is carefully controlled and standardised to avoid the introduction of inter-observer error, therefore data collection procedures should be developed, and draft copies of the procedures disseminated among collaborators for feedback; this feedback should be incorporated into a detailed protocol to ensure that data are collected consistently by collaborators. A virtual meeting could also be arranged to provide a visual demonstration of the data collection process for collaborators.

### 6.3.1. Photography protocols

Photography protocols were developed to enable the digitization of a range of data, such as metric measurements, landmarks, and outlines. The photography equipment required by all collaborators includes: a digital camera, a macro lens, a copy stand or tripod, photography lights, flashes or a light box, a spirit level, materials for holding the artefacts down, a small photography scale and either a remote control, computer software for remote capture or a timer built into the camera. This equipment is commonly found within museums; however, funding should be sought to ensure that each collaborator has the necessary apparatus for the project. If purchased for the project, the equipment can be donated to the museums for future research and engagement opportunities, following guidance from the Wenner Gren Foundation. Figure 13 demonstrates an illustration of an example photography equipment set-up; each collaborator set-up should be checked by the PI through a video meeting and sample images produced for feedback before initiation of the full data collection period.

#### *6.3.1.1. Artefact position*

Each artefact should be photographed to capture both the dorsal (upper) and ventral (lower) surface. The artefacts should be secured to a contrasting background (usually white or grey coloured) and levelled so they can be laid completely flat. Lithics with uneven ventral surfaces are likely to wobble onto one side; this should be corrected for by nesting the object using wedges to stabilise the artefact or by situating the artefact into sand, beads, or lab plasticine. It is important to not leave the artefact to rock, as any outlines or landmarks digitized from the photographs will not be homologous and make assumptions about the surface causing the rocking, with disproportionate and non-linear effects depending on the size of ridges causing wobble. Moreover, linear measurements taken from the photographs will also be impacted by

distortion if the artefact is not secured completely flat. Finally, the artefact should be centred within the camera frame to minimise parallax error in addition to a scale, which should be placed in the same plane as the artefact at a far enough distance to not interfere with data capture (Fig. 14).

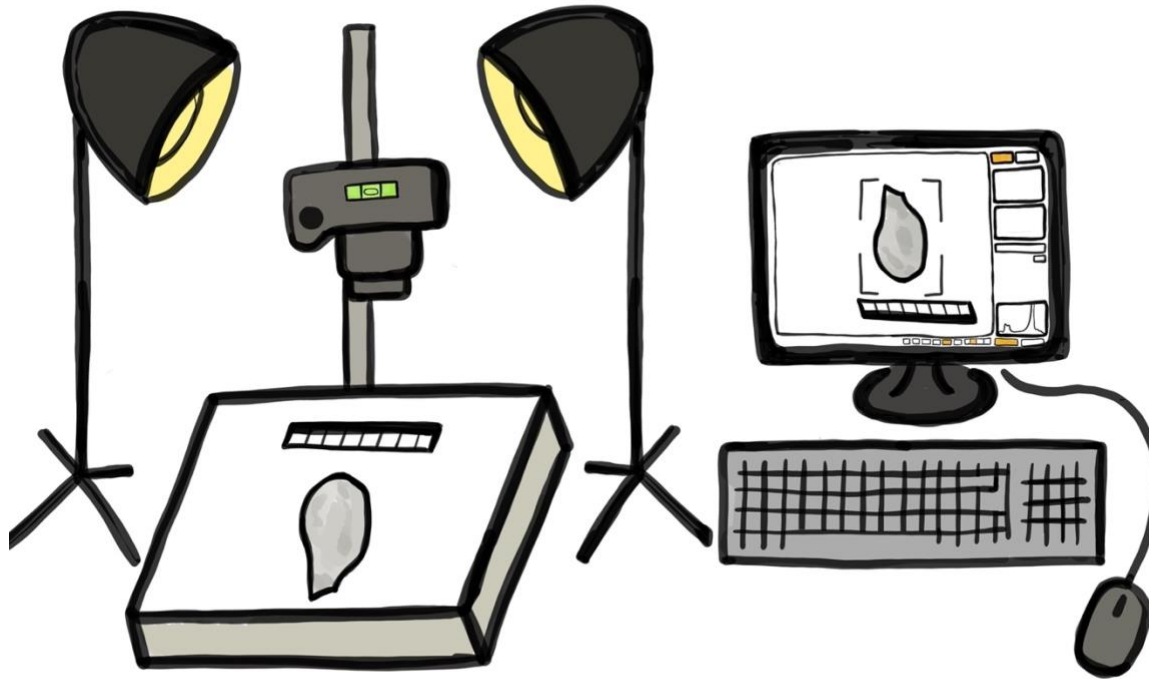


**Figure 13.** Cartoon of an example photography set-up, including a digital camera, a macro lens, a copy stand, photography lights, a spirit level, materials for holding the artefacts down, a small photography scale, and computer software for remote data capture.

### *6.3.1.2. Camera position and settings*

The posterior surface of the camera should be positioned at a set distance away from the artefact using a copy stand or a tripod. The camera needs to be levelled using the spirit level and recalibrated around once an hour to ensure it remains completely flat for the duration of the data capture. Each collaborator should use a macro lens to take the photographs, with corresponding focal lengths wherever possible. Macro lenses tend to produce less lens distortion than regular lens because the sensor produces an image of exact size and proportions of the artefact. Any distortion correction settings should be turned off and aperture priority mode turned on; this results in an appropriate shutter speed for the lighting conditions specific to

the location so that the artefact remains in focus whilst capturing the detail of the artefact. Camera shake should be minimised by using remote capture computer software, a digital remote, or the timer built into the camera.



**Figure 14.** Example photos of lithic points from Omo Kibish, Ethiopia. All points are photographed with their dorsal surface facing the camera. Photos taken by Dr Behailu Habte, National Museum of Ethiopia.

### 6.3.1.3. Lighting

Lights should be positioned depending on the individual situation of the collaborator and the material properties of the artefact, with the primary aim of minimising shadows around the artefact and highlighting features of interest. This usually means lighting the artefact from multiple different angles or with a light box. Shadows should be minimised as much as possible as they can interfere with image processing; for example, for outline based GMM, images should be binarized so that the outline can be clearly demarked, however when shadows are dark around the artefact, the binary threshold between what should be black (artefact) and what should be white (background) becomes harder to discern (Fig. 15). Shadows can also be minimised by placing the artefacts on top of an elevated transparent box – if this method is adopted, then the camera must be elevated at the specific height above the elevated artefacts rather than from the table. Lights should be carefully positioned to ensure that the artefact is well-defined, non-reflective and completely in focus.

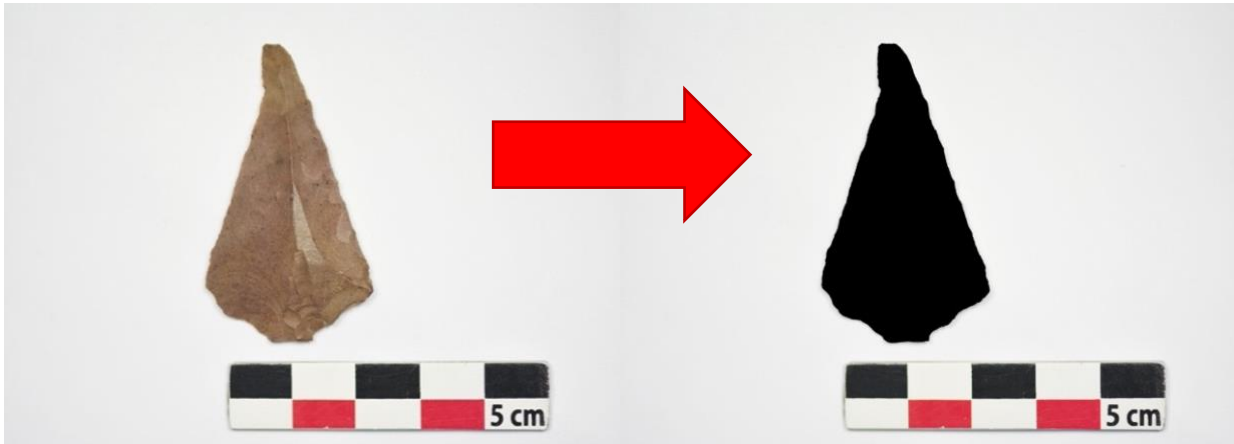


**Figure 15.** Image binarization process of a lithic point from Ifri n’Ammar, Morocco. Photo taken by Mouna Qazzih, Institut National des Sciences de l’Archéologie et du Patriome, Morocco.

### 6.3.2. Measurement protocols

In general, when measuring lithic artefacts, they should be orientated so that striking platform is at the proximal end of the flake and the distal end is where the detaching fracture terminates. Measurements should be clearly defined and illustrated visually within the protocol documents to demonstrate the exact dimensions of interest. This is because measurements can either be defined by the technological characteristics of the lithic or by its morphology (Shea, 2020). For example, technological length of a flake relates to the distance between the fracture initiation point on the ridge between the ventral surface and the striking platform and the distal edge of the ventral surface at a perpendicular angle. On the other hand, morphological measurements, which are of more relevance to lithic shape, relate to the maximum dimensions of a flake— maximum length, maximum width (which is usually perpendicular to length, though note this can vary [Dogandžić, Braun and McPherron, 2015] and so requires clear specification within the protocols), and maximum thickness (which is perpendicular to the dorsal/ventral plane). Morphological measurements of the platform also relate to the maximum values. The resolution of the measurements should be specified to ensure that the data is at a comparable precision; in most cases, a resolution of either 0.1 or 0.01mm should be sufficient (Lyman and VanPool, 2009).

### 6.3.3. Data recording, storage and sharing

A spreadsheet should be provided to ensure metadata is recorded in a comparable format across collaborators, including details on the collection numbers, stratigraphy, context, raw material, and

preservation of each artefact as well as the metric data and corresponding photograph numbers. Data can be stored on a communal data storage platform (such as a Google Drive) that each collaborator has access to, and external hard drives can be provided for data back-up. Following a discussion with each museum regarding the publication of the data, the resulting data could be uploaded onto an open-access digital archive if all parties give consent. All publications resulting from the data collected by the collaborators should elicit co-authorship and should be submitted to journals that are accessible to the collaborators – for example, for a project with African collaborators, articles should be submitted to *African Archaeology Review* and *Journal of African Archaeology*, and/or under a Gold or Green Open Access publishing agreement to ensure maximum accessibility (Marwick *et al.*, 2017).

## 6.4. Discussion

This article has presented photography protocols for lithic shape documentation which can be implemented under a research model involving multiple observers. Whilst this approach has provided an initial strategy for overcoming COVID-19 related disruptions to museum or laboratory-based research on lithic assemblages, remote models of science that foster equitable international collaborations offer multiple benefits for the field far beyond the current crisis if adopted more widely. As such, the COVID-19 pandemic has the potential to offer an effective alternative to the way we usually conduct scientific research within museum settings by encouraging dual-project development across the Global North-South divide.

### 6.4.1. ‘Helicopter research’ in the museum context

Douglass (2020) proposes that the events of the COVID-19 pandemic should invite archaeologists to consider the concept of resilience as it relates to their research practices as well as their day-to-day life. This article argues that collaborative data collection with museum partners fosters research resilience by inviting local curators, researchers, and volunteers to be directly involved with international research projects conducted there. Often, foreign researchers travel to museum collections without extended interaction with museum staff or the local communities that have ancestral connections to the collections, even though these people likely possess the most contextual knowledge about the objects. Neo-colonial research, commonly known as ‘helicopter research’, limits the scientific knowledge gained from the data collection process, as conclusions from visiting scientists may be misinformed or simply perpetuate the assumptions of previous scholars (Nordling, 2021). More recently there has been increased awareness



around such practices – for example, detailed engagement plans are required to undertake research at the Iziko Museums of South Africa. Moving forward, collaborative data collection models have the potential to provide local researchers with opportunities to assume prominent roles in the international research being conducted in their countries. African-led initiatives, such as those coordinated by the Turkana Basin Institute (Nordling, 2021), the Middle Awash Project (Sahle, 2021) and the Human Evolution Research Institute, University of Cape Town, have been extremely effective for building capacity within Africa; collaborative projects can contribute by allowing local scholars to benefit from international projects, though this needs to be coupled with more direct funding and support to further facilitate African-led research.

Collaborative data collection should only be undertaken with the understanding that local researchers are included in all phases of the work, from planning to the research outputs, including co-authorship on publications resulting from the data collected. Douglass (2020) describes the fully collaborative framework adopted by the Morombe Archaeological Project, working in the Vezo territories of coastal southwest Madagascar, where power-sharing initiatives have enabled research to persist throughout the COVID-19 pandemic. Such frameworks from the field can be applied within museum settings in order to mitigate pandemic-related disruptions, as well as to improve the quality and equity of the science produced, with input from all collaborators adding value and increasing diversity in understanding of the artefacts. Moreover, collaboration encourages local researchers to assume a central voice in the narrative of international archaeological research, which is especially important in places where the story of the past has been told by predominately Western scholars, who were typically white and male (Ackermann, 2019; Athreya and Ackermann, 2019; Sahle, 2021), such as within Africa, Australia, and North America. It is often in these regions where community building and respecting the cultural beliefs of local communities becomes particularly salient, as strong ancestral links to archaeological material persist. For example, First Nation groups in Canada have the power to decline archaeologists' requests to study their ancestors' remains (Nicholas, 2007), thus taking control over the narrative of their own heritage.

To accommodate COVID-19 related disruptions, most major research funders have allowed maximum flexibility and the reallocation of grants to meet the cost of working remotely (Stoye, 2020). Within a museum context, grants traditionally cover the training, travel, accommodation, and bench fees of foreign researchers to carry out research projects. This ultimately benefits the foreign PI and their development as a researcher, but also the wider community through the money spent by the PI during an in-country research visit. However, under a collaborative model, funding instead can be reallocated to ensure that local collaborators have the necessary equipment, training, skills, and provisioning to undertake the

project. If equipment is purchased, it can then be ‘donated’ to the museum after the project has finished (as proposed under the guidance of the Wenner Gren Foundation) and used for future research and engagement projects led by local researchers. Investing in the training and development of students, interns and volunteers working at museum collections, perhaps in-person by a senior curator or virtually by international collaborators, is vital for ensuring that local early career researchers are equipped to conduct further research on museum collections and can provide long-term opportunities for often disadvantaged scholars (Nordling, 2021). Therefore, any spending that is inevitably lost through the PI not visiting physically can be made up for, or even superseded by, a direct investment into the country’s heritage sector by providing funded research opportunities for local scholars, which are rare in most countries. As proposed Scerri *et al.* (2020), investing in the location of the data, not the location of the PI, is ultimately more sustainable for the field.

#### 6.4.2. Reducing the carbon footprint of museum research

Archaeology, as a field-based science, has long been concerned by its carbon footprint (Reynold, 2018). Interestingly, despite many archaeologists working with paleoenvironmental data and understanding the devastating effects climate change has had on past societies (e.g., Jackson, Dugmore and Riede, 2018), archaeologists often travel abroad multiple times a year, be it for fieldwork, conferences, or international collaborations. Museum-based research is no exception, with researchers sometimes flying to multiple countries within a single project to collect data on often very small samples. The sudden halt to domestic and international travel, and the slowing down of other human activities in the first half of 2020 saw a decrease in global carbon dioxide emissions by 8.8% (Liu *et al.*, 2020) - whilst this is gradually increasing again as restrictions are released, the pandemic has revealed that reducing travel can have a significant beneficial impact on climate change and our planet.

Whilst concerned with the carbon footprint of their research, often archaeologists feel they have no choice but to conform to this research structure. Traditionally, to progress one’s academic career, one would need to generate new data, excavate a new archaeological site, or make new discoveries to produce publications. This pressure is especially felt by early career researchers, who have faced particular challenges during the COVID-19 pandemic due to the increased restrictions on time, funding and access to samples, yet they face competition in the job market with those who have not faced similar disruptions. Indeed, there is great value in analysing and aggregating pre-existing data (Timbrell, 2020b), and nowadays most researchers are willing to share data thanks to the Open Science movement within archaeology (Marwick *et al.*, 2017). Collaborative models of data collection can offer another solution for

environmentally conscious researchers by facilitating the development of international networks of collaborators, providing an alternative means of gaining access to disparate collections.

The recent International Panel on Climatic Change report has warned that climate change is ‘widespread, rapid and intensifying’ thanks to human activity with urgent action necessary to change the course of future climate change (IPCC, 2021), making it hard to justify the pre-pandemic level of travel undertaken by archaeologists. Therefore, adopting a collaborative model, whereby travel is not a necessity and data is shared as part of the collaboration, ensures that as much is gained from the data collection process as possible with relatively little cost to the environment. This article does not advocate that all travel related to archaeological research has to be avoided, but that a more mindful, nuanced, and considered approach should be taken when initiating international projects; upon reflection, the adoption of a collaborative data collection model could be more appropriate in many scenarios, particularly when samples are small, numerous, and disparate. In sum, future climate change itself has the potential to cause disruption to international archaeological research, therefore it is in our best interest as a field to find effective ways to reduce our carbon footprint.

#### 6.4.3. Building resilience through collaborations with museums

Although the scholarly and professional value of engaging with artefacts and gaining practical research skills within a physical museum is priceless, the potential value that can be gained through remote collaboration and knowledge production makes the collaborative data collection model an effective alternative for accessing international lithic samples. Whether cooperative science produces data comparable to that typically collected by a single researcher remains currently untested (though see Chapter 7, Timbrell *et al.*, 2022b); indeed, Scerri *et al.* (2020) propose that funding should be redirected to test the validity of remote methods of data generation. It is likely that the development of protocols to ensure consistency corrects for many, but not all, potential sources of error. For example, using lenses of different length, despite maintaining the height above the artefact, can still cause parallax issues, but this is largely a logistical limitation of the collaborative model whereby each museum either uses equipment that is already available is easy to source, or can be purchased within the financial scope of the project. Assessments of error in lithic studies involving multiple collaborators, particularly those of poorly standardised artefacts, require the careful application of specific methods that are able to partition variance between specimens from that which derives from error, in order to determine the effects of inter-observer variability on the results (see Ulijaszek and Kerr, 1999; Lyman and VanPool, 2009; Fruciano, 2016; Timbrell *et al.*, 2022b; Chapter 7 in this thesis).

The protocols described in this article focus on the standardised digitization of lithic artefacts that can enable a variety of analyses (e.g., Timbrell *et al.*, 2022c). High-resolution photographs of lithics can be used to analyse morphological shape, as well as identify flake scars and wear damage. Moreover, photographs are a useful resource for digital archives and museum displays when artefacts are taken out on loan. In fact, many museums are in the process of creating online archives through the digitisation of their collections, and therefore collaborative research models have the potential to offer support for local researchers by facilitating this process, whilst also generating data on lithic collections. Online databases of photographs may become vital for the training of students who are unable to get in-person field or museum experience, ultimately making archaeology more accessible. Additionally, photographic databases can also be used in a variety of research contexts such as for photogrammetry; this is relatively cheap and easy to teach virtually, and therefore has been proposed as another imaging method that could be suitable for remote science (Scerri *et al.*, 2020). Both metric and photographic data generated under a collaborative model can also be re-used by local early career researchers for their own research purposes, such as for a university dissertation.

However, not all photographs will be suitable to be shared across a collaborative data collection framework; for example, images of human remains and culturally sensitive artefacts require a more nuanced data sharing agreement to ensure that the necessary communities retain control over who accesses the data (Walter *et al.*, 2020; Tsosie *et al.*, 2020). Any data generated under a collaborative research framework should be considered the responsibility of all parties involved, and therefore its publication, be it in a journal article, online repository, or museum website, should be discussed at length prior to project initiation to ensure that all parties have given the necessary consent. In general, however, data sharing (such as through an online repository; Marwick *et al.*, 2017) should be encouraged as part of the collaborative data collection model, as not only does this reduce the potential for future artefact damage, increase the accessibility of data for those who are unwilling and/or unable to travel extensively to access samples, encourage transparency and replicability which should be central to scientific practice, but it also may invite repatriation in some cases.

## 6.5. Conclusion

Human responses to past epidemics can be illuminated through archaeological research (Gamble *et al.* 2020); however, now we must use the COVID-19 pandemic to interrogate the way in which we conduct international archaeological research. This article presents an alternative to in-person research visits via a

collaborative data collection model, which encourages the digitization of lithic artefacts that are remotely accessed through an equitable collaboration with local researchers. Under this model, data generation is decarbonised and decolonialised through a meaningful dual-partnership approach to data collection. Collaborative data collection provides a promising alternative to in-person research visits, with the COVID-19 pandemic providing the much-needed catalyst for the development of new remote frameworks of science that can ultimately make international research practices more accessible, resilient, sustainable, and equitable.

## Chapter 7: Testing inter-observer error under a collaborative research framework for studying lithic shape variability

This chapter was published in *Archaeological and Anthropological Sciences* on the 1<sup>st</sup> of October 2022 under a Gold Open Access Agreement (Timbrell *et al.*, 2022b). It was co-authored by myself (lead author), Christopher Scott (University of Liverpool), Behailu Habte (National Museum of Ethiopia), Yosef Tefera (National Museum of Ethiopia), H el ene Monod (Mus ee de l'Homme), Mouna Qazzih (Institut National des Sciences de l'Arch eologie et du Patrimoine), Benjamin Marais (Iziko Museums of South Africa), Wendy Black (Iziko Museums of South Africa), Christine Maroma (National Museums of Kenya), Emmanuel Ndiema (National Museums of Kenya), Struan Henderson (Mossel Bay Archaeological Project), Katherine Elmes (Mossel Bay Archaeological Project), Kimberly Plomp (University of the Philippines, Simon Fraser University) and Matt Grove (University of Liverpool).

### Abstract:

Evaluating error that arises through the aggregation of data recorded by multiple observers is a key consideration in many metric and geometric morphometric analyses of stone tool shape. One of the most common approaches involves the convergence of observers for repeat trials on the same set of artefacts: however, this is logistically and financially challenging when collaborating internationally and/or at a large scale. We present and evaluate a unique alternative for testing inter-observer error, involving the development of 3D printed copies of a lithic reference collection for distribution among observers. With the aim of reducing error, clear protocols were developed for photographing and measuring the replicas, and inter-observer variability was assessed on the replicas in comparison with a corresponding data set recorded by a single observer. Our results demonstrate that, when the photography procedure is standardized and dimensions are clearly defined, the resulting metric and geometric morphometric data are minimally affected by inter-observer error, supporting this method as an effective solution for assessing error under collaborative research frameworks. Collaboration is becoming increasingly important within archaeological and anthropological sciences in order to increase the accessibility of samples, encourage dual-project development between foreign and local researchers and reduce the carbon footprint of collection-based research. This study offers a promising validation of a collaborative research design whereby researchers remotely work together to produce comparable data capturing lithic shape variability.

## 7.1. Introduction

Shape analyses are becoming an increasingly popular methodology for examining lithic variability in the archaeological record. As such, traditional linear metrics and geometric morphometrics (GMM) are often employed to capture morphological information on stone tools (Cardillo, 2010; Lycett and von Cramon-Taubadel, 2015; Matzig, Hussain and Riede, 2021). Combining morphological data from multiple observers is frequently necessary in studies of lithic assemblages, to increase sample size and/or to perform inter-site / inter-assemblage analyses, yet this can be problematic due to the possibility of introducing inter-observer error into the data (Lyman and VanPool, 2009). Such error has multiple potential sources, can be introduced at various stages in the workflow, and can skew results by obscuring any ‘real’ signals in the data (Fruciano, 2016); examining the magnitude of inter-observer error is therefore imperative to validate whether meta-analyses are robust. International researchers are increasingly being encouraged to work collaboratively in order to remotely produce archaeological and anthropological datasets (Chang and Alfaro, 2015; O’Leary and Kaufman, 2011; Scerri *et al.*, 2020; Timbrell, 2020, 2022) – in some case even crowdsourcing morphometric data (Chang and Alfaro, 2015). However, it is frequently impossible for observers to converge on the same material to record repeat trials for an inter-observer repeatability assessment. Such tests therefore need to be appropriate for the specific research design, and customized solutions for evaluating error under collaborative research frameworks should be developed (Fruciano, 2016). Here we present an innovative analysis of inter-observer error involving the compilation of standardized photographs and measurements of lithics from multiple observers for metric and GMM analysis (Timbrell, 2022).

Traditionally, lithic shape variation has been examined through qualitative descriptions (Inizan *et al.*, 1999), typological classification (Bordes, 1961), and/or linear measurements (Roe, 1964; McNabb, 2017). Advancements in biological morphometrics and computing have meant that geometric morphometrics are now also routinely applied in the analysis of lithic morphologies (Bookstein, 1991; Buchanan *et al.*, 2018; Cardillo, 2010; Lycett, 2009; Serwatka and Riede, 2016). GMM approaches are split into methods that use landmarks and outlines, the former representing shape through homologous points (landmarks) superimposed on a two-dimensional (2D) or three-dimensional (3D) object and the latter applying geometric descriptions of homologous outlines or surfaces (Mitteroecker, 2021). Landmark based methods allow for specific aspects of morphology to be captured without the inclusion of random noise (i.e., shape dimensions that are not pertinent to the research question), however, their application to certain non-biological structures, such as lithics and other archaeological artefacts, is often more difficult as the identification of homologous landmarks can be subjective (Okumura and Araujo, 2018). Outline

based GMM, on the other hand, avoids certain issues of homology through quantifying the gross shape of each specimen (Klingenberg, 2008), making them ideal for describing shape variation of lithics in archaeological studies (e.g., Iovita, 2009, 2011; Ivaonovaité *et al.*, 2020; Matzig *et al.*, 2021; Mesfin *et al.*, 2020; Wang and Marwick, 2020).

Assessment of the levels of inter- and intra-observer error under different methodological approaches to studying lithic shape is vital, and several studies have examined error in metric and GMM analyses at different phases of the workflow (Evin, Bonhomme and Claude, 2020; Fagerton *et al.*, 2014; Lyman and VanPool, 2009; Macdonald, Royal and Buchanan, 2020; Menedez, 2017; Osis *et al.*, 2015; Perini *et al.*, 2005; Robinson and Terhune, 2017; von Cramon-Taubadel, Frazier and Mirazón Lahr, 2007; Yezerinac, Lougheed and Handford, 1992). Problematic landmarks, i.e., those that are difficult to consistently locate, can be a source of error in landmark based GMM analysis (Fagerton *et al.*, 2014; Menedez, 2017; Robinson and Terhune, 2017; von Cramon-Taubadel, Frazier and Mirazón Lahr, 2007), even for experienced observers (Chang and Alfaro *et al.*, 2015). von Cramon-Taubadel, Frazier and Mirazón Lahr, (2007) found that repeating the digitization procedure was the most suitable method for assessing the precision of landmarks, with adequate landmark definitions imperative for reducing error. Yezerinac, Lougheed and Handford (1992) also found that ill-defined measurements were a factor increasing error in metric data, in addition to operator experience, the precision of the measuring device, and the conditions under which the measurements are made, such as lighting. Combining metric measurements from more than one observer therefore is likely to be suitable only when the dimensions are standardized and easily measured, and the conditions, the precision and quality of the equipment, and the technique of recording the data are comparable (Lyman and VanPool, 2009).

Comparatively, fewer studies have examined the levels of inter-observer error in outline based GMM methods. Evin, Bonhomme and Claude (2020), in an investigation of error between morphometric approaches, found that although methods that employ landmarks were the most sensitive to error, outline data saw relatively lower levels of intra-observer error compared to inter-observer error, with photography being an influential source of variance between observers. Digital photography is widely used in 2D GMM as it is inexpensive, easy to perform, and does not require extremely specialist knowledge or equipment, with the digitization of landmarks and/or outlines on the resulting images providing a 2D representation of the 3D object. The focal length and specifications of the lens used can, however, cause parallax error, optical distortion that occurs when the specimen is too close or not directly centered beneath the lens (fisheye). Nonetheless, several studies employing both landmark and outline methods suggest that 2D GMM data are minimally affected by parallax error, especially when the camera



set-up is standardized and calibrated, with deviations small and constant enough for accurate analyses (Caple, Byrd and Stephan, 2018; Macdonald, Royal and Buchanan, 2020; Mullin and Taylor, 2002; Riano, Jaramillo and Dujardin., 2009). Overall, outline-based methods are likely more suitable for collaborative research designs in studies of lithic shape, due to the objectivity of data capture, the fact that landmark methods have high rates of inter-observer error, though this is more pertinent during landmark digitization than object photography (Evin, Bonhomme and Claude, 2020), and the potential to reduce inter-observer error through the standardization of the photography procedure.

Although inter-observer error is a concern in any collaborative research design, collating data from multiple observers is often necessary in archaeological research, be it to increase sample sizes, facilitate interdisciplinary research and/or enable access to disparate data (Timbrell, 2020b). The latter is especially important when considering issues of income-disparity, childcare, and disability that can disproportionately disadvantage researchers who are unable to travel extensively to collect data. Global catastrophes, such as pandemics, climate change, and conflict, can also temporarily delay international research through the constraints imposed on travel and safety, requiring researchers to develop scientifically-sound remote models of data generation (Scerri *et al.*, 2020). Timbrell (2022) presents such a framework, which involves the documentation of lithic shape by multiple collaborators. These types of approaches have additional benefits for decreasing the carbon footprint associated with accessing multiple international samples and fostering knowledge-sharing through dual project development and the division of responsibilities so that both foreign and local researchers take on principal roles within a given project, which is particularly crucial across the Global North-South divide (Chirikure, 2015; Douglass, 2020; Else, 2022). Indeed, collaborative approaches accord with the open science initiative in archaeology, which advocates that data stewardship should be centered around researchers collecting and sharing data on behalf of the scientific community, as opposed for the betterment of a single individual's career (Marwick *et al.*, 2017).

While collaborative data collection offers a promising new framework for generating and sharing data internationally, the analysis of inter-observer error is imperative to validate such an approach. Here, we present a unique control test that involves the production of 3D printed replicas of a lithic reference collection, which can be distributed among observers and measured following the same protocols used to collect the actual data. We then examine the differences between the datasets, knowing that each collaborator has recorded the same data from identical copies of the artefacts. Using this approach, we evaluate whether the compilation of data from multiple observers is conducive to error, and thus could negatively bias the results of a collaborative study.

## 7.2. Materials

Six lithic points were knapped using fine-grained flint from Caistor Quarry, Caister St Edmunds, UK, and scanned for 3D printing at the University of Liverpool (Fig. 16). The reference tools varied in both size and shape, encapsulating a range of morphologies characteristic of the empirical sample to be studied in the main project (African Middle Stone Age assemblages). While flint is not a feature of African lithic assemblages, it could be considered representative of the finer-grained materials, such as obsidian, chert, and heat-treated silcrete, exploited during the Middle Stone Age (Key, Pargeter and Schmidt, 2021; Sahle *et al.*, 2013). The tools were produced on flakes and retouched using: (1) direct freehand hard hammer percussion (quartzite hammerstones); (2) direct soft free hand hammer percussion using an antler hammer; (3) handheld pressure flaking using an antler tine supported in a tanned leather pad. Each tool was colored blue using craft enamel spray paint to aid scanning.

Next, each lithic was scanned with a freshly calibrated Einscan Pro 2X structured light scanner with colour camera, using combined feature and texture mapping in the high-resolution setting. Initial scans were performed with the lithics placed vertically in a foam holder using fixed scan mode aligned with an automated turntable and coded targets (scans taken every 11.25 degrees, i.e., 32 scans). The models were then completed by switching to the 'align by' feature using the turntable (32 scans) and the lithic was rescanned (2-3 times) until a complete model was achieved. All alignment was automatic to produce a watertight mesh; no holes were filled. Each model was sharpened using the Einscan high-setting and saved as .obj files without decimation (see Appendix 2: Supplementary Table S1 for further data on each model).

The 3D models were processed for printing using Chitubox v1.8.1. Medium-sized automated supports were applied using this software at 90% total coverage to provide a strong foundation for the 3D prints. We used an Elegoo Mars 2 Resin printer, with a new printer film, using standard grey Elegoo LCD UV curing 405 Nm photopolymer resin with recommended Elegoo settings (Fig. 17). The prints were extracted from the print bed and the supports were removed by hand prior to being rinsed in ethanol and cured in direct sunlight. Each tool was printed six times to create six copies of the assemblage, resulting in 36 prints in total.



**Figure 16.** The six 3D printed replica tools. Original lithics were knapped and scanned by CS in preparation for 3D printing. Example photos were taken by SH. Scale = 3cm.

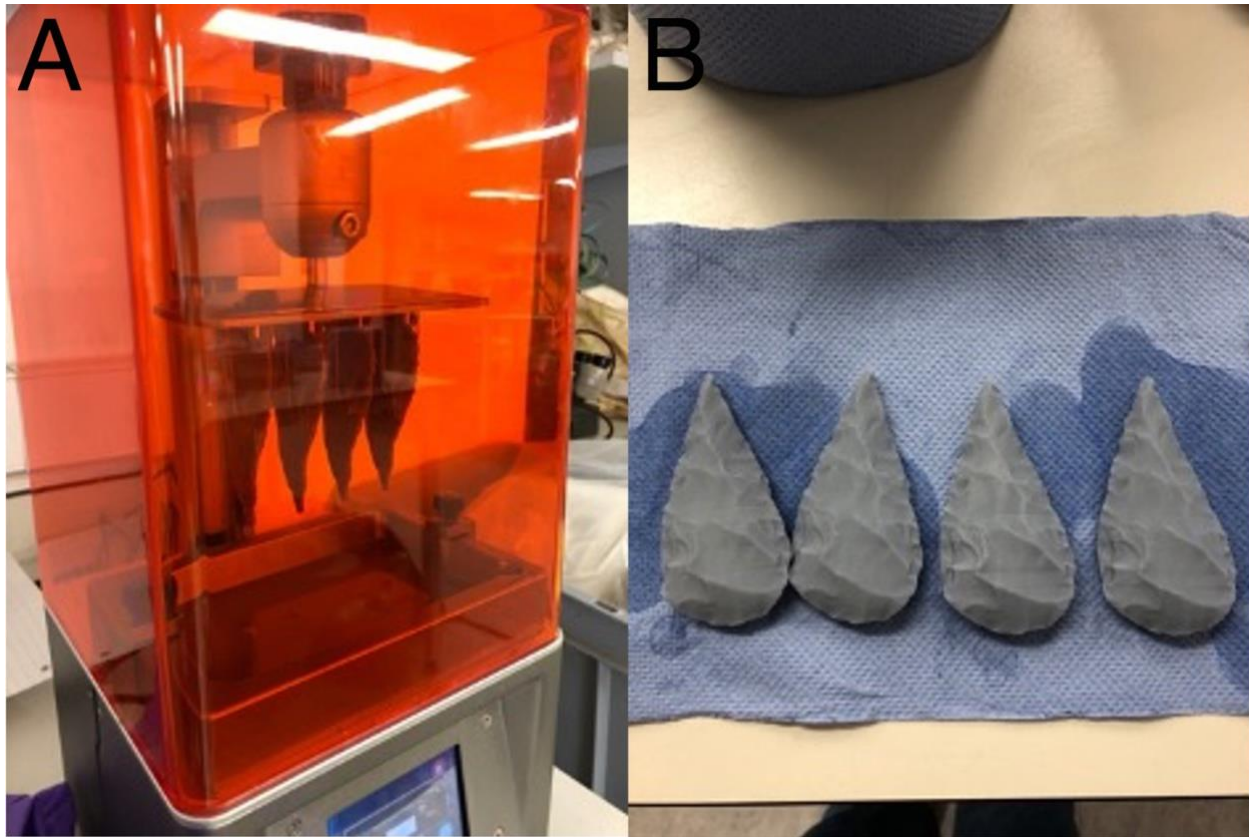


**Figure 17.** Photographs from the 3D printing process. A) The 3D model of the tool is sent to the machine for printing. B) The resulting 3D prints once removed from the supports are cleaned using ethanol. 3D printing was carried out by LT and CS.

### 7.3. Methods

Each tool was assigned a number (Tool 1-6; Fig. 16) and a replica copy of the assemblage was sent to researchers at six independent institutions (Table 9). Data collection protocols, outlined in detail by Timbrell (2022) and described in Chapter 6, were developed to standardize the documentation of lithic shapes through photography and measurements. These procedures were followed by all observers across the study to produce equivalent data. Instructions for object position, camera position and settings, and lighting were specified and tightly controlled (see Chapter 6). In addition, a scale (sourced in situ by the observers) was placed in each photograph to ensure a measure of size was recorded. Table 9 reports the camera and lenses used to capture each replica assemblage in the study; high quality equipment was accessed by all observers either through their institution directly or through funding provided by the project. Three basic measurements on each tool were also taken to record morphological length, width, and thickness (see Appendix 2: Supplementary Fig. S1 for a schematic) at a resolution of 0.1mm. We

defined length as the maximum dimension of the point, width as the maximum measurement in the perpendicular dimension to length, and thickness as the maximum measurement in the third dimension, following Shea (2020).

**Table 9.** Summary of the observers and the photography equipment used. This equipment was sourced locally; in most cases, the institutions already had access to the necessary apparatus, however in some cases it was rented and/or purchased and donated to the institution after the project, following guidelines provided by The Wenner Gren Foundation.

| Assemblage number | Institution  | Abbreviation | Country      | Camera body         | Camera lens                       |
|-------------------|--|--------------|--------------|---------------------|-----------------------------------|
| 1                 | Institut National des Sciences de l'Archéologie et du Patrimoine | INSAP        | Morocco      | Nikon D7100         | Nikon AF-S Micro Nikkor 105mm     |
| 2                 | Iziko Museums of South Africa                                    | IM           | South Africa | Canon 6D II         | Canon 100mm 2.8 Macro             |
| 3                 | Mossel Bay Archaeological Project                                | MBAP         | South Africa | Nikon D300s         | Nikon AF Micro Nikkor 60mm 1:2.8D |
| 4                 | National Museum of Ethiopia                                      | NME          | Ethiopia     | Canon EOS DSLR 200D | Canon Tamron 60mm Macro Di II     |
| 5                 | National Museums of Kenya  | NMK          | Kenya        | Nikon D5300         | Nikon AF-S Micro Nikkor 40mm      |
| 6                 | Musée de l'Homme   | MH           | France       | Nikon D5200         | Nikon AF-S Nikkor 24-70mm         |

Prior to distribution among institutions, all 36 replicas were also recorded by a single observer (LT) to produce a comparative dataset. Photography was performed using a Canon M50 camera with an EF-S 60mm f/2.8 Macro USM lens and the three measurements were taken using digital callipers. This enabled us to determine the magnitude of intra-observer measurement error, for comparison with the magnitude of inter-observer error, had the project been carried out by a single individual under a traditional research framework.

Data were uploaded onto a communal data sharing platform (Google Drive) by each observer for processing and analysis by a single observer (LT). Analyses were performed in the R software environment (R Core Team 2020). Data and code can be found on the GitHub repository for the project:

[https://github.com/lucyimbrell/error\\_analysis\\_lithics/](https://github.com/lucyimbrell/error_analysis_lithics/)

### 7.3.1. Metric analyses

We first computed the intra-class correlation coefficient (*ICC*) using the ‘psych’ R package (Revelle, 2022) to assess the agreement between the six observers in measuring the six tools for length, width, and thickness. The *ICC* compares the variability within repeat measurements whilst contrasting variability between groups of measurements (Bartlett and Frost, 2008; Fruciano, 2016; Koo and Li, 2016; Shrout and Fleiss, 1979). Specifically, we used a two-way mixed effects model to compute the *ICC*, with the set of observers considered a fixed effect. To assess the reliability of data collection, we next calculated and compared the mean, variance, technical error of measurement (*TEM*) and percentage technical error of measurement (*%TEM*). The mean and variance (expressed as the standard deviation) were calculated for each measurement on each tool, with the *TEM* and *%TEM* calculated to compare pairs of observers across all measurements on all tools. The *TEM* reflects measurement precision between observers, and is calculated as:

$$TEM = \sqrt{\frac{(\sum_1^N (\sum_1^K M^2)) - ((\sum_1^K M)^2 / K)}{N(K - 1)}} \quad [7.1]$$

where *N* is the number of subjects, *K* is the number of observers, and *M* is the measurement (modified from Ulijaszek and Kerr [1999]). The *%TEM* represents the magnitude of the error as a percentage of the mean of the measurement/variable studied. It is calculated as:

$$\%TEM = 100 \left( \frac{TEM}{\bar{v}} \right) \quad [7.2]$$

where  $\bar{v}$  is the average value of the raw measurements, taken across all measurements on all tools by multiple observers. The values obtained for these metrics must be subjectively assessed according to the research question, as there is no standard applied threshold of error deemed to be ‘acceptable’. Following Lyman and VanPool (2009)’s analyses of projectile points, we propose that a *%TEM* of <4 could be an acceptable level of error without negative consequences on the results. Lastly, we calculated the coefficient of reliability (*R*), which ranges from 0 to 1, with 1 indicating very high congruence between measures. We used the following formula outlined in Lyman and VanPool (2009):

$$R = \sigma_v^2 / (\sigma_v^2 + \sigma_d^2)$$

where  $\sigma_v^2$  is the variance of all raw measurements on all tools taken by two observers and  $\sigma_d^2$  is the variance of the difference between those two sets of measurements. Similarly to the *ICC*, the coefficient of reliability distinguishes between the variability between the specimens and that which results from random measurement error. However, whilst *R* can only be calculated between pairs of observers, the *ICC* represents an overall metric for measurement error across all observers.

Random error can inflate the amount of variance within a sample, resulting in a loss of statistical power as noise obscures true differences in means (Fruciano, 2006; Yezerinac, Lougheed and Handford, 1992). To evaluate the levels of error in the multiple observer data in relation to the single observer data, we used two-sample t-tests to compare differences in mean and F-tests to compare differences in variance. If there is high inter- and/or intra-observer error, variation within replicas of the same tool will be increased and differences in the mean values for each tool will be significantly different.

### 7.3.2. Two-dimensional geometric morphometric analysis

In preparation for GMM analysis, each image was processed using the ‘object select’ tool in Adobe Photoshop, which automatically determines the contour of the object. Once the contour was highlighted, the object was filled with solid black to help facilitate the extraction of outline data. All processed images were then synthesized into a single thin-plate spline (.tps) file using tpsUtil, and the outline data were extracted using tpsDig2. The outline of each artefact was represented by an average of 2856 equidistant points, which were scaled through the specification of the pixel to centimeter ratio for each image (see Appendix 2: Supplementary Fig. S2 for a visualization of the data). The outline data were saved as (x,y) coordinates within the .tps file and imported into R.

Using the ‘Momocs’ R package (Bonhomme *et al.*, 2014), the outlines were standardized following Bonhomme *et al.* (2017) by normalizing to a common centroid, scaling to centroid size, and aligning along the long axis of the object. We then performed elliptic Fourier Analysis (EFA) to convert the geometric data to frequency data, with the outline decomposed into a series of repeating trigonometric functions, referred to as harmonics (Cagle, Byrd and Stephan, 2017; Fig. 18). The appropriate number of harmonics were identified to capture sufficient information on shape; this was deemed to be 8 harmonics, achieving 99% harmonic power (Cagle, Byrd and Stephan, 2017).

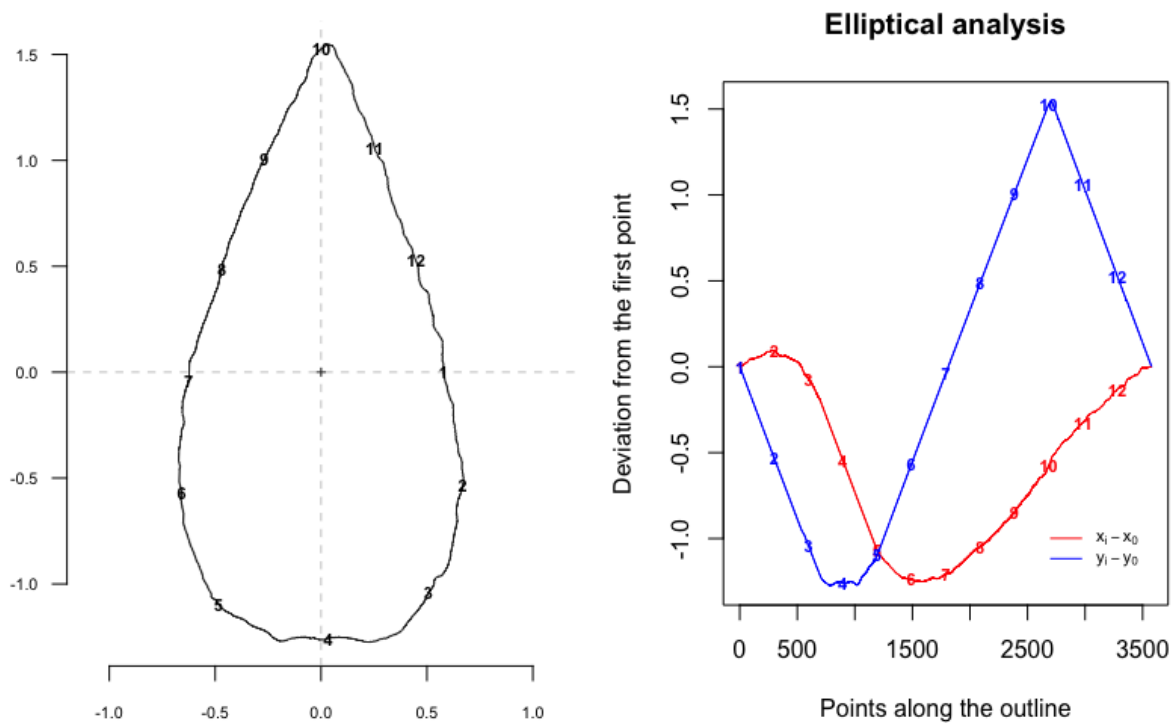


**Figure 18.** A schematic of the Elliptic Fourier fitting process that generates the raw shape data for geometric morphometrics. Coefficients of sine and cosine terms (harmonics) are computed to reconstruct the x (blue) and y (red) coordinates from an arbitrary starting point moving along the outline.

Next, we performed a principal components analysis (PCA) on the elliptic Fourier coefficients to reduce the dimensionality of the data. Principal components (PCs) are constructed to highlight the main axes of morphological variance (Zelditch *et al.*, 2004). Like with the metric data, we calculated the *ICC* and *R* values to partition the variance from the inter-observer error for the PC scores of repeat captures (Daboul *et al.*, 2018; Fruciano, 2006). Due to the nature of PC scores, we were unable to obtain an informative relative measure of dispersion (*%TEM*) and instead refer to the standard deviation (calculated as the square root of the variance) as absolute measures of dispersion. This is because, when the mean of a set of repeat captures falls close to the mean of a PC ( $\sim 0$ ) and has a low standard deviation ( $\sim 0$ ), the *%TEM* would be very high despite the tight clustering of the repeated measures along that PC. In addition, we applied linear discriminant analysis (LDA) to the PC scores, with the equal sample sizes used as the prior group probabilities (1/6) of a repeat belonging to a certain group based on their outline shape alone (Mitteroecker and Bookstein, 2011). In this analysis, we tested firstly whether the tools could be distinguished based on their shape alone, and then whether the observers could be identified. One would



expect high classification results when discriminating between tools and low classification results when discriminating between observers if inter-observer error is low.

## 7.4. Results

All data and R code can be found on the project's repository, and was made available for the peer-review of this article: [https://github.com/lucyimbrell/error\\_analysis\\_lithics/](https://github.com/lucyimbrell/error_analysis_lithics/)

### 7.4.1. Linear metric analysis

We first explored whether the measurements were recorded consistently on the replicas between observers. Figure 19 shows the distribution of the multiple observer data through boxplots; most of the measurements have very limited variance around the mean, and all tools were significantly different to each other across all measurements when tested using Tukey's Honestly Significant Difference (HSD;  $p < 0.001$ ). Thickness is the most variable dimension recorded, probably because it is more difficult to orient the tool for this measurement than it is for length or width. Calculation of the coefficient of reliability between each pair of observers found that all values of  $R$  were  $>0.999$ , suggesting that over 99% of the variance in each measurement is due to variability between the specimens as opposed to error. We calculated the  $TEM$  as 0.368 and the  $\%TEM$  as 0.908, supporting that less than 1% of the variance in the dataset is related to measurement error. Finally, the  $ICC$  score confirmed that there is very high absolute agreement between the observers ( $ICC = 1$ ,  $p < 0.001$ ).

We then compared the measurements taken by multiple observers with those taken by a single observer as a means of comparing intra- and inter-observer error. We first calculated the coefficient of reliability for the single observer for each pair of replica assemblages – we found that all values were  $>0.999$ , indicating very high congruence between repeat captures by the single observer. Table 10 reports the mean and standard deviation of length, width, and thickness for the single observer compared to multiple observers; two-sample t-tests found that there were almost no statistically significant differences in means between the data sets ( $1/36 = p < 0.05$ ; Table 11). However, F-tests found that half of the measurements show statistically significant differences in variance, particularly along length and width (Table 11). This demonstrates that the single observer is generally less prone to error, which is likely due to a combination of the familiarity of this observer to both the metric definitions and the assemblage and the fact that the same equipment was used to measure all of the replicas. Nonetheless, that fact that these differences in

variance only resulted in a single instance of significant difference in mean, plus the standard deviation does not exceeds 0.7 mm, suggests that the effects of inter-observer error are minimal on the results.

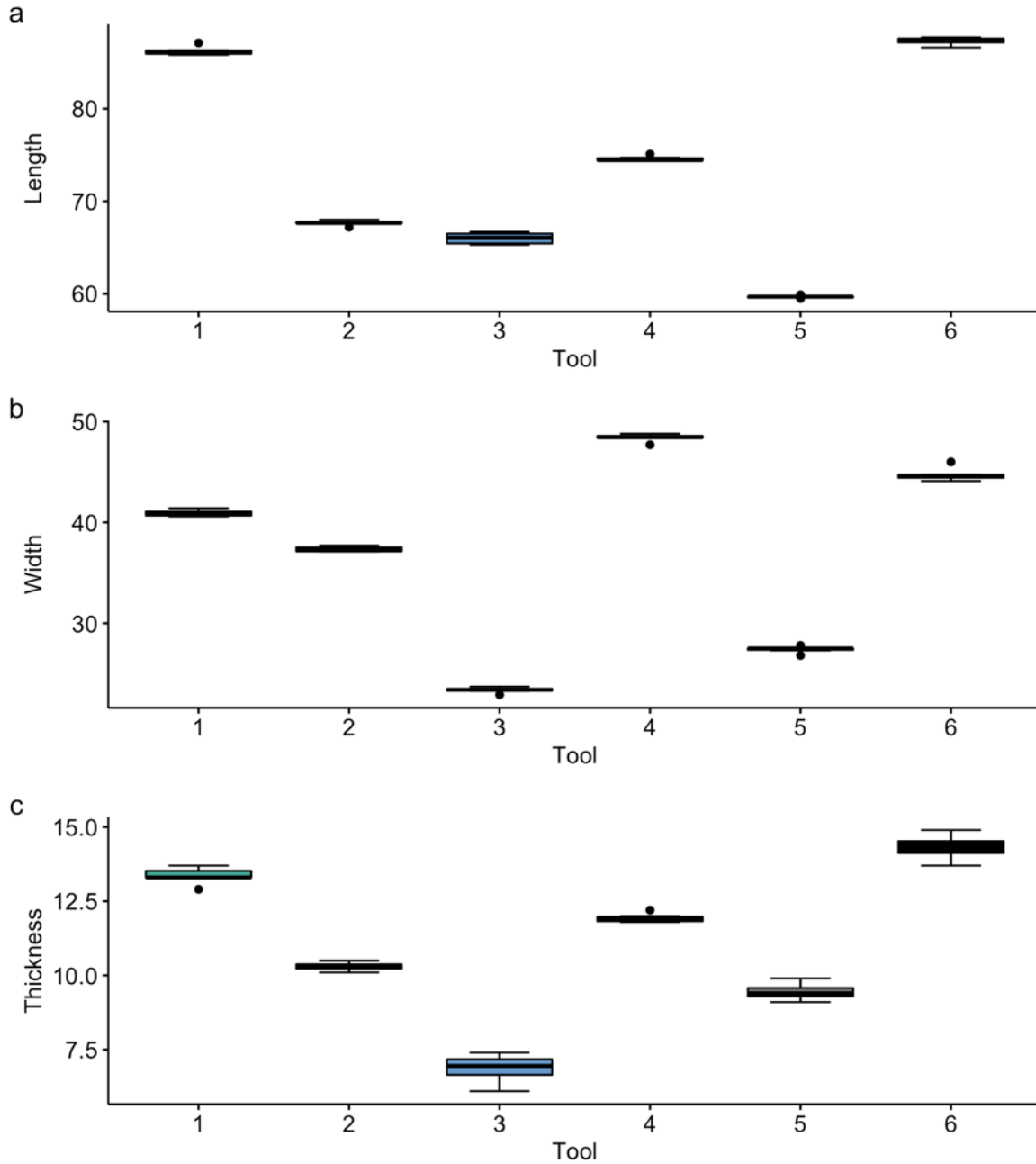


**Figure 19.** Boxplots demonstrating the distribution of length, width, and thickness (mm) collected by multiple observers for each tool (1-6).

**Table 10.** Summary statistics reporting the mean (m) and standard deviation (sd) obtained for length, width and thickness, recorded by multiple observers versus a single observer for each tool (1-6). Standard deviation values have been rounded to 3 decimal places.

|   | Length (mm) |           |          |           | Width (mm) |           |          |           | Thickness (mm) |           |          |           |
|---|-------------|-----------|----------|-----------|------------|-----------|----------|-----------|----------------|-----------|----------|-----------|
|   | Multiple    |           | Single   |           | Multiple   |           | Single   |           | Multiple       |           | Single   |           |
|   | <i>m</i>    | <i>sd</i> | <i>m</i> | <i>sd</i> | <i>m</i>   | <i>sd</i> | <i>m</i> | <i>sd</i> | <i>m</i>       | <i>sd</i> | <i>m</i> | <i>sd</i> |
| 1 | 86.2        | 0.471     | 86.3     | 0.175     | 40.9       | 0.308     | 40.9     | 0.103     | 13.4           | 0.281     | 13.3     | 0.248     |
| 2 | 67.6        | 0.266     | 67.6     | 0.089     | 37.3       | 0.258     | 37.5     | 0.228     | 10.3           | 0.141     | 10.4     | 0.075     |
| 3 | 66.0        | 0.613     | 66.3     | 0.137     | 23.4       | 0.266     | 23.3     | 0.225     | 6.87           | 0.472     | 6.72     | 0.075     |
| 4 | 74.6        | 0.279     | 74.4     | 0.299     | 48.4       | 0.374     | 48.5     | 0.103     | 11.9           | 0.151     | 11.8     | 0.105     |
| 5 | 59.7        | 0.133     | 59.7     | 0.075     | 27.4       | 0.335     | 27.6     | 0.082     | 9.45           | 0.281     | 9.48     | 0.147     |
| 6 | 87.3        | 0.405     | 87.4     | 0.063     | 44.7       | 0.659     | 44.6     | 0.126     | 14.3           | 0.415     | 14.2     | 0.117     |

**Table 11.** P-values from t-tests (difference in mean) and F-tests (difference in variance) comparing the metrics (length, width, and thickness) for each tool (1-6) measured by multiple observers versus a single observer. Statistical significance ( $p < 0.05$ ) is marked by an asterisk (\*). All values have been rounded to 3 decimal places.

|   | Length (mm) |        | Width (mm) |        | Thickness (mm) |        |
|---|-------------|--------|------------|--------|----------------|--------|
|   | T           | F      | T          | F      | T              | F      |
| 1 | 0.815       | 0.049* | 0.632      | 0.032* | 0.673          | 0.792  |
| 2 | 0.678       | 0.032* | 0.264      | 0.792  | 0.240          | 0.193  |
| 3 | 0.342       | 0.005* | 0.498      | 0.724  | 0.475          | 0.001* |
| 4 | 0.342       | 0.879  | 0.689      | 0.013* | 0.037*         | 0.446  |
| 5 | 0.608       | 0.238  | 0.152      | 0.008* | 0.804          | 0.182  |
| 6 | 0.575       | 0.001* | 0.646      | 0.002* | 0.653          | 0.015* |

#### 7.4.2. Geometric morphometric analysis

PCA was used to highlight variance in the multiple observer data. The first 3 PCs represented >90% of the variation between the replicas, and thus were explored in this study. Figure 20 demonstrates the shape differences highlighted by PC1-3. PC1 represents 59.7% of the total variance, whilst PC2 and PC3

account for 33.4% and 3% respectively (see Appendix 2: Supplementary Fig. S3 for scree plot of PC loadings and cumulative variance).

When the first 3 PCs are plotted against each other, clear clustering occurs, demonstrating that replicas of the same tool tend to share more similarities than that of different tools (Fig. 21). However, there is notable variation within tools along PC3, suggesting that inter-observer error deriving from photography equipment and set-up is prevalent in this dimension. PC3 is an axis of variation represented by slight asymmetries in convexity at the proximal end (Fig. 20), thus likely reflecting parallax error between observers. Additionally, we note some overlap between certain tool groups, although this is primarily because these tools share similar shapes once size is removed (Appendix 2: Supplementary Figure S2). For example, Tool 5 sometimes plots within the range of variation for Tool 1 and only shows statistically significant differences in mean from this tool along PC2 ( $p < 0.008$ ; see Appendix 2: Supplementary Table S2 for Tukey's HSD results comparing differences in mean between tools). To tease apart the variation between the tools and that associated with error, we calculated the coefficient of reliability between each pair of observers, which ranged between 0.960 and 0.999 (Table 12), suggesting that <4% of the variance is due to inter-observer error, which lies within our acceptable threshold. The *ICC* was computed using the first 3 PC scores to determine levels of similarity between the six observers, whilst taking into account the variability between the tools, and found an almost perfect agreement ( $ICC = 0.99$ ,  $p < 0.001$ ). Finally, we found that an LDA could discriminate accurately between the replica groups (94% classification accuracy) and could not differentiate between observers (0% classification accuracy).

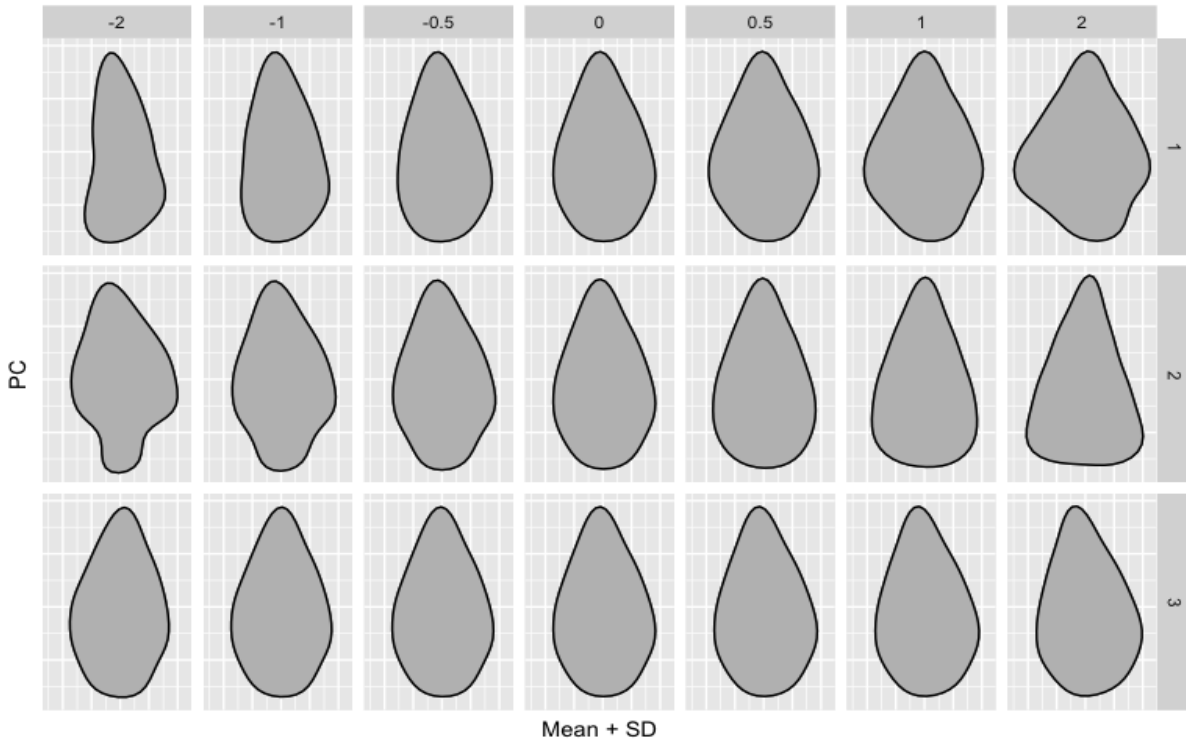


**Figure 20.** Principal component (PC) contributions along the first 3 axes of variance within the multiple observer outline data.

**Table 12.** Coefficient of reliability (R) values for pair-wise combinations of observers using the first 3 PC scores. For observer abbreviations and associated assemblage numbers, see Table 1. All values have been rounded to 3 decimal places.

|      | INSAP | IM    | MBAP  | NME   | NMK   |
|------|-------|-------|-------|-------|-------|
| IM   | 0.988 |       |       |       |       |
| MBAP | 0.978 | 0.960 |       |       |       |
| NME  | 0.984 | 0.975 | 0.995 |       |       |
| NMK  | 0.969 | 0.969 | 0.985 | 0.992 |       |
| MH   | 0.989 | 0.978 | 0.993 | 0.999 | 0.990 |

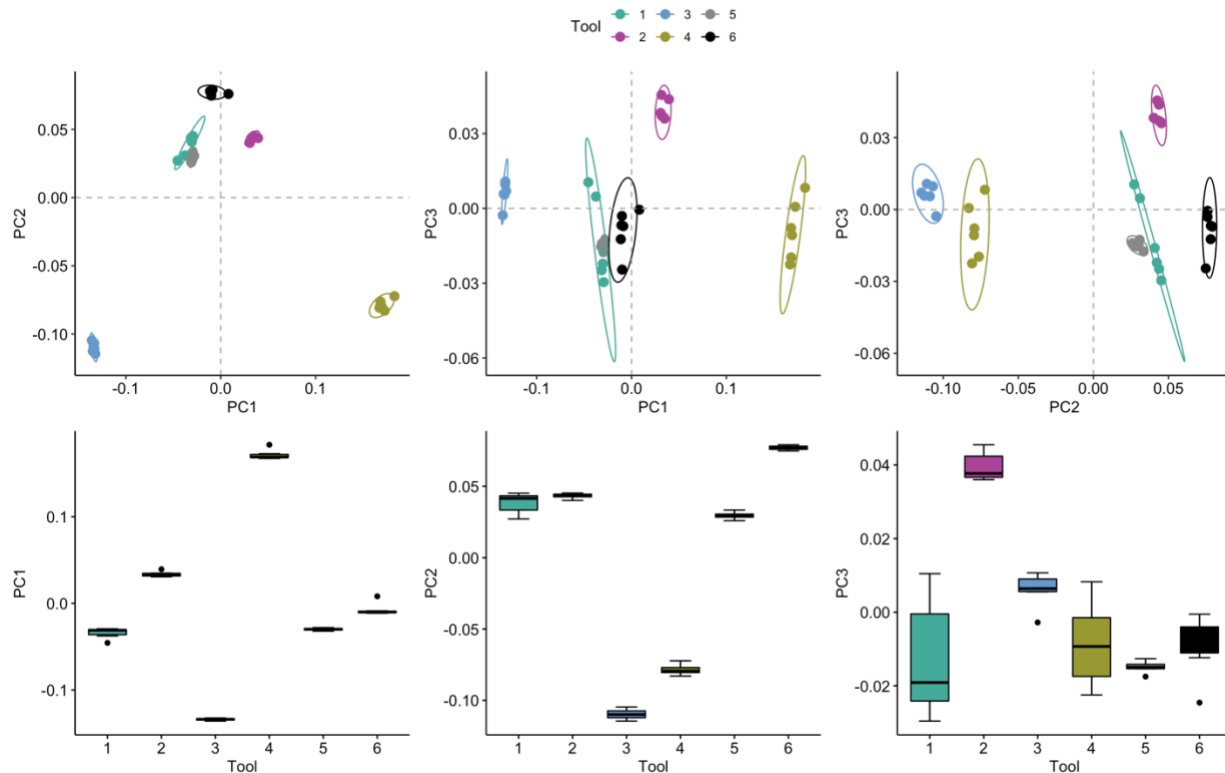


**Figure 21.** Scatterplots (top row) and boxplots (bottom row) of repeat capture scores along principal components (PC) 1-3, demonstrating the clustering within tools (1-6). PC1 represents 59.7% of the total variance, whilst PC2 and PC3 account for 33.4% and 3% respectively.

Next, we compared the levels of error obtained when collating photographs from multiple observers and that which arises when all replicas are photographed by the same observer. We performed another PCA with data acquired from both sets of images (see Appendix 2: Supplementary Fig. S4-5 for PC contributions and loadings) and produced scatterplots of PC1-3. Figure 22 demonstrates clear clustering between tools recorded in both sets of data along PC1 and PC2. However, along PC3 there is clear variability within repeats when grouped by observer (multiple vs single). F-tests found that the variance among certain tools was only significantly higher for the multiple observers in three cases, i.e., Tool 4 and 1 along PC3 and Tool 4 along PC1 (Table 13). Two sample-t-tests found statistically significant differences in means between the data sets, but these are limited ( $5/36 = p < 0.05$ ; Table 13). Table 14 and Figure 22 demonstrate that the data collected by a single observer returns lower variance, though this pattern is not strong, and, in a few cases, it is slightly higher under this strategy, though not significantly so. We finally calculated the coefficient of reliability for the single observer between each of capture of the replica assemblages – Appendix 2: Supplementary Table S3 shows that the *R* values ranged from 0.994 to 0.999, suggesting that <1% of the variance in the single observer data is due to intra-observer error.

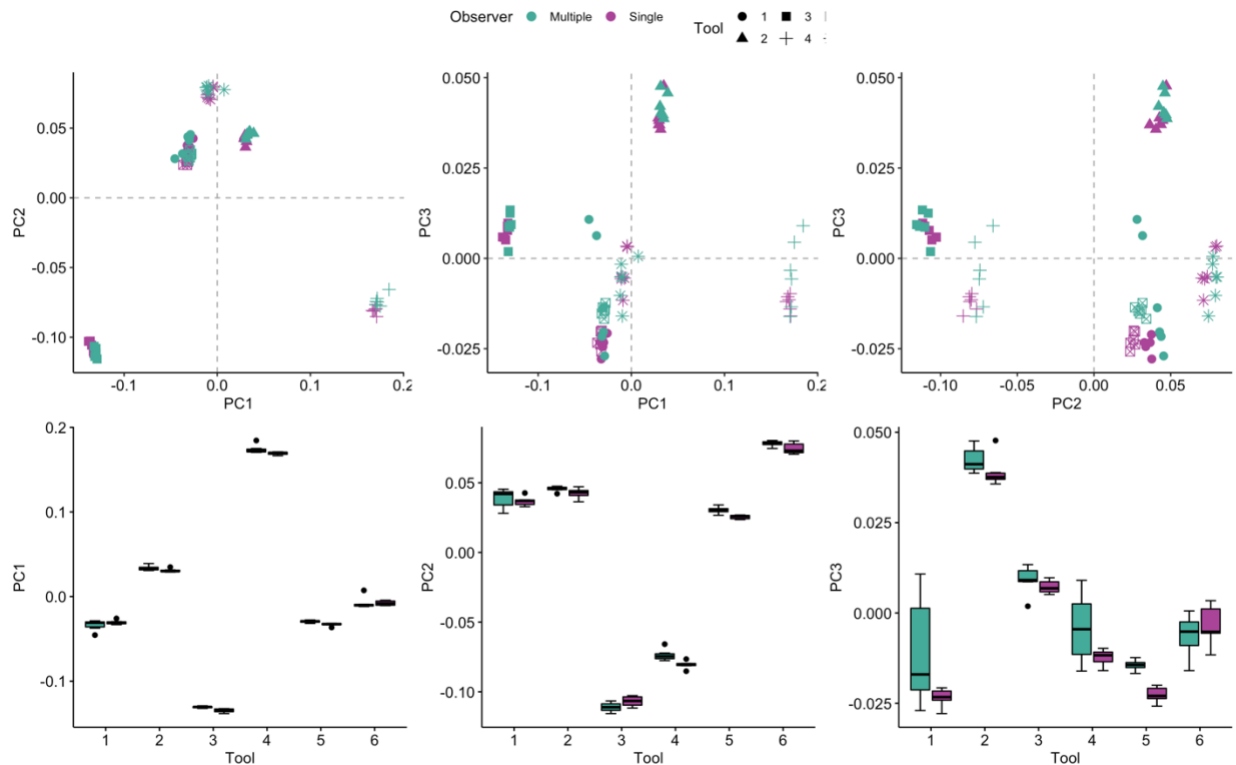


**Figure 22.** Scatterplots (top row) and boxplots (bottom row) of repeat capture scores along principal components (PC) 1-3, demonstrating the clustering within tools (symbols) and between data sets (colors). PC1 represents 60.4 % of the total variance, whilst PC2 and PC3 account for 33.5% and 3.3% respectively.

**Table 13.** P-values from t-tests (difference in mean) and F-tests (difference in variance) comparing the principal component (PC) scores of the repeats of each tool (1-6) captured by multiple observers versus a single observer. Statistical significance ( $p < 0.05$ ) is marked by an asterisk (\*). All values have been rounded to 3 decimal places.

|   | PC1    |        | PC2    |       | PC3    |        |
|---|--------|--------|--------|-------|--------|--------|
|   | T      | F      | T      | F     | T      | F      |
| 1 | 0.282  | 0.068  | 0.556  | 0.141 | 0.110  | 0.001* |
| 2 | 0.091  | 0.463  | 0.114  | 0.162 | 0.188  | 0.671  |
| 3 | 0.006* | 0.119  | 0.067  | 0.873 | 0.335  | 0.115  |
| 4 | 0.082  | 0.029* | 0.009* | 0.384 | 0.099  | 0.006* |
| 5 | 0.004* | 0.663  | 0.003* | 0.257 | 0.000* | 0.411  |
| 6 | 0.954  | 0.056  | 0.095  | 0.157 | 0.441  | 0.939  |

**Table 14.** Summary statistics reporting mean (*m*) and standard deviation (*sd*) of principal component (PC) scores of the repeats of each tool (1-6), captured by multiple observers versus a single observer. All values have been rounded to 3 decimal places.

|   | PC1      |           |          |           | PC2      |           |          |           | PC3      |           |          |           |
|---|----------|-----------|----------|-----------|----------|-----------|----------|-----------|----------|-----------|----------|-----------|
|   | Multiple |           | Single   |           | Multiple |           | Single   |           | Multiple |           | Single   |           |
|   | <i>m</i> | <i>sd</i> | <i>m</i> | <i>sd</i> | <i>m</i> | <i>sd</i> | <i>m</i> | <i>sd</i> | <i>m</i> | <i>sd</i> | <i>m</i> | <i>sd</i> |
| 1 | -0.034   | 0.006     | -0.031   | 0.003     | 0.039    | 0.007     | 0.037    | 0.003     | -0.011   | 0.016     | -0.023   | 0.003     |
| 2 | 0.034    | 0.003     | 0.031    | 0.002     | 0.046    | 0.002     | 0.042    | 0.004     | 0.042    | 0.004     | 0.039    | 0.004     |
| 3 | -0.131   | 0.001     | -0.135   | 0.002     | -0.111   | 0.003     | -0.107   | 0.004     | 0.009    | 0.004     | 0.007    | 0.002     |
| 4 | 0.174    | 0.005     | 0.169    | 0.002     | -0.074   | 0.004     | -0.081   | 0.003     | -0.004   | 0.01      | -0.012   | 0.002     |
| 5 | -0.03    | 0.001     | -0.033   | 0.002     | 0.03     | 0.003     | 0.025    | 0.001     | -0.014   | 0.001     | -0.023   | 0.002     |
| 6 | -0.008   | 0.007     | -0.008   | 0.003     | 0.078    | 0.002     | 0.074    | 0.004     | -0.006   | 0.006     | -0.004   | 0.006     |

## 7.5. Discussion

Here we present a control study that validates the use of the collaborative data collection protocol presented in Timbrell (2022), which can now be used more extensively by other researchers to reduce travel and carbon emissions, as well as to bring researchers from other geographical areas into the collaborative process more directly. Our results demonstrate that the levels of inter-observer error permeating shape data collated under a collaborative research framework fall within the acceptable threshold, thanks to the establishment of clear research protocols followed by each collaborator. We found that, inevitably, increases in error occur as a consequence of relying on multiple observers, who each have access to different equipment, yet we do not deem this to be significant enough to highly distort the results towards a different conclusion about the data. Therefore, our innovative 3D printing approach and the results reported here have important implications for error assessments of linear metric and GMM data when recording lithic shape as well as the aggregation of data collected by multiple observers.

Outline based GMM was found to be slightly more sensitive to inter-observer error than metric methods. As Caple, Byrd and Stephan (2018) point out, EFA involves global descriptors capturing around 99% of the variance in the outline shape, and therefore discrepancies between images lead to error in the



coefficients dispersed throughout the full outline. Therefore, even if the error is not equally distributed, it is measured as such and consequently outline methods are often more sensitive to error than linear methods that capture only certain dimensions of an object. 2D outline based GMM provides comprehensive morphological information on the gross outline shape of an object, whereas linear metrics are able to capture aspects of the 3D shape but in much less detail; the increase in the morphological information captured, plus the added potential for automated data capture (e.g. Bonhomme *et al.*, 2014; Matzig, 2021) and impressive shape visualization (e.g. Fig. 20), will be worth the potential increase in error with 2D GMM in many scenarios.

Our use of PCA to highlight axes of variance within lithic shape assemblages also demonstrates that inter-observer error does not affect all PCs equally. As outlined by Page (1976), subtle errors in each variable are combined in multivariate analyses and can be extracted by a single or small set of PCs, although they may also describe real aspects of covariance and so require careful consideration as to their source. When undertaking metric analyses, it is possible to assess error in each individual measurement; if the metrics are combined via dimension reduction methods such as PCA, the contributions of each individual measurement to each PC are readily identifiable through the PCA coefficients. This is less feasible with GMM data, particularly when using outlines and semi-landmarks, and in such cases, it is preferable to assess error on each of the leading PCs, as demonstrated above, rather than on each set of coordinates, which can be very numerous. Overall, error is impossible to avoid completely, and indeed the imperfect fidelity of cultural transmission means that copying errors can naturally occur during the knapping process and inflate variance between and within assemblages (Eerkens and Lipo, 2005; Schillinger, Mesoudi and Lycett, 2014). In this sense, error is certain to arise within a data set capturing lithic variability; however, steps can be taken to ensure it is minimized, such as standardization of data acquisition, processing, and analytical procedures, calibration, high quality equipment, and assessment of error through repeat measures (Evin, Bonhomme and Claude, 2020; Lyman and VanPool, 2009; Robinson and Terhune, 2017; Yezerinac, Loughheed and Handford, 1992). In the case of the current study, we determine that inter-observer error is low enough for accurate analyses under both methods, especially as the high *ICC* and *R* values demonstrate acceptable levels of congruence between the six observers.

Through the development of clear research protocols, our results demonstrate that multiple observers can successfully work together to produce sets of comparable data for aggregation. We believe that collaborative research designs, such as the one reported in Timbrell (2022), play an integral role in addressing the vulnerabilities of international research to disruption, revealed most recently in 2020 by the outbreak of coronavirus (COVID-19), which halted both domestic and international travel as well as

social interaction. Our results suggest that, as well as single researchers visiting multiple collections to independently access lithic samples, international colleagues are also able to work together *in situ* to generate data, thereby building resilience in archaeological practice (Douglass, 2020; Scerri *et al.*, 2020). We stress though that collaborative research designs should involve an equitable partnership in relation to the data, following the imminent Cape Town statement (see Else, 2022), with all researchers being involved in all stages of the research, from planning and protocol development to publication and dissemination (Chirikure, 2015; Douglass, 2020). In this way, dual project development can enable local researchers to benefit from international archaeological research, thereby avoiding some (but not all) of the neo-colonial ‘helicopter’ practices that have been hugely criticized in archaeological and anthropological sciences, particularly in Africa (Ackermann, 2019; Athreya and Ackermann, 2019; Sahle, 2021). We have provided here an initial pilot test of collaborative data collection using a 3D printing approach. This approach is unique and, to our knowledge, has not yet been applied in the context of lithic variability nor inter-observer error assessments. We propose that future studies should aim to reproduce our approach with more expanded samples of replica artefacts and discuss three important aspects of potential future study design below.

The first aspect relates to the use of statistics and simple metrics for reporting inter-observer error. Statistics such as the *ICC* and *%TEM* express the error variance relative to the overall variance of the sample; variance is decomposed into that due to genuine variation among the artefacts and that due to variation among the observers (including that due to different individuals, their different cameras, lenses, etc.). Whilst this approach has many advantages, one immediate drawback is that these statistics are directly affected by the magnitude of genuine variation in both the sample of artefacts and in the dimensions measured. A given, constant level of measurement error will appear large when the artefacts measured are highly standardized, but small when the artefacts measured are highly variable. Even if one were to measure the widths and lengths of a set of highly standardized artefacts, a given level of measurement error would appear smaller the further the ratio of width to length is from unity, as this would increase the magnitude of genuine variation in the measurements taken. For this reason, it is always valuable to present simple indices of *absolute* error (such as standard deviation or variance) for *single* measurements alongside the indices of relative error variance across all measurements provided by the *ICC* and *%TEM*. Such simple indices are valuable in assessing inter-observer error even when the ultimate study involves more sophisticated morphological analyses, such as those based on GMM. In the current study, Table 2 presents such indices, and demonstrates that levels of error are minimal (the largest standard deviation among multiple observers for a single measurement = 0.613mm).

The second aspect relates to the exploration of the effects of the raw material used for production of the reference collection on the results of comparative studies. In this study, we used flint because it was available and accessible at the University of Liverpool, where the materials were prepared. This fine-grained raw material tends to produce well-defined features and edges, and so it would be interesting to replicate the approach with a more coarse-grained material, such as quartzite, chert, calcrete or sandstone. This is especially pertinent in our case as the shapes obtained from these materials are likely to be more representative of the actual African stone tools that have been recorded in the main project. However, we note that heat-treated silcrete may achieve a grain as fine as flint (Key *et al.*, 2021), and that obsidian can be even finer-grained than flint; since both silcrete and obsidian are raw materials commonly found in African Middle Stone Age assemblages, we suggest that the flint used here acts as a suitable middle ground in terms of granularity and can therefore be considered as broadly comparable to those raw materials studied in the main project.

Finally, an aspect of variation between individual replicas that we did not explicitly measure is that which can arise through 3D printing. Zeng and Zou (2019) outline some of the factors that can affect the precision of 3D printing, which include slicing and support errors. However, we propose that, even if there are printing errors present in our replicas, these are likely minimal due to the highly comparable data obtained across the project. Additionally, printing errors should not contribute to differences between the two data collection strategies as both the multiple observers and the single observer recorded measurements from the same set of replicas. Depending on the local accessibility of 3D printers, our approach to inter-observer testing could be further streamlined through the direct sharing of the virtual 3D models, with each collaborator printing their own copies to measure. This would alleviate potential logistical problems with global distribution, both via mail or directly, though further research is required to ascertain the variation in objects printed using different models of 3D printers.

## 7.6. Conclusion

Aggregating lithic shape data requires careful consideration in order to reduce potential sources of inter-observer error that can result in detrimental consequences on the results and their interpretation. Our analysis of metric and outline-based 2D GMM data from multiple observers found that the former performed slightly better than the latter in our tests of inter- and intra-observer error, primarily due to differences in the nature and detail of the morphological information obtained, though both approaches returned levels of error deemed acceptable for accurate analyses. Standardization of the data collection procedure is vital for ensuring that congruence between observers is maintained, though we note that this

alone cannot completely eradicate error as we find that variability between observers can still be detected within our data to a (sometimes) significant extent. Nonetheless, we believe that producing replica samples through 3D printing could have many useful applications within archaeological and anthropological sciences beyond the study of error in the analysis of lithic assemblages and should be adopted more widely in assessments of inter-observer error as an integral component of international collaborations between institutions.

## Chapter 8. Eastern African Middle Stone Age point shape variability

### 8.1. Introduction

Across the world, stone points are routinely used by archaeologists to chronologically and spatially order the prehistoric record (Shott, 2020). Since its inception, the MSA (and its industries) has been defined based on the presence of regionally variable points, among other features (Goodwin and van Riet Lowe, 1929). In north Africa, the Aterian industry is recognised by the presence of tanged points (Iovita, 2011), whilst in southern Africa affiliation to the Still Bay requires the presence of bifacial foliate points (Archer et al., 2016). Such distinctive point styles have been argued to represent the spatiotemporal distribution of regional cultures during the MSA (McBrearty and Brooks, 2000). In eastern Africa, Clark (1988) asserted that the form of MSA points varies considerably, whilst also being distinctive from other regions. For example, he noted that, in the Rift Valley, unifacial and bifacial foliate and triangular points dominated MSA assemblages, while in the Horn of Africa, there is much more technological and typological variability, such as leaf-shaped points from Porc-Epic and Levallois points from Midhishi (Clark, 1988). Although these early observations highlight that eastern African MSA points demonstrate marked patterns of formal variability, points from eastern Africa have received relatively less attention as proxies for shared group identity compared to other regions of the continent.

Although archaeologists have proposed MSA industries for eastern Africa, these are usually limited to individual sites or simply borrow nomenclature from other regions (Shea, 2020). As a result, eastern Africa does not have highly distinctive and widely applied cultural variants that divides its MSA record. This makes eastern Africa a particularly important laboratory for testing hypotheses about the casual mechanisms of variation observed in the ‘generic’ MSA record, i.e., assemblages that are deemed to be MSA but without any further cultural division. The MSA is polythetic, meaning that it is defined by a number of criteria, not all of which need to be met to be considered part of the group. Points are considered to be one of the defining features of the MSA, yet the rarity of points is not sufficient to exclude attribution of an assemblage to the MSA (e.g., Mumbwa Caves [Barham, Pinto and Andrews, 2000]). However, because certain point technologies/typologies are seen to be indicative of specific cultural industries, assemblages without distinct signs of regionalisation, such as specific MSA point variants, are somewhat understudied. The underlying structure of variation throughout the MSA is unknown, making it somewhat impossible to ascertain whether the MSA at a continental or even regional level is even a coherent unit of analysis. Due to the significance of points for defining the MSA, and the apparent link between standardised point forms and shared traditions

between interacting populations, this chapter will present a metric and geometric morphometric analysis of eastern African MSA points and then evaluate the potential causal mechanisms of variation observed in the record.

### 8.1.1. Function of eastern African MSA points

'Point' is often used synonymously for 'projectile' due to the initial widespread belief that they were hafted components of thrown hunting armatures during the MSA (e.g., McBrearty and Brooks, 2000). In eastern Africa, there is considerable evidence that points were indeed manufactured for projectile weaponry. For example, Sisk and Shea (2011) found that the bifacial and unifacial points at Porc-Epic had similar metrical properties to ethnographic dart tips, reinforcing a proposed projectile function. At Mumba Rockshelter, Tanzania, evidence of hafting modifications, such as thinning and notching at the distal end, and macroscopic tip damage has also been suggested to demonstrate that MSA points were designed and hafted for insertion into wooden shafts to create arrows and spears (Bushozi, 2011; Brezke, Marks and Conard, 2006). Brezke, Marks and Conard (2006) compared the weight and tip cross-sectional area (TCSA) values of the Mumba Cave points with a published ethnographic dataset of thrown and thrusting spears, spear-thrower projectiles, and arrows. Their results showed that, although not all examples could be confidently assigned to one of the groups, the variation in these parameters was interpreted to indicate the co-existence of multiple weapons systems. Yet they found that point shapes did not co-vary with size, and therefore concluded that point morphology does not equate or relate to function, with only size being informative about the delivery system of the tool. Notably, the authors did not test for any other potential uses of the points like cutting, incising, and sawing, undermining the evidence for points being used in this way during the MSA (e.g., Lombard, 2007; Rots, van Peer and Vermeersch, 2011). A homogenous conception of the 'point' as a projectile is likely an overgeneralisation as it fails to capture the full range of variability falling under this shared generic concept which seemed to have had some emic significance for hominin populations during the MSA, as shown by the proliferation of pointed flake technology across Africa following the ESA.

Douze and Delagnes (2016), in their technological analysis of the early MSA points from the Gademotta and Kulkuletti site complex, differentiated between point production involving shaping of undetermined blanks and that involving the retouching of predetermined blanks. They suggest that pointed forms achieved by shaping were likely multi-purpose tools, due to the presence of multiple functional edges, whilst those achieved via pre-determination and retouch were likely projectile technology due to the penetrative potential of the tip. Such techno-typological approaches (e.g., Conard, Porraz and Wadley, 2012; Slater, 2016; Douze *et al.*, 2020; Timbrell *et al.*, 2022c; Maier *et*

*al.*, 2023) are likely more effective for determining potential use than those reliant on typology alone. For example, in analyses of the MSA assemblages at Aduma (Ethiopia), Sahle and Brooks (2019) found that point forms at the site change through time, with the oldest points showing larger dimensions and TCSA values than ethnographic spears. The authors suggested that this may represent a shift from simple spear technologies to more refined and complex projectiles. However, whilst it is true that Sahle and Brooks (2019) also considered impact fractures, just 23% of the analysed points demonstrated potential signs of impact-related damage, with only half of those exhibiting damage fractures commonly considered diagnostic of that found on hunting armature tips. Rots and Plisson (2014) drew attention to the problematic nature of using such diagnostic features of impact damage, stating that without detailed analyses of large reference collections of experimental tools, the reliability of the analogy is impossible to determine. Recently Lombard *et al.* (2022) expanded ethnographic datasets obtained from hafted weapon tips and/or weapon tips of known use, mostly from sub-Saharan Africa, and found that TCSA ranges were in fact useful for identifying different types of hafted weaponry.

Rots (2016), however, argues that evidence of hafting is essential for determining ‘points’ and their function, with the TCSA only useful following microwear and residue analyses. Yet, traces of microwear and residue are only rarely preserved, and the time-consuming process of detecting them limits large scale analysis. Shea and Sisk (2011) also highlight that making references to ethnographic collections requires careful consideration, as ‘points’ in museums are often biased towards those that are more heavily retouched, yet experimental work has demonstrated that unretouched, minimally retouched and wooden points may also have functioned adequately as projectiles (Sisk and Shea, 2009; Waguespack *et al.*, 2009), thus leading to an under-appreciation of technological strategies for manufacturing hafted point technology in archaeological populations. Overall, the identification of hafted point technology in the archaeological record is difficult, with little agreement over whether typological characteristics of pointed tools, such as the TCSA, hold merit in these discussions about function.

### 8.1.2. Technology and typology of eastern African MSA points

Point designs during the MSA were likely constrained by the functional requirements of the tool, with the type and quality of raw material and reduction method used also potentially influencing the range of shapes that could be produced (McBrearty and Brooks, 2000). Points are fundamentally components of hunting technology; however, they have also been argued to represent the single artefact category within MSA toolkits that most likely reflects group identity and population structure (McBrearty and Brooks, 2000; Wilkins, 2010). This is because, ethnographically, points are traded

between groups that come into contact across the hunting landscape, with comparable designs among co-operating neighbours maintained to ensure that they can be used by several hunters within the 'hxaro' exchange system (Yellen, 1977; Wiessner, 1982, 1983, 1985; Nicholas and Kramer, 2001). Therefore, whilst typology is unlikely to be useful for determining point function as a hunting armature, their technological and typological characteristics are likely to be informative to some extent about group style and thus interaction. Bushozi (2011) in his doctoral dissertation analysed 261 points from the MSA and MSA/LSA transitional layers at Nasera, Mumba and Magubike in Tanzania. Triangular blanks were found to have been selected for point production, due to the minimal modification required to obtain a desirable shape, with unifacial points making up over half of the sample, Levallois points comprising around 33% and bifacial points 14% respectively. His results demonstrate that, at all sites, a consistent range of butt modification strategies and retouch modifications are present in both MSA and transitional assemblages, interpreted to represent continuity in regional traditions and the presence of complex population networks which shared technological knowledge.

Geometric morphometric analyses of the full MSA sequence at Mumba found consistently high morphological variability and no significant changes in shape through time (Brezke and Conard, 2017). Yet, these authors suggest that this pattern demonstrates technological flexibility and the development of multiple hunting systems, rather than evidence for the maintenance of regional traditions. It is possible that such differences in interpretation derive from the variable information ascertained by technological and typological analyses, whilst taking a site-based approach over that which considers regional patterns of variability may also influence the conclusions drawn, with the supplementary spatial dimension by Bushozi (2011) indicating that certain aspects of variability were not only maintained from generation to generation but also across large areas. Additionally, temporal variation within a site can represent a number of processes, such as technological flexibility within a single population, adaptation to the environment within a single population, and/or multiple populations with different technologies (Foley, Mirazón Lahr and Mailio-Fernandez, 2013), the latter two echoing the famous Bordes-Binford debate (Bordes, 1950; Binford and Binford, 1966). Patterns of chronological variability can therefore reflect a number of processes, as opposed to being purely functional (Sahle and Brooks, 2019) or stylistic.

Methods for determining function from typology are heavily debated and the alternative of systematic micro-use-wear and residue analyses is extremely labour intensive, limiting our understanding of how reliably archaeologists can identify points in lithic assemblages and what information is conveyed by their variability. However, whilst the delivery system of a point (i.e., as a hand-thrown spear, spear thrower, bow and arrow etc.) likely affects the characteristics of the tool (Coppe, Leper and Rots,



2022), ethnographic observations, in conjunction with the evidence for sporadic point form standardisation in the MSA, implies that point morphology is likely indicative, at least to some extent, of MSA social networks. Whether all ‘points’ are equally as informative in this context still remains unclear and careful consideration is required about the theoretical expectations of variation deriving from socially transmitted style as opposed to that which is functional, as well as spatial or temporal autocorrelation, as discussed below.

## 8.2. Theoretical expectations of population structure and point variability

Archaeological similarities and differences in relation to population structure need to take into account that neutral forms of cultural evolution can also generate patterns of variability. Isolation-by-distance (IBD), isolation-by-time (IBT) and isolation-by-environment (IBE), originally developed from genetic theory (Wright, 1943), can thus be utilised as null models. IBD is the observation that decreases in genetic similarity among populations occurs as the geographic distance between them increases due to the negative effect of distance on rates of gene flow (Wright, 1943). Similarly, IBT is defined as decreasing genetic similarity between two populations as the chronological distance between them increases (Wright, 1943). IBE can be defined as the pattern of increased genetic differentiation with increased environmental differences, independent of geographic distances; unlike the first two, which relate to patterns of gene flow and drift, IBE is usually related to adaptation to localised environmental pressures.

Within the context of archaeological data, cultural transmission and the transfer of skills depends on close interaction between individuals through space (Tostevin, 2012); interaction declines with geographic distance thus, when controlling for other confounding factors, similarity in transmitted cultural diversity has also been found to decrease (Neiman, 1995; Shennan, 2020). Under IBD in archaeology, similarities are expected between proximal sites, as the generation of novel variation (innovation) in one place is less likely to be transmitted to populations further away than those at proximity. Temporal change results from the random loss of variants during transmission through time (drift), with archaeological similarities expected between sites of similar ages under IBT (Shennan, 2020). Similarities in assemblages may also represent comparable adaptive solutions to similar environmental (or social) contexts (IBE). Patterns of IBD and IBE are likely highly correlated as populations that share the same geography likely also share similar environments, which may generate similar patterns. Moreover, archaeological diversity is both spatially and temporally autocorrelated; differences between any two entities increases as a function of the temporal and spatial distance between them (Loog *et al.*, 2017). The extent to which spatial differences contribute to cultural diversity relies heavily on population structure and mobility, with low mobility leading to

strong spatial structure. This means that differences are more likely to be correlated with space relative to time (Loog *et al.*, 2017). Applying this logic, Blinkhorn and Grove (2021) used a highly correlated ‘timespace’ variable that recognised the combined influence of space and time and found that it exhibits a stronger and independent correlation to eastern African MSA variability than other spatial variables, emphasising the potential role of cultural transmission and inheritance on innovation during the MSA.

Another particular issue when considering cultural data is that convergence has the potential to confound interpretations of variability under these null models. Convergence describes the appearance of similar ideas or technological solutions arising from independent innovation – i.e., without interaction and cultural transmission. Convergent culture may arise as similar evolutionary answers to adaptive forces within similar environmental or social contexts (such as Nubian-style points; Hallinan and Shaw, 2020), or as a result of their similar function, or simply just by chance (Will and Mackay, 2020). Large-scale patterns of IBE could be considered to be a form of environmentally driven convergence in some (but not all) cases, with cultural similarities appearing in comparable environments that are too geographically or temporally distant to be explained by transmission and therefore arise as comparable technological solutions to those environmental conditions. Distinguishing convergence from spatial, temporal, and environmental autocorrelation is another important step in understanding patterns of archaeological diversity, with comparative analyses over wide geographic areas and chronological timespans key for identifying similarities that could not have arisen through cultural transmission.

Because points are fundamentally tools, certain aspects of their morphology are likely to be influenced by the selective environment in which design choices affect performance. During the MSA (and indeed other chronological periods), point designs were likely modified over time due to small copying errors that arise during trial and error. Those modifications that increased performance during the intended task would have likely been ‘selected for’ and passed on to the next generation (Dunnell, 1978). Stylistic variability concerns the aspects of shape that are not functional (Sackett, 1982), and therefore are not directly conditioned by the selective environment. These aspects of point typology are therefore more prone to random drift through the accumulation of copying errors over time. Style can, however, be both active and passive; MSA populations may have actively incorporated style into their point designs to demonstrate group affiliation and facilitate trading for meat, as seen in the hunter-gatherer gift exchange system ‘hxaro’ (Wiessner, 1983), or certain styles may have emerged as a result of the technological and cultural traditions of a group (Sackett, 1982; Dunnell, 1978).

Historically, a strict dichotomy between style, which represents neutral aspects of variation, and function, which is the aspects of variation under selection, has been argued by evolutionary

archaeologists (Dunnell, 1978; Neiman, 1995). Shennan and Wilkinson (2001), however, argue that there is not a radical distinction between style and function, and in reality, both drift and selection likely operate within a broad spectrum of possibilities. Moreover, unlike genetics, cultural change can occur very quickly (i.e., in a single or few generations) and therefore often it simply cannot be the result of natural selection and drift *sensu stricto* (Collard *et al.*, 2008). Nonetheless, ascertaining which aspects of point shape are more likely to be linked to functional versus stylistic variability is an important task when using tool morphology as a proxy. White (2013) hypothesised that the width and thickness of the hafted end are most likely to relate to functional variability due to the requirement of the point to be inserted into a shaft, with stylistic attributes appearing more variable due to random drift causing differentiation through time and space without constraint by the selective environment.

Another important consideration is that the specific life histories of individual tools can also affect morphological variability in assemblages, with retouching and re-use often leading to more elongated and/or asymmetrical shapes (Dibble *et al.*, 2017). It is rare to find a lithic in its final form, and thus when recovered by an archaeologist, it represents one moment on the continuum of its life history, and thus not necessarily the desired-end product. For example, in the Lake Naivasha basin, unifacial points are found to have long use-lives, demonstrated by high frequencies of use-wear traces (Slater, 2016). Conard *et al.* (2012) defined several point morphotypes at Sibhudu, South Africa, based on the specific techno-functional characteristics and life cycle of individual tools. However, establishing both use and intentionality is not an easy feat at a regional scale and often requires whole-assemblage analysis. Point shape depends on myriad, often co-dependent, factors, and future research is required to develop methods for teasing these apart in order to evaluate and maximise the potential of points as proxies in the archaeological record.

### 8.2.1. Hypotheses setting

Scerri *et al.*'s (2018) SAM model is now widely accepted as a promising explanation for some of the complex patterns observed in archaeological, fossil, genetic and palaeoecological evidence from the Late-Middle Pleistocene, with 'complete (group) isolation seen as the exception, and not the rule' (Scerri, Chikhi and Thomas, 2019). Though time-averaging is a problematic issue (Dibble *et al.*, 2017), Scerri (2013a) suggested that population structure is best inferred archaeologically through analyses conducted at the assemblage level as the complexity of group boundaries may manifest in similarities between some assemblage components with differences in others. Under this model, group boundaries are most clearly structured when there are strong differences in hafted stylistic tools between assemblages whilst blank manufacture and hand-held and heavy toolkit morphology remains similar. However, when similarities in hafted tools exist between assemblages, group structure is

either weak/permeable or spatially autocorrelated. This confirms that, whilst assemblage-level studies potentially give a more holistic account, hafted tools (like points) are particularly informative about cultural transmission and group identity and are a key driver of patterns relating to population structure in archaeological assemblages.

Hypotheses have thus been developed that distinguish between point diversity related to various types of autocorrelations (H0), which act as null models. Figure 23 illustrates how archaeological variability can be explained in relation to the null models (H0a, b, c). It must be noted that the null models represent idealised theoretical states; the imperfect nature of the archaeological record means that it is largely impossible to have assemblages that are completely isolated along only one dimension or represent a single moment in time. Nonetheless, regression statistics can identify independent relationships between cultural variability and space, time and environments through controlling for the effects of other confounding variables and can therefore effectively test these hypotheses.

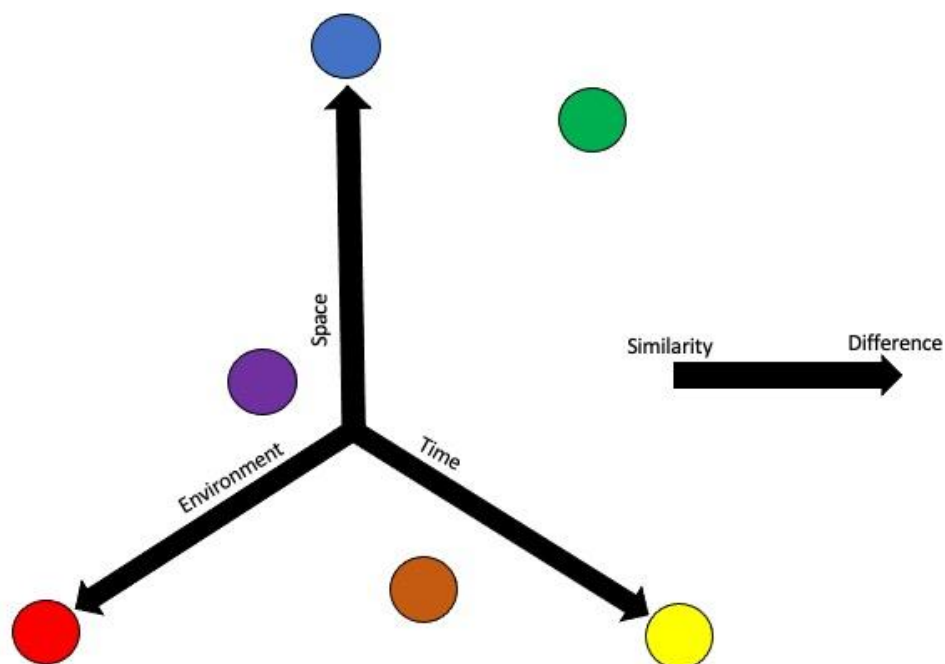


**Figure 23.** 3D visualisation of the null hypotheses in relation to how they explain archaeological diversity, adapted from Scerri (2013a). The arrows represent archaeological variability with the circles at the end of each arrow representing an assemblage conforming to a particular null model's assumptions. Isolation by distance (H0a) represents diversity through space when controlling for time and environment (blue). Isolation by time (H0b) is marked by the yellow circle, variation only occurring through time. Isolation by environment (H0c) is marked by the red circle, with the environmental dimension the only influence over patterns of diversity.

Cultural variation is likely explained by a combination of these factors, i.e., variation through timespace is represented by the green circle, and the correlation between space and environment means that assemblages that share the same environment and are close together are likely to be archaeologically similar (purple).

*Null hypotheses:*

H0<sub>a</sub>: Isolation by distance

Differences between points will not tend to be observed in assemblages that are geographically proximal, controlling for the effects of time and environments.

H0<sub>b</sub>: Isolation by time

Differences in points will not tend to be observed in assemblages that are chronologically proximal, controlling for the effects of space and environments.

H0<sub>c</sub>: Isolation by environments

Differences in points will not tend to be observed between assemblages occupying similar environments, controlling for the effects of time and space.

### 8.3. Materials

To study the structure of eastern African MSA point variability, artefact samples were accessed remotely via the collaborative data collection framework (Chapter 6-7) from the National Museums of Kenya (NMK) and the National Museum of Ethiopia (NME). Table 15 describes the sample, which includes artefacts from both dated and undated layers, with date ranges rounded to the nearest 1,000 years. In total, 218 eastern African MSA points were studied from six sites: Porc-Epic, Goda Buticha, Kapthurin Formation, Prospect Farm, Prolonged Drift and Omo Kibish. Some points were surface finds and/or did not have information regarding which assemblage they belong to, and therefore they were omitted from any analyses conducted beyond the site-level. Thirteen assemblages from six sites were studied, many with only a few points; power analysis, following recommendations from Cohen (1988), revealed that the sample sizes studied were often not large enough to return robust results (Appendix 3; Supplementary Methods S1). Caution must therefore be taken when generalising from these results given the sample sizes. MSA points, despite being a defining feature of the period, are often at relatively low densities compared to other tool types, making it difficult to reach the sample size threshold required to detect statistical effects with high confidence. Nonetheless, the results obtained from these small samples can be used to indicate trends that should be tested with further data, be it from future excavations or the analysis of existing collections.

**Table 15.** A summary of the eastern African Middle Stone Age point sample studied in this thesis, accessed via remote data collection. Samples without information regarding assemblage attribution and/or are surface finds are left unassigned and were removed from analyses beyond the site-level.

| Site                        | Coll. | Permit holder or contact                    | Lat.  | Lon.  | Assemblage        | Min age | Mid age | Max age | n                            | Ref                                |
|-----------------------------|-------|---|-------|-------|-------------------|---------|---------|---------|------------------------------|------------------------------------|
| Kaphurin Formation (N = 13) | NMK   | Sally McBrearty Nick Blegen Christian Tryon | 0.52  | 35.9  | GnJh-15           | 396     | 431     | 465     | 5                            | Deino and McBrearty (2002)         |
|                             |       |   |       |       | GnJh-78           |         | 100     |         | 9                            | Blegen, Jicha and McBrearty (2018) |
| Prolonged Drift (N = 8)     | NMK   | NA  | -0.48 | 36.1  | GrJi 11           | 30      | 51      | 72      | 8                            | Merrick (1975)                     |
| Prospect Farm (N = 78)      | NMK   | Barbara Anthony Stanley Ambrose             |       |       | GsJi 8            | 50      | 85      | 120     | 56                           | Anthony (1978)                     |
|                             |       |   |       |       | GsJi 7            | 50      | 85      | 120     | 22                           | Anthony (1978)                     |
| Goda Buticha (N=32)         | NME   | Zelalem Assefa                              | -0.59 | 36.18 |                   |         |         |         |                              |                                    |
|                             |       |   | 9.54  | 41.63 | Complex II IIc-a  | 4       | 6       | 8       | 8                            | Tribolo <i>et al.</i> (2017)       |
|                             |       |   |       |       | Complex II II d-f | 33      | 41      | 48      | 13                           | Tribolo <i>et al.</i> (2017)       |
|                             |       |   |       | N/A   |                   |         |         | 13      | Tribolo <i>et al.</i> (2017) |                                    |
| Omo Kibish (N =12)          | NME   | John Shea                                   | 5.41  | 35.9  | BNS               | 93      | 111     | 123     | 4                            | Shea (2008)                        |
|                             |       |   |       |       | AHS               | 195     | 200     | 205     | 6                            | Shea (2008)                        |
|                             |       |   |       |       | N/A               |         |         |         | 2                            | Shea (2008)                        |
| Porc-Epic (N = 74)          | NME   | David Pleurdeau                             | 9.63  | 41.87 | 08N-07W IIIa      |         | 40      |         | 22                           | Pleurdeau (2005)                   |
|                             |       |   |       |       | 08N-07W IIIb      |         | 40      |         | 23                           | Pleurdeau (2005)                   |
|                             |       |   |       |       | 08N-07W IIIc      |         | 40      |         | 10                           | Pleurdeau (2005)                   |
|                             |       |   |       |       | 08N-07W IIId      |         | 40      |         | 4                            | Pleurdeau (2005)                   |
|                             |       |   |       |       | 06N-14W 60-200cm  |         | 40      |         | 14                           | Pleurdeau (2005)                   |
|                             |       |   |       |       | N/A               |         |         |         | 2                            | Pleurdeau (2005)                   |

Several other relevant sites yield large samples of eastern African MSA points from well-dated and stratified sites, such as Aduma (Sahle and Brooks, 2019; Brooks *et al.*, 2006) and Gademotta (Douze and Delagnes, 2016) in Ethiopia, Olorgesailie (Brooks *et al.*, 2018) and Marmonet Drift (Slater, 2016) in Kenya, and Mumba, Nasera and Magubike in Tanzania (Bushozi, 2011), making them ideally placed to be studied in relation to null models. Figure 24 demonstrates the spatial distribution of the eastern African MSA sites studied in this analysis. This highlights that, although additional samples would have extended the geographic coverage of the analysis, the sites included in this thesis provide good geographic representation of the Ethiopian Highlands and Central EARS, which acts as the unit of analysis.

Points were selected following the definition outlined by Shea (2020): “broadly triangular flakes with retouched lateral edges that converge at their distal edge”. This definition, whilst primarily a typological one with the addition of retouching as a technological requirement, considers that even though points do not necessarily have to be retouched (Douze *et al.*, 2020; Timbrell *et al.*, 2022c), retouching exerts a control over shape. Scerri (2013a) proposed that variability in hafted tools is most likely to be indicative of group dynamics, and whilst experimental work has indicated that points do not have to be heavily retouched in order to be hafted (Sisk and Shea, 2009; Waguespack *et al.*, 2009), hafting motivates standardized tool designs in order for the tool to fit within the shaft. Points that are retouched are thus somewhat more likely to be hafted tools, though ultimately micro-use wear and residue analyses are required to confirm this. Shea (2020) also refers to points as being ‘bilaterally symmetrical’. Only pieces with extreme asymmetry were removed from this analysis - whilst this was a somewhat arbitrary process, a degree of asymmetry was deemed acceptable to account for the fact that the life history of points can affect symmetry, with side-to-side variability observed in MSA hafted tools (Iovita, 2011). Such asymmetrical pieces could be classified as hafted ‘knives’ or ‘scrapers’ using Bordesian systematics, but subjective labels that conflate typology with function (without use-wear analyses) should be avoided, especially as these differing classifications could primarily be a question of semantics when considering that pointed forms were probably used for a variety of tasks in the MSA (Douze *et al.*, 2020).

The collaborators collected the data from each site and uploaded it to a communal Google Drive. I visually assessed each artefact to ensure I agreed that it met the definition of a point as described by Shea (2020). A number of Acheulean bifaces were recorded from Kapthurin Formation because they met the definition of Shea (2020) due to a morphological continuum between this tool type and MSA points. Those that were labelled ‘handaxe’ and which were deemed not to be hafted due to their large size were omitted from the analysis. Though not the focus of this study, further work should be done to explore this dichotomy (with the inclusion of examples from other sites), as it would be interesting to ascertain whether bifacial points and handaxes indeed fall along the same morphological and

technological continuum, which also has been proposed at Kilombe in Kenya (Gowlett *et al.*, 2017) with important cognitive implications. All samples that met the criteria were given an ID with the prefix “E\_point”. The data were grouped into assemblages based on both information provided by the collaborators from the specimen bags and from the literature. To ensure that all aspects of the outline were culturally significant, any points with tip damage or blunting were removed.

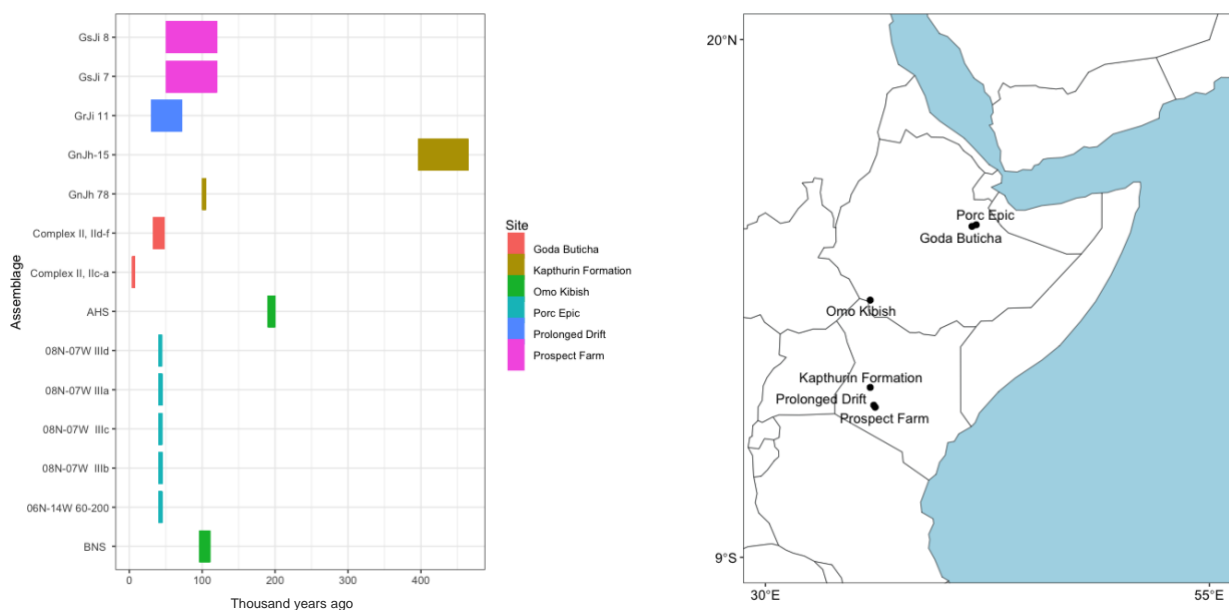


**Figure 24.** The chronological (left) and spatial (right) extent of the eastern African Middle Stone Age points studied in this analysis.

Raw materials were determined macroscopically by the collaborators based on their expertise and/or information provided on the sample bags. The points were predominately made from obsidian (n=106), basalt (n=46) and chert (n=61), with much smaller frequencies of quartzite (n=1), rhyolite (n=3) and fossilized wood (n=1).

### 8.3.1. Background to the sites studied

Porc-Epic is situated in Ethiopia around 3 km south of Dire Dawa, between the Somali Plateau and the Afar Depression. It was first discovered by H. De Monfried and P. Teilhard de Chardin in 1920 (Teilhard de Chardin, 1930) and has since been excavated by H. Breuil and P. Wernert in 1933 (Breuil, Teilhard de Chardin and Wernert, 1951), J. Desmond Clark and K. D. Williamson from 1975-1976 (Clark and Williamson, 1984) as well as in 1998 as part of a collaborative project between Authority for Research and Conservation of Cultural Heritage of Ethiopia and the French Muséum National d'Histoire Naturelle. The site is divided into seven stratigraphic units, with MSA artefacts recovered from Levels 2, 3 and 4A/B, from 60 to 220-230cm below datum (Clark and Williamson,



1984). Points studied in this analysis derive from two squares: 06N-14W (60-200cm) and 08N-07W, which is divided into the following sub-units: IIIa (from 90-120 cm), IIIb (from 120- 150cm), IIIc (from 150- 170cm) and IIId (from 170-210cm), following Pleurdeau (2005). A sample of MSA artefacts were dated to 61-71 kya using obsidian hydration (Michaels and Marean, 1984), however, the precise stratigraphic provenance of artefacts analysed is unknown and the reliability of the method has since been questioned. Accelerator mass spectrometry dates of three gastropod opercula from different MSA levels located 160–170 cm, 180–190cm and 270–280cm below datum obtained uncalibrated ages of  $33.7 \pm 0.3$  kya,  $35.6 \pm 0.4$  kya, and  $> 43.2$  kya (Assefa, 2006). It is unknown, however, how these relate to the assemblages studied here, as the gastropod samples were collected from different squares. New optically stimulated luminescence dates are expected imminently (Pleurdeau, pers.comm), and can be used to refine the analysis in future work; however, in the meantime, all of the assemblages have been given the same date estimation of ~40 kya following Rosso, d’Errico and Zilhao (2014), who note that the MSA deposits likely accumulated over a relatively short period of time based on the distribution of ochre fragments.

Goda Buticha is similarly located in the Dire Dawa district in southeastern Ethiopia, near Kunama in the administrative district of Serkama village (Pleurdeau *et al.* 2014). There are two major stratigraphic divisions, labelled as Complex I (Lower Complex) from 0-180cm above datum and Complex II (Upper Complex) from 180-230cm above datum. Within Complex II, there are two further sedimentological subsets between Layers IIf-d and Layers IIc-a. All of the points studied here derive from Complex II. Tribolo *et al.* (2017), based on 14 AMS radiocarbon analyses, found that the phase of occupation marked by Layers IIf-d dated from at least  $46.3 \pm 2.1$  kya to  $33.8 \pm 0.4$  kya, thus falling within MIS 3, with the upper sub-unit of Complex II yielding a Holocene age from  $7.8 \pm 0.1$  kya to  $4.7 \pm 0.1$  kya. The dates suggest a large stratigraphic gap within Complex II without abrupt technological change; both sub-units are described as showing clear MSA features, though the upper sub-unit has more LSA attributes, such as blades and non-geometric microliths (Pleurdeau *et al.* 2014).

The Omo Kibish Formation is situated in the Lower Omo Valley of southwestern Ethiopia, consisting of three main archaeological sites: Kamoya's Hominid Site (KHS), Awoke's Hominid Site (AHS) and Bird's Nest Site (BNS). Leakey, Butzer and Day (1969) first excavated at Omo Kibish, discovering hominin remains and lithics, with J. J. Shea and colleagues renewing excavations in 2001 and 2003. Points studied in this analysis derive from AHS and BNS. Based on McDougall *et al.*'s (2005) chronology of the site, Shea (2008) estimates that Level 3 at BNS has a minimum age of  $104 \pm 1$  kya, whereas the AHS assemblage has a date of  $195 \pm 5$  kya, based on the dating of KHS Levels 2-3. The KHS tuff has recently been redated to  $233 \pm 22$  kya (Vidal *et al.*, 2022), though the previous dates are maintained as it is unclear how/if this datum relates to AHS. Importantly, AHS is described as being a

multicomponent site whilst BNS is a single-level site (Shea, 2008); though there are large similarities between levels at AHS, the assemblage inevitably conflates artefacts from different occupations but, as Shea (2008) points out, this is a general reflection of the uncertainties of the archaeological record, and thus is probably the case for many of the assemblages studied.

Prolonged Drift (GrJi 11) is situated within the Central Kenyan Rift on the lower reaches of the Enderit River in the Lake Nakuru basin. MSA artefacts are reported to occur throughout the stratigraphy of the site but are mostly concentrated in three horizons. There are few recent publications about this site, with the only dates produced by Merrick (1975) of 30-72 kya using obsidian hydration. Clark (1988) suggested that the high concentration of MSA points at Prolonged Drift indicates it may have been a seasonal hunting camp used for only short periods of time, making it particularly relevant for this study.

Prospect Farm is also situated within the Central Kenyan Rift, on the slopes of Mount Eburru overlooking Lakes Elmenteita and Nakuru. It yields multiple MSA horizons described by Anthony (1978) in three locations (I-III), with artefacts in this analysis deriving from Locality I (GsJi 7) and Locality II (GsJi 8). Anthony (1978) described the MSA artefacts as being an eastern African variant of the Still Bay industry, which she refers to as the Prospect Industry, due to the presence of bifacially worked points and Levallois technology. From the stratigraphy, Anthony (1978) distinguished four phases within the Prospect Industry, with obsidian rehydration dating of phase IV artefacts from Locality I ranging between  $45.7 \pm 0.24$  and  $53.5 \pm 0.3$  kya and those from phase III Locality I indicating a further three occupational phases dating from  $46.5 \pm 1.7$  to  $53.1 \pm 4.2$  kya (overlapping with the dates from the overlying phase IV artefacts),  $106.3 \pm 3.2$  to  $108.6 \pm 2.9$  kya and around  $119.6 \pm 1.7$  kya. Points from both localities have been given a broad date range encompassing all of these dates (following Tryon and Faith, 2013) as their stratigraphic positioning is unclear, though the fact that the other MSA phases (I and II) have to be older than 120 kya suggests that these artefacts could have been manufactured much earlier.

The Kapthurin Formation is located in the Tugen Hills within the Kenyan Rift, west of Lake Baringo. Multiple archaeological sites have been exposed along the 150 km formation, with excavations led by E. Cornelissen and S. McBrearty since the 1990s. The Kapthurin Formation marks the transition from the Acheulean to the MSA, with high variability reported due to the presence of handaxes, cleavers, points, and blades at penecontemporaneous sites. The stratigraphy of the sites has been separated into members, which have been dated using  $^{40}\text{Ar}/^{39}\text{Ar}$  (Deino and McBrearty, 2002). Of relevance here, K3 is directly dated to  $509 \pm 9$  kya, K4 has produced two dates of  $284 \pm 12$  kya and  $235 \pm 2$  kya and K5 is  $< 200$  kya. Transitional ESA/MSA assemblages from Kapthurin Formation have been loosely associated with K3 and K4; GnJh-15, a non-diagnostic site with both MSA and ESA features, has

been stratigraphically associated with K3 however, because of upfaulting and erosion, this has not been confirmed (Tryon, 2003). This locality (also known as Kapthurin Site "A") and GnJh-78 (Keraswanin), described as being MSA by Blegen *et al.* (2018), are studied in this research.

#### 8.4. Methods

The methods used for this analysis build upon and combine those applied in Chapters 4, 5, 6 and 7.

Following the protocols outlined in Chapter 6, three basic measurements on each artefact were taken to record morphological length, width, and thickness at a resolution of 0.1mm. I defined length as the maximum dimension of the point, width as the maximum measurement in the perpendicular dimension to length, and thickness as the maximum measurement in the third dimension, following Shea (2020). One point (E\_point\_142) from Kapthurin Formation did not have metric measurements recorded for an unknown reason, and thus was removed from the metric analysis.

I also performed 2D GMM on the photographs of the points taken via collaborative data collection as outlined and validated in Chapters 6-7. The protocols followed by the collaborators at the NMK and NME use a number of steps to optimize the photos for outline-based GMM, such as including a scale in the image and minimising shadows around the object. Each image was processed following the procedures outlined in Chapter 7. Outline extraction was performed in tpsDig2, with each artefact represented by an average of 1755 equidistant points.

As in Chapter 7, I performed elliptic Fourier analysis (EFA) to produce outline data and standardised each outline following Bonhomme *et al.* (2017). I retained 10 harmonics for 99% harmonic power. To explore the potential drivers of shape variability within the eastern African MSA point sample, I applied a range of statistical techniques. First, I performed a Principal Components Analysis (PCA) to reduce the dimensionality of the data. To assess the relationship between centroid size and the most heavily weighted principal components (PCs), as well as length and width metrics established in the technological analysis, I also performed correlation and linear regression analyses. I performed multivariate analysis of variance (MANOVA), analysis of variance (ANOVA) and Tukey's Honestly Significant Difference (HSD) tests on the PC scores to further assess the statistical significance of differences between raw materials, sites and assemblages. I performed a hierarchical cluster analysis, specifically the complete method to ascertain the structure of variation according to different factors. Finally, I calculated the mean shape of each assemblage using the 'mshapes' function in Momocs (Bonhomme *et al.*, 2014) and extracted the mean PC scores to act as the cultural data for each assemblage in the subsequent matrix regressions.

To evaluate point shape variability in terms of isolation by distance, time, and environment, I first produced a costpath using Tobler's Hiking Function (Tobler, 1993) between the site coordinates using the formula outlined in Chapter 5 to ascertain the spatial distance between the sites. For chronology, I used the mid-point in the dating error range as a simple estimation of age for each assemblage, though note that for some assemblages, this spans several tens of thousands of years (Table 15). The mismatch between the resolution of archaeological and palaeoclimatological data is discussed in Chapter 10. Lastly, to produce a characterisation of the environment of each assemblage, I extracted the temperature and precipitation values from the climate model of Krapp *et al.* (2021) at the site coordinates in the time-slice representative of the simple age, following the methodology outlined in Chapter 4.

Together, these provided measures of distance, time and environment that were then assessed against mean point shape for each assemblage (characterised by the PCs) using multiple matrix regressions, controlling for size (characterised by the metric measurements) and raw material. Raw materials were converted to binary data, following Blinkhorn and Grove (2018), to demonstrate the presence and absence of each within each point assemblage.

## 8.5. Results

PCA was performed and 6 principal components (PCs) were found to represent >90% of the total variance in the data. Figure 25 highlights the shape differences along each PC. PC1 represents 63.4% of the total variance and is an axis of elongation, with negatively scoring points demonstrating long, thin shapes and positively scoring points having wide, short morphologies. PC2 and PC3 represent 11.2% and 8.7% of the total variance respectively and mark an asymmetrical shape difference between more triangular morphologies with acute tips and more rectangular morphologies with obtuse tips, with mirrored convexities along each lateral edge. PC4 represents 4.6% of the total variance and represents asymmetrical shape differences between points with acute tips with convexity on the left or right lateral edge. PC5 represents an axis of tip narrowing from negative to positive, with slight convexity of the base in the positive direction, which makes up 2.6% of the total variance. PC6 also represents 2.6% of the total variance and reflects a similar axis of variance to PC5 though the convexity of the base is expressed more asymmetrically, and also occurs on negatively scoring points with obtuse tip angles.

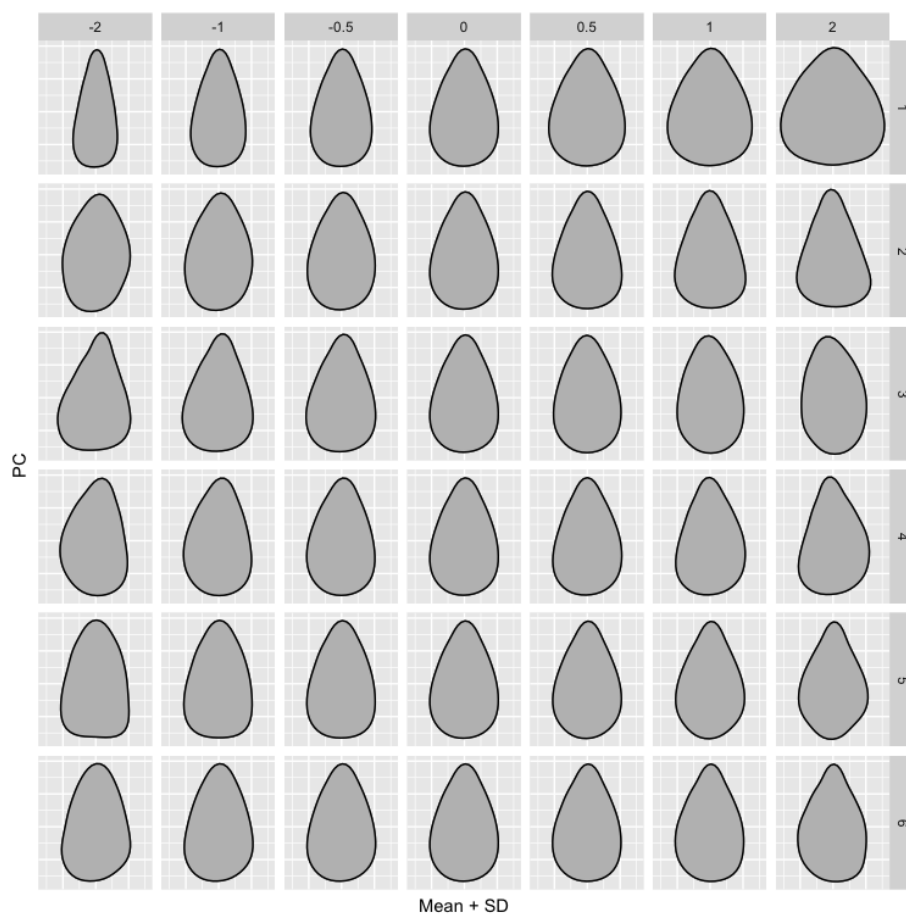


**Figure 25.** Principal component (PC) contributions, highlighting the mean and standard deviation (SD) shape changes along PC1-6.

### 8.5.1. Relationship between shape and size

To understand how size and shape are related, I regressed centroid size against each PC (Fig. 26, Appendix 3: Supplementary Table S1). PC1 demonstrates a statistically significant relationship with centroid size, with points demonstrating wider morphologies tending to be larger than those with thinner shapes. The  $R^2$  value (0.1) highlights that size accounts for around 13% of the variance in elongation. PC2 through PC5 also show statistically significant relationships with centroid size, though these relationships are much weaker. There are also some clear outliers in terms of size from these plots. E\_point\_122 and E\_point\_166 have the smallest centroid sizes, however their shape clearly meets the definition of a point (Appendix 3: Supplementary Fig. S1), therefore they were retained in the analysis. Overall, the results highlight that allometry is present within the data and that point form (shape + size) should be tested using the metric variables as well as shape.

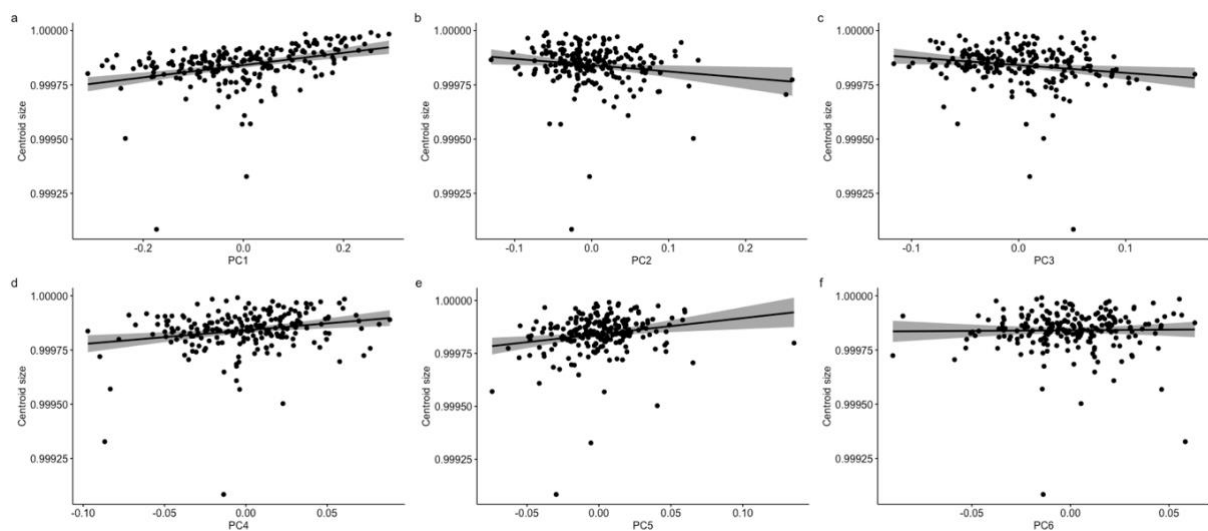


**Figure 26.** Regressions of principal components (PC) 1-6 on centroid size, with 95% confidence intervals.

### 8.5.2. Raw materials

Next, I tested for the effects of raw material on point form. Points manufactured from basalt and rhyolite tended to show the largest variability in point shape and size (Fig 27, Table 16). Yet, the three categories with large enough samples for analyses (basalt, chert, and obsidian) demonstrate similar means for all three dimensions (Table 16). ANOVA and post-hoc Tukey HSD tests suggested that raw materials have a significant effect on point length ( $p < 0.001$ ) and width ( $p = 0.01$ ), however these relationships are primarily driven by differences seen in the raw material types with very small samples, thus the result is not robust (Appendix 3; Supplementary Table S2). Thickness does not

show significant differences between raw material types. There are no statistically significant differences between the main raw material types, basalt, chert, and obsidian, suggesting the raw material has little effect on point form (Appendix 3: Supplementary Table S2).

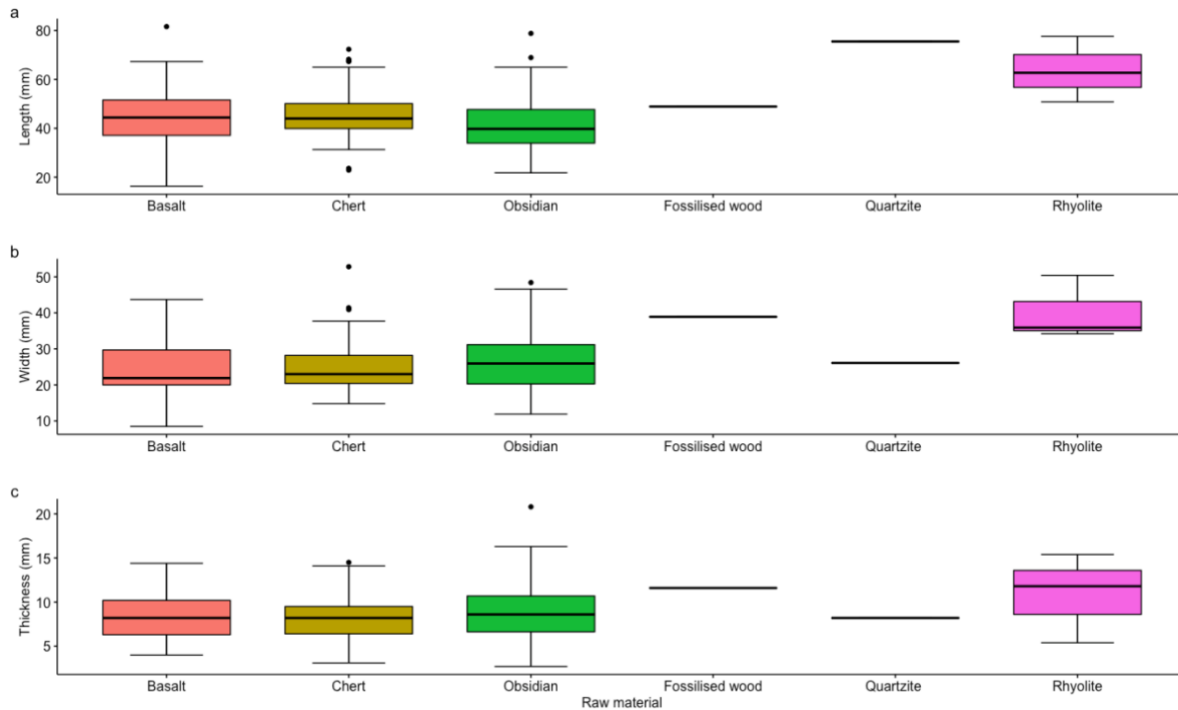


**Figure 27.** Boxplots of point length, width, and thickness (mm) in relation to raw material.

**Table 16.** Summary statistics for point length, width, and thickness (mm) for each raw material, highlighting the sample size (n), mean (m) and standard deviation (sd)

|                 | Length (mm) |          |           | Width (mm) |           | Thickness (mm) |           |
|-----------------|-------------|----------|-----------|------------|-----------|----------------|-----------|
|                 | <i>n</i>    | <i>m</i> | <i>sd</i> | <i>m</i>   | <i>sd</i> | <i>m</i>       | <i>sd</i> |
| Basalt          | 45          | 44.1     | 12.6      | 25.3       | 8.2       | 8.3            | 2.3       |
| Chert           | 61          | 45.5     | 10.3      | 24.7       | 6.8       | 8.2            | 2.6       |
| Fossilised Wood | 1           | 48.9     | NA        | 38.9       | NA        | 11.6           | NA        |
| Obsidian        | 106         | 41.7     | 10.8      | 26.3       | 7.9       | 9.0            | 3.1       |
| Quartzite       | 1           | 75.5     | NA        | 26.1       | NA        | 8.2            | NA        |
| Rhyolite        | 3           | 63.7     | 13.4      | 40.2       | 8.9       | 10.9           | 5.1       |

Figure 28 demonstrates the distribution of each raw material in relation to PC1-6. MANOVA confirmed a statically significant relationship between raw material and point morphology (Hotelling-Lawley = 0.427, approx  $F = 2.126$ ,  $p < 0.001$ ), however when investigated with ANOVA and post-hoc Tukey HSD tests (Appendix 3: Supplementary Table S2), this relationship is driven solely by shape differences between obsidian and chert along PC1 ( $p < 0.001$ ) and PC3 ( $p < 0.001$ ). I also found that obsidian and chert show significant differences in centroid size ( $p = 0.002$ ; Appendix 3: Supplementary Table S2). This highlights how obsidian points tend to be larger and wider than chert

points. Overall, whilst raw material does have an effect on point shape, this effect is deemed to be minimal and restricted to certain raw material types. It must also be taken into account that any differences between raw materials could be linked to stylistic differences between sites; for example, the vast majority of the obsidian points (n = 76) come from Prospect Farm whilst almost all of the chert points (n = 43) are from Porc-Epic. Raw material use also has the potential to confound patterns of IBD and IBE, as rock types are unequally distribution across the landscape, and thus requires exploration within a multivariate framework.

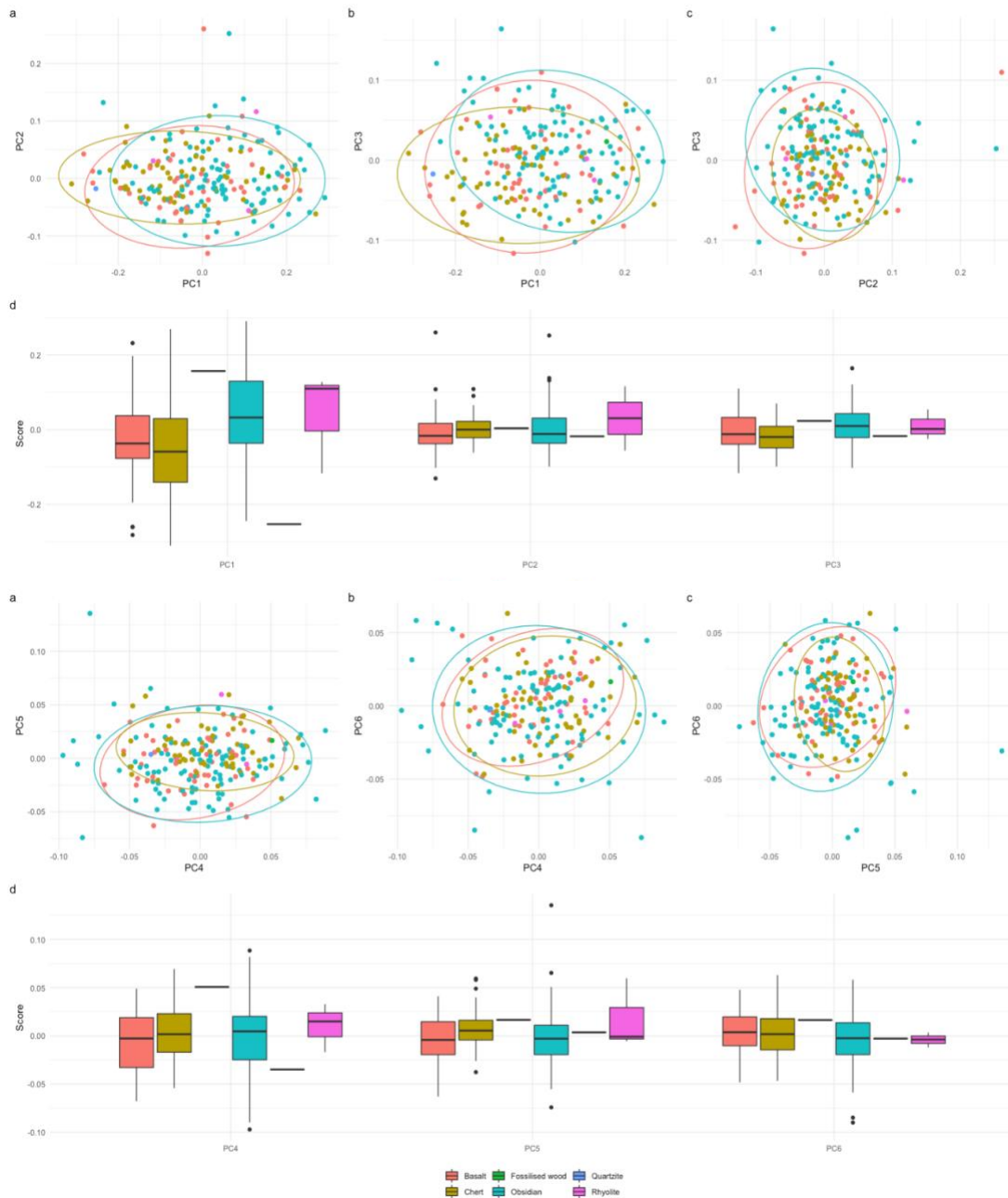


**Figure 28.** Principal components analysis (PCA) scatterplots (a-c) and boxplots (d) of principal component (PC) 1-3 (top) and PC 4-6 (bottom) against raw materials.



Next, I analysed whether there are shape and size differences between points from different sites. Figure 29 and Table 17 describe the distribution of length, width, and thickness according to the sites. Kapthurin Formation is the most variable site, and Prolonged Drift is the least variable (Fig. 29, Table 17). Tukey HSD confirmed that points from Goda Buticha are significantly shorter than those from Omo Kibish and less wide than those from Omo Kibish, Kapthurin Formation and Prospect Farm (Table 18). Points from Kapthurin Formation and Goda Buticha also show significant differences in width, as do Prospect Farm and Porc-Epic (Table 18). In terms of thickness, Goda Buticha show significantly lower values than points from Omo Kibish and Prospect Farm, with Porc-Epic points also being significantly thinner than Prospect Farm (Tables 17-18).

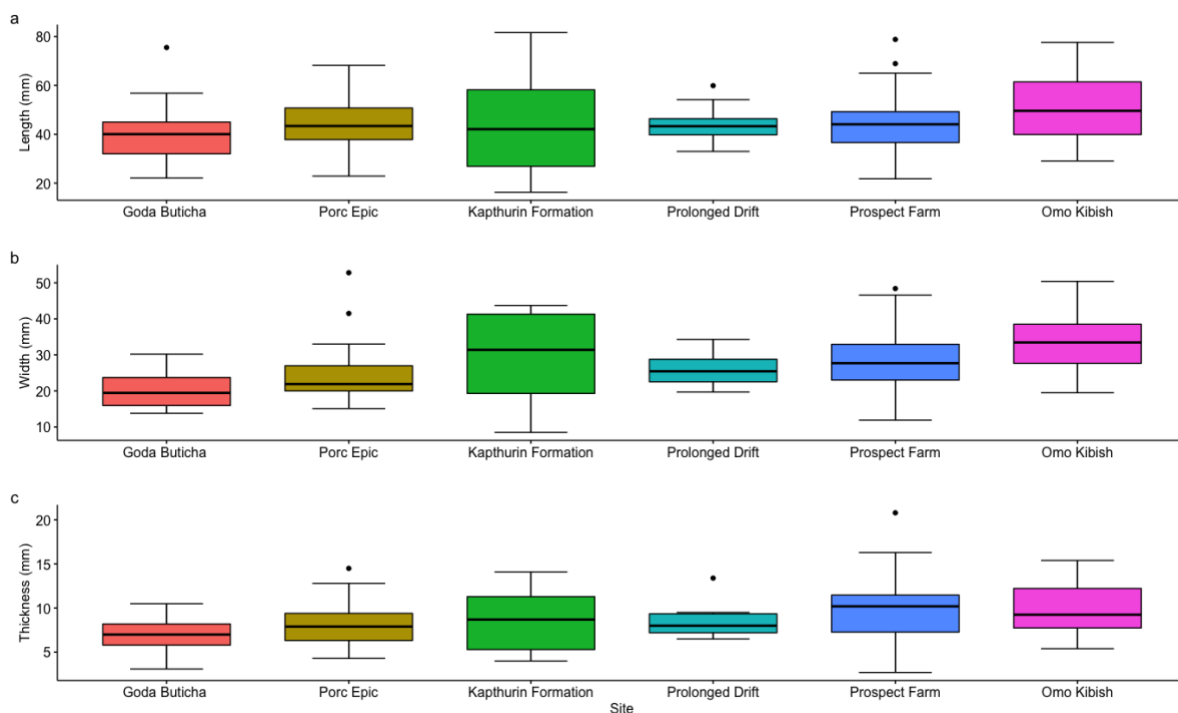


**Figure 29.** Boxplots of point length, width, and thickness (mm) for each site.

**Table 17.** Summary statistics for point length, width, and thickness (mm) for each site, highlighting the sample size (n), mean (m) and standard deviation (sd)

|                     | Length (mm) |          |           | Width (mm) |           | Thickness (mm) |           |
|---------------------|-------------|----------|-----------|------------|-----------|----------------|-----------|
|                     | <i>n</i>    | <i>m</i> | <i>sd</i> | <i>m</i>   | <i>sd</i> | <i>m</i>       | <i>sd</i> |
| Goda Buticha        | 32          | 39.8     | 10.9      | 20.3       | 4.8       | 6.9            | 1.9       |
| Kapthurin Formation | 13          | 43.2     | 20.4      | 28.9       | 12.3      | 8.7            | 3.3       |
| Omo Kibish          | 12          | 50.9     | 14.9      | 33.6       | 8.4       | 9.8            | 3.3       |
| Porc-Epic           | 74          | 44.3     | 9.7       | 23.6       | 5.9       | 8.0            | 2.2       |
| Prolonged Drift     | 8           | 44.6     | 8.6       | 26.1       | 5.0       | 8.6            | 2.2       |
| Prospect Farm       | 78          | 43.7     | 10.9      | 28.5       | 7.8       | 9.8            | 3.2       |

GMM analysis confirmed statistically significant differences in point shape between the sites (MANOVA: Hotelling-Lawley = 1.0062, approx  $F = 5.116$ ,  $p < 0.001$ ). Figure 30 highlights that Goda Buticha and Porc-Epic score more negatively along PC1 compared to the other sites, as they tend to show more elongated morphologies. Along PC3, Prospect Farm and Kapthurin Formation tend to score more positively suggesting that points from these sites tend to demonstrate more obtuse tip angles (Fig. 30). Along PC6, Prolonged Drift tends to score more negatively compared to the other sites (Fig. 30), Tukey HSD results on ANOVA scores for each PC are listed in Table 18, highlighting many key differences between sites across multiple dimensions.

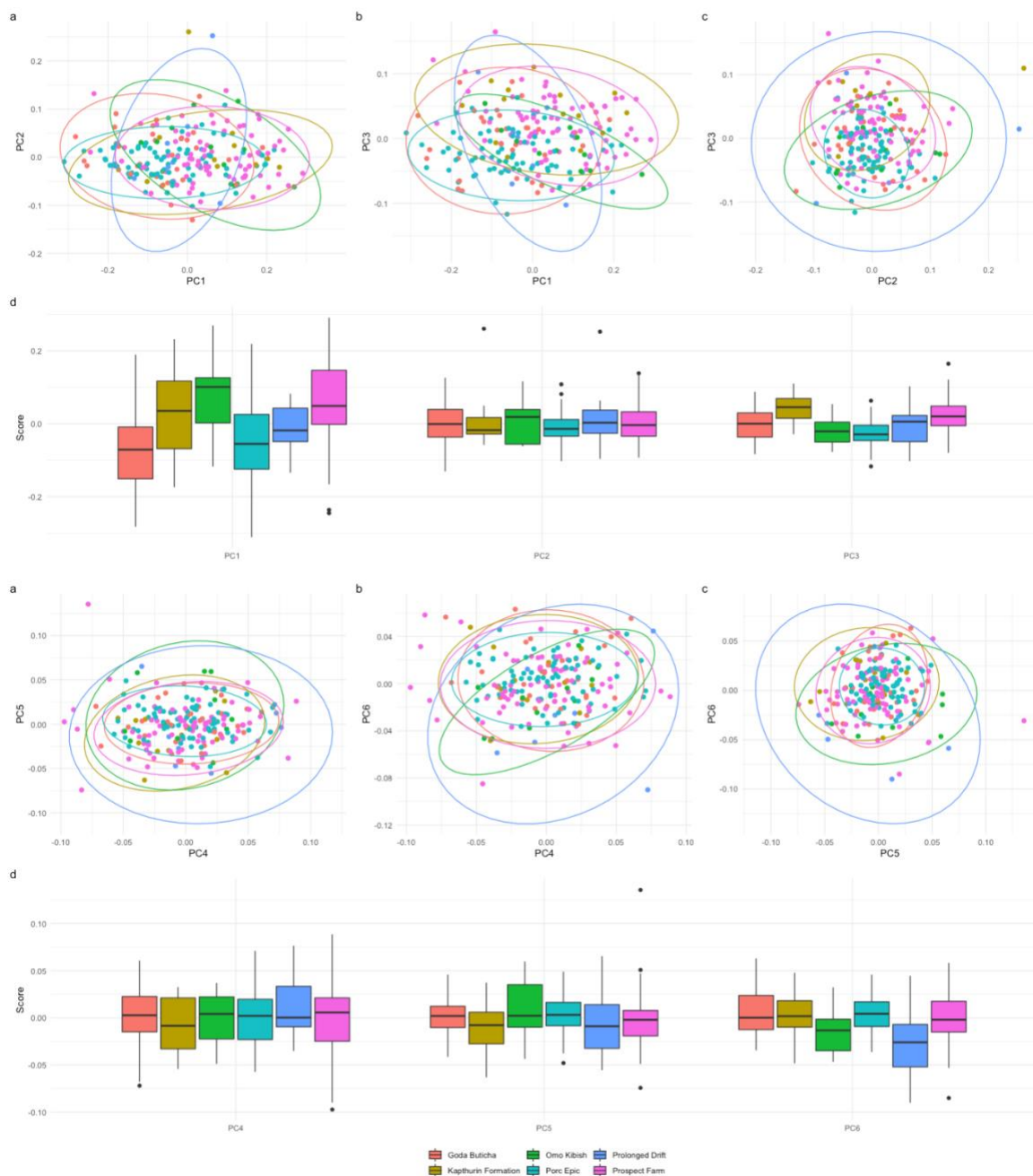


**Figure 30.** Principal components analysis (PCA) scatterplots (a-c) and boxplots (d) of principal component (PC) 1-3 (top) and PC 4-6 (bottom) for each site.

**Table 18.** P-values from Tukey Honestly Significant Difference analyses for length, width, and thickness as well as principal component (PC)1, 3 and 6. Statistical significance is highlighted at  $p < 0.05$  (\*) and at  $p < 0.01$  (\*\*). All values have been rounded to 3 decimal places.

|                                       | Length | Width    | Thickness | PC1      | PC3      | PC6    |
|---------------------------------------|--------|----------|-----------|----------|----------|--------|
| Kapthurin Formation - Goda Buticha    | 0.945  | 0.004**  | 0.314     | 0.058    | 0.007**  | 0.999  |
| Omo Kibish – Goda Buticha             | 0.049* | <0.001** | 0.021*    | 0.004**  | 0.925    | 0.129  |
| Porc-Epic – Goda Buticha              | 0.408  | 0.230    | 0.400     | 0.925    | 0.215    | 0.991  |
| Prolonged Drift – Goda Buticha        | 0.895  | 0.310    | 0.618     | 0.753    | 0.999    | 0.013* |
| Prospect Farm – Goda Buticha          | 0.567  | <0.001** | <0.001**  | <0.001** | 0.052*   | 0.664  |
| Omo Kibish – Kapthurin Formation      | 0.535  | 0.554    | 0.919     | 0.955    | 0.004**  | 0.403  |
| Porc-Epic – Kapthurin Formation       | 0.999  | 0.150    | 0.944     | 0.166    | <0.001** | 0.999  |
| Prolonged Drift – Kapthurin Formation | 1.000  | 0.956    | 1.000     | 0.962    | 0.115    | 0.0711 |
| Prospect Farm - Kapthurin Formation   | 1.000  | 1.000    | 0.806     | 0.946    | 0.471    | 0.976  |
| Porc-Epic – Omo Kibish                | 0.435  | <0.001** | 0.262     | 0.013*   | 0.997    | 0.192  |
| Prolonged Drift – Omo Kibish          | 0.827  | 0.195    | 0.919     | 0.635    | 0.981    | 0.910  |
| Prospect Farm – Omo Kibish            | 0.326  | 0.196    | 1.000     | 0.999    | 0.035    | 0.524  |
| Prolonged Drift – Porc-Epic           | 1.000  | 0.939    | 0.992     | 0.949    | 0.805    | 0.020* |
| Prospect Farm – Porc-Epic             | 0.999  | <0.001** | 0.001**   | <0.001** | <0.001** | 0.852  |
| Prospect Farm – Prolonged Drift       | 1.000  | 0.943    | 0.852     | 0.539    | 0.574    | 0.081  |

A cluster analysis found that there is some structuring by site, with points from certain sites clustering closely together (Fig. 31). Splitting the tree into six clusters (the number of sites) demonstrates that points from Kapthurin Formation and Prolonged Drift form tight groups within cluster 5 and those from Omo Kibish form a tight group within cluster 3. However, points from Prospect Farm appear in 5 clusters, Goda Buticha points appear in 4, and Porc-Epic in 3, suggesting that the main structure of variability within the sample does not necessarily correspond with site attribution, implicating other potential factors, such as environmental factors.

#### 8.5.4. Inter-assembly variability

I then analysed point variance between assemblages. Table 19 reports summary statistics for each assemblage, and Figure 32 demonstrates boxplots of length, width, and thickness. Interestingly, some sites (i.e., Goda Buticha) demonstrate relatively low variance between assemblages (Table 19), whereas others (Kapthurin Formation, Prospect Farm) show much higher diversity between assemblages, which was confirmed to be statistically significant by post-hoc Tukey HSD tests (Kapthurin assemblages:  $p < 0.001$ , Prospect Farm assemblages:  $p = 0.02$ ; Table 20). Points from GnJh-78 and GsJi 8 are relatively longer, wider, and thicker than those from GnJh-15 and GsJi 7

respectively (Table 19). Research at Aduma has suggested that points found in earlier contexts were larger, likely due to a shift from thrusting spear technology (which is less constrained by hafting requirements) to projectile weaponry (Sahle and Brooks, 2019). Yet the earliest sample explored here (GnJh-15, Kaputhurin Formation) has some of the smallest points, with the much younger assemblage from the same site (GnJh-78) having consistently larger dimensions. This could attest to the asynchronous adoption of different point technologies across the region or the problematic nature of using point dimensions for inferring changes in function through time. Table 20 also highlights how differences tend to be seen between assemblages from the Ethiopian Rift and the Kenyan Rift, and also those within the Kenyan Rift, indicating a degree of spatial structure to the variability.

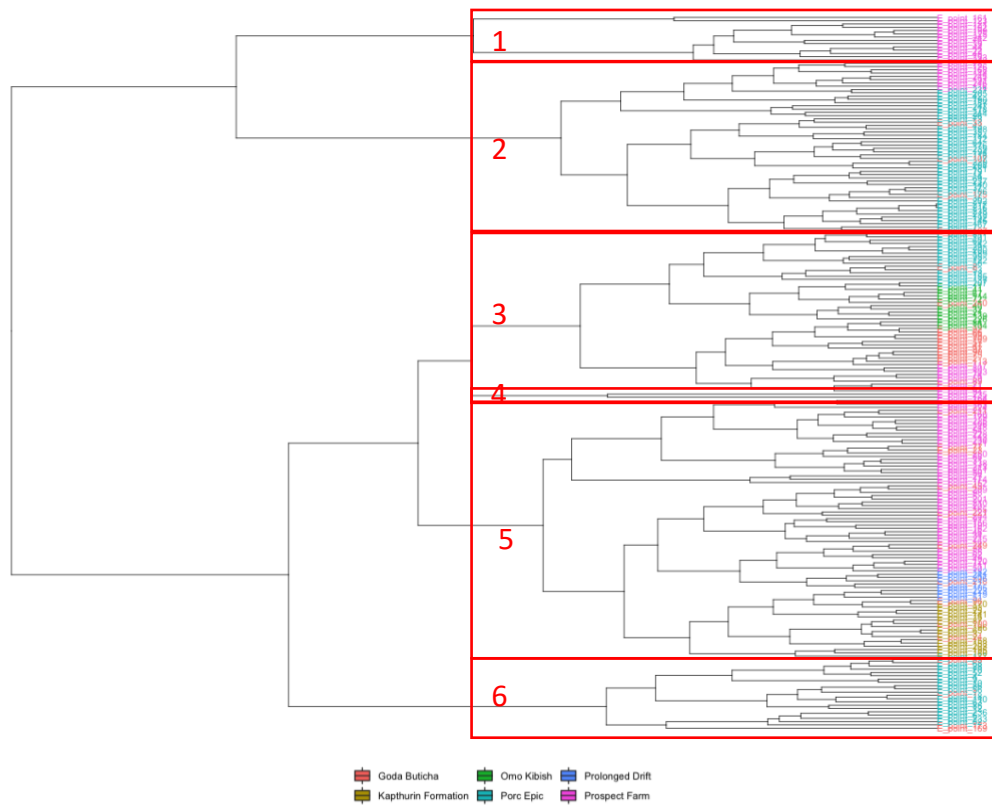


**Figure 31.** Hierarchical cluster analysis demonstrating the structure of point shape variability between sites. The dendrogram has been split into six clusters ( $n$  = number of sites) which are highlighted by the red boxes.

**Table 19.** Summary statistics for point length, width, and thickness (mm) for each assemblage, highlighting the sample size ( $n$ ), mean ( $m$ ) and standard deviation ( $sd$ )

| Site       | Assemblage | $n$ | Length (mm) |      | Width (mm) |      | Thickness (mm) |      |
|------------|------------|-----|-------------|------|------------|------|----------------|------|
|            |            |     | $m$         | $sd$ | $m$        | $sd$ | $m$            | $sd$ |
| Omo Kibish | AHS        | 6   | 53.7        | 14.1 | 34.0       | 4.5  | 9.9            | 3.1  |
| Omo Kibish | BNS        | 4   | 46.4        | 19.0 | 30.7       | 10.3 | 9.3            | 3.2  |

|                     |                   |    |      |      |      |      |      |     |
|---------------------|-------------------|----|------|------|------|------|------|-----|
| Prospect Farm       | GsJi 7            | 22 | 36.7 | 7.9  | 24.2 | 6.2  | 8.7  | 3.0 |
| Prospect Farm       | GsJi 8            | 56 | 46.5 | 10.8 | 30.2 | 7.8  | 10.2 | 3.2 |
| Goda Buticha        | Complex II, IIc-a | 8  | 40.4 | 16.5 | 19.3 | 3.9  | 7.4  | 1.6 |
| Goda Buticha        | Complex II, IIc-f | 13 | 36.2 | 6.8  | 19.1 | 4.8  | 6.5  | 1.8 |
| Kapthurin Formation | GnJh 78           | 8  | 54.1 | 16.8 | 35.5 | 8.4  | 10.2 | 2.4 |
| Kapthurin Formation | GnJh 15           | 5  | 25.6 | 11.2 | 18.2 | 10.2 | 6.4  | 3.3 |
| Prolonged Drift     | GrJi 11           | 8  | 44.6 | 8.6  | 26.1 | 5.0  | 8.6  | 2.2 |
| Porc-Epic           | 08N-07W IIIa      | 22 | 44.7 | 10.1 | 23.7 | 4.6  | 8.6  | 2.4 |
| Porc-Epic           | 08N-07W IIIb      | 23 | 44.5 | 10.6 | 22.5 | 4.6  | 7.5  | 2.1 |
| Porc-Epic           | 08N-07W IIIc      | 9  | 45.6 | 10.3 | 26.1 | 10.6 | 7.6  | 2.7 |
| Porc-Epic           | 08N-07W IIIc      | 4  | 45.4 | 11.5 | 31.2 | 7.6  | 8.6  | 1.5 |
| Porc-Epic           | 06N-14W 60-200cm  | 14 | 40.9 | 4.6  | 21.8 | 3.0  | 8.1  | 1.6 |

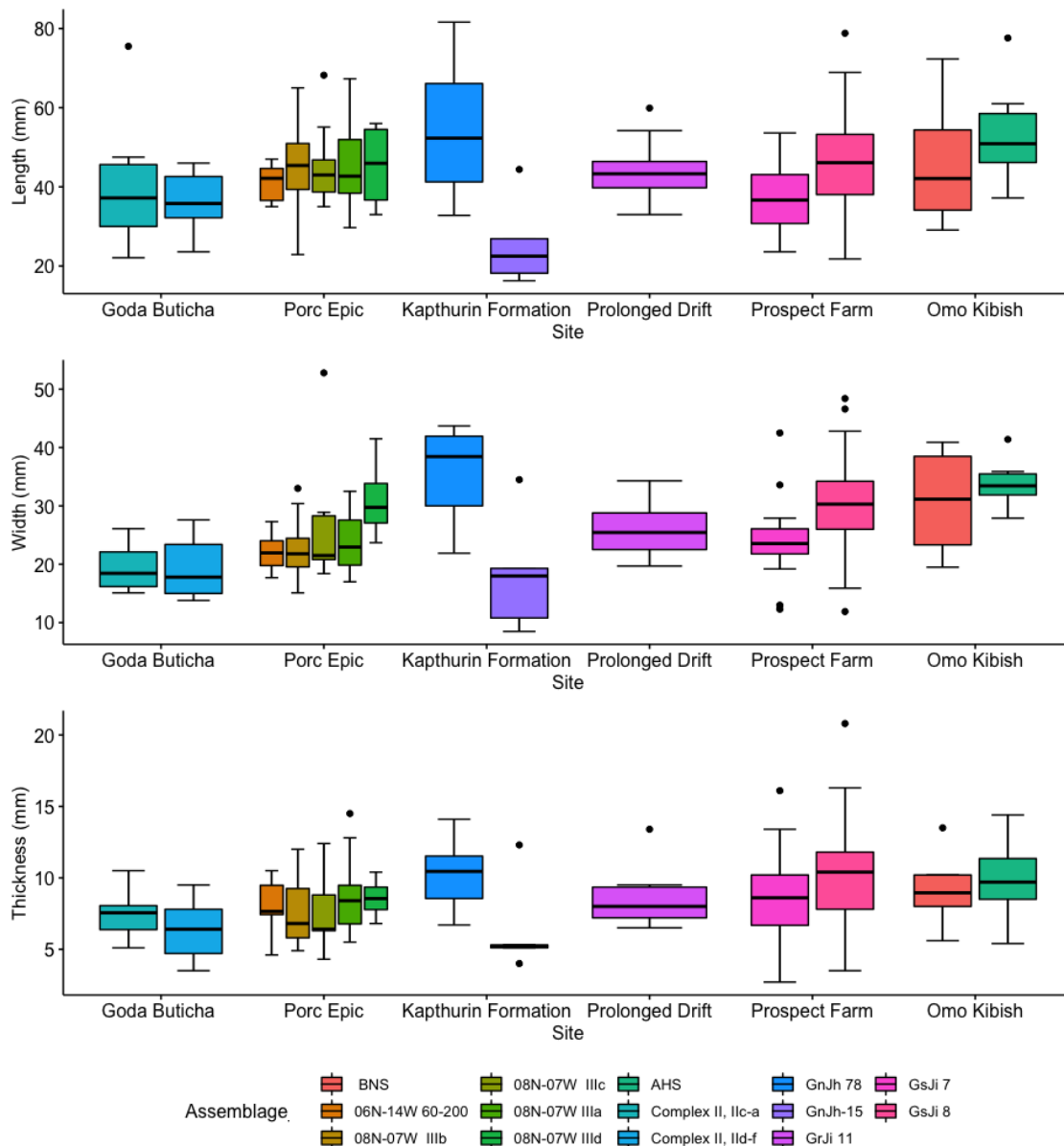


**Figure 32.** Boxplots of point length, width, and thickness (mm) for each assemblage.

**Table 20.** P-values from Tukey Honestly Significant Difference analyses for length, width, and thickness, as well as principal component (PC)1, 3 and 6 and centroid size (CS) for each pair of assemblages. Statistical significance is highlighted at  $p < 0.05$  (\*) and at  $p < 0.01$  (\*\*) and cells have been shaded grey to assist identification. All values have been rounded to 2 decimal places.

|                     | Length | Width | Thickn<br>ess | PC1  | PC3  | PC6  | CS   |
|---------------------|--------|-------|---------------|------|------|------|------|
| 06N-14W 60-200- BNS | 1.00   | 0.50  | 1.00          | 0.72 | 1.00 | 0.92 | 1.00 |
| 08N-07W IIIb- BNS   | 1.00   | 0.55  | 0.99          | 0.43 | 1.00 | 0.92 | 1.00 |
| 08N-07W IIIc- BNS   | 1.00   | 1.00  | 1.00          | 0.92 | 1.00 | 0.74 | 1.00 |
| 08N-07W IIIa- BNS   | 1.00   | 0.79  | 1.00          | 0.86 | 1.00 | 0.35 | 1.00 |
| 08N-07W III d- BNS  | 1.00   | 1.00  | 1.00          | 1.00 | 1.00 | 1.00 | 1.00 |

|                                     |       |        |        |        |        |      |        |
|-------------------------------------|-------|--------|--------|--------|--------|------|--------|
| AHS- BNS                            | 1.00  | 1.00   | 1.00   | 1.00   | 1.00   | 1.00 | 1.00   |
| Complex II, IIC-a- BNS              | 1.00  | 0.22   | 1.00   | 0.48   | 1.00   | 0.90 | 1.00   |
| Complex II, IId-f- BNS              | 0.92  | 0.12   | 0.86   | 0.77   | 0.91   | 0.22 | 0.98   |
| GnJh 78- BNS                        | 1.00  | 1.00   | 1.00   | 1.00   | 0.37   | 0.97 | 1.00   |
| GnJh-15- BNS                        | 0.19  | 0.22   | 0.94   | 1.00   | 0.51   | 0.52 | 0.04*  |
| GrJi 11- BNS                        | 1.00  | 1.00   | 1.00   | 0.99   | 1.00   | 1.00 | 0.11   |
| GsJi 7- BNS                         | 0.92  | 0.88   | 1.00   | 1.00   | 0.39   | 1.00 | 1.00   |
| GsJi 8- BNS                         | 1.00  | 1.00   | 1.00   | 1.00   | 0.90   | 0.62 | 0.55   |
| 08N-07W IIIb-06N-14W<br>60-200      | 1.00  | 1.00   | 1.00   | 1.00   | 1.00   | 1.00 | 1.00   |
| 08N-07W IIIc-06N-14W 60-<br>200     | 1.00  | 0.96   | 1.00   | 1.00   | 1.00   | 1.00 | 1.00   |
| 08N-07W IIIa-06N-14W 60-<br>200     | 1.00  | 1.00   | 1.00   | 1.00   | 1.00   | 0.99 | 1.00   |
| 08N-07W IIId-06N-14W 60-<br>200     | 1.00  | 0.41   | 1.00   | 0.64   | 1.00   | 1.00 | 1.00   |
| AHS-06N-14W 60-200                  | 0.44  | 0.01** | 0.98   | 0.78   | 1.00   | 1.00 | 0.98   |
| Complex II, IIC-a-06N-14W<br>60-200 | 1.00  | 1.00   | 1.00   | 1.00   | 1.00   | 1.00 | 1.00   |
| Complex II, IId-f-06N-14W<br>60-200 | 1.00  | 1.00   | 0.95   | 1.00   | 0.57   | 0.90 | 1.00   |
| GnJh 78-06N-14W 60-200              | 0.24  | 0.00** | 0.85   | 0.98   | 0.05*  | 1.00 | 1.00   |
| GnJh-15-06N-14W 60-200              | 0.26  | 1.00   | 0.99   | 0.82   | 0.20   | 1.00 | 0.03*  |
| GrJi 11-06N-14W 60-200              | 1.00  | 0.97   | 1.00   | 1.00   | 1.00   | 0.51 | 0.08   |
| GsJi 7-06N-14W 60-200               | 1.00  | 1.00   | 1.00   | 0.10   | 0.02*  | 0.87 | 1.00   |
| GsJi 8-06N-14W 60-200               | 0.90  | 0.00** | 0.30   | 0.07   | 0.31   | 1.00 | 0.48   |
| 08N-07W IIIc-08N-07W<br>IIIb        | 1.00  | 0.98   | 1.00   | 1.00   | 1.00   | 1.00 | 1.00   |
| 08N-07W IIIa-08N-07W<br>IIIb        | 1.00  | 1.00   | 0.98   | 1.00   | 1.00   | 0.93 | 1.00   |
| 08N-07W IIId-08N-07W<br>IIIb        | 1.00  | 0.45   | 1.00   | 0.34   | 1.00   | 1.00 | 1.00   |
| AHS-08N-07W IIIb                    | 0.83  | 0.01** | 0.80   | 0.43   | 1.00   | 1.00 | 0.97   |
| Complex II, IIC-a-08N-07W<br>IIIb   | 1.00  | 1.00   | 1.00   | 1.00   | 1.00   | 1.00 | 1.00   |
| Complex II, IId-f-08N-07W<br>IIIb   | 0.59  | 0.97   | 1.00   | 1.00   | 0.21   | 0.75 | 1.00   |
| GnJh 78-08N-07W IIIb                | 0.63  | 0.00** | 0.40   | 0.76   | 0.01** | 1.00 | 1.00   |
| GnJh-15-08N-07W IIIb                | 0.03* | 0.99   | 1.00   | 0.51   | 0.08   | 0.99 | 0.01** |
| GrJi 11-08N-07W IIIb                | 1.00  | 0.99   | 1.00   | 0.98   | 1.00   | 0.43 | 0.04*  |
| GsJi 7-08N-07W IIIb                 | 0.45  | 1.00   | 0.96   | 0.00** | 0.00** | 0.79 | 1.00   |
| GsJi 8-08N-07W IIIb                 | 1.00  | 0.00** | 0.00** | 0.00** | 0.02*  | 1.00 | 0.16   |
| 08N-07W IIIa-08N-07W<br>IIIc        | 1.00  | 1.00   | 1.00   | 1.00   | 1.00   | 1.00 | 1.00   |
| 08N-07W IIId-08N-07W<br>IIIc        | 1.00  | 0.99   | 1.00   | 0.87   | 1.00   | 1.00 | 1.00   |
| AHS-08N-07W IIIc                    | 0.98  | 0.59   | 0.93   | 0.96   | 1.00   | 1.00 | 1.00   |
| Complex II, IIC-a-08N-07W<br>IIIc   | 1.00  | 0.67   | 1.00   | 1.00   | 1.00   | 1.00 | 1.00   |

|  |        |        |      |       |        |        |        |
|--|--------|--------|------|-------|--------|--------|--------|
| Complex II, IId-f-08N-07W<br>IIIc      | 0.73   | 0.44   | 1.00 | 1.00  | 0.13   | 1.00   | 1.00   |
| GnJh 78-08N-07W IIIc                   | 0.93   | 0.17   | 0.72 | 1.00  | 0.01** | 1.00   | 1.00   |
| GnJh-15-08N-07W IIIc                   | 0.06   | 0.67   | 1.00 | 0.96  | 0.04*  | 1.00   | 0.02*  |
| GrJi 11-08N-07W IIIc                   | 1.00   | 1.00   | 1.00 | 1.00  | 0.95   | 0.27   | 0.07   |
| GsJi 7-08N-07W IIIc                    | 0.69   | 1.00   | 1.00 | 0.53  | 0.00** | 0.59   | 1.00   |
| GsJi 8-08N-07W IIIc                    | 1.00   | 0.90   | 0.26 | 0.55  | 0.04*  | 1.00   | 0.45   |
| 08N-07W IIIId-08N-07W IIIa             | 1.00   | 0.70   | 1.00 | 0.79  | 1.00   | 1.00   | 1.00   |
| AHS-08N-07W IIIa                       | 0.86   | 0.05*  | 1.00 | 0.91  | 1.00   | 0.91   | 0.99   |
| Complex II, IIc-a-08N-07W<br>IIIa      | 1.00   | 0.94   | 1.00 | 1.00  | 1.00   | 1.00   | 1.00   |
| Complex II, IId-f-08N-07W<br>IIIa      | 0.56   | 0.77   | 0.56 | 1.00  | 0.14   | 1.00   | 0.98   |
| GnJh 78-08N-07W IIIa                   | 0.68   | 0.00** | 0.97 | 1.00  | 0.00** | 0.99   | 1.00   |
| GnJh-15-08N-07W IIIa                   | 0.03*  | 0.92   | 0.92 | 0.93  | 0.05*  | 1.00   | 0.01** |
| GrJi 11-08N-07W IIIa                   | 1.00   | 1.00   | 1.00 | 1.00  | 1.00   | 0.02*  | 0.01** |
| GsJi 7-08N-07W IIIa                    | 0.42   | 1.00   | 1.00 | 0.15  | 0.00** | 0.03*  | 1.00   |
| GsJi 8-08N-07W IIIa                    | 1.00   | 0.01** | 0.50 | 0.08  | 0.01** | 1.00   | 0.05*  |
| AHS-08N-07W IIIId                      | 0.99   | 1.00   | 1.00 | 1.00  | 1.00   | 1.00   | 1.00   |
| Complex II, IIc-a-08N-07W<br>IIIId     | 1.00   | 0.16   | 1.00 | 0.40  | 1.00   | 1.00   | 1.00   |
| Complex II, IId-f-08N-07W<br>IIIId     | 0.97   | 0.09   | 0.98 | 0.70  | 0.35   | 0.97   | 0.98   |
| GnJh 78-08N-07W IIIId                  | 0.99   | 1.00   | 1.00 | 1.00  | 0.05*  | 1.00   | 1.00   |
| GnJh-15-08N-07W IIIId                  | 0.27   | 0.17   | 0.99 | 1.00  | 0.11   | 0.99   | 0.05*  |
| GrJi 11-08N-07W IIIId                  | 1.00   | 0.99   | 1.00 | 0.98  | 0.96   | 0.98   | 0.14   |
| GsJi 7-08N-07W IIIId                   | 0.97   | 0.80   | 1.00 | 1.00  | 0.04*  | 1.00   | 1.00   |
| GsJi 8-08N-07W IIIId                   | 1.00   | 1.00   | 1.00 | 1.00  | 0.28   | 1.00   | 0.61   |
| Complex II, IIc-a-AHS                  | 0.56   | 0.00** | 0.91 | 0.53  | 1.00   | 1.00   | 0.97   |
| Complex II, IId-f-AHS                  | 0.06   | 0.00** | 0.36 | 0.84  | 0.94   | 0.76   | 0.69   |
| GnJh 78-AHS                            | 1.00   | 1.00   | 1.00 | 1.00  | 0.36   | 1.00   | 0.99   |
| GnJh-15-AHS                            | 0.00** | 0.01** | 0.66 | 1.00  | 0.54   | 0.95   | 0.00** |
| GrJi 11-AHS                            | 0.95   | 0.63   | 1.00 | 1.00  | 1.00   | 0.99   | 0.01** |
| GsJi 7-AHS                             | 0.04*  | 0.09   | 1.00 | 1.00  | 0.35   | 1.00   | 0.99   |
| GsJi 8-AHS                             | 0.95   | 0.99   | 1.00 | 1.00  | 0.93   | 0.99   | 0.07   |
| Complex II, IId-f-Complex<br>II, IIc-a | 1.00   | 1.00   | 1.00 | 1.00  | 0.74   | 0.99   | 1.00   |
| GnJh 78-Complex II, IIc-a              | 0.38   | 0.00** | 0.68 | 0.83  | 0.13   | 1.00   | 1.00   |
| GnJh-15-Complex II, IIc-a              | 0.45   | 1.00   | 1.00 | 0.58  | 0.30   | 1.00   | 0.12   |
| GrJi 11-Complex II, IIc-a              | 1.00   | 0.71   | 1.00 | 0.98  | 1.00   | 0.53   | 0.33   |
| GsJi 7-Complex II, IIc-a               | 1.00   | 0.86   | 1.00 | 0.06  | 0.09   | 0.88   | 1.00   |
| GsJi 8-Complex II, IIc-a               | 0.97   | 0.00** | 0.26 | 0.05* | 0.63   | 1.00   | 0.94   |
| GnJh 78-Complex II, IId-f              | 0.02*  | 0.00** | 0.10 | 0.99  | 0.99   | 0.93   | 1.00   |
| GnJh-15-Complex II, IId-f              | 0.84   | 1.00   | 1.00 | 0.86  | 1.00   | 1.00   | 0.19   |
| GrJi 11-Complex II, IId-f              | 0.89   | 0.50   | 0.88 | 1.00  | 0.99   | 0.01** | 0.48   |
| GsJi 7-Complex II, IId-f               | 1.00   | 0.60   | 0.49 | 0.15  | 1.00   | 0.02*  | 0.99   |



|                          |        |        |        |      |      |      |        |
|--------------------------|--------|--------|--------|------|------|------|--------|
| GsJi 8-Complex II, IId-f | 0.10   | 0.00** | 0.00** | 0.12 | 1.00 | 0.96 | 1.00   |
| GnJh-15-GnJh 78          | 0.00** | 0.00** | 0.38   | 1.00 | 1.00 | 0.99 | 0.06   |
| GrJi 11-GnJh 78          | 0.88   | 0.21   | 0.99   | 1.00 | 0.55 | 0.73 | 0.19   |
| GsJi 7-GnJh 78           | 0.01** | 0.00** | 0.98   | 1.00 | 1.00 | 0.98 | 1.00   |
| GsJi 8-GnJh 78           | 0.83   | 0.68   | 1.00   | 1.00 | 0.87 | 1.00 | 0.79   |
| GrJi 11-GnJh-15          | 0.11   | 0.70   | 0.97   | 1.00 | 0.73 | 0.17 | 1.00   |
| GsJi 7-GnJh-15           | 0.70   | 0.85   | 0.89   | 1.00 | 1.00 | 0.40 | 0.01** |
| GsJi 8-GnJh-15           | 0.00** | 0.01** | 0.12   | 1.00 | 0.97 | 1.00 | 0.44   |
| GsJi 7-GrJi 11           | 0.88   | 1.00   | 1.00   | 0.92 | 0.54 | 1.00 | 0.02*  |
| GsJi 8-GrJi 11           | 1.00   | 0.93   | 0.95   | 0.95 | 0.99 | 0.07 | 0.84   |
| GsJi 8-GsJi 7            | 0.02*  | 0.03*  | 0.60   | 1.00 | 0.82 | 0.08 | 0.07   |

GMM analyses also highlighted significant variability in shape between the assemblages (MANOVA: Hotelling-Lawley = 1.540, approx.  $F = 2.67$ ,  $p < 0.001$ ), with PC1, PC3 and PC6 yielding significant differences (Fig. 33, Table 20). Along PC1, 08N-07W IIIb (Porc-Epic) and the two assemblages from Prospect Farm (GsJi 7 and GsJi 8) show significant differences, with the assemblage from Porc-Epic having elongated points compared to those from Prospect Farm (Fig. 33). GsJi 8 also shows significant differences to Complex II, IId-a from Goda Buticha (Table 20). Along PC3, all five of the assemblages from Porc-Epic show significant differences to GsJi 7 from Prospect Farm, with 08N-07W IIIa-c also displaying differences to GsJi 8, also Prospect Farm (Table 20). All of the Porc-Epic assemblages additionally show distinctions to GhJh 78 from Kapthurin Formation along PC3 with 08N-07W IIIa and 08N-07W IIIc also exhibiting differences to GnJh 15, Kapthurin Formation (Table 20). Along PC6, the assemblage from Prolonged Drift, GrJi 11, and GsJi 7 from Prospect Farm both show disparities to 08N-07W IIIa from Porc-Epic and Complex II, IId-f from Goda Buticha (Table 20).

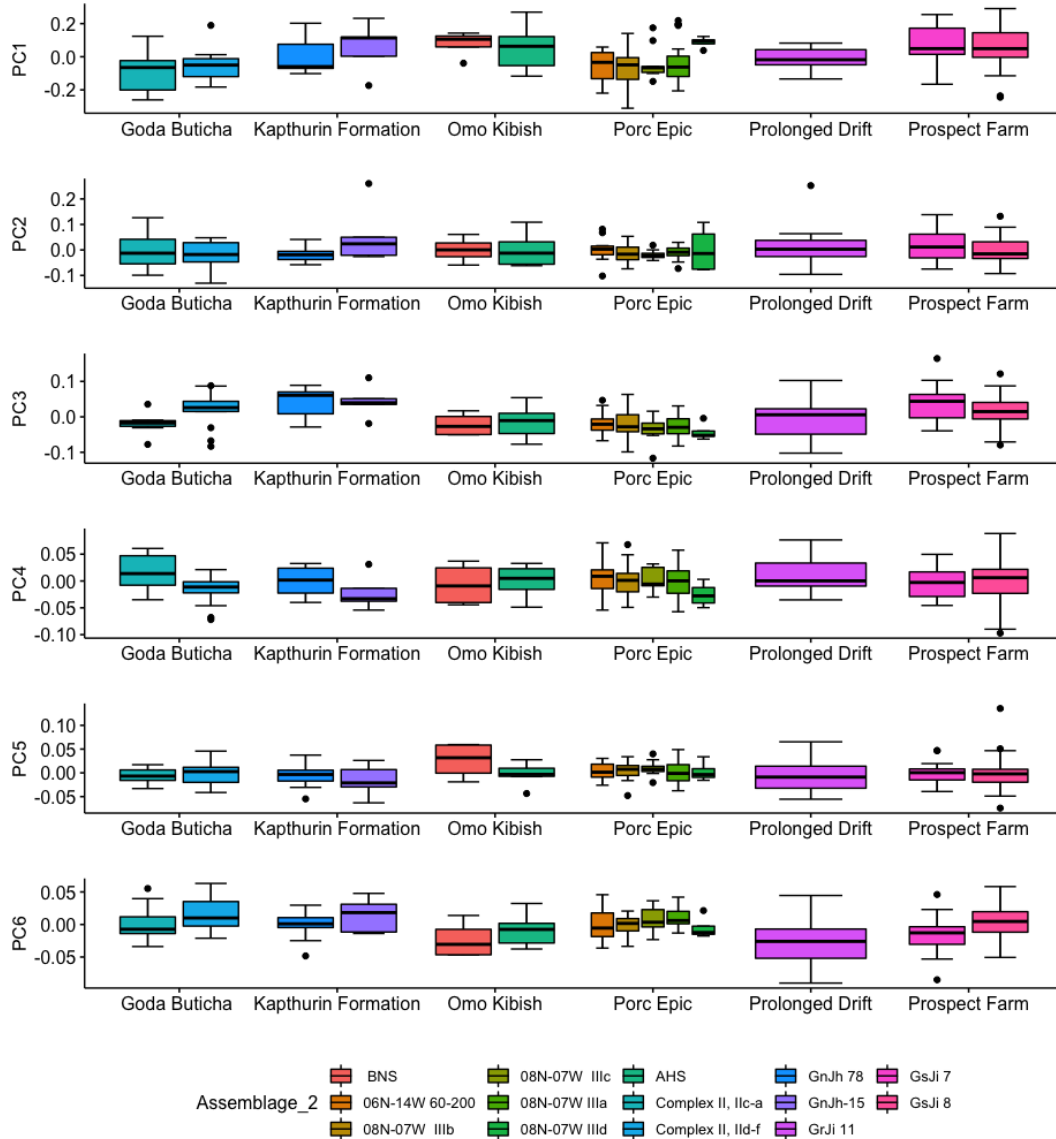


**Figure 33.** Boxplots of principal component (PC) scores along PC1-6 for each assemblage.

I then calculated the mean point shape for each assemblage (Table 21 and Appendix 3: Supplementary Fig. S2). Point shape appears relatively regular at Porc-Epic, with highly symmetrical elongated morphologies with acute tips seen in 4/5 assemblages. 08N-07W III d is differentiated to the other Porc-Epic assemblages, appearing much wider, more asymmetrical, and triangular shaped, as well as more standardised along PC1 ( $sd = 0.035$ ) yet more variable along PC2 ( $sd = 0.035$ ) than the other assemblages from the site (Table 21). Similar mean shapes to that just described are also reported for AHS (Omo Kibish) and GsJi 7 (Prospect Farm), with BNS sharing some similarities but also having further convexity in the base. Mean shapes for both Goda Buticha assemblages are elongated and thin, bearing similarities to the other assemblages at nearby Porc-Epic (Table 21; Appendix 3: Supplementary Fig. S2). Both assemblages from Kapthurin Formation demonstrate mean point shapes with relatively obtuse tip angles, with GnJh 15 in particular being asymmetrical; GnJh 15

is the least standardised assemblage along PC1 and PC2 (PC1 sd = 0.153, PC2 sd = 0.118; Table 21). GsJi 11 from Prolonged Drift exhibits a unique mean shape in that it exhibits extended right lateral convexity, though the rest of its morphology bears similarities to the assemblages from Kapthurin Formation (Table 21; Appendix 3: Supplementary Fig. S2).

**Table 21.** Principal component (PC) scores for the mean (m) shapes of each assemblage. Standard deviation (sd) is also reported demonstrating the variability of each assemblage in each dimension. All values have been rounded to 2 decimal places.

|                | PC1   |      | PC2   |      | PC3   |       | PC4   |      | PC5   |      | PC6   |      |
|----------------|-------|------|-------|------|-------|-------|-------|------|-------|------|-------|------|
|                | m     | sd   | m     | sd   | m     | sd    | m     | sd   | m     | sd   | m     | sd   |
| AHS            | 0.06  | 0.14 | 0.00  | 0.07 | -0.01 | 0.05  | 0.00  | 0.03 | -0.00 | 0.02 | -0.01 | 0.03 |
| BNS            | 0.08  | 0.08 | 0.00  | 0.05 | -0.02 | 0.03  | -0.01 | 0.04 | 0.03  | 0.04 | -0.02 | 0.03 |
| 06N-14W 60-200 | -0.06 | 0.10 | -0.00 | 0.05 | -0.02 | 0.03  | 0.01  | 0.04 | 0.00  | 0.02 | -0.00 | 0.03 |
| 08N-07W IIIb   | -0.08 | 0.12 | -0.01 | 0.03 | -0.02 | 0.04  | -0.00 | 0.03 | 0.01  | 0.02 | -0.00 | 0.02 |
| 08N-07W IIIc   | -0.04 | 0.10 | -0.02 | 0.02 | -0.04 | 0.04  | 0.00  | 0.02 | 0.01  | 0.02 | 0.01  | 0.02 |
| 08N-07W IIIa   | -0.04 | 0.13 | -0.01 | 0.03 | -0.03 | 0.028 | -0.00 | 0.03 | 0.00  | 0.02 | 0.01  | 0.02 |
| 08N-07W III d  | 0.09  | 0.04 | 0.00  | 0.09 | -0.04 | 0.03  | -0.03 | 0.02 | 0.00  | 0.02 | -0.01 | 0.02 |
| Complex IIc-a  | -0.09 | 0.14 | -0.00 | 0.07 | -0.02 | 0.03  | 0.02  | 0.04 | -0.01 | 0.02 | 0.00  | 0.03 |
| Complex II d-f | -0.05 | 0.10 | -0.02 | 0.05 | 0.02  | 0.05  | -0.02 | 0.03 | 0.00  | 0.03 | 0.02  | 0.08 |
| GnJh-78        | 0.02  | 0.12 | -0.02 | 0.03 | 0.04  | 0.04  | 0.00  | 0.03 | -0.01 | 0.03 | -0.00 | 0.02 |
| GnJh-15        | 0.06  | 0.15 | 0.06  | 0.12 | 0.04  | 0.05  | -0.02 | 0.03 | -0.02 | 0.03 | 0.01  | 0.03 |
| GrJi 11        | -0.01 | 0.07 | 0.02  | 0.10 | -0.01 | 0.07  | 0.01  | 0.04 | -0.01 | 0.04 | -0.03 | 0.04 |
| GsJi 7         | 0.07  | 0.13 | 0.01  | 0.06 | 0.04  | 0.05  | -0.00 | 0.03 | -0.00 | 0.02 | -0.02 | 0.03 |
| GsJi 8         | 0.06  | 0.11 | -0.00 | 0.05 | 0.02  | 0.04  | 0.00  | 0.04 | -0.00 | 0.03 | 0.00  | 0.02 |

### 8.5.5. Evaluation of point shape in relation to null models

To tease apart potential independent drivers of variation between point assemblages, such as those deriving from isolation by distance, time and environments, I performed a series of multiple matrix regressions using the mean point shapes (Table 21, Appendix 3: Supplementary Fig. S2). Table 22 reports the results for each PC as well as an overall model for all of the PCs. PC1 was found to have significant independent relationships with time ( $p = 0.001$ ), space ( $p = 0.002$ ) and environment ( $p = 0.006$ ), with time and space having similar positive effects (time coeff = 0.43, space coeff = 0.47), with precipitation having a negative effect (-0.38; Table 22). A negative relationship suggests that as diversity in one variable increases (PC1), the other decreases (precipitation). Because PC1 represents 63% of the total variance, the model for this PC explains 28% of the variance in the data, calculated using the  $R^2$  value (Table 22). PC3 has an independent significant relationship with space ( $p = 0.036$ ), and PC5 has an independent significant relationship with time (Table 22). Length and width have significant independent effects on PC1 (an axis characterised by elongation) and PC3 (an axis characterised by tip narrowing; Table 22). Raw material does not have a significant independent

effect on any of the PCs (Table 22). The final model found that distance through time, space and environment have significant independent effects on point shape variability, with all the variables together explaining 44.7% of the variance in the shape data (Table 22). This highlights the importance of isolation by distance, time, and environments, as well as point size and raw material use, in generating patterns of diversity between spatiotemporally disparate assemblages.

**Table 22.** Multiple matrix regression standardised test statistics and adjusted  $R^2$  for principal components (PC) 1-6, as well as an overall model incorporating all 6 PCs. Variance explained by each PC is given as well as the percentage of shape data explained by each PC is given as well as the percentage of shape data explained by the overall model (%), calculated by multiplying the percentage variance of each PC with the models  $R^2$  value. Those relationships that are significant at  $p \leq 0.05$  are shaded grey.

|                           | Length | Width  | Thickness | Raw<br>mat | Time   | Space  | Precip | Temp   | $R^2$ | %    |
|---------------------------|--------|--------|-----------|------------|--------|--------|--------|--------|-------|------|
| PC1<br>(63%)              | -0.674 | 0.720  | -0.353    | -0.066     | 0.436  | 0.477  | -0.379 | -0.101 | 0.445 | 28.0 |
| PC2<br>(11.2%)            | 0.283  | -0.152 | 0.027     | 0.195      | 0.418  | -0.171 | 0.344  | -0.171 | 0.692 | 7.8  |
| PC3<br>(8.7%)             | 0.786  | -0.350 | -0.083    | -0.158     | -0.133 | 0.245  | 0.187  | -0.137 | 0.435 | 3.8  |
| PC4<br>(4.6%)             | -0.050 | -0.019 | 0.044     | -0.076     | 0.294  | -0.155 | 0.109  | 0.018  | 0.102 | 0.4  |
| PC5<br>(2.6%)             | -0.297 | 0.060  | -0.044    | -0.229     | 0.617  | -0.028 | 0.065  | 0.262  | 0.387 | 1.0  |
| PC6<br>(2.6%)             | -0.290 | -0.122 | 0.442     | 0.208      | 0.113  | -0.016 | 0.172  | 0.175  | 0.243 | 0.6  |
| Overall<br>shape<br>(90%) | -0.419 | 0.591  | -0.295    | -0.052     | 0.495  | 0.411  | -0.243 | -0.103 | 0.497 | 44.7 |

Next, I ran multiple matrix regressions on the metric dimensions to ascertain the independent effects of space, time, environment, and raw material on point form. Table 23 reports the test statistics for each dimension as well as overall point form. Width ( $p = 0.001$ ) and time ( $p = 0.027$ ) have a significant independent effect on length (Table 23). Length ( $p = 0.001$ ), thickness ( $p = 0.002$ ) and raw material types ( $p = 0.045$ ) all have independent significant relationships with width (Table 23). Correlations between these measures of size affirms the common triangular shape of points, because as one metric increases the others also increase. Thickness has a significant relationship with width ( $p = 0.02$ ) and space ( $p = 0.02$ ; Table 23). The final model, incorporating all three dimensions to characterise overall point form, found only time to have a significant independent effect, with the overall model also being significant ( $p = 0.001$ ; Table 23).

**Table 23.** Multiple matrix regression standardised test statistics and adjusted  $R^2$  for length, width, and thickness in addition to the other variables, as well as an overall model incorporating all three dimensions (form). Those relationships that are significant at  $p \leq 0.05$  are shaded grey.

|        | Length | Width | Thickness | Raw<br>material | Time  | Space  | Precip | Temp   | $R^2$ |
|--------|--------|-------|-----------|-----------------|-------|--------|--------|--------|-------|
| Length | NA     | 0.421 | 0.103     | 0.160           | 0.371 | -0.139 | 0.127  | -0.145 | 0.695 |

|              |       |       |       |        |        |        |        |        |       |
|--------------|-------|-------|-------|--------|--------|--------|--------|--------|-------|
| Width        | 0.608 | NA    | 0.468 | -0.206 | -0.208 | 0.034  | -0.049 | 0.201  | 0.640 |
| Thickness    | 0.183 | 0.576 | NA    | 0.002  | 0.076  | 0.189  | -0.150 | -0.07  | 0.568 |
| Overall form | NA    | NA    | NA    | -0.050 | 0.445  | -0.002 | 0.002  | -0.013 | 0.320 |

## 8.6. Discussion

Early observations by Clark (1988) noted that MSA point shape and form varies substantially across eastern Africa. Results from a series of univariate and multivariate quantitative analyses here confirm the presence of statistically significant differences in point shape and form, both between and within eastern African MSA sites. Spatial distance, time, and precipitation are found to be key, independent drivers of point shape variability. However, not all diversity seen in eastern African MSA points can be explained by these null models. In fact, over half of the variability in point shape is unexplained by the variables studied, which could imply that the majority of point typology reflects other aspects of cultural variation. Stylistic traits are likely to be structured through space and time as a result of cultural transmission between interacting individuals, though the patterning observed here indicates that random cultural variation also contributes heavily to point diversity between eastern African MSA assemblages.

Raw material use was not found to have a significant independent effect of point shape diversity between assemblages, as has been suggested elsewhere in the literature (Andrefsky, 1994; Manninen and Knutson, 2014; cf. Timbrell *et al.*, 2022c). Instead, significant differences between the shapes of obsidian and chert points results from the unequal spatial distribution of raw materials across the landscape. Spatial variability is found to be an independent driver of point shape variability between assemblages, particularly along the latitudinal axis. Shea (2008) compared the whole MSA assemblage from Omo Kibish and Porc-Epic, in addition to Gademotta/Kulkuletti and the Middle Awash, and found notable technological similarities, including the formal characteristics of points, proposing that early *H. sapiens* were practising similar technological behaviour throughout southern and central Ethiopia between 80-200 kya. Indeed, GMM analysis confirmed no significant differences between point shapes from this area of eastern Africa. For example, points from Goda Buticha, southeastern Ethiopia, were found to exhibit similar morphologies despite a large chronological gap between the occupations, potentially indicating the maintenance of MSA cultural traditions extending into the Holocene (Pleurdeau *et al.* 2014). Point morphologies from within the Central Kenyan Rift were also not found to be significantly different from each other in any shape dimension (i.e., the PCs). Broadly, latitudinal differences in point shapes can be characterised as ranging between long, thin points and short wide points, though this trend is not maintained for all samples. This dichotomy in eastern African point variability seen here could indicate the presence of at least two sub-regional traditions in point style throughout the EARS system, supporting a degree of cultural coherence and

demographic stability through space and time. Obsidian sourcing studies at Prospect Farm found that, despite it being very close to local raw material sources, exotic obsidian was utilised at the site, leading the authors to suggest the presence of long-distance trade networks through the Rift Valley (van Baelen *et al.* 2019). Moreover, cultural continuity and the maintenance of traditions has also been proposed from analyses of point technology at Nasera, Mumba and Magubike by Bushozi (2011); these assemblages were not studied in this analysis, but it would be interesting to explore how far the regionalisation of traditions extended throughout eastern Africa, particularly in different biogeographic zones.

Contrastingly, the metric data revealed several statistically significant differences within and between sites from these two sub-regions, as well as differences between assemblages from the same site. This indicates that form (shape and size) rather than just shape is more useful for differentiating between MSA points from different assemblages. This is supported by differences in centroid size being significantly different between multiple assemblages with similarly shaped points. Differences in size likely also relates to functional element of the tool, thus supporting GMM as more useful for capturing variability in style rather than function. An additional benefit of including both metric and GMM data within the analysis is that thickness captures variability in the third dimension, an aspect of point form not accounted for in the outline. Thickness was found to have an independent significant relationship with space in the multiple matrix regressions, suggesting that points from assemblages further away from each other also have different point thicknesses. Thickness has been linked to the ballistics of the point and hafting, with thinner points allowing better penetration and thicker points having higher impact resistance and variability constrained by shaft configuration (White, 2013); this is seen ethnographically with projectiles used to hunt small birds being broad and flat, which kill without penetrating the skin (Clark, 1952; Hodder, 1982). PC5, an axis of variance that characterises diversity in the shape of the hafted end, shows a significant relationship with thickness, supporting a potential link between base morphology and overall thickness that could be linked to functionality such as type of propulsion (White, 2013; Coppe, Leper and Rots, 2022). This may speak to the multifunctional nature of points, as has been proposed for the MSA (Douze *et al.*, 2020; Timbrell *et al.*, 2022c) and/or that the taxon as defined by Shea (2020) contains diverse tools. That said, functionality should also correlate with climatic variables to some extent, as these are what condition the selective environment for tool manufacture (White, 2013). Overall, this highlights the complex considerations required when using point typology without technological and use-wear analysis to understand patterns of point manufacture, with further exploration ultimately needed on bigger samples.

Multiple matrix regressions found that point shape diversity between assemblages can be explained by the distance between them through time, space and in relation to environments, particularly

precipitation. These relationships can be further explored through individual linear regressions to better understand the nature and direction of the relationship (Fig. 34). The results show that assemblages that differ in terms of point elongation tend to be found at further distances and in different chronological periods, with wider, shorter morphologies found in older contexts and/or at lower latitudes (Fig. 34a-b). Wider points also tend to be associated with higher precipitation environments (Fig. 34c). The negative coefficient for precipitation in the multiple matrix regression for PC1 and the final model suggests that, as points get more similar, the precipitation values they experience diverge. This is captured by the shape of the data in Fig. 34c – variance between the points along the Y axis (precipitation) increases as variance between the points along the X axis (PC1) decreases. All of the assemblages studied are found in sub-humid landscapes (>600mm precipitation) which are considered to be suitable habitats for hominin occupation, yet Figure 34c suggests that, within this bracket, higher precipitation environments allow for a greater variety of point shapes whereas those with relatively little rainfall may act as a constraint on point shape. Because aridity generally elicits more open landscapes like xerophytic shrubland, a standardised point style may emerge as a specific ecological adaptation, for example to ensure ballistic efficiency when thrown across open spaces. Smaller, elongated point morphologies were likely more aerodynamic than those with wider morphologies, and thus perhaps used for lightweight weapons projected through the air across long distances (Lombard *et al.*, 2022). Additionally, more standardised shapes may suggest that, within these relatively arid tropical biomes, populations traded standardised points within a group network, as seen ethnographically (Wiessner, 1982, 1983, 1985). Assemblages that demonstrate diversity in patterns of tip narrowing (PC3) tend to be further apart in space, with points at lower latitudes appearing more triangular with acute tips (Fig. 34d), a trend first noted by Clark (1988). Figure 34e highlights that diamond-shaped points (i.e., those with acute tips and convexity in the proximal end) tend to be found in younger contexts, though the correlation is not strong.

Together, these results indicate that a large proportion of diversity in eastern African MSA points can be explained by null models of isolation by distance, time and environments (precipitation). Cultural transmission tends to occur between groups that are proximal in time and space through interaction, structuring patterns of diversity as a result of copying and learning. Independent significant relationships between point shapes and precipitation, and not temperature, also indicate a potential role for environmentally mediated convergence in driving point shape variability, with certain point styles potentially representing adaptive responses to different palaeoecological contexts. The effects of temperature and rainfall on the ecosystem are difficult to disentangle, though precipitation has been found to profoundly impact food availability in the tropics due to the effects of rainfall on plant phenology, with major repercussions for fauna, foraging behaviour, and reproductive and population growth rates (Boyle, Shogren and Brawn, 2020). On a global scale, Torrence (2001) predicts that, in tropical environments that are less affected by seasonality, a more generalised point form used for

hunting a variety of animals should prevail, compared to higher latitude environments where specialised forms that minimise risk due to shorter periods of game availability are observed. Applying these hypotheses to the African MSA, point shape, size, and frequency could all be seen as adaptive to variable precipitation regimes that affect the range of prey available and thus the type of delivery system(s) adopted. For example, in South Africa, Still Bay bifacial points have been proposed to have been designed to be multi-functional and to economise raw material, which may have been useful in unpredictable and variable ecological zones (McCall and Thomas, 2012). Additionally, bifacial lanceolate points found in Lupemban assemblages in Central Africa have been suggested to represent a rainforest adaptation to wood-working (Taylor, 2022). Our results indicate that, even beyond these highly stylistic styles, MSA point morphology was likely affected by variable rainfall patterns across Africa in order to facilitate the engagement with different environmental contexts, with perhaps more elaborate styles an adaptive response under certain environmental or demographic conditions.

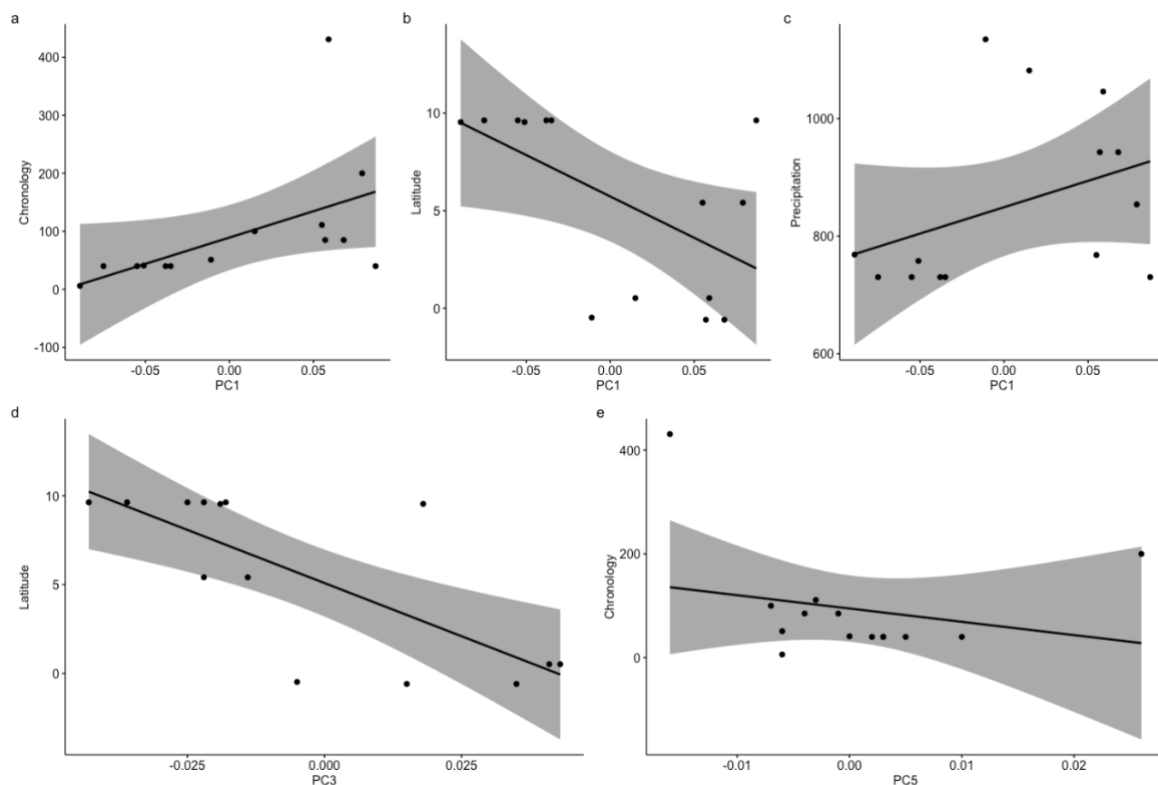


**Figure 34.** Regressions of principal components (PC) 1, 3 and 5 against chronology, latitude, and precipitation according to which demonstrated independent relationships in the multiple matrix regression (see Table 22). 95% confidence intervals have been highlighted in grey.



## 8.7. Conclusion

Overall, eastern African MSA points are differentiated in both shape and form, with null models of space, time and environment, as well as the effects of raw material and size, found to explain around 45% of the total variance in point shapes between assemblages. This suggests that eastern African MSA populations were structured considerably via autocorrelation through time and space and in relation to precipitation, but not temperature, though over 50% of the total variance relates predominately to random aspects of cultural or stylistic diversity. Indeed, it is these aspects of variance that we, as archaeologists, tend to be interested in capturing in analyses of cultural and behavioural evolution, such as those modelling inter-group dynamics and the development of cultural complexity, yet they are somewhat obscured through compounding effects of autocorrelation. Overall, points are imperfect proxies for shared cultural traditions in archaeological populations due to myriad factors affecting their size, shape and technological characteristics. However, multivariate regression provides a promising approach for isolating these different influences on lithic morphology, with systematic use-wear analyses fundamentally required to ascertain whether the ‘point’ itself is indeed a coherent technological concept across MSA assemblages.

## Chapter 9: Integrating the habitability model with point shape variability

### 9.1. Introduction

Hunter-gatherers obtain resources via central place foraging, which means acquiring food in a radius surrounding a residential base. When the resources have been depleted, Binford (1982) proposed that hunter-gatherers should move at least twice the foraging radius of that of the current residential base to avoid foraging in exhausted territory. This feature of hunter-gatherer mobility strategies tends to mean that any individual population's home-range can be geographically extensive, making the likelihood of interactions between and within regional networks of hunter-gatherer groups relatively high. Hunter-gatherer population density and connectivity is hypothesised to have increased during the MSA, with the appearance and spread of novel behaviours potentially leading to the transition to the LSA and dispersals across and out of Africa (McBrearty and Brooks, 2000; Gunz *et al.*, 2009; Powell, Shennan, Thomas, 2009; Tryon *et al.*, 2016).

Habitat quality, and its implications for resource abundance, has been argued to be a key influence over hunter-gatherer mobility strategies and consequently population structure. For example, Dyson-Hudson and Smith (1978) proposed that territoriality occurs when resources are sufficiently abundant and predictable in space and time, so that costs of exclusive use and defence of an area are outweighed by the benefits gained from resource control. Analyses by Kelly (1993, 1995) indicate that the frequency of moves observed in ethnographic populations correlates with the available biomass in the environment, with low amounts of consistently accessible edible plant foods tending to lead to frequent mobility. Grove (2009) also found that climatic variables are limiting factors on hunter-gatherer mobility strategies as well as group sizes, with larger hunter-gatherer groups able to be sustained in better habitats and tending to move short distances. Extension of the modelling by Grove (2018) then found that hunter-gatherer groups adjust their levels of mobility to maintain contact with neighbours, ensuring that opportunities for cultural transmission and interaction are maintained regardless of climatic fluctuations. Recent work by Garg *et al.* (2021) goes further to suggest that the heterogeneity of resources across the landscape, under certain mobility regimes, may itself encourage the development of a complex population structure, characterised by tightly clustered subgroups within a more extensive regional network. These authors also found that central place foraging demonstrated increased propensity for information transmission in larger populations than point-to-point foraging strategies of non-human great apes. Overall, whilst it is perhaps unsurprising that environmental variables, given their effect on resource quality and availability, have a strong

influence over hunter-gatherer behaviour, these results stress the importance of the physical landscape in driving hunter-gatherer mobility patterns, as well as the potential role of mobility in facilitating opportunities for innovation and increased behavioural complexity through its impact on interaction and cultural transmission.

As previously discussed in Chapter 8, archaeological diversity is often both spatially and temporally autocorrelated, with differences between any two entities increasing as a function of the temporal and spatial distance between them (Loog *et al.*, 2017). The extent to which spatial differences contribute to cultural diversity has been hypothesised to rely heavily on population structure and mobility, with low mobility leading to strong spatial structure and thus differences are more likely to be correlated with space relative to time (Loog *et al.*, 2017). When mobility is high, time tends to explain a larger proportion of variability due to the homogenising effects of interaction across space. Convergence, as a result of isolated populations arriving at a similar technological or behavioural solution through adaptation to specific climatic conditions or by chance, also increases variation within a region independent of cultural transmission. However, aspects of the physical landscape not only provide the selective environment that can drive patterns within the archaeological record, but also influence the distribution and density of hunter-gatherer populations through space and time. Like ethnographic populations, MSA hunter-gatherers were also highly mobile, therefore the articulation between dispersal patterns, paleoclimatic change and the spatiotemporal structuring and variability of populations has the potential to provide interesting insight into early *H. sapiens* demography and evolution.

Chapter 5 describes an archaeologically validated habitability model that incorporates spatial, chronological, and environmental dimensions into a single index that predicts how suitable certain areas of eastern Africa would have been for habitation by MSA hunter-gatherers. This index will be used in this final chapter in two ways. First, it will be directly applied to understand the effects of habitat suitability on point shape variability. Because the primary function of stone tools is to assist with the procurement of food, the forms of lithics are likely influenced by type of animal and delivery system. For example, technological adaptations that increase hunting performance may be a response to resource risk, with highly specialised tools designed to kill as many prey as possible in a short period likely in areas of unstable food availability and more generalised toolkits in areas of less pronounced seasonality, like the tropics (Torrence, 2001). Additionally, in these more stable and abundant environments, fewer retouched tools with low levels of standardisation were likely manufactured on an ad-hoc basis for a varied task and thus discarded after use, whereas curated tools would have required more skill to make and were resharpened and reused repeatedly (Parry and Kelly, 1987). All of the points studied in this research come from sub-humid landscapes, thus these environmental influences are likely to be less pronounced than at a global scale. Nonetheless, Chapter

8 found that more arid areas tended to demonstrate a convergence in point shapes with wetter areas having more variation between assemblages, indicating that such patterns can be observed even at a regional scale. Point shape variability could thus also be linked to environmental suitability. Therefore, through this first analysis, I will ascertain the effects of habitat suitability on point form and shape.

Secondly, the habitability model will be used to map habitable corridors between chronologically corresponding assemblages through heterogeneous landscapes. Resulting routes can then be interpreted in terms of how likely they are to have facilitated dispersal and, potentially, interaction between spatially disparate populations. Though it is highly unlikely that any of the populations represented by the assemblages studied in this analysis directly interacted with each other due to the large chronological span of the eastern African MSA, they offer a palimpsest of cultural variability for a broad moment in space/time. Despite the limitations of the archaeological record, this analysis will facilitate the integration of the ecology of eastern Africa during the Late-Middle Pleistocene with MSA archaeological diversity through a novel combined approach, enabling exploration of intra-regional dispersals and mobility.

## 9.2. Materials and Methods

To integrate the point shape data from Chapter 8 with the habitability model (Chapter 5), I extracted the habitability values for each assemblage from the time-slice representative of the simple age (following methods established in Chapter 4); this value gives an indication of whether the assemblage was in a marginal or optimal environment. To understand the impact of dating error, 1000 iterations were performed, permuting across the age range of each point assemblage. The results are reported in Appendix 4 and, whilst chronological uncertainty does increase the variance of the coefficient estimates, iterating across the dating range does not alter the original results (Appendix 4: Supplementary Figure S1-2).

Multiple matrix regressions were used to assess the impact of habitability on point shape. As the habitability model incorporates the environmental characteristics of the assemblage, the raw values of precipitation and temperature were removed from the modelling. Chronology is also somewhat captured by the habitability model in that it is time-specific, however simple age was retained in the model as an absolute measure of the distance of the assemblages through time.

I determined which assemblages had overlapping dating ranges (see Fig. 24 in the previous chapter), defined as occupations whose duration, captured by the minimum and maximum absolute dates for

that assemblage, are corresponding for at least 1,000 years. Then, I modelled habitable corridors between them via a least-cost path analysis. To accomplish this, I took the time-slice from the habitability model representative of the midpoint of the chronological overlap between two assemblages. For example, BNS has a date range of 93-123 kya and GsJi 7 has a date range of 50-120 kya; for these two sites, I used the raster from the habitability model representative of 107 kya as this is the mid-point between 93 and 120 kya (the period that the sites could have co-existed). When an assemblage only has a single date associated to it (i.e., GnJh 78 has a rough date of 100 kya [Blegen *et al.*, 2018]), and if this single date falls within another assemblage’s date range, the time slice for that single date was used. The rasters from the habitability model were turned into a cost surface, where the value in each cell represents the cost of occupying that area. Table 24 summarises the cost surface utilised for each pair of overlapping assemblages.

**Table 24.** Summary of the overlapping assemblages studied in this analysis, with a justification of which time slice was chosen for the model.

| Assemblage 1     | Assemblage 2   | Time slice of cost surface | Justification                     |
|------------------|----------------|----------------------------|-----------------------------------|
| BNS              | GsJi 7         | 107                        | Mid-point of overlap (93-120 kya) |
| BNS              | GsJi 8         | 107                        | Mid-point of overlap (93-120 kya) |
| BNS              | GnJh 78        | 100                        | Age estimation of KF assemblage   |
| GsJi 7           | GnJh 78        | 100                        | Age estimation of KF assemblage   |
| GsJi 7           | GrJi 11        | 61                         | Mid-point of overlap (50-72 kya)  |
| GsJi 8           | GrJi 11        | 61                         | Mid-point of overlap (50-72 kya)  |
| Complex II IId-f | GrJi 11        | 41                         | Mid-point of overlap (33-48 kya)  |
| Complex II IId-f | 06N-14W 60-200 | 40                         | Age estimation of PE assemblage   |
| Complex II IId-f | 08N-07W IIIa   | 40                         | Age estimation of PE assemblage   |
| Complex II IId-f | 08N-07W IIIb   | 40                         | Age estimation of PE assemblage   |
| Complex II IId-f | 08N-07W IIIc   | 40                         | Age estimation of PE assemblage   |
| Complex II IId-f | 08N-07W IIId   | 40                         | Age estimation of PE assemblage   |

The calculation of cost distances requires the transformation of the raster (i.e., a time slice from the habitability model) into a matrix whereby cell centres are connected to each other via nodes. Connections between the nodes are weighted according to the probability of transition (van Etten, 2019). For calculating the cost of movement in Chapter 5, the difference in altitude values of the DEM was used as the probability of transition between cells; here, the mean of the two connecting cells was used, and the optimal route was then calculated to increase conductance. This means that the route was calculated to maximise the accrued values when travelling between site locations rather than minimise, as the accumulation of high values equates to the tracking habitability. To calculate cost paths through the cost surfaces, I used the ‘gdistance’ (van Etten, 2019) and ‘leastcostpath’ (Lewis, 2022) R packages.

### 9.3. Results

Table 25 reports the habitability index scores of each assemblage. Assemblages from Omo Kibish, Kapthurin Formation and Prolonged Drift occupy the most suitable landscapes (index > 0.90), with assemblages from Prospect Farm located at a slightly sub-optimal suitability due to its position at high altitude (index = 0.63). Goda Buticha and Porc-Epic assemblages are located within the least suitable landscapes (index ≤ 0.44). Although Omo Kibish and Goda Buticha demonstrate considerable chronological variability between assemblages, the habitability index at both sites remains relatively stable through time, suggesting that either optimal and marginal environments have a deep-rooted spatial structure across eastern Africa or the persistent preferences of humans for more certain areas of the landscape, with occupations only occurring when the site falls within the habitable range (Tribolo et al., 2017). Modelling by Blinkhorn *et al.* (2022) implicates the area as being within the narrow definition of a refugia on the border between stable open and changing forest environments, thus it may even be a combination of the two. When comparing point form variability with suitability, there does not appear to be a relationship between intra-assemblage diversity and habitat quality, as both optimal and marginal environments sustain the full range of variability, from standardised assemblages (low standard deviations) to unstandardised assemblages (high standard deviations). This likely attests to the region’s relative stability as a refugia (Blinkhorn et al., 2022) with much of the landscape habitable throughout the MSA, as suggested by modelling in Chapter 5. In this sense, whilst some sites appear more habitable than others, habitability may not have exerted a strong influence over intra-assemblage point variability at this scale.

**Table 25.** Habitability index values of each assemblage alongside the standard deviations of length, width and thickness (mm) for that assemblage.

| Assemblage        | Index | Length (sd) | Width (sd) | Thickness (sd) |
|-------------------|-------|-------------|------------|----------------|
| 06N-14W 60-200    | 0.435 | 4.6         | 3.0        | 1.6            |
| 08N-07W IIIa      | 0.435 | 10.1        | 4.6        | 2.4            |
| 08N-07W IIIb      | 0.435 | 10.6        | 4.6        | 2.1            |
| 08N-07W IIIc      | 0.435 | 10.3        | 10.6       | 2.7            |
| 08N-07W III d     | 0.435 | 11.5        | 7.6        | 1.5            |
| AHS               | 0.956 | 14.1        | 4.5        | 3.1            |
| BNS               | 0.956 | 19.0        | 10.3       | 3.2            |
| Complex II, IIc-a | 0.362 | 16.5        | 3.9        | 1.6            |
| Complex II, IId-f | 0.354 | 6.8         | 4.8        | 1.8            |
| GnJh 78           | 0.912 | 16.8        | 8.4        | 2.4            |
| GnJh-15           | 0.936 | 11.2        | 10.2       | 3.3            |
| GrJi 11           | 0.959 | 8.6         | 5.0        | 2.2            |
| GsJi 7            | 0.633 | 7.9         | 6.2        | 3.0            |
| GsJi 8            | 0.633 | 10.8        | 7.8        | 3.2            |

Multiple matrix regression of the PCs found that many of the significant relationships noted in Chapter 8 were retained (Table 26). Habitability was found to have a significant effect on certain aspects of point shape, particularly PC3 and PC6. When comparing the  $R^2$  values for the final model from Chapter 8 and here, this model captures more of the shape variability at 47% compared to the earlier model where environments were characterised by the raw climatic values (Table 26). For the multiple matrix regression of the metric dimensions, habitability had a significant effect on width (Table 27). Importantly, neither temperature nor precipitation was found to have a significant effect on point form in Chapter 8 (Table 27); this result therefore suggests that the suitability of the overall landscape rather than climatic variables themselves influences point form, specifically width.

I then calculated habitable corridors through the landscape for each pair of overlapping sites/assemblages (see above explanation of how overlapping occupations were determined). Figure 35 maps the least cost pathways through the habitability model. The resulting routes demonstrate how habitable corridors closely track water networks, probably because water networks follow the lowest topographic gradients, with interaction between northern and southern localities likely mediated by Lake Turkana (Cuthbert *et al.*, 2017). Routes through habitable corridors would have certainly been longer than Euclidean distances (i.e., straight line distances between sites), as demonstrated by Figure 35 where uninhabitable zones are circumnavigated in favour of more habitable zones.

**Table 26.** Multiple matrix regression standardised test statistics, including the habitability index rather than the raw climatic variables, and adjusted  $R^2$  for principal components (PC) 1-6, as well as an overall model incorporating all 6 PCs. Variance explained by each PC is given as well as the percentage of shape data explained by each PC is given as well as the percentage of shape data explained by the overall model (%), calculated by multiplying the percentage variance of each PC with the models  $R^2$  value. Those relationships that are significant at  $p \leq 0.05$  are shaded grey.

|                        | Length | Width  | Thickn<br>ess | Raw<br>mat | Time   | Space  | Hab    | $R^2$ | %      |
|------------------------|--------|--------|---------------|------------|--------|--------|--------|-------|--------|
| PC1 (63%)              | -0.778 | 0.745  | -0.271        | -0.148     | 0.481  | 0.283  | -0.071 | 0.367 | 23.121 |
| PC2<br>(11.2%)         | 0.421  | -0.196 | 0.046         | 0.099      | 0.451  | 0.068  | -0.059 | 0.611 | 6.843  |
| PC3 (8.7%)             | 0.819  | -0.272 | -0.171        | -0.282     | -0.005 | 0.555  | 0.332  | 0.502 | 4.368  |
| PC4<br>(4.6%)          | -0.028 | -0.005 | 0.010         | -0.069     | 0.305  | -0.061 | -0.045 | 0.096 | 0.044  |
| PC5 (2.6%)             | -0.034 | 0.125  | -0.083        | -0.076     | 0.589  | 0.026  | -0.004 | 0.336 | 0.087  |
| PC6 (2.6%)             | -0.243 | -0.190 | 0.436         | 0.356      | -0.006 | -0.215 | 0.273  | 0.280 | 0.073  |
| Overall<br>shape (90%) | -0.493 | 0.635  | -0.257        | -0.142     | 0.564  | 0.345  | -0.145 | 0.472 | 42.48  |

**Table 27.** Multiple matrix regression standardised test statistics and adjusted  $R^2$  for length, width, and thickness in addition to the other variables including the habitability index, as well as an overall model incorporating all three dimensions (form). Those relationships that are significant at  $p \leq 0.05$  are shaded grey.

|              | Length | Width | Thickness | Raw<br>mat | Time   | Space  | Hab    | $R^2$ |
|--------------|--------|-------|-----------|------------|--------|--------|--------|-------|
| Length       | NA     | 0.420 | 0.085     | 0.079      | 0.430  | -0.043 | -0.048 | 0.673 |
| Width        | 0.568  | NA    | 0.487     | -0.070     | -0.271 | -0.071 | 0.140  | 0.639 |
| Thickness    | 0.144  | 0.614 | NA        | -0.056     | 0.119  | 0.146  | -0.082 | 0.557 |
| Overall form | NA     | NA    | NA        | -0.046     | 0.433  | -0.037 | 0.057  | 0.324 |



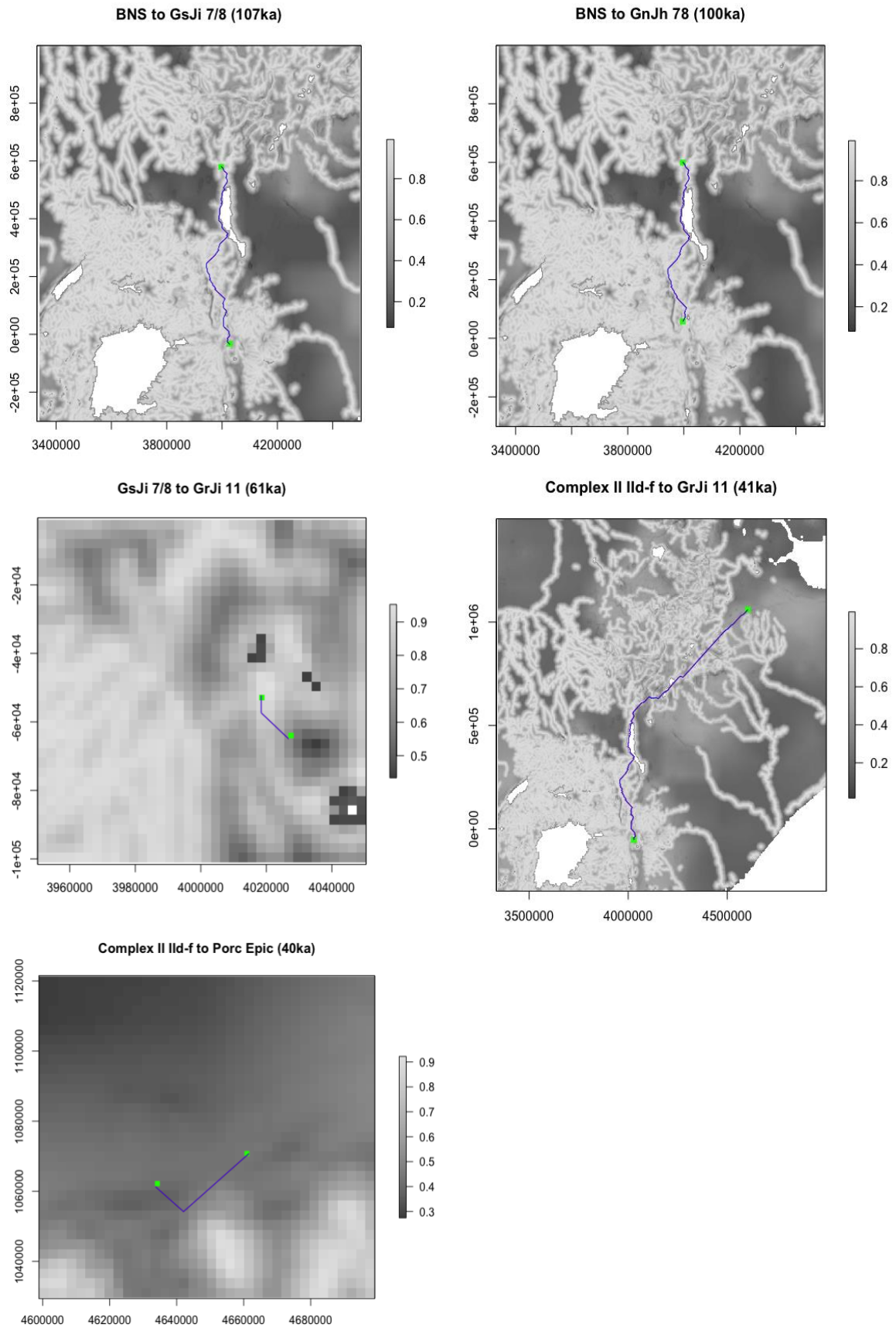


**Figure 35.** Predicted dispersal corridors, calculated using least-cost pathways through the habitability index cost-surface corresponding to the mid-point between the chronological overlap of two assemblages.

## 9.4. Discussion

Habitat suitability has a significant influence over MSA toolkits, potentially both through the adaptation to similar habitats (IBE and convergence) as well as its influence over hunter-gather distribution and density, thus mediating cultural transmission between groups across heterogeneous landscapes (a form of IBD). The results here highlight that, whilst habitat suitability does not affect the standardisation of point forms *within* an assemblage as predicted, the habitability index does have an independent significant effect on certain aspects of eastern African MSA point form *between* assemblages. I plotted the significant relationships between habitability and point shape, characterised by the PCs established in Chapter 8, and point form. Figure 36 demonstrates that, as habitability increases, PC3 and width increase whilst PC6 decreases. This highlights that points that have more obtuse tips and/or are wider tend to be found in more habitable environments, whilst those that have more reduced tip and/or are narrower tend to be found in less habitable environments (see Fig. 25 in Chapter 8 for a visualisation of the shape differences captured by PC1-6). Whilst the correlation coefficients are high (see Fig. 36 for results), none of the individual models are found to be statistically significant, suggesting that the relationship between habitat suitability and point form/shape is weak based on the current sample. This is also reflected in the fact that, in the final model (accounting for 90% of the shape variance), habitability is not found to have a significant independent effect on overall point shape. In Chapter 8, the results suggested that wetter sub-humid landscapes may have led to wider variance in point shapes between assemblages, perhaps to facilitate the occupation of wooded/ecotonal landscapes with more variable food resources and where prey can be ambushed at close quarters, whereas populations living in more arid areas may have seen a convergence in point shape around aerodynamic designs that facilitate long-distance hunting across open spaces. This could suggest that the raw effects of precipitation on point shape diversity are more influential than that exerted by the overall suitability of the landscape. However, because the correlation is high between habitat suitability and point diversity, it is likely that significance would be achieved with larger samples of assemblages.

Least cost-path analyses have highlighted potential routes through habitable corridors between chronologically corresponding sites. Whilst this analysis is inherently limited by the chronological resolution and associated dating error of the assemblages, and the fact that the long duration of the MSA means that only a few assemblages potentially overlap in time, interesting points of comparison can be made in relation to the patterns of point shape variability observed. The first point of comparison is between BNS (Omo Kibish), GsJi 7 and 8 (Prospect Farm) and GnJh 78 (Kaphthurin Formation). Prospect Farm and Kaphthurin Formation are at a similar distance to Omo Kibish and occur along the same habitable corridor around about the same time (~100/107 kya). Table 28 reports

the scaled distance matrix of point shapes, characterised by PC1-6, between assemblages. BNS from Omo Kibish demonstrates relatively similar point shapes to the Prospect Farm assemblages (GsJi 7 – 0.36; GsJi 8 – 0.32; Table 28). Yet this similarity is not expressed as strongly at the slightly closer GnJh 78 (0.55; Table 28). Nonetheless, BNS is found to be more similar to this Kapthurin Formation assemblage than almost all of those from Porc-Epic and both assemblages from Goda Buticha (shape distance > 0.67; Table 28). This could support the interpretation that population networks from the Central African Rift Valley extended northwards beyond Lake Turkana and into southwestern Ethiopia through the Lower Omo Valley, but no further. Shea (2008) describes how MSA assemblages from East Turkana demonstrate some similarities (but also differences) to the Omo Kibish assemblages, though Figure 35 suggests that routes south may have circumnavigated Lake Turkana to the west rather than the east. This is likely because the Kibish Formation extends southwards from the Lower Omo valley along the northwestern side of Lake Turkana. Few MSA sites from West Turkana have been reported due to a combination of poor preservation and political instability in the region, though a rare site at Nakechichok 1 (GdJh 5) has been reported to demonstrate marked technological differences to the Omo Kibish assemblages, such as a complete absence of bifacial retouched tools (Shea and Hildebrand, 2010). This site yields hippopotamus remains and rhizolith components that indicate it as a potential water source during the time of occupation, therefore it would be interesting to include the points from this site in future analyses. Lake Turkana has been deemed vital in Pleistocene refugia modelling by Cuthbert *et al.* (2017), facilitating movement along palaeohydrological networks even during the most extreme climatic conditions. This interpretation is supported by these results.

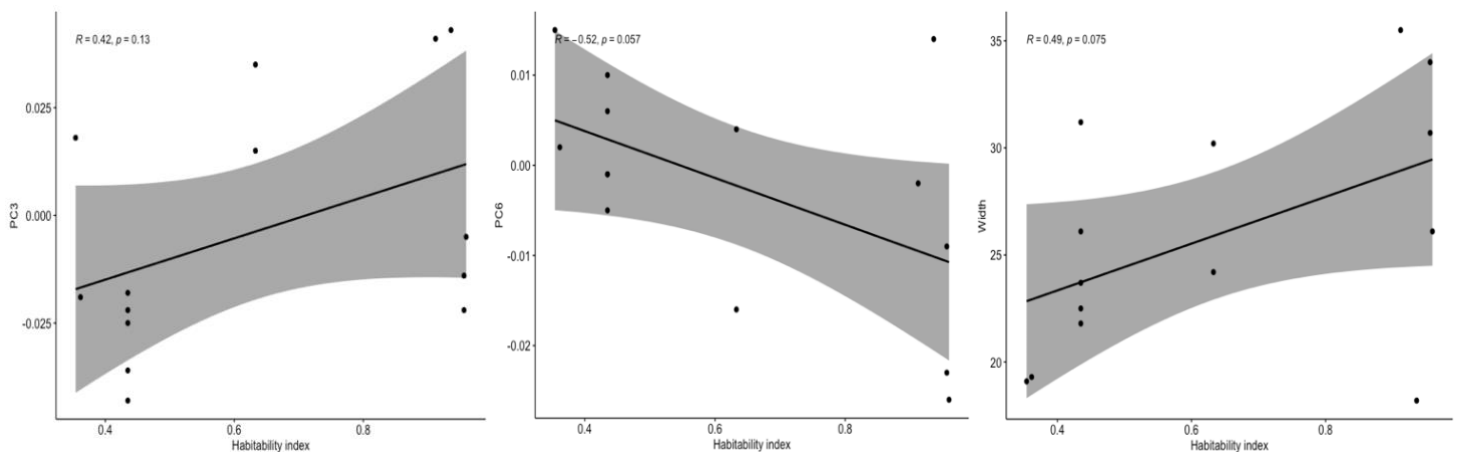


**Figure 36.** Spearman's correlation of the habitability index against principal component (PC)3 (left), PC6 (centre) and width (right). A regression line has been drawn with 95% confidence intervals.

**Table 28.** Scaled distance matrix highlighting the degree of point shape variation (as captured by principal components 1-6) between assemblages.

|                | 06N-14W<br>60-200 | 08N-07W<br>IIIb | 08N-07W<br>IIIc | 08N-07W<br>IIIa | 08N-07W<br>IIIId | AHS  | BNS  | Complex<br>IIc-a | Complex<br>IIId-f | GnJh 78 | GnJh-15 | GrJi 11 | GsJi 7 | GsJi 8 |
|----------------|-------------------|-----------------|-----------------|-----------------|------------------|------|------|------------------|-------------------|---------|---------|---------|--------|--------|
| 06N-14W 60-200 | NA                | 0.14            | 0.18            | 0.15            | 0.81             | 0.61 | 0.76 | 0.20             | 0.27              | 0.52    | 0.80    | 0.32    | 0.74   | 0.64   |
| 08N-07W IIIb   | 0.14              | NA              | 0.22            | 0.23            | 0.91             | 0.72 | 0.86 | 0.15             | 0.29              | 0.61    | 0.92    | 0.45    | 0.86   | 0.76   |
| 08N-07W IIIc   | 0.18              | 0.22            | NA              | 0.09            | 0.71             | 0.54 | 0.68 | 0.33             | 0.33              | 0.52    | 0.82    | 0.39    | 0.73   | 0.60   |
| 08N-07W IIIa   | 0.15              | 0.23            | 0.09            | NA              | 0.70             | 0.51 | 0.67 | 0.32             | 0.27              | 0.46    | 0.75    | 0.34    | 0.68   | 0.55   |
| 08N-07W IIIId  | 0.81              | 0.91            | 0.71            | 0.70            | NA               | 0.28 | 0.23 | 1.00             | 0.84              | 0.64    | 0.60    | 0.64    | 0.47   | 0.39   |
| AHS            | 0.61              | 0.72            | 0.54            | 0.51            | 0.28             | NA   | 0.23 | 0.80             | 0.64              | 0.39    | 0.48    | 0.41    | 0.29   | 0.17   |
| BNS            | 0.76              | 0.86            | 0.68            | 0.67            | 0.23             | 0.23 | NA   | 0.95             | 0.79              | 0.55    | 0.58    | 0.56    | 0.36   | 0.32   |
| Complex IIc-a  | 0.20              | 0.15            | 0.33            | 0.32            | 1.00             | 0.80 | 0.95 | NA               | 0.36              | 0.67    | 0.96    | 0.48    | 0.92   | 0.82   |
| Complex IIId-f | 0.27              | 0.29            | 0.33            | 0.27            | 0.84             | 0.64 | 0.79 | 0.36             | NA                | 0.41    | 0.74    | 0.44    | 0.70   | 0.61   |
| GnJh 78        | 0.52              | 0.61            | 0.52            | 0.46            | 0.64             | 0.39 | 0.55 | 0.67             | 0.41              | NA      | 0.51    | 0.41    | 0.35   | 0.29   |
| GnJh-15        | 0.80              | 0.92            | 0.82            | 0.75            | 0.60             | 0.48 | 0.58 | 0.96             | 0.74              | 0.51    | NA      | 0.58    | 0.33   | 0.38   |
| GrJi 11        | 0.32              | 0.45            | 0.39            | 0.34            | 0.64             | 0.41 | 0.56 | 0.48             | 0.44              | 0.41    | 0.58    | NA      | 0.50   | 0.45   |
| GsJi 7         | 0.74              | 0.86            | 0.73            | 0.68            | 0.47             | 0.29 | 0.36 | 0.92             | 0.70              | 0.35    | 0.33    | 0.50    | NA     | 0.18   |
| GsJi 8         | 0.64              | 0.76            | 0.60            | 0.55            | 0.39             | 0.17 | 0.32 | 0.82             | 0.61              | 0.29    | 0.38    | 0.45    | 0.18   | NA     |

These results also suggest that any interaction between the Central African Rift Valley and the Lower Omo Valley likely did not extend as far north as the Ethiopian Highlands, and thus was probably constrained to the northern limits of the Turkana Basin. Almost all Ethiopian Highland assemblages share similarities in point shapes (distances < 0.33; Table 28), which could be expected due to the geographical proximity of Porc-Epic and Goda Buticha at only 30km, however assemblage 08-07W-IIIId shows strong differences to both other assemblages from Porc-Epic (distances = 0.70-0.91) and to those from Goda Buticha (distances = 0.84-1.0; Table 28). Interestingly, the points from this assemblage instead share the most similarities with those from Omo Kibish. This result could indicate that at certain times interaction may have extended further south to the Lower Omo Valley, perhaps as a consequence of climatic deterioration at higher latitudes, leading to the breakdown of local networks and an increase in mobility in order to mitigate resource risk (Wiessner, 1982; Whallon, 2006; Grove, 2018). Table 25 shows that the habitability index scores of these sites are relatively low compared to others at lower latitudes, therefore perhaps the sub-optimal environments of these regions required higher levels of mobility, leading to sporadic interaction with populations from other regions at different times. Differences in raw material procurement strategies and use between Goda Buticha and Porc-Epic may also play a part in generating differences between them, with the former using obsidian more frequently and for all retouched tool types compared to the latter, which relied more heavily on basalt, and only tended to use obsidian for the production of blades (Pleurdeau *et al.*, 2014). Both sites have been proposed to have adopted a strategy of ‘provisioning of place’, following Kuhn (1995), which proposes that raw material would have been brought to the site as a result of an

extended occupational span. Whilst Kuhn (1995) hypothesises such a strategy would have led to less resharpening of tools, which is not reflected in the more reduced, elongated shape of points at these sites, these observations could suggest that the differences in raw material use and preference at Goda Buticha and Porc-Epic could relate to raw material-specific transport strategies. Like Porc-Epic, populations occupying Omo Kibish similarly rely on basalt as a key raw material source, therefore it could be suggested that groups searching for similar raw materials may have had more opportunity to interact and trade with other sub-regional population networks, particularly during times of environmental or social instability, potentially explaining why their tools appear more similar to disparate sites than closer sites at certain times but not others, though this interpretation is tentative and requires further exploration.

## 9.5. Conclusion

Interaction and trade between populations was likely mediated by habitat quality and resource availability. Indeed, the !Kung prefer to exchange points with groups living 60-100 km away in areas providing complementary resources than with those closest to them (Wiessner, 1977). The results here show some support of this in eastern African MSA populations, though increased chronological resolution, particularly at Porc-Epic, will no doubt provide a better framework for understanding the variation in point styles within the region in relation to environmental variability. Nonetheless, the results presented here support the conclusion that both environmental and physical variables likely played a key role in driving variability in eastern African MSA assemblages, both through adaptation and its influence over the organisation of group networks through space and time. Point morphology can be impacted by a multitude of factors, with the delivery system of the tool likely also a key driver of variability in this sample though this is likely captured to some extent by the modelling as the quality of the habitat likely exerts selective pressure over tool morphology and thus should correlate with functionality.

## Chapter 10: Concluding remarks

This chapter presents a summary of the findings of this thesis, as well as its contributions to our understanding of modern human origins in Africa. I will also outline some limitations and challenges faced whilst carrying out the project and provide suggestions for further directions that future research should explore.

### 10.1. Summary of findings and key results

Scerri *et al.* (2018) recently proposed that our own species, *H. sapiens*, emerged across the continent through a complex pattern of mosaic evolution (the SAM model), with interaction between and within regions likely mediated by asynchronously fluctuating climatic conditions that afforded and precluded connectivity at different moments through space and time. Only eight Late-Middle Pleistocene sites have yielded potential early *H. sapiens* fossils (Table 5), each with considerable age uncertainties and debated apomorphies. The fossil record is thus too sparse and uncertain for testing hypotheses about the effects of climatic change on *H. sapiens* distribution and demography across Africa, despite arguably providing some of the most concrete evidence for population structure prior to African dispersals. Currently, the MSA record offers the most fruitful sample for analysis, with the eastern Africa preserving a particularly rich archaeological record for this period, thus making it an excellent laboratory for testing such hypotheses.

This thesis investigated the articulation between early human habitats and material culture during the eastern African MSA, a key period and region for understanding modern human evolution and intra and extra-African dispersals. It is split into two main sections that are integrated in the final chapter. The first part of the thesis involved the characterisation of eastern African MSA habitats and the second part involved an analysis of eastern African MSA behavioural diversity via the single artefact class theorised to be the most reflective of group identity: MSA points. Together, these two components offer unique insight into Scerri *et al.*'s (2018) SAM model as applied to eastern Africa, which can later be extended to other regions and indeed the whole continent.

Proxy records, whilst dramatically improved in chronological resolution over the last decade, offer only limited insights into climatic change during the eastern African MSA. This is because lake core records are often not stratigraphically associated with archaeological finds, and therefore provide isolated snaps-shots of climate variability across the landscape, usually without clear links to spatiotemporal patterns of MSA archaeological diversity. Moreover, paleoenvironmental proxies can be highly diverse in nature, are often non-linear, sometimes with opaque relationships to the variables

they are supposed to be proxies for and usually act as relative wet-dry indicators of past conditions, making it difficult to translate them into tangible parameters that can be used within a comprehensive paleoenvironmental framework for the region. Considering this, Chapter 4 set out to integrate the eastern African MSA record with novel high-resolution climatic simulations to produce a spatiotemporally explicit representation of the environments inhabited during this key period. I found that eastern African MSA occupations tend to be limited to sub-humid landscapes within or close to tropical xerophytic shrubland, with preferential occupation of ecotonal areas between open and forested biomes. During warmer, interglacial phases, there was an increase in occupation density and corresponding expansions beyond these core landscapes, with MIS 5 seeing the movement into hot, low-altitude landscapes and MIS 3 conversely seeing a trend towards cool, high-altitude environments being occupied. Exploration of the effects of climatic variables on MSA archaeology demonstrated that precipitation, but not temperature, had an important influence over toolkit composition, as did other geographical variables like altitude and topographic roughness.

Through modelling the potential extent of eastern African populations via the climatic envelope of MSA occupations, the analyses in Chapter 4 indicated that much of the region could have been suitable for habitation. However, these phased climate envelope models were not validated against independent evidence and were limited to interglacial/glacial cycles. Chapter 5 saw the development of a more nuanced habitability model for the MSA of eastern Africa, which was independently validated against the MSA archaeological record (Blinkhorn and Grove, 2021). Whilst climate suitability (based on ethnographic data) was found to be a relatively good predictor of site presences compared to random background samples, the model was vastly improved when access to water and the effects of heterogenous topography were included. MSA sites tend to be found close to water sources, which likely acted as corridors for movement through the landscape (Scerri *et al.*, 2014; Cuthbert *et al.*, 2017). Such palaeohydrological passageways have been found to be key ecological drivers of population structure in other regions, such as northern (Scerri *et al.*, 2014) and southern Africa (von der Meden *et al.*, 2022). The Lake Victoria region and to the south appear to be consistently habitable zones during the MSA due to the high density of river networks and increased levels of precipitation, potentially facilitating stable occupation and thus greater point shape diversity (as predicted by the modelling in Chapters 8-9). Interestingly, the model also predicted areas of the landscape that could have been suitable for occupation where few MSA archaeological sites are currently documented such as the Sudanese region of the Nile Valley, and thus this work could help focus future excavation efforts in order to improve our understanding of modern human behaviour outside the EARS, where most sites are currently found due to a combination of research history and preservation biases as well as the probable suitability of this region for human habitation (Blinkhorn *et al.*, 2022).

Previous analyses have tended to focus on MSA toolkit composition to represent archaeological diversity in studies of regional population structure (Scerri *et al.*, 2014; Blinkhorn and Grove, 2018; 2021; Timbrell *et al.*, 2022a). Whilst this is the most holistic approach for capturing patterns of cultural behaviour, different stone tool types likely conserve different information, with hafted technology (and specifically MSA points) theorised to be the lithic category most indicative of group identity during prehistory (Shott, 2020). MSA point typology was therefore used as a proxy for cultural dynamics in this thesis. Because this project was carried out during the COVID-19 pandemic, my access to MSA point samples became severely restricted due to limitations on travel, making in-person research on MSA lithic collections impossible within the timeframe of my Ph.D. To try to mitigate these disruptions, I developed a remote collaborative model of data collection, which involved an equitable partnership between myself and early career researchers, students, and volunteers at five African and one European institutions, predominately museums. This new model for collaborative data collection is reported in Chapter 6. I found that there were additional benefits of this alternative approach for museum-based research in terms of actively engaging local researchers within international projects, as well as avoiding carbon emissions associated with extensive overseas travel for research purposes. Using a collaborative data collection model may become increasingly vital in archaeological, and indeed any field-based science, as future disruptions become ever more likely due to climate change, conflict, and other pandemics.

In order to validate my novel collaborative data collection approach, I developed a unique control test to assess the levels of inter-observer variability introduced by combining data from multiple collaborators. Because the collaborators could not converge on the same set of artefacts to record repeat measures, I produced and distributed 3D prints of a reference collection, which were recorded by the collaborators following the same set of protocols (outlined in Chapter 6) used to collect the real data. My findings in Chapter 7 demonstrated that the levels of error were low enough for accurate analyses, suggesting that MSA point variability can be captured reliably by multiple collaborators under tightly controlled conditions. I tested the robusticity of two methodologies – physical metric measurements and artefact photography – of which the latter can be used as the raw data for outline-based GMM analysis. I found that the metric data was less prone to error than the resulting GMM data, however this is primarily due to differences in the level of detail that each method captures shape. Overall, 3D printing could offer an important avenue for error testing across collaborative projects in the future.

Having developed and validated a new data collection approach, I then exploratorily analysed the metric and GMM data of the eastern African MSA points from the museum collaborators using a range of statistical techniques. Key differences were noted both between sites and between assemblages, particularly in the metric data suggesting that point form (shape and size) is more useful



for distinguishing between assemblages than shape alone. Null models of isolation by distance, time, and environment, as well as additional factors such as size, explain a key proportion of eastern African MSA point variability. However, over 50% of the variability in the sample is unexplained by these variables, and one could argue that it is this that we are primarily interested in as archaeologists. Portioning out the effects of spatial, temporal, and environmental autocorrelation is an important step in archaeological analyses of lithic forms in order to ensure that the variability being explored relates to cultural/social factors. Moreover, functional variation is likely related, at least to an extent, to climate and the physical environment, therefore analyses such as these can contribute to the classic style vs function arguments by factoring out some of the functional requirements of the morphology of tools, leaving stylistic and socially mediated aspects of variation. In the absence of systematic use-wear analyses, which offer more reliable data regarding function though are time and labour intensive, such methods may prove useful in analyses of broad lithic categories like 'MSA points' that likely encompass different types of technology but capture generic behavioural trends with some evolutionary significance in the past (Maier *et al.*, 2023).

The final chapter combined the habitability model developed in Chapter 5 with the point shape and form data to explore the effects of habitat suitability on eastern African MSA behavioural variability. Diversity in habitat suitability was found to have a weak but significant relationship with point shape variability between assemblages, likely because living in variable environmental contexts would exert different selective pressures on tool manufacture and performance. Predicted routes between assemblages in relation to the habitability model were then compared with patterns of point shape variability. The results suggest that interaction may have occurred within the Central Rift Valley and extended to the northerly limits of the Turkana Basin, with Lake Turkana acting as a point of mediation between the Kenyan and Ethiopian Rift Valleys as a result of habitable corridors through the landscape. Similarities between proximal sites in the Ethiopian highlands could suggest spatially structured group interaction within this area; there is also some potential evidence for a periodic breakdown of this network with some groups potentially extending contact to lower latitude regions, however the current chronological resolution precludes further assessment at the assemblage/occupation level. Ultimately, the lithics studied here offer a palimpsest of archaeological variability in the eastern African MSA, with time averaging an important limitation for understanding population dynamics at this time depth. Nonetheless, this research offers methodological and theoretical insights that can be expanded on with larger samples, though fundamentally simulation studies offer the best avenue for ascertaining the expectations of population structure against null models, which will render these ideas and methods fully operational when applied to the archaeological record.

## 10.2. Summary of contributions

The first major contribution of this research is that it makes a vital leap in our understanding of regional patterns of environmental diversity in relation to the eastern African MSA record. Previous work has struggled to comprehensively assess the extent, diversity, and implications of early human habitats on the earliest members of our species as a result of inherent limitations of the climatic data previously available. This thesis is one of the first instances of the application of novel high-resolution climatic simulations to human evolution studies, bridging the gap between the archaeological record and palaeoenvironments in a previously impossible way. Proxy records still remain the most accurate methodology for capturing the environmental context of site occupations, yet until all sites across the whole region yield correspondingly high-resolution paleoenvironmental data, and each site has a proxy record that captures comparable climatic variables, simulations provide the most promising avenue for analyses at the regional scale, as well as for relating climate to hunter-gatherer behaviour as per Binford's (2001) and Kelly's (1993) work on modern ethnographic populations. Although site-based research forms the crux of our knowledge as evolutionary anthropologists and archaeologists, a lack of understanding about the regional patterns of archaeological and environmental diversity has likely contributed to the disjointed nature research in the region, such as that of stone tool nomenclature: what Shea (2020) refers to as "lithic systems anarchy". It is only with comprehensive analyses of both archaeological and environmental diversity at this scale that we can start to answer the overarching questions about human evolution, with site-based analysis vital for building these larger syntheses but providing only limited information on broader evolutionary trends without quantitative assessment within the wider context.

Moreover, the characterisation of both habitat and archaeological diversity during the eastern African MSA is vital for understanding modern human evolution prior to extra-African dispersals. The results here suggest that humans were already occupying a range of habitats by the end of the MSA and therefore our species likely possessed the capacity to survive in a range of conditions experienced in Eurasia. Plasticity evolving in response to environmental variability has been argued to have been key for *H. sapiens* evolution, dispersal, and survival (Potts, 1998), though these results go further to suggest that not only did the first modern human populations demonstrate behavioural flexibility in response to climatic fluctuation through time but also that they were able to mediate spatial fluctuations in environmental diversity. In this sense, MSA toolkits were key for facilitating the occupation of a wide range of environmental conditions, though specific constellations of tools, as well as specific tool typologies, were likely adaptive in certain climatic contexts, as shown by the results of this thesis. MSA sites are unequally distributed across the landscape in favour of the more habitable areas particularly close to water sources, indicating that a combination of favourable-

habitat-tracking and adaptation allowed for the inhabitation of diverse and fluctuating ecologies within the range of conditions suitable for hunter-gatherers, as hypothesised by Vrba (1992). Beyer *et al.* (2021) found that rivers served a potentially vital role in eastern Africa for providing corridors for dispersal out of Africa; this is also supported by Cuthbert *et al.* (2017) in terms of intra-regional mobility patterns along water courses. This research supports access to water in being key for mediating population structure within eastern Africa, and thus likely beyond too.

This research represents the first application of complex shape analysis techniques to capture patterns of variability in eastern African point shapes and forms at a regional scale. Although the eastern African MSA is generally very well studied, particularly compared to other regions like West Africa, points from the region have been largely overlooked in GMM studies, probably because of their variable nature (i.e., lacking well-defined and distinctive stylistic qualities found across multiple sites) compared to those of more well-established northern and southern African MSA variants. Indeed, there appears to be underlying continuity in variation of material cultural in eastern Africa (Groucutt *et al.*, 2015b) with many eastern African MSA assemblages showing no obvious signals of regionalisation. However, it is this lack of distinctive point typologies that makes the region an ideal arena for testing hypotheses about typological diversity without preconceived ideas regarding the underlying structure of variability and in relation to null models, which should form the baseline of analyses of prehistoric population dynamics. Only by partitioning variance associated with autocorrelation can we more directly access the aspects of variance that we, as archaeologists, tend to be interested in, as it is this which most likely relates to cultural variation, innovation, and socially mediated style.

Interestingly, the results from the GMM analysis in Chapter 8 accord well with the findings from Chapter 4. Precipitation, and not temperature, is consistently supported as having significant effects on MSA diversity. The fact that, both at the assemblage-level (characterised by presences and absences of tool types) and at the artefact level (characterised by point typology), precipitation is found to be a key driver of diversity between assemblages suggests that different rainfall regimes require specific suites of behaviours, which are either adaptations for a particular set of functions or result in tools that can be traded between groups occupying similar biogeographic zones, or both. Although temperature influences ecological variability with consequences for hunter-gatherer populations (Kelly 1993, 1995), precipitation is arguably more important for survival in tropical environments where there is less temperature seasonality (Boyle, Shogren and Brawn, 2020), hence with a stronger selection pressure on hunting technology and resource procurement. In the case of the MSA, hafted points facilitate subsistence acquisition in a variety of ecological contexts, and thus their production and functionality should be affected by the availability and diversity of food across the landscape. More open xerophytic landscapes likely required thin, aerodynamic points for projecting

across large distances, whilst wetter tropical landscapes in eastern Africa tended to exhibit more variable tree-cover, due to interannual variation in precipitation affecting leaf, flower, fruit and seed production (Boyle, Shogren and Brawn, 2020) thus, in these contexts, points may have been less constrained by aerodynamics due to the ability to procure prey from close proximity and thus potentially were functional in a wider variety of tasks. Variable ecologies across Africa may also explain why points are rare in some MSA assemblages, particularly those found today in deciduous forest zones, such as Mumbwa Caves in Zambia (Barham, Pinto and Andrews, 2000). This thesis focusses on the stone tool MSA record; it would also be interesting to explore whether temperature influences other aspects of material culture (i.e., not stone tools); for example, populations in hot areas may require different shelter types and forms of bodily protection than those in colder areas, i.e., ochre as sunblock (Rifkin *et al.*, 2015).

### 10.2.1. Point shape, demography and refugia

Overall, the findings of this thesis tentatively suggest that eastern Africa could have supported consistent occupation throughout the MSA. Aspects of the environment likely mediated the distribution, density, and connectivity of groups across the landscape, though eastern Africa has been proposed to have been a relatively stable in terms of climate change compared to other regions (Blome *et al.*, 2012). Eastern Africa has therefore been thought to represent a refugial zone within Africa, providing consistently suitable conditions for human occupation (Blinkhorn *et al.*, 2022). This is because, although the types of environments inhabited were variable both through time and through space, populations occupying this area were buffered against the extremes of climatic change due to the unique features of the region's physical environment, climatic system, and hydrological networks (Blome *et al.*, 2012; Cuthbert *et al.*, 2017).

The relative stability of eastern Africa could be why it does not exhibit stylistic MSA point types like that seen in other regions. Torrence (2001) predicts that a more generalised point form, which could be used for hunting a variety of animals, should prevail in lower risk environments compared to higher risk environments where specialised forms should be observed. Sub-regions, like that along the Maghreb and the southern Cape, may have experienced more demographic instability in relation to climate change than eastern Africa, with more detrimental consequences of restricted availability of suitable habitats on population distribution and density. Stewart and Stringer (2012) suggest that vicariance between isolated populations encourages cultural diversification, therefore higher within-region diversification in lithic typologies may have occurred through both drift and adaptation, as populations retreating to different areas experienced diverse selection pressures leading to distinct and specialised cultural adaptations. Following Wright's (1982) shifting balance theory, during periods of

fragmentation, spatial heterogeneity should increase as innovations occur in individual groups, whereas in, alternate periods of coalescence, independent innovations would have been shared and thus spatial heterogeneity would have declined.

Yet within these isolated refugia, there may have been social pressure on populations to ensure cohesion during periods of stress and thus a wider range of contacts may have been maintained, as seen in the 'hxaro' system, leading to similarities between disparate sites (Wiessner, 1977, 1982, 1983). This suggestion was proposed for the Still Bay and Howiesons Poort industries (Ambrose and Lorenz 1990; McCall, 2007; Powell, Shennan and Thomas, 2009) though was refuted by Blome *et al.* (2012) who found that site numbers increased, rather than decreased, in South Africa during arid intervals. During these periods of deterioration, fragmentation of forested landscapes revealed resource-rich ecotonal zones, which were likely ideal habitats for humans (Kaboth-Bahr *et al.*, 2022). Indeed, d'Errico *et al.* (2017) demonstrated that Howiesons Poort populations expanded their ecological niche during the arid conditions of MIS 4 through developing a flexible but adaptive technology. It is unclear whether the appearance of certain MSA industries was mediated by climatic change during the Late Pleistocene. Yet analyses of language diversity indicate that when climate variability is greater, increased social networks are required to maintain adequate subsistence and therefore communication systems become more geographically widespread (Nettle, 1998). Indeed, Gamble (1982) proposed a similar hypothesis to explain the extensive distribution of similarly designed 'Venus' figurines across Europe during the Upper Palaeolithic. It is thought that increases in cultural complexity depend on the degree of interaction between sub-populations rather than overall population size (Powell, Shennan and Thomas, 2009), therefore populations may have increased connectivity to act as a 'safety net' to buffer against stress in areas of demographic and ecological instability (Whallon, 2006).

Relevant here is the question of whether certain forms of points can be considered to be more 'innovative' or 'complex' than others, especially as pointed technology is observed consistently throughout the MSA and thus is an (albeit variably expressed) technological behaviour that was established early in the evolution of our species. Point style should therefore be considered to be a dynamic and adaptative technological system, with the underlying capacity for more stylistic forms likely present in most (if not all) MSA populations though the demographic and ecological trajectories of specific regions likely resulted in the variable manifestation of the capacity in the archaeological record. This thesis showed that point shape and form variability in eastern Africa is autocorrelated to an extent through space, time and in relation to precipitation regimes, though over 50% of the variation links to diversity in behaviours between populations occupying different sites. Without comparative analyses in other regions of Africa, it is difficult to interpret the magnitude and significance of this result. For example, following Powell, Shennan, and Thomas (2009), the cultural

consequences of living in a relatively ecologically stable region like eastern Africa may have encouraged innovation through social signalling via variable point styles, with such manifestations of territoriality suggested to be more likely in regions of resource abundance and predictability (Dyson-Hudson and Smith, 1978). Yet, even though eastern African MSA points are deemed to be variable (Clark, 1978), the region has been argued to demonstrate an underlying consistency in material culture (Groucutt *et al.*, 2015b), with few sites demonstrating signals of regionalisation like specific point designs. In this way, it could be more likely that highly standardised point forms seen in other regions (like the Still Bay) are more representative of active forms of signalling, incorporated into point manufacture between interacting populations to either minimise resource risk during a period of stress or to maintain inter-connectivity across wide areas through defining group boundaries (Hodder, 1982; Wilkins, 2010). Like habitual ochre use (Dapschaskas *et al.*, 2022), such practises likely benefitted early human cooperation, promote sociality between neighbours, and increase information sharing throughout the broader social network, perhaps thus also facilitating sporadic bursts of cultural evolution and demographic expansion (Henrich *et al.*, 2016). More autocorrelated patterns of point shape diversity may instead reflect passive style that is inadvertently passed on through consistent cultural transmission between interacting individuals. Future work should look to perform comparative analyses with other regions of Africa to fully understand the casual mechanisms underlying point shape variability in the MSA.

Overall, the scale and type of refugia, as well as demographic factors like population size and connectivity, likely have important and variable impacts on aspects of lithic typology, with small-scale climatic change, population instability and resource risk within isolated refugia likely key for encouraging within-region differentiation, adaptation, and specialisation (Stewart and Stringer, 2012). Refugia on a wider regional scale likely had a more stabilising effect over archaeological diversity as a result of sustained occupation and cultural transmission through space and time. More habitable regions with stable levels of rainfall may have allowed for the development of more generalised toolkits that facilitated the procurement of a wide range of resources; indeed, this could be why MSA assemblages appear to persist in eastern Africa without stylistic point forms. However, ultimately further work is required to ascertain the effects of ecological parameters on population structure and size, and how these influence the overall rate and spatial structuring of innovations in the archaeological record of different regions.

### 10.2.2. Collaborative and remote science

Another major contribution of this thesis is that of the collaborative data collection model. Scerri *et al.* (2020) stated that, to ensure future resilience for the field, archaeology needs to develop more robust

remote models for conducting science. Whilst these authors were primarily referring to excavation and field-based activities, this statement should also refer to museum-based research. Museum-based research is riddled with many of the same issues as international excavation; in some cases, it could be argued to be worse. For example, often museum-based research involves a single individual visiting multiple collections across the world within a project, sometimes to access very small samples or single artefacts/fossils. Unlike excavation, where the data generated is entirely novel, often these museum collections have been studied multiple times before using very similar methods and research frameworks. Though this is improving in recent years, archaeology has an unfortunate history and culture of gatekeeping, with the ‘ownership’ of sites and data ultimately lying with the site permit holder rather than the scientific community. This thesis provides a solution for how researchers can work together to collect and share archaeological data; it advocates that data should be collected in a collaborative manner with the main responsibility lying with the museum institution housing the artefacts. The data can then be shared in an open-access format for use by all collaborators, and indeed anyone interested in analysing the artefacts in the same way. Collaborative research projects involving the in-situ collection and amalgamation of data from multiple sources (potentially even with variable initial research aims) can utilise the 3D printing approach presented in Chapter 7 to conduct a relatively simple and cheap control test to test the integrity of such meta-analyses. Indeed, Will *et al.* (2019) concluded from CoMSAfrica that in order to standardize pan-African comparisons, a unified analytical approach is necessary, making robust collaborative methods such as the one presented here vital for advances in our understanding of human evolution.

Another contribution of this approach is that by involving local researchers in the data collection process, the collaborative data approach can help to address the unequal research dynamic that permeates archaeology. In the context of museum research, ‘helicopter’ research practises involve a foreign researcher flying into a country, studying the artefacts, and leaving again without engagement with local researchers who curate the artefacts. Often, foreign researchers do not acknowledge or involve local museum personnel in the research and/or publication process. Across the world, there are few funded research opportunities to routinely work with prehistoric collections; often these roles must be undertaken on a volunteer basis or with support from funding bodies whose reach tends to be biased towards the Global North. Undertaking work on a volunteer basis is particularly difficult for researchers in certain areas of the Global South, who face additional struggles such as unreliable public transport, safety issues travelling to museums and a general lack of resources to support their professional development, on top of needing to financially support themselves and their families. Through providing funding to museum volunteers to support their participation in international projects, collaborative data collection has the potential to provide invaluable opportunities for local researchers to develop their skills and build upon their experience, thus helping to decolonize archaeological research. Furthermore, the collaborators were, and will continue to be, involved with

the publication of analyses deriving from this thesis; many have told me that they have referred to our project and resulting publications in applications for further study and/or employment.

Whilst it was somewhat unfortunate that I was unable to visit the museum collections myself, the COVID-19 pandemic provided me with the opportunity to develop a novel and arguably much needed approach to international collaboration between academic and museum institutions that will hopefully be built upon and refined in future years by other researchers. Although there are a number of scientific advances to come out of this thesis, this contribution to the future archaeological practice is perhaps the most important, and definitely the one I am most proud of.

### 10.3. Limitations of research and future directions

There are several considerations that require further discussion and explorations. Some of these are limitations inherent to all archaeological analyses and can only be alleviated with more samples, better methods, and more collaboration between and within projects, but some can be actively addressed with future research. I provide suggestions for such future avenues of interesting study below.

#### 10.3.1. The question of resolution

The first point of contention is the resolution of the climatic simulations and the archaeological data, both in the spatial and chronological dimensions. Archaeological data of this antiquity has inherently large dating errors due to the imprecise nature of chronometric dating. Whilst this has greatly improved in recent years, each assemblage in this analysis has a wide chronological window, meaning that a simple age estimate must be taken at the mid-point to anchor the assemblage within the climatic model. Permutation analyses in Chapter 9 (Appendix 4) demonstrate that the simple age estimate is robust against chronological uncertainty, with the habitability model effective at capturing the suitability of each site across the dating error range. Despite proving robust to error, the modelling would no doubt be improved with higher chronological resolution. For example, many of the assemblages studied in Chapter 8-9 rely on unreliable and obsolete dating methodologies, like obsidian rehydration. Unfortunately, therefore, the chronological control of this analysis is poor. For example, the Porc-Epic assemblages all have the same age estimate due to the lack of high-resolution accurate dating of the site (though the publication of improved dating is imminent; Pleurdeau, pers. comms), plus different age estimates for the site have been produced by different methods from different sources. However, because the analysis is performed at a regional scale, a compromise on chronological resolution is somewhat necessary in order to expand the temporal window to get a big



enough sample of sites for robust analyses. An additional factor is that some of the assemblages likely represent more than one occupational phase. Time averaging is an important and inherent aspect of formational processes that can complicate the behavioural inferences drawn from assemblages. This is a general issue of archaeological research, which is exacerbated by poor excavation and data recording practises. Unfortunately, in some cases, information about the assemblage attribution was not sufficiently recorded under the collaborative data collection framework; although a spreadsheet was provided for the local collaborators, it should have been more specific to each museum collection and further training should have been provided to ensure that all relevant information from the archives was captured.

The spatial scale of site-based reconstructions using climate simulations also requires consideration. Using simulations at their native resolution has the potential to produce biases when compared to on-site proxies due to the underlying complexity of the physical landscape, particularly in areas of high elevation and that are proximal to the coast (Maraun *et al.*, 2018). Resultant errors can be on the order of several degrees for temperature and tens of percent for precipitation, which would lead to substantially different biome classifications (Kottek, Grieser and Beck, 2006). I therefore explored the effects of downscaling on my results in Chapter 4 (see Appendix 1: Supplementary Methods S3); I found that bilinear interpolation was the most conservative in terms of the statistical analyses conducted, however the delta method likely is better for producing accurate characterisations of past climate due to its ability to incorporate topographic effects on local climates (Beyer, Krapp and Manica, 2020), which is particularly pertinent in eastern Africa. Further work should look at determining the impact of downscaling on past climate reconstructions, particularly in comparison to on-site proxies.

A final point of discussion is the decision to characterise past environments across landscapes rather than at the site level. The concept of the 'site' is important in archaeology, particularly given the role that targeted excavation plays in recovering material culture and associated samples with which to explore past behaviour. Arguably a 'site' is reliant on modern observation, rather than past action, for definition and is filtered through myriad natural and human taphonomic factors (McCoy, 2020). There has long been recognition among archaeologists that the 'site' is merely an anomalously high concentration of anthropogenic material existing against the backdrop of near-continuous, lower density deposition (Isaac, Harris and Marshall, 1984). Similarly, whilst some stone tool assemblages may encapsulate an entire reduction sequence at one site, from raw material acquisition, tool production, use and discard, many include artefacts imported from elsewhere in the landscape and discarded at the site as well as indicating potential export of tools produced at the site but used and discarded elsewhere in the landscape (Clarkson, 2008). In short, no site is the sole location of activity associated with the hominins that produced it, and I argue that no useful palaeoecological

reconstruction can be achieved without reference to the surrounding landscape; these are basic tenets of palaeoecological investigation established in archaeology by Vita-Finzi and Higgs over 50 years ago (Vita-Finzi and Higgs, 1970). Indeed, Rob Foley (1978) coined the term ‘off-site’ archaeology after working in the Amboseli in Kenya; he found clusters of material – what one might call ‘sites’ – but also observed scatters across the landscape representing activities beyond areas of aggregation. My choice to use a 50km radii to characterise the geographic, climatic, and ecological landscape within which a site is situated is grounded in both ethnographic and archaeological research and is an approach used elsewhere by Blinkhorn and Grove (2018, 2021). Site-focused studies can be complementary to this landscape approach, but differences in climate variables derived from point locations, such as individual sites, and the average of the landscape in which they are situated, are highly plausible. Overall, the approaches taken to capture spatiotemporal variability across the eastern African MSA are robust and conservative, with further potential to be refined and validated through corroboration with site-based reconstructions and downscaling.

### 10.3.2. Costs and benefits of inhabiting heterogenous landscapes

Chapter 5 raised the issue of the complex and somewhat contradictory effects that heterogenous topography has on determining habitat suitability. Often when simulating hunter-gatherer mobility using agent-based modelling and least cost-path modelling approaches, the energetic cost of movement is utilised as a condition that determines the direction, speed, and route of movement across rough terrain. In this sense, areas with large slopes, often at high altitude, are circumnavigated in favour of flatter, lower altitude regions. Yet during particularly hot and dry phases, mountains can offer shelter for hominins as higher altitudes tend to be colder and wetter than lower lying regions. Indeed, in eastern Africa, during times of climatic deterioration, it is thought that hominins would have moved into higher landscapes (Ambrose, 2001), as is reported in Chapter 4 when MSA populations shifted to higher altitude settings in MIS 3, potentially in response to erratic high temperatures. Additionally in ethnographic and archaeological studies, it has been noted that such heterogenous landscapes are beneficial for human occupation due to the diverse variety of resources and protection they provide. This made it difficult to incorporate the effects of topography within a single index of habitability, particularly when it is currently unclear under what circumstances the benefits of mountains outweigh the potential energetic cost it requires to migrate into and inhabit these areas.

It may be that these two factors operate on different temporal and spatial scales; for instance, smaller scale topographic features are likely those that provide immediate tangible benefits to hominin survival through providing diverse resources and protection from predators, whilst the large scale

slopes, typically captured through the topographic maps that form the basis of cost of movement surfaces, pose an obvious challenge for human mobility despite providing a buffer against the harshest effects of climatic change. Hunter-gatherers may opt to circumnavigate very high-altitude regions during wet phases, particularly for longer residual moves, though logistical mobility could be largely unconstrained by the cost of movement, as abundant resources may act as a pull into these regions for food acquisition. During more arid phases, hunter-gatherers may extend residual mobility into higher altitudes to buffer the effects of climatic change, as is seen at Fincha Habera (Ossendorf *et al.*, 2019). Overall, the effects of mountainous terrain have been incorporated into the model at a basic level, however future research should focus on exploring the nuances of hunter-gatherer mobility and settlement strategies across complex landscapes, particularly in relation to climatic change.

#### 10.4. Final thoughts

Future climate change will likely be catastrophic for human populations. Using prehistoric societies as models enables us to understand our evolutionary responses to climate perturbation, providing important insight into the links between environment and human behaviour. The MSA is arguably the most pertinent case study, given these populations likely reflect the first members of our own species and these populations persisted through periods of dramatic climatic fluctuations, like the Late-Middle Pleistocene transition.

This thesis has highlighted how the earliest members of our species were diverse, resilient, and adaptable in the face of climate disruption, maintaining and extending social relationships with their neighbours to get them through tough times. Upon reflection, this core principle of working together in the face of adversity is exactly what enabled the continuation of this research throughout the COVID-19 pandemic.

We live in a disconnected modern world, detached both from each other and the climate emergency we are causing. Yet our earliest ancestors offer a beacon of hope in that it seems that the very essence of what makes us human is rooted in flexibility, sociality, and cooperation. I suggest that it is exactly these traits that will enable us to continue to adapt to, and even reverse, our environmental destruction.

## References

- Ackermann, R.R. (2019). Reflections on the history and legacy of scientific racism in South African paleoanthropology and beyond. *Journal of Human Evolution* 126, pp. 106-111, doi: 10.1016/j.jhevol.2018.11.007.
- Ackermann, R. R., Athreya, S., Black, W. *et al.* (2019). Upholding “good science” in human origins research: A response to Chan *et al.* (2019). *Matters Arising to Nature*. doi: 10.31730/osf.io/qtjfp
- Ambrose, S. H. (1998a). Late Pleistocene Human Population Bottlenecks, Volcanic winter, and Differentiation of Modern Humans. *Journal of Human Evolution* 34(6), pp. 623–651.
- Ambrose, S. H. (1998b). Chronology of the later stone age and food production in East Africa, *Journal of Archaeological Science* 25(4), pp. 377–392. doi: 10.1006/jasc.1997.0277.
- Ambrose, S. H. (2001). Middle and Later Stone Age Settlement Patterns In The Central Rift Valley, Kenya: Comparisons And Contrasts. In: Conard, N. J. (eds) *Settlement Dynamics of the Middle Palaeolithic and Middle Stone Age*. pp. 21–43.
- Ambrose, S. H. (2012). Obsidian dating and source exploitation studies in Africa: implications for the evolution of human behaviour. In: Liritzis, I. and Stevenson, C. (eds). *Obsidian and Ancient Manufactured Glasses*. University of New Mexico Press, Albuquerque pp. 56-72, (2012).
- Ambrose, S. H. and Lorenz, K. G. (1990). Social and ecological models for the Middle Stone Age in southern Africa. In: Mellars, P. (eds) *The emergence of modern humans: an archaeological perspective*. Edinburgh: Edinburgh University Press, pp. 3–33.
- Ambrose, S. H. and Sikes, N. E. (1991). Soil carbon isotope evidence for holocene habitat change in the Kenya Rift Valley. *Science* 253(5026), pp. 1402–1405. doi: 10.1126/science.253.5026.1402.
- Andrefsky, W. (1994). Raw-material availability and the organization of technology, *American Antiquity* 59, p.21e34.
- Anthony, B. W. (1978). *The Prospect Industry—a definition*. Ph.D. dissertation, Harvard University, Cambridge.
- Anthony, N. M., Johnson-Bawe, M., Jeffery, K. *et al.* (2007). The role of Pleistocene refugia and rivers in shaping gorilla genetic diversity in central Africa. *Proceedings of the National Academy of Sciences of the United States of America* 104(51), pp. 20432–20436. doi: 10.1073/pnas.0704816105.
- Araujo, M.B. and Guisan, A. (2006). Five (or so) challenges for species distribution modelling. *Journal of Biogeography* 33(10), pp. 1677-1688, doi: 10.1111/j.1365-2699.2006.01584.x
- Archer, W., Gunz, P., van Niekerk, K. L. *et al.* (2015). Diachronic change within the Still Bay at Blombos Cave, South Africa. *PLoS One* 10(7): e0132428. doi: 10.1371/journal.pone.0132428
- Archer, W., Pop, C. M., Gunz, P. and McPherron, S. P. (2016). What is Still Bay? Human biogeography and bifacial point variability, *Journal of Human Evolution* 97, pp. 58–72. doi: 10.1016/j.jhevol.2016.05.007.
- Armitage, S. Jasim, S. A., Marks, A. E. *et al.* (2011). The Southern Route “Out of Africa”: Evidence for an Early Expansion of Modern Humans into Arabia. *Science: Reports* 331(1), pp. 453–6. doi: 10.1594/PANGAEA.755114.
- Arsuaga, J. L., Martinez, I., Arnold, L. J. *et al.* (2014). Neandertal roots: Cranial and chronological evidence from Sima de los Huesos. *Science* 344(6190), pp. 1358–1363. doi: 10.1126/science.1253958.
- Assefa, Z. (2006). Faunal remains from Porc-Epic: Paleoecological and zooarchaeological investigations from a Middle Stone Age site in southeastern Ethiopia. *Journal of Human Evolution* 51(1), pp. 50–75. doi: 10.1016/j.jhevol.2006.01.004.
- Assefa, Z., Lam, Y. M. and Mienis, H. K. (2008). Symbolic use of terrestrial gastropod opercula during the Middle Stone Age at Pore-Epic cave, Ethiopia. *Current Anthropology* 49(4), pp. 746–756. doi: 10.1086/589509.
- Athreya, S. and Ackermann, R. R. (2019). Colonialism and narratives of human origins in Asia and Africa. In: Porr, M. and Matthews, J. M. (eds.) *Interrogating Human Origins: Decolonisation and the Deep Past*. Routledge, London, doi: 10.4324/9780203731659-4
- Atkinson, Q. D. (2011). Phonemic diversity supports a serial founder effect model of language expansion from Africa. *Science* 332(6027), pp. 346–349. doi: 10.1126/science.1199295.
- Aubert, M., Pike, A. W. G., Stringer, C. *et al.* (2012). Confirmation of a late middle Pleistocene age for the Omo Kibish 1 cranium by direct uranium-series dating. *Journal of Human Evolution* 63(5), pp. 704–710. doi: 10.1016/j.jhevol.2012.07.006.

- Backwell, L. R., d'Errico, F., Banks, W. E. *et al.* (2018). New Excavations at Border Cave, KwaZulu-Natal, South Africa. *Journal of Field Archaeology* 43, 417–436. doi: 10.1080/00934690.2018.1504544
- Bailey, G. N., Reynolds, S. C. and King, G. C. P. (2011). Landscapes of human evolution: Models and methods of tectonic geomorphology and the reconstruction of hominin landscapes. *Journal of Human Evolution* 60(3), pp. 257–280. doi: 10.1016/j.jhevol.2010.01.004.
- Banks, W. E., d'Errico, F., Townsend Peterson, A. *et al.* (2008). Reconstructing ecological niches and geographic distributions of caribou (*Rangifer tarandus*) and red deer (*Cervus elaphus*) during the Last Glacial Maximum. *Quaternary Science Reviews* 27(27-28), pp. 2568-2575, doi: /10.1016/j.quascirev.2008.09.013
- Barham, L. S. (1998). Possible early pigment use in south-central Africa. *Current Anthropology* 39(5), pp. 703–710. doi: 10.1086/204793.
- Barham, L. (2000). *The Middle Stone Age of Zambia, South Central Africa*. Western Academic & Specialist Press.
- Barham, L. (2001). Central Africa and the emergence of regional identity in the Middle Pleistocene. In: Barham, L. and Robson-Brown, K. (eds) *Human Roots: Africa and Asia in the Middle Pleistocene*. Bristol: Western Academic and Specialist Press, pp. 65–80.
- Barham, L. S. and Smart, P. L. (1996). Current events: An early date for the Middle Stone Age of central Zambia. *Journal of Human Evolution* 30(3), pp. 287–290. doi: 10.1006/jhev.1996.0023.
- Barham, L. S. and Mitchell, P. J. (2008). *The First Africans: African Archaeology from the Earliest Toolmakers to Most Recent Foragers*. Cambridge: Cambridge University Press. doi: 10.1017/CBO9780511817830.
- Barham, L. S., Pinto, A. C., and Andrews, P. (2000). The Mumbwa Caves behavioural record. In L. S. Barham (Ed.), *The Middle Stone Age of Zambia, South Central Africa* (pp. 81–148). Western Academic & Specialist Press.
- Barham, L., Tooth, S., Duller, G. A. *et al.* (2015). Excavations at Site C North, Kalambo Falls, Zambia: New Insights into the Mode 2/3 Transition in South-Central Africa. *Journal of African Archaeology*, 13(2), 187-214. doi: <https://doi.org/10.3213/2191-5784-10270>
- Bartlett, J. W. and Frost, C. (2008). Reliability, repeatability and reproducibility: analysis of measurement errors in continuous variables. *Ultrasound in Obstetrics and Gynecology* 31, pp. 466–75, doi: 10.1002/uog.5256
- Basell, L. S. (2008). Middle Stone Age (MSA) site distributions in eastern Africa and their relationship to Quaternary environmental change, refugia and the evolution of *Homo sapiens*. *Quaternary Science Reviews* 27(27–28), pp. 2484–2498, 10.1016/j.quascirev.2008.09.010
- Behrensmeyer, A. K. and Hill, A. P. (1980). *Fossils in the Making: Vertebrate Taphonomy and Palaeoecology*. The University of Chicago Press.
- Belmaker, M. and Hovers, E. (2011). Ecological change and the extinction of the Levantine Neanderthals: Implications from a diachronic study of micromammals from Amud Cave, Israel. *Quaternary Science Reviews* 30(21–22), pp. 3196–3209. doi: 10.1016/j.quascirev.2011.08.001.
- Bennet, M. J. (2021). On the nature of extreme close-range photogrammetry: visualisation and measurement of North African Stone Points. *Code4Lib Journal*. 51. ISSN 1940-5758
- Berger, L. R., Hawks, J., de Ruiter, D. *et al.* (2015). *Homo naledi*, a new species of the genus *Homo* from the Dinaledi Chamber, South Africa. *eLife* 4:e09560. doi: 10.7554/eLife.09560.001
- Bertola, L. D., Jongbloed, H., van der Gaag, K. J. *et al.* (2016). Phylogeographic Patterns in Africa and High Resolution Delineation of Genetic Clades in the Lion (*Panthera leo*). *Scientific Reports* 6(1), p. 30807. doi: 10.1038/srep30807.
- Bescoby, D. J. (2006). Detecting Roman land boundaries in aerial photographs using Radon transforms. *Journal of Archaeological Science* 33(5), pp. 735–743, doi: 10.1016/j.jas.2005.10.012.
- Betti, L., Balloux, F., Amos, W. *et al.* (2009). Distance from Africa, not climate, explains within-population phenotypic diversity in humans. *Proceedings of the Royal Society: B* 276(1658), pp. 809-14. doi: 10.1098/rspb.2008.1563.
- Beyer, R., Krapp, M., and Manica, A. (2020). An empirical evaluation of bias correction methods for palaeoclimate simulations. *Climate Past* 16, pp. 1493-1508, doi: 10.5194/cp-16-1493-2020
- Beyer, R. M., Krapp, M., Eriksson, A. *et al.* (2021). Climatic windows for human migration out of Africa in the past 300,000 years. *Nature Communications* 12, 4889, doi: 10.1038/s41467-021-24779-1
- Beyin, A. (2016). The Relevance of the Abdur and Asfet Middle Stone Age Sites from the Red Sea Coast of

- Eritrea. Conference: 81st Annual Meeting of the Society for American Archaeology.
- Bibi, F. and Kiessling, W. (2015). Continuous evolutionary change in Plio-Pleistocene mammals of eastern Africa. *Proceedings of the National Academy of Sciences of the United States of America* 112(34), pp. 10623–10628. doi: 10.1073/pnas.1504538112.
- Binford, L. R. (1982). The archaeology of place. *Journal of Anthropological Archaeology* 1 (1), pp. 5-31.
- Binford, L. R. (2001). *Constructing Frames of Reference: An Analytical Method for Archaeological Theory Building Using Ethnographic and Environmental Data Sets*. University of California Press.
- Binford, L. R. and Binford, S. R. (1966). A Preliminary Analysis of Functional Variability in the Mousterian of Levallois Facies. *American Anthropologist* 68, pp. 238-295
- Blegen, N. (2017). The earliest long-distance obsidian transport: Evidence from the ~200 ka Middle Stone Age Sibilo School Road Site, Baringo, Kenya. *Journal of Human Evolution* 103, pp. 1–19, doi: 10.1016/j.jhevol.2016.11.002
- Blegen, N., Jicha, B. R. and McBrearty, S. (2018). A new tephrochronology for early diverse stone technologies and long distance raw material transport in the Middle to Late Pleistocene Kapthurin Formation, East Africa. *Journal of Human Evolution* 121, pp. 75-103, doi: 10.1016/j.jhevol.2018.03.005
- Blinkhorn, J. and Grove, M. (2018). The structure of the Middle Stone Age of eastern Africa. *Quaternary Science Reviews* 195, pp. 1–20. doi: 10.1016/j.quascirev.2018.07.011.
- Blinkhorn, J. and Grove, M. (2021). Explanations of variability in Middle Stone Age stone tool assemblage composition and raw material use in Eastern Africa. *Archaeological and Anthropological Sciences* 13(14). doi: 10.1007/s12520-020-01250-8
- Blinkhorn, J., Timbrell, L., Grove, M. and Scerri, E. M. L. (2022). Evaluating refugia in recent human evolution in Africa. *Philosophical Transactions of the Royal Society B* 377, 1849. doi: 10.1098/rstb.2020.0485
- Blome, M. W., Cohen, A. S., Tryon, C. A. *et al.* (2012). The environmental context for the origins of modern human diversity: A synthesis of regional variability in African climate 150,000–30,000 years ago. *Journal of Human Evolution* 62(5), 563–592, 10.1016/j.jhevol.2012.01.011
- Bobe, R., Behrensmeyer, A. K. and Chapman, R. E. (2002). Faunal change, environmental variability and late Pliocene hominin evolution. *Journal of Human Evolution* 42(4), pp. 475–497. doi: 10.1006/jhev.2001.0535.
- Bock, F., Fennessy, J., Bidon, T. *et al.* (2014). Mitochondrial sequences reveal a clear separation between Angolan and South African giraffe along a cryptic rift valley. *BMC Evolutionary Biology* 14(1). doi: 10.1186/s12862-014-0219-7.
- Bonhomme, V., Picq, S., Gaucherel, C. and Claude, J. (2014). Momocs: Outline Analysis Using R, *Journal of Statistical Software* 56, pp. 1–24, doi: 10.18637/jss.v056.i13
- Bonhomme, V., Forster, E., Wallace, M. *et al.* (2017). Identification of Inter- and Intra-species Variation in Cereal Grains Through Geometric Morphometric Analysis, and its Resilience under Experimental Charring. *Journal of Archaeological Science* 86, pp. 60–67, doi: 10.1016/j.jas. 2017.09.010
- Bookstein, F. L. (1991). *Morphometric tools for landmark data: geometry and biology*. Cambridge University Press, Cambridge
- Booth, T. H., Nix, H. A., Busby, J. and Hutchinson, M. F. (2014). BIOCLIM: the first species distribution modelling package, its early applications and relevance to most current MaxEnt studies. *Biodiversity Review* 20(1), pp. 1-9, doi: 10.1111/ddi.12144
- Borches, H. (2022). *pracma: Practical Numerical Math Functions*. CRAN R Package. <https://cran.r-project.org/web/packages/pracma/pracma.pdf>
- Bordes, F. (1950). L'évolution buissonnante des industries en Europe occidentale. Considérations théoriques sur le Paléolithique ancien et moyen. *L'Anthropologie* 54, pp.393-420
- Bordes F (1961). *Typologie du Paléolithique Ancien et Moyen*. Bordeaux
- Boucher, D.H. (1985). The idea of mutualism, past and future. In: *The Biology of Mutualism: Ecology and Evolution*, Oxford University Press, pp. 1-27
- Brace, C. L. (1969). *The Stages of Human Evolution: Human and Cultural Origins, Man*. Englewood Cliffs (N.J.) Prentice-Hall. doi: 10.2307/2799277.
- Brandt, S. A. (1986). The Upper Pleistocene and early Holocene prehistory of the Horn of Africa. *The African Archaeological Review* 4(1), pp. 41–82. doi: 10.1007/BF01117035.
- Brandt, S. A., Hildebrand, E., Vogelsand, R. *et al.* (2017). A new MIS 3 radiocarbon chronology for Mochena

- Borago Rockshelter, SW Ethiopia: Implications for the interpretation of Late Pleistocene chronostratigraphy and human behaviour. *Journal of Archaeological Science: Reports* 11, pp. 352–369, doi: 10.1016/j.jasrep.2016.09.013
- Bräuer, G. (2012). Middle Pleistocene Diversity in Africa and the Origins of Modern Humans. In: Hublin, J.-J. and McPherron, S. P. (eds) *Modern origins. Vertebrate Paleobiology and Paleoanthropology*. Dordrecht: Springer.
- Bräuer, G. and Leakey, R. E. (1986). The ES-11693 Cranium from Eliye Springs, West Turkana, Kenya. *Journal of Human Evolution* 15, pp. 289–312.
- Bretzke, K. and Conard, N. J. (2016). Mumba Cave and the development of regional point styles. Conference poster
- Bretzke, K., Marks, A. E., Conard, N. J. (2006). Projektiltechnologie und kulturelle Evolution in Ostafrika. *Mitteilungen der Gesellschaft für Urgeschichte* 15, pp. 63–81.
- Breuil, H., Teilhard de Chardin, P., and Wernert, P. (1951). Le Paléolithique du Harrar. *L'Anthropologie* 55, pp. 219–228.
- Brooks, A. S. and Yellen, J. E. (1977). Archaeological Excavations at Gi, (Western Ngamiland, Botswana): A Report on the First Two Field Seasons. *Botswana Notes and Records*, 9, pp. 21–30.
- Brooks, A. S., Hare, P. E., Kokis, J. E. *et al.* (1990). Dating pleistocene archeological sites by protein diagenesis in ostrich eggshell. *Science* 248(4951), pp. 60–64. doi: 10.1126/science.248.4951.60.
- Brooks, A. S., Nevell, L., Yellen, J. E. and Hartman, G. (2006). Projectile Technologies of the African MSA. In: Hovers, E. and Kuhn, S. L. (eds) *Transitions Before the Transition Evolution and Stability in the Middle Paleolithic and Middle Stone Age*. New York: Springer, pp. 233–255. doi: 10.1007/0-387-24661-4\_13.
- Brooks, A. S., Yellen, J. E., Potts, R. *et al.* (2018). Long-distance stone transport and pigment use in the earliest Middle Stone Age. *Science* 360(6384), pp. 90–94. doi: 10.1126/science.aao2646.
- Brown, E. T. (2011). Lake Malawi's response to “megadrought” terminations: Sedimentary records of flooding, weathering and erosion, *Palaeoecology* 303(1-4), pp. 120–125. doi: 10.1016/j.palaeo.2010.01.038
- Brown, K. S., Marean, C. W., Jacobs, Z. *et al.* (2012). An early and enduring advanced technology originating 71,000 years ago in South Africa. *Nature* 491(7425), pp. 590–593. doi: 10.1038/nature11660.
- Browning, S. R., Browning, B. L., Zhou, Y. *et al.* (2018). Analysis of Human Sequence Data Reveals Two Pulses of Archaic Denisovan Admixture. *Cell* 173(1), pp. 53–61.e9. doi: 10.1016/j.cell.2018.02.031.
- Bruner, E. and Pearson, O. (2013). Neurocranial evolution in modern humans: the case of Jebel Irhoud 1, *Anthropological Science*, 121(1), pp. 31–41. doi: 10.1537/ase.120927.
- Bruno, J. F., Stachowicz, J. J. and Bertness, M. D. (2003). Inclusion of Facilitation into Ecological Theory. *Trends in Ecology and Evolution* 18 (3), pp. 119–25.
- Buchanan, B., Andrews, B., O'Brien, M, and Eren, M. I. (2018). An assessment of stone weapon tip standardization during the Clovis–Folsom transition in the Western United States, *American Antiquity* 83, pp. 721–734, doi: 10.1017/aaq.2018.53
- Buchanan, B. and Collard, M. (2010). A geometric morphometrics-based assessment of blade shape differences among Paleoindian projectile point types from western North America. *Journal of Archaeological Science* 37, pp. 350–359, doi: 10.1016/j.jas.2009.09.047
- Buchanan, B., Collard, M. and O'Brien, M. J. (2020). Geometric morphometric analyses support incorporating the Goshen point type into plainview. *American Antiquity* 85(1), pp. 171–181, doi: 10.1017/aaq.2019.89
- Burke, A., Kageyama, M., Latombe, G. *et al.* (2017). Risky business: The impact of climate and climate variability on human population dynamics in Western Europe during the Last Glacial Maximum. *Quaternary Science Reviews* 164, pp. 217–229, doi: 10.1016/j.quascirev.2017.04.001
- Bushozi, P. G. M. (2011). Lithic technology and hunting behaviour during the Middle Stone Age in Tanzania. Doctoral Dissertation, University of Alberta.
- Butzer, K. W., Beaumont, P. B. and Vogel, J. C. (1978). Lithostratigraphy of Border Cave, KwaZulu, South Africa: a Middle Stone Age sequence beginning c. 195,000 b.p. *Journal of Archaeological Science* 5(4), pp. 317–341. doi: 10.1016/0305-4403(78)90052-3.
- Cann, R. L., Stoneking, M. and Wilson, A. C. (1987). Mitochondrial DNA and Human Evolution. *Nature* 325(6099), pp. 31–36. doi: 10.1038/325031a0.
- Caple, J., Byrd, J. and Stephan, C. N. (2017). Elliptical Fourier Analysis: Fundamentals, Applications, and

- Value for Forensic Anthropology. *International Journal of Legal Medicine* 131, pp. 1675–1690, doi: 10.1007/s00414-017-1555-0
- Caple, J., Byrd, J. and Stephan, C. N. (2018). The utility of elliptical Fourier analysis for estimating ancestry and sex from lateral skull photographs. *Forensic Science International* 289, pp. 352–362, doi: 10.1016/j.forsciint.2018.06.009
- Cardillo, M. (2010). Some Applications of Geometric Morphometrics to Archaeology. In A.M.T. Elewa (ed.) *Morphometrics for Nonmorphometricians*. Springer, Berlin, Heidelberg. 325–341, doi: 10.1007/978-3-540-95853-6\_15
- Cerasoni, J. N. (2021). Vectorial application for the illustration of archaeological lithic artefacts using the “Stone Tools Illustrations with Vector Art” (STIVA) Method. *PLoS ONE* 16(5): e0251466, doi: 10.1371/journal.pone.0251466
- Cerasoni, J. N., Hallet, E. Y., Orijemie, E. A. et al. (2023). Human interactions with tropical environments over the last 14,000 years at Iho Eleru, Nigeria. *IScience*, doi: 10.1016/j.isci.2023.106153.
- Chan, E. K. F., Timmermann, A., Baldi, B. F. et al. (2019). Human origins in a southern African palaeowetland and first migrations, *Nature* 575(7781), pp. 185–189. doi: 10.1038/s41586-019-1714-1.
- Chang, J. and Alfaro, M. E. (2015). Crowdsourced geometric morphometrics enable rapid large-scale collection and analysis of phenotypic data, *Methods in Ecology and Evolution* 7(4), pp. 472–482, doi: 10.1111/2041-210X.12508
- Chikhi, L., Rodriguez, W., Grusea, S. et al. (2018). The IICR (inverse instantaneous coalescence rate) as a summary of genomic diversity: Insights into demographic inference and model choice. *Heredity* 120(1), pp. 13–24. doi: 10.1038/s41437-017-0005-6.
- Chirikure, S. (2015). “Do as I Say and Not as I Do”. On the Gap Between Good Ethics and Reality in African Archaeology. In A. Haber & N. Shepherd (eds.) *After Ethics. Ethical Archaeologies: The Politics of Social Justice*, vol 3. Springer, New York, doi: 10.1007/978-1-4939-1689-4\_3.
- Clark, J. D. (1952). Prehistoric Europe: the Economic Basis. London: Methuen.
- Clark, J. D. (1982). *The Cultures of the Middle Palaeolithic/Middle Stone Age*. Cambridge: Cambridge University Press. doi: <https://doi.org/10.1017/CHOL9780521222150.005>.
- Clark, J. D. (1988). The Middle Stone Age of East Africa and the beginnings of regional identity. *Journal of World Prehistory* 2(3), pp. 235–305. doi: 10.1007/BF00975618.
- Clark, J. D., and Williamson, K. D. (1984). A middle stone age occupation site at Porc-Epic Cave, Dire Dawa (east-central Ethiopia), Part I. *African Archaeological Review* 2, pp. 37–64.
- Clark, J. D., Beyene, Y., WoldeGabriel, G. et al. (2003). Stratigraphic, chronological and behavioural contexts of Pleistocene Homo sapiens from Middle Awash, Ethiopia. *Nature* 423(6941), pp. 747–752. doi: 10.1038/nature01670.
- Clarkson, C. (2008). Lithics and landscape archaeology. In: Davis, B. and Thomas, N. (eds.), *Handbook of Landscape Archaeology*, Left Coast Press, Walnut Creek pp. P490-501
- Clarkson, C., Jacobs, Z., Marwick, B. et al. (2017). Human Occupation of Northern Australia by 65,000 years ago. *Australian Archaeology* 83(3), pp. 162–163. doi: 10.1080/03122417.2017.1408198.
- Clement, A. C. and Peterson, L. C. (2008). Mechanisms of abrupt climate change of the last glacial period. *Reviews of Geophysics* 46(4), doi: 10.1029/2006rg000204
- Cole, S. (1954). *The Prehistory of East Africa*. New York: Mentor.
- Collard, M., Shennan, S. J., Buchanan, B. and Bentley, R. A. (2008). Evolutionary biological methods and cultural data. In: Bentley, R. A., Maschner, H. D. G., Chippindale, C. (eds.) *Handbook of Archaeological Theories*, pp. 203–223. Lanham: Altamira Press
- Conard, N. J. (2004). An overview of the patterns of behavioural change in Africa and Eurasia during the Middle and Late Pleistocene. In: d’Errico, F. and Backwell, L. R. (eds) *From Tools to Symbols: From Early Hominids to Modern Humans*. Witswatersrand, South Africa: Witswatersrand University Press, pp. 294–332. doi: 10.18772/22005064174.24.
- Conard, N. J., Porraz, G. and Wadley, L. (2012). What is in a name? Characterising the ‘post-Howiesons Poort’ at Sibudu. *South African Archaeological Review* 67(196), pp. 180–199.
- Coon, C. S. (1962). *The Origin of Races*. Edited by J. Cape. London: Lowe and Brydone Ltd.
- Coppe, J., Lepers, C. and Rots, V. (2022). Projectiles Under a New Angle: a Ballistic Analysis Provides an Important Building Block to Grasp Paleolithic Weapon Technology. *Journal of Archaeological Method and Theory* 29, pp. 1131–1157. doi: 10.1007/s10816-022-09551-z
- Cowling, S. A., Cox, P. M., Jones, C. et al. (2007). Simulated glacial and interglacial vegetation across



- Africa: Implications for species phylogenies and trans-African migration of plants and animals. *Global Change Biology* 14(4), pp. 827–840. doi: 10.1111/j.1365-2486.2007.01524.x.
- Crassard, R. and Hilbert, Y. H. (2013). A Nubian Complex Site from Central Arabia: Implications for Levallois Taxonomy and Human Dispersals during the Upper Pleistocene. *PLoS ONE* 8(7), p. e69221. doi: 10.1371/journal.pone.0069221.
- Crevaschi, M., Di Lernia, S. and Garcea, E. A. (1998). Some insights on the Aterian in the Libyan Sahara: chronology, environment, and archaeology. *African Archaeological Review* 15(4), pp. 261–86, doi: 10.1023/A:1021620531489
- Crevecoeur, I., Rougier, H., Grine, F. and Froment, A. (2009). Modern Human Cranial Diversity in the Late Pleistocene of Africa and Eurasia: Evidence from Nazlet Khater, Peștera cu Oase, and Hofmeyr. *American Journal of Physical Anthropology* 140(2), pp. 347–358. doi: 10.1002/ajpa.21080.
- Cuthbert, M. O., Gleeson, T., Reynolds, S. *et al.* (2017). Modelling the role of groundwater hydro-refugia in East African hominin evolution and dispersal. *Nature Communications* 8, 15696, doi: 10.1038/ncomms15696
- d’Errico, F., Banks, W. E., Warren, D. L. *et al.* (2017). Identifying early modern human ecological niche-expansions and associated cultural dynamics in the South African Middle Stone Age. *Proceedings of the National Academy of Sciences of the United States of America* 114(30), pp. 7869–7876. doi: 10.1073/pnas.1620752114.
- d’Errico, F., Marti, A. P., Shipton, C. *et al.* (2020). Trajectories of cultural innovation from the Middle to Later Stone Age in Eastern Africa: Personal ornaments, bone artifacts, and ochre from Panga ya Saidi, Kenya. *Journal of Human Evolution* 141, p. 102737. doi: 10.1016/j.jhevol.2019.102737.
- Daboul, A., Ivanovska, T., Bülow, R. *et al.* (2018). Procrustes-based geometric morphometrics on MRI images: An example of inter-operator bias in 3D landmarks and its impact on big datasets. *PLoS ONE* 13(5): e0197675, doi: 10.1371/journal.pone.0197675
- Dalén, L., Nystrom, V., Valdiosera, C. *et al.* (2007). Ancient DNA reveals lack of postglacial habitat tracking in the arctic fox. *Proceedings of the National Academy of Sciences of the United States of America* 104(16), pp. 6726–6729. doi: 10.1073/pnas.0701341104.
- Dapschuska, R., Göden, M.B., Sommer, C. *et al.* (2022). The Emergence of Habitual Ochre Use in Africa and its Significance for The Development of Ritual Behavior During The Middle Stone Age. *Journal of World Prehistory* 35, pp. 233–319, doi: 10.1007/s10963-022-09170-2
- Dart, R. A. (1925). *Australopithecus africanus*: the man-ape of South Africa. *Nature* 115, pp. 195–199, doi: 10.1038/115195a0
- Dart, R. A. (1953). The predatory transition from ape to man. *International Anthropology and Linguistics Review* 1, pp. 201–218
- Davis, D. S. and Douglass, K. (2020). Aerial and Spaceborne Remote Sensing in African Archaeology: A Review of Current Research and Potential Future Avenues. *African Archaeological Review* 37, pp. 9–24, doi: 10.1007/s10437-020-09373-y
- Day, M. H. (1969). Early Homo sapiens remains from the Omo River region of South-west Ethiopia: Omo human skeletal remains. *Nature* 222(5199), pp. 1135–1138. doi: 10.1038/2221135a0.
- Day, M. H. and Stringer, C. B. (1982). A Reconsideration of the Omo Kibish Remains and the Erectus-Sapiens Transition.. *Prétirage First Intérrnational Congress of Human Palaeontology*, pp. 814–846.
- Day, M. H., Leakey, M. D. and Magori, C. (1980) A new hominid fossil skull (L.H. 18) from the NgaJoba Beds, Laetoli, northern Tanzania, *Nature* 284(5751), pp. 55–56. doi: 10.1038/284055a0.
- de la Peña, P. (2015). Refining our understanding of Howiesons Poort lithic technology: the evidence from Grey rocky layer in Sibudu cave (KwaZulu-Natal, South Africa). *PloS One* 10(12), p.e0143451.
- DeGiorgio, M., Jakobsson, M. and Rosenberg, N. A. (2009). Explaining worldwide patterns of human genetic variation using a coalescent-based serial founder model of migration outward from Africa. *Proceedings of the National Academy of Sciences of the United States of America* 106(38), pp. 16057–16062. doi: 10.1073/pnas.0903341106.
- Deiano, A. L. and McBrearty, S. (2002). 40Ar/39Ar dating of the Kapthurin Formation, Baringo, Kenya. *Journal of Human Evolution* 42(102), pp. 185–210, doi: 10.1006/jhev.2001.0517
- Deino, A. L., Behrensmeier, A. K., Brooks, A. C. *et al.* (2018). Chronology of the Acheulean to Middle Stone Age transition in eastern Africa. *Science* 360(6384), pp. 95–98. doi: 10.1126/science.aao2216.
- deMenocal, P. B. (2004). African climate change and faunal evolution during the Pliocene-Pleistocene. *Earth and Planetary Science Letters*. 220(1–2), pp. 3–24. doi: 10.1016/S0012-821X(04)00003-2.

- Dennell, R. W., Marinón-Torres, M. and Bermúdez de Castro, J. M. (2011). Hominin variability, climatic instability and population demography in Middle Pleistocene Europe. *Quaternary Science Reviews* 30(11-12), pp. 1511-1534
- Deshpande, O., Batzoglou, S., Feldman, M. W., Cavalli-Sforza. (2009). A Serial Founder Effect Model for Human Settlement Out of Africa. *Proceedings of the Royal Society: B* 276(1655), pp. 291–300. doi: 10.1098/rspb.2008.0750.
- Dibble, H. L., Holdaway, S. J., Lin, S. C. *et al.* (2017). Major Fallacies Surrounding Stone Artifacts and Assemblages. *Journal of Archaeological Method and Theory* 24, pp. 813–851, doi: 10.1007/s10816-016-9297-8
- Dirks, P. H., Roberts, E. M., Hilbert-Wolf, H. *et al.* (2017). The age of *Homo naledi* and associated sediments in the Rising Star Cave, South Africa. *eLife* 6:e24231. doi: 10.7554/eLife.24231.001.
- Dogandžić, T., Braun, D. R. and McPherron, S. P. (2015). Edge Length and Surface Area of a Blank: Experimental Assessment of Measures, Size Predictions and Utility. *PLoS ONE* 10(9): e0133984.
- Döll, P. & Fiedler, K. (2008). Global-scale modeling of groundwater recharge. *Hydrological Earth System Science* 12, pp. 863–885, doi: 10.5194/hess-12-863-2008
- Domingo, I., Villaverde, V., López-Montalvo, E. *et al.* (2013). Latest developments in rock art recording: towards an integral documentation of Levantine rock art sites combining 2D and 3D recording techniques. *Journal of Archaeological Science* 40(4), pp. 1879-1889, doi: 10.1016/j.jas.2012.11.024
- Domingo, I., Carridon, B., Blanco, S. and Lerma, J. L. (2015). Evaluating conventional and advanced visible image enhancement solutions to produce digital tracings at el Charche rock art shelter. *Digital Applications in Archaeology and Cultural Heritage* 2 (2-3), pp. 79-88, doi: 10.1016/j.daach.2015.01.001
- Domínguez-Rodrigo, M., Mabulla, A., Luque, L. *et al.* (2008). A new archaic *Homo sapiens* fossil from Lake Eyasi, Tanzania. *Journal of Human Evolution* 54(6), pp. 899–903. doi: 10.1016/j.jhevol.2008.02.002.
- Douglass, K. (2020). Amy ty lilin-draza'ay: Building archaeological practice on principles of community, *African Archaeological Review* 37, pp. 481-485, doi: 10.1007/s10437-020-09404-8
- Douze, K. and Delagnes, A. (2016). The pattern of emergence of a Middle Stone Age tradition at Gademotta and Kulkuletti (Ethiopia) through convergent tool and point technologies. *Journal of Human Evolution* 91, pp. 93–121.
- Douze, K., Igraja M., Rots, V., Cnuts, D. and Porraz, G. 2020. Technology and Function of Middle Stone Age Points. Insights from a Combined Approach at Bushman Rock Shelter, South Africa. In: Groucutt, H. (eds) *Culture History and Convergent Evolution. Vertebrate Paleobiology and Paleoanthropology*. Springer, Cham. doi: 10.1007/978-3-030-46126-3\_7
- Douze, K., Lespez, L., Rasse, M. *et al.* (2021). A West African Middle Stone Age site dated to the beginning of MIS 5: Archaeology, chronology, and paleoenvironment of the Ravin Blanc I (eastern Senegal). *Journal of Human Evolution* 154, 102951. doi: 10.1016/j.jhevol.2021.102952
- Drake, N. A., Blench, R. M., Armitage, S. *et al.* (2011). Ancient watercourses and biogeography of the Sahara explain the peopling of the desert. *Proceedings of the National Academy of Sciences of the United States of America*, 108(2), pp. 458–462. doi: 10.1073/pnas.1012231108.
- Drake, N. A., Breeze, P. and Parker, A. (2013). Palaeoclimate in the Saharan and Arabian Deserts during the Middle Palaeolithic and the potential for hominin dispersals. *Quaternary International* 300, pp. 48–61. doi: 10.1016/j.quaint.2012.12.018.
- Drake, N. and Breeze, P. (2016). Climate Change and Modern Human Occupation of the Sahara from MIS 6-2. In: Jones, S. and Stewart, B. A. (eds) *African from MIS6-2: Population Dynamics and Palaeoenvironments, Vertebrate Paleobiology and Paleoanthropology*, pp. 103–122. doi: 10.1007/978-94-017-7520-5\_6.
- Dunnell, R. C. (1978). Style and Function: A Fundamental Dichotomy, *American Antiquity* 43(2), pp. 192-202, doi: 10.2307/279244
- Durvasula, A. and Sankararaman, S. (2020). Recovering signals of ghost archaic introgression in African populations. *Science Advances* 6(7), p. eaax5097. doi: 10.1126/sciadv.aax5097.
- Dyson-Hudson, R. and Smith, E. A. (1978). Human Territoriality: An Ecological Reassessment. *American Anthropology* 80(1), pp. 21-41. doi: 10.1525/aa.1978.80.1.02a00020
- Earl, G., Basford, P. J, Bischoff, A. S. *et al.* (2011). Reflectance transformation imaging systems for ancient documentary artefacts. In Bowen, J. P., Dunn, S. and Ng, K. (eds.) *EVA London 2011: Electronic Visualisation and the Arts*. BCS, pp. 147-154.

- Eerkins, J. W. and Lipo, C. P. (2005). Cultural transmission, copying errors, and the generation of variation in material culture and the archaeological record. *Journal of Anthropological Archaeology* 24(2005), pp. 316–334, doi: 10.1016/j.jaa.2005.08.001
- Else, H. (2022). African researchers lead campaign for equity in global collaborations. *Nature News*. <https://www.nature.com/articles/d41586-022-01604-3>
- Eren, M. I., Diez-Martin, F. and Dominguez-Rodrigo, M. (2013). An empirical test of the relative frequency of bipolar reduction in Beds VI, V, and III at Mumba Rockshelter, Tanzania: Implications for the East African Middle to Late Stone Age transition. *Journal of Archaeological Science* 40(1), pp. 248–256. doi: 10.1016/j.jas.2012.08.012.
- Eriksson, A. and Manica, A. (2012). Effect of ancient population structure on the degree of polymorphism shared between modern human. *Proceedings of the National Academy of Sciences of the United States of America* 109(35), pp. 13956–13960. doi: 10.1073/pnas.1200567109.
- Esri Inc. (2020). ArcGIS Pro (Version 2.5). <https://www.esri.com/en-us/arcgis/products/arcgis-pro/overview>.
- Evin, A., Bonhomme, V. and Claude., J. (2020). Optimising digitalization effort in morphometrics. *Biology Methods and Protocols* 5(1) bpaa023, doi: 10.1093/biomethods/bpaa023.
- Fagerton, J., Harder, S., Rosengren, A. et al. (2014). 3D facial landmarks: inter-operator variability of manual annotation. *BMC Med Imaging* 14:35, doi: 10.1186/1471-2342-14-35
- Faith, J. T., Domínguez-Rodrigo, M. and Gordon, A. D. (2009). Long-distance carcass transport at Olduvai Gorge? A quantitative examination of Bed I skeletal element abundances. *Journal of Human Evolution* 56(3), pp. 247–256. doi: 10.1016/j.jhevol.2008.12.008.
- Faith, J. T., Tryon, C. A., Peppe, D. J. et al. (2015). Paleoenvironmental context of the Middle Stone Age record from Karungu, Lake Victoria Basin, Kenya, and its implications for human and faunal dispersals in East Africa. *Journal of Human Evolution* 83, pp. 28–45, doi: 10.1016/j.jhevol.2015.03.004
- Faulkner, P., Miller, J. M., Quintana Morales, E. M. et al. (2021) 67,000 years of coastal engagement at Panga ya Saidi, eastern Africa. *PLoS ONE* 16(8): e0256761. doi: 1371/journal.pone.0256761
- Féblot-Augustins, J. (1993). Mobility strategies in the late middle palaeolithic of central europe and western europe: Elements of stability and variability. *Journal of Anthropological Archaeology* pp. 211–265. doi: 10.1006/jaar.1993.1007.
- Fernandes, V., Alshamali, F., Alves, M. et al. (2012). The Arabian cradle: Mitochondrial relicts of the first steps along the Southern route out of Africa. *American Journal of Human Genetics* 90(2), pp. 347–355. doi: 10.1016/j.ajhg.2011.12.010.
- Field, J. S. and Mirazón Lahr, M. (2005). Assessment of the Southern Dispersal: GIS-Based Analyses of Potential Routes at Oxygen Isotopic Stage 4. *Journal of World Prehistory* 19(1), pp. 1–45. doi: 10.1007/s10963-005-9000-6.
- Finlayson, C., Pacheco, F. G., Rodriguez-Vidal, J. et al. (2006). Late survival of Neanderthals at the southernmost extreme of Europe, *Nature* 443(7113), pp. 850–853. doi: 10.1038/nature05195.
- Foerster, V., Asrat, A., Ramsey, C. B. et al. (2022). Pleistocene climate variability in eastern Africa influenced hominin evolution. *Nature Geoscience* 15, pp. 805–811. doi: 10.1038/s41561-022-01032-y
- Foley, R. A. (1978). Incorporating sampling into initial research design: some aspects of spatial archaeology. In JF Cherry, C Gamble & S Shennan (Eds) *Sampling in Contemporary British Archaeology*, pp 49–65. Oxford: British Archaeological Reports.
- Foley, R. A. (1995). *Humans Before Humanity*. UK: Blackwell Publishing Inc.
- Foley, R. and Mirazón Lahr, M. (1997). Mode 3 Technologies and the Evolution of Modern Humans. *Cambridge Archaeological Journal* 7(1), pp. 3–36. doi: 10.1017/s0959774300001451.
- Foley, R., Mirazón Lahr, M. and Mailio-Fernandez, J. M. (2013). The Middle Stone Age of the Central Sahara: Biogeographical Opportunities and Technological Strategies in Later Human Evolution. *Quaternary International* 300, pp. 153–170
- Forni, G., Mantovani, A., and COVID-19 Commission of Accademia Nazionale dei Lincei, Rome. (2021). COVID-19 vaccines: where we stand and challenges ahead. *Cell Death Differ* 28, pp. 626–639, doi: 10.1038/s41418-020-00720-9.
- Fowler, M. J. (2018). Aerial Photography. *The Encyclopedia of Archaeological Sciences*, doi: 10.1002/9781119188230.saseas0007.
- Franklin, J., Potts, A. J., Fisher, E. C. et al. (2015). Paleodistribution modelling in archaeology and palaeoanthropology. *Quaternary Science Reviews* 110, pp. 1–14, doi: 10.1016/j.quascirev.2014.12.015

- Frazer, D., Wolpoff, M. H., Thorne, A. G. *et al.* (1993). Theories of Modern Human Origins: The Paleontological Test. *American Anthropologists* 95(1), pp. 14–50. doi: 10.1525/aa.1993.95.1.02a00020.
- Fritz, H. and Duncan, P. (1994). On the carrying capacity for large ungulates of African savanna ecosystems. *Proceedings of Biological Sciences* 256, pp. 77–82
- Fruciano, C (2016). Measurement error in geometric morphometrics. *Development Genes and Evolution* 226, pp. 139–158, doi: 10.1007/s00427-016-0537-4
- Fu, Q., Li, H., Moorjani, P. *et al.* (2014). Genome sequence of a 45,000-year-old modern human from western Siberia. *Nature* 514, 445–449 doi: 10.1038/nature13810
- Gamble, C. (1982). Interaction and Alliance in Palaeolithic Society. *Man* 17(1), pp. 91-107.
- Gamble, L., Claassen, C., Eerkens, J. *et al.* (2021). Finding Archaeological Relevance during a Pandemic and What Comes After. *American Antiquity* 86(1), pp. 2-22, doi: 10.1017/aaq.2020.94.
- Garg, K., Padilla-Iglesias, C., Ochoa, N. R. and Knight, V. B. (2021). Hunter-gatherer foraging networks promote information transmission. *Royal Society Open Science* 8(12), doi: 10.1098/rsos.211324
- Genomes Project C, Auton, A., Brooks, L. D. *et al.* (2015). A global reference for human genetic variation. *Nature* 526, pp. 68–74.
- Ghirotto, S., Penso-Dolfin, L. and Barbujani, G. (2011). Genomic Evidence for an African Expansion of Anatomically Modern Humans by a Southern Route. *Human Biology* 83(4), pp. 477–489. doi: 10.3378/027.083.0403.
- Gliganic, L. A., Jacobs, Z., Roberts, R. G. *et al.* (2012). New ages for Middle and Later Stone Age deposits at Mumba rockshelter, Tanzania: Optically stimulated luminescence dating of quartz and feldspar grains. *Journal of Human Evolution* 62(4), pp. 533–547. doi: 10.1016/j.jhevol.2012.02.004.
- Gomes, V. H., IJff, S. D., Raes, N. *et al.* (2018). Species Distribution Modelling: Contrasting presence-only models with plot abundance data. *Scientific Reports* 8, 1003, doi: 10.1038/s41598-017-18927-1
- Gonder, M. K., Mortensen, H. M. and Reed, F. A. (2007). Whole-mtDNA genome sequence analysis of ancient african lineages. *Molecular Biology and Evolution* 24(3), pp. 757–768. doi: 10.1093/molbev/msl209.
- Goodwin, A. J. H. and van Riet Lowe, C. (1929). *The Stone Age Cultures of South Africa.*, Man. Trustees of the South African Museum. doi: 10.2307/2789873.
- Gowlett, J.A.J., Brink, J.S., Herries, A.I.R., Hoare, S., and Rucina, S.M. (2017). The small and short of it: mini-bifaces and points from Kilombe, Kenya, and their place in the Acheulean. In: Wojtczak, D., Al Najjar, M., Jagher, R., Elsuede, H., and Wegmüller, F. (eds.) *Vocation Préhistoire: Homage à Jean-Marie Le Tensorer.* ERAUL 148, Liège, 121-132.
- Gravel-Miguel, C., Murray, J. K., Schoville, B. J., Wren, C. D. and Marean, C. W. (2021). Exploring variability in lithic armature discard in the archaeological record. *Journal of Human Evolution* 155, 102981, doi: 10.1016/j.jhevol.2021.102981
- Groos, A. R., Akçar, N., Yesilyurt, S. *et al.* (2021). Nonuniform Late Pleistocene glacier fluctuations in tropical Eastern Africa. *Scientific Advances* 7(11), doi: 10.1126/sciadv.abb6826 .
- Groucutt, H. S., Petraglia, M. D., Bailey, G. *et al.* (2015a). Rethinking the Dispersal of Homo sapiens Out of Africa. *Evolutionary Anthropology: Issues, News, and Reviews* 24(4), pp. 149–164. doi: 10.1002/evan.21455.
- Groucutt, H. S., Scerri, E. M. L., Lewis, L. *et al.* (2015b) Stone tool assemblages and models for the dispersal of Homo sapiens out of Africa. *Quaternary International* 382, pp. 8–30. doi: 10.1016/j.quaint.2015.01.039.
- Groucutt, H.S., Grün, R., Zalmout, I.A.S. *et al.* (2018). Homo sapiens in Arabia by 85,000 years ago. *Nature Ecology Evolution* 2, pp. 800–809. doi: 10.1038/s41559-018-0518-2
- Grove, M. (2009). Hunter-gatherer movement patterns: Causes and constraints. *Journal of Anthropological Archaeology* 28(2), pp. 222-233, doi: 10.1016/j.jaa.2009.01.003
- Grove, M. (2011). Change and variability in Plio-Pleistocene climates: Modelling the hominin response, *Journal of Archaeological Science* 38(11), pp. 3038–3047. doi: 10.1016/j.jas.2011.07.002.
- Grove, M. (2015). Palaeoclimates, plasticity, and the early dispersal of Homo sapiens. *Quaternary International* 369, pp. 17–37. doi: 10.1016/j.quaint.2014.08.019.
- Grove, M. (2018). Hunter-gatherers adjust mobility to maintain contact under climatic variation. *Journal of Archaeological Science: Reports* 19, pp. 588-595, doi: 10.1016/j.jasrep.2018.04.003
- Grove, M. and Blinkhorn, J. (2020). Neural networks differentiate between Middle and Later Stone Age lithic

- assemblages in eastern Africa. *PLoS ONE* 15, pp. 1–27. doi: 10.1371/journal.pone.0237528.
- Grove, M. and Blinkhorn, J. (2021). Testing the integrity of the Middle and Later Stone Age Cultural Taxonomic division in Eastern Africa. *Journal of Palaeolithic Archaeology* 4 (14). doi: 10.1007/s41982-021-00087-4 (2021).
- Grove, M., Lamb, H., Roberts, H. *et al.* (2015). Climatic variability, plasticity, and dispersal: A case study from Lake Tana, Ethiopia. *Journal of Human Evolution* 87, 32–47, doi: 10.1016/j.jhevol.2015.07.007
- Grove, M., Timbrell, L., Jolley, B. *et al.* (2022). The importance of noise colour in simulations of evolutionary systems. *Artificial Life* 27(3), doi: 10.1162/artl\_a\_00354
- Grun, R. (2016). Direct dating of Florisbad hominid. *Journal of Human Evolution*, 43(147), pp. 27–32.
- Grün, R., Pike, A., McDermott, F. *et al.* (2020). Dating the skull from Broken Hill, Zambia, and its position in human evolution. *Nature* 580(7803), pp. 1–4. doi: 10.1038/s41586-020-2165-4
- Gunz, P. and Mitteroecker, P. (2013). Semilandmarks: a method for quantifying curves and surfaces. *Hystrix: the Italian Journal of Mammalogy* 24(1), pp. 103-109, doi: 10.4404/hystrix-24.1-6292
- Gunz, P., Mitteroecker, P., Stadlmayr, A. *et al.* (2009). Early modern human diversity suggests subdivided population structure and a complex out-of-Africa scenario. *Proceedings of the National Academy of Sciences of the United States of America* 106(15), pp. 6094–6098. doi: 10.1073/pnas.0808160106.
- Haddon, A. C. (1905). Presidential address, Section H. *Reports of the British Association for the Advancement of Science (South Africa)*, 1905, pp. 511–527.
- Hallinan, E. and Shaw, M. (2020). Nubian Levallois reduction strategies in the Tankwa Karoo, South Africa. *PLoS One* 15(10):e0241068. doi: 10.1371/journal.pone.0241068.
- Hammer, M. F., Woerner, A. E., Mendez, F. L. *et al.* (2011). Genetic evidence for archaic admixture in Africa. *Proceedings of the National Academy of Sciences of the United States of America* 108(37), pp. 15123–15128. doi: 10.1073/pnas.1109300108.
- Harding, R. M. and McVean, G. (2004). A structured ancestral population for the evolution of modern humans. *Current Opinion in Genetics and Development* 14(6), pp. 667–674. doi: 10.1016/j.gde.2004.08.010.
- Harpending, H. and Rogers, A. (2000). Genetic Perspectives on Human Origins and Differentiation', *Annual Review of Genomics and Human Genetics* 1, pp. 361–385. doi: 10.1146/annurev.genom.1.1.361.
- Harpending, H. C., Sherry, S. T., Rogers, A. R. and Stoneking, M. (1993). The Genetic Structure of Ancient Human Populations. *Current Anthropology* 34(4), pp. 483–496. doi: 10.1086/204195.
- Harvati, K., Hublin, J. J. and Gunz, P. (2010). Evolution of middle-late Pleistocene human cranio-facial form: A 3-D approach. *Journal of Human Evolution* 59(5), pp. 445–464. doi: 10.1016/j.jhevol.2010.06.005.
- Harvati, K., Stringer, C., Grün, R. *et al.* (2011) The Later Stone Age Calvaria from Iwo Eleru, Nigeria: Morphology and Chronology. *PLoS ONE* 6(9): e24024. doi: 10.1371/journal.pone.002402
- Harvati, K., Roding, C., Bosman, A. M. *et al.* (2019). Apidima Cave fossils provide earliest evidence of *Homo sapiens* in Eurasia. *Nature* 57, pp. 500-504. doi: 10.1038/s41586-019-1376-z.
- Hays, J. D., Imbrie, J. and Shackleton, N. J. (1976). Variations in the earth's orbit: Pacemaker of the ice ages, *Science* pp. 1121–1132. doi: 10.1126/science.194.4270.1121.
- Henn, B. M., Gignoux, C. R., Jobin, M. *et al.* (2011). Hunter-gatherer Genomic Diversity Suggests a Southern African Origin for Modern Humans. *Proceedings of the National Academy of Sciences of the United States of America* 108(13), pp. 5154–62. doi: 10.1073/pnas.1017511108.
- Henrich, J., Boyd, R., Derex, M. *et al.* (2016). Understanding cumulative cultural evolution. *Proceedings of the National Academy of Sciences of the United States of America* 113(44), pp. E6724–E6725. doi: 10.1073/pnas.1610005113.
- Henshilwood, C. S., d'Errico, F., Yates, R. *et al.* (2002). Emergence of modern human behavior: Middle stone age engravings from South Africa. *Science*, 295(5558), pp. 1278–1280. doi: 10.1126/science.1067575.
- Hershkovitz, I., Marder, O., Ayalon, A. *et al.* (2015). Levantine cranium from Manot Cave (Israel) foreshadows the first European modern humans. *Nature*. 520(7546), pp. 216–219. doi: 10.1038/nature14134.
- Hershkovitz, I., Weber, G. W., Quam, R. *et al.* (2018). The Earliest Modern Humans Outside Africa. *Science* 359(6374), pp. 456–459. doi: 10.1126/science.aap8369.
- Hewitt, G. (2000). The genetic legacy of the quaternary ice ages. *Nature* 405 pp. 907–913. doi: 10.1038/35016000.
- Higham, T., Ramsey, C. B., Karavanic, I. *et al.* (2006). Revised direct radiocarbon dating of the Vindija G1

- Upper Paleolithic Neandertals. *Proceedings of the National Academy of Sciences of the United States of America* 103(3), pp. 553–557. doi: 10.1073/pnas.0510005103.
- Hijmans, R. J., van Etten, J., Sumner, M. *et al.* (2021). raster: Geographic Data Analysis and Modeling. CRAN: R Packages: <https://cran.r-project.org/web/packages/raster/index.html>.
- Hodder, I. (1982). *Symbols in Action: Ethnoarchaeological Studies of Material Culture*. Cambridge: Cambridge University Press.
- Holt, R.D. (2009). Bringing the Hutchinsonian niche into the 21<sup>st</sup> Century: Ecological and evolutionary perspectives. *Proceedings of the National Academy of Sciences of the United States of America* 106, pp. 19659–19665, doi: 10.1073/pnas.0905137106
- Howell, D. (2018). The potential of hyperspectral imaging for researching colour on artefacts. In Kelley, K. and Wood, R. L. (eds.) *Digital Imaging of Artefacts: Developments in Methods and Aims*. Archaeopress: Access Archaeology.
- Hublin, J. J., Ben-Ncer, A., Bailey, S. E. *et al.* (2017). New fossils from Jebel Irhoud, Morocco and the pan-African origin of Homo sapiens. *Nature* 546(7657), pp. 289–292. doi: 10.1038/nature22336.
- Hutchinson, G. E. (1957). Concluding Remarks, Cold Spring Harbor Symposium. *Quantitative Biology* 22, pp. 415–27.
- Imbrie, J. and Imbrie, J. Z. (1980). Modeling the climatic response to orbital variations. *Science* 207(4434), pp. 943–953. doi: 10.1126/science.207.4434.943.
- Inizan, M. L., Reduron-Ballinger, M., Roche, H. and Tixier, J. (1999). *Technology and Terminology of Knapped Stone*. Cercle de recherches et d'études préhistoriques.
- Iovita, R. (2009). Ontogenetic scaling and lithic systematics: Method and application. *Journal of Archaeological Science* 36(7), pp. 1447–1457, doi: 10.1016/j.jas.2009.02.008.
- Iovita, R. (2011). Shape variation in Aterian Tanged Tools and the Origins of Projectile Technology: A Morphometric Perspective on Stone Tool Function. *PLOS One* 6(12): e29029. doi: 10.1371/journal.pone.0029029
- Iovita, R., Braun, D. R., Douglass, M. J. *et al.* (2021). Operationalizing niche construction theory with stone tools. *Evolutionary Anthropology Issues, News and Reviews* 30(1), pp. 28–39, doi: 10.1002/evan.21881
- IPCC (2021). *Climate Change 2021: The Physical Science Basis. Contribution of Working Group I to the Sixth Assessment Report of the Intergovernmental Panel on Climate Change* [Masson-Delmotte, V., P. Zhai, A. Pirani, S.L. Connors, C. Péan, S. Berger, N. Caud, Y. Chen, L. Goldfarb, M.I. Gomis, M. Huang, K. Leitzell, E. Lonnoy, J.B.R. Matthews, T.K. Maycock, T. Waterfield, O. Yelekçi, R. Yu, and B. Zhou (eds.)]. Cambridge University Press. In Press.
- Isaac, G.L., Harris, J.W.K. and Marshall, F (1981). Small is informative: the application of the study of mini-sites and least-effort criteria in the interpretation of the Early Pleistocene archaeological record at Koobi Fora, Kenya. In: Clark, J. D. and Isaac, G. L. (eds). *Las Industrias mas Antiguas, Mexico City: X Congreso Union Internacional de Ciencias Prehistoricas y Protohistoricas*, pp. 101–119
- Ivanovaité, L., Serwatka, K., Hoggard, C. S. *et al.* (2020). All these fantastic cultures? Research history and regionalization in the Late Palaeolithic tanged point cultures of Eastern Europe. *European Journal of Archaeology* 23(2), pp. 162–185, doi: 10.1017/ea.2019.59
- Ivory, S. J., Lezine, A. M-, Vincens, A. and Cohen, A. S. (2018). Waxing and waning of forests: Late Quaternary biogeography of southeast Africa. *Global Change Biology* 24(7), pp. 2939–2951, doi: 10.1111/gcb.14150
- Jackson, R. C., Dugmore, A. J., & Riede, F. (2018). Rediscovering lessons of adaptation from the past. *Global environmental change* 52, pp. 58–65, doi: 10.1016/j.gloenvcha.2018.05.006
- Jacobs, Z., Roberts, R. G., Galbraith, R. F. *et al.* (2008). Ages for the Middle Stone Age of southern Africa: Implications for human behavior and dispersal, *Science* 322(5902), pp. 733–735. doi: 10.1126/science.1162219.
- Jacobs, Z., Hayes, E. H., Roberts, R. G. *et al.* (2013). An improved OSL chronology for the Still Bay layers at Blombos Cave, South Africa: Further tests of single-grain dating procedures and a re-evaluation of the timing of the Still Bay industry across southern Africa. *Journal of Archaeological Science* 40(1), pp. 579–594. doi: 10.1016/j.jas.2012.06.037
- Johnson, T. C., Werne, J. P., Brown, E. T. *et al.* (2016). A progressively wetter climate in southern East Africa over the past 1.3 million years. *Nature* 537(7619), pp. 220–224. doi: 10.1038/nature19065
- Jones, M. B., Brandt, S. A. and Marshall, F. (2017). Hunter-gatherer reliance on inselbergs, big game, and

- dwarf antelope at the Rifle Range Site, Buur Hakaba, southern Somalia ~20,000-5,000 BP. *Quaternary International* 471(A), pp. 55-65, doi: 10.1016/j.quaint.2017.09.030
- Joordens, J. C. A., Vonhof, H. B., Feibel, C. S. *et al.* (2011). An astronomically-tuned climate framework for hominins in the Turkana Basin. *Earth Planet Science Letters* 307, pp. 1–8, doi: 10.1016/j.epsl.2011.05.005
- Jouzel, J., Masson-Delmotte, V., Cattani, O. *et al.* (2007). Orbital and Millennial Antarctic Climate Variability over the Past 800,000 Years. *Science* 317(5839), pp. 793-796, doi: 10.1126/science.1141038
- Kaifu, Y. (2017). Archaic Hominin Populations in Asia before the Arrival of Modern Humans: Their Phylogeny and Implications for the “Southern Denisovans”. *Current Anthropology* 58(S17), pp. S418–S433. doi: 10.1086/694318.
- Kaifu, Y., Aziz, F., Indriati, E. *et al.* (2008). Cranial morphology of Javanese Homo erectus: new evidence for continuous evolution, specialization, and terminal extinction. *Journal of Human Evolution* 55(4), pp. 551-80. doi: 10.1016/j.jhevol.2008.05.002.
- Kelly, R. L. (1983). Hunter–gatherer mobility strategies. *Journal of Anthropological Research*, 39 277-306
- Kelly, R. L. (1995). *The Foraging Spectrum: Diversity in Hunter–Gatherer Lifeways*. Smithsonian Institution Press, Washington.
- Keppel, G., van Niel, K. P., Wardell-Johnson, G. W. *et al.* (2012). Refugia: identifying and understanding safe havens for biodiversity under climate change. *Global Ecology and Biogeography* 21(4), pp. 393–404. doi: 10.1111/j.1466-8238.2011.00686.x.
- Kersten, T. P. and Lindstaedt, M. (2012). Image-based low-cost systems for automatic 3D recording and modelling of archaeological finds and objects. In Ioannides, M., Fritsch, D., Leissner, J., Davies, R., Remondino, F. and Caffo, R. (eds.) *Progress in Cultural Heritage Preservation*. Springer, Berlin, Heidelberg, pp. 1-10, doi: 10.1007/978-3-642-34234-9\_1
- Key, A., Pargeter, J. and Schmidt, P. (2021) Heat treatment significantly increases the sharpness of silcrete stone tools, *Archaeometry* 63(3), pp. 447-466, doi: 10.1111/arcm.12619
- King, G. and Bailey, G. N. (2006). Tectonics and human evolution. *Antiquity* 80(308), pp. 265–286, doi: 10.1017/S0003598X00093613
- Klein, R. G. (2019). Population structure and the evolution of Homo sapiens in Africa. *Evolutionary Anthropology* 28(4), pp. 179–188. doi: 10.1002/evan.21788.
- Kleindienst, M. (1967). Questions of terminology in regard to the study of stone age industries in Eastern Africa: “Cultural stratigraphic units”. In: Bishop, W. W. and Clark, J. D. (eds) *Background to evolution in Africa*. Chicago: University of Chicago Press, pp. 861–878.
- Kleindienst, M. (2006). On Naming Things. In: Hovers, E. and Kuhn, S.L. (eds) *Transitions Before the Transition. Interdisciplinary Contributions To Archaeology*. Springer, Boston, MA. doi: .1007/0-387-24661-4\_2
- Klingenberg, C. (2008). Novelty and ‘Homology-free’ Morphometrics: What’s in a Name? *Evolutionary Biology* 35, pp. 186-190, doi: 10.1007/s11692-008-9029-4.
- Koo, T. and Li, M. (2016). A Guideline of Selecting and Reporting Intraclass Correlation Coefficients for Reliability Research. *Journal of Chiropractic Medicine* 15, doi: 10.1016/j.jcm.2016.02.012
- Kosmidis, I. (2007). brglm: Bias Reduction in Binomial-Response Generalized Linear Models. CRAN R Package. <https://cran.r-project.org/web/packages/brglm/brglm.pdf>
- Kottek, M., Grieser, J. and Beck, C. (2006). World Map of the Köppen-Geiger climate classification updated. *Gebüder Borntraeger*, Berlin, Stuttgart, doi: 10.1127/0941-2948/2006/0130
- Krapp, M., Beyer, R. M., Edmondson, S. L. *et al.* (2021). A statistics-based reconstruction of high-resolution global terrestrial climate for the last 800,000 years. *Scientific Data* 8, 228, doi: 10.1038/s41597-021-01009-3
- Krause, P., Szekely, O., Bloom, M. *et al.* (2021). COVID-19 and Fieldwork: Challenges and Solutions. *PS - Political Science & Politics* 54(2), pp. 264-269, doi: 10.1017/S1049096520001754.
- Kuhn, S. L. (1995). *Mousterian lithic technology. An ecological perspective*. Princeton, NJ: Princeton University Press.
- Kuhn, S. L. (2004). Upper Paleolithic raw material economies at Üçağizli cave Turkey. *Journal of Anthropological Archaeology* 23(4), pp. 431–448. doi: 10.1016/j.jaa.2004.09.001.
- Kuhn, S. L. and Stiner, M. (2001). The antiquity of hunter-gatherers. In: Panter-Brick, C., Layton, R. H., and Rowley-Conwy, P. (eds) *Hunter-gatherer: an interdisciplinary perspective*. Cambridge University Press, pp. 99–142.

- Lamb, H. F., Bates, C. R., Bryant, C. L. *et al.* (2018). 150,000-year palaeoclimate record from northern Ethiopia supports early, multiple dispersals of modern humans from Africa. *Scientific Reports* 8, 1077, doi: 10.1038/s41598-018-19601-w
- Lasker, J., Robutel, P., Joutel, F. *et al.* (2004). A long-term numerical solution for the insolation quantities of the Earth. *Astronomy Astrophysics* 238(1), pp. 261–285, doi: 10.1051/0004-6361:20041335
- Latter, B. D. H. (1980). Genetic Differences Within and Between Populations of the Major Human Subgroups. *The American Naturalist* 116(2), pp. 220–237. doi: 10.1086/283624.
- Leakey, R. E. F., Butzer, K. W. and Day, M. H. (1969). Early Homo sapiens remains from the Omo River region of south-west Ethiopia, *Nature* 222, pp. 1132–1138
- Leplongeon, A. (2016). Middle Stone Age and early Late Stone Age lithic assemblages at Enkapune Ya Muto (Kenya). In: *Proceedings of the European Society for the study of Human Evolution. Vol. 5. ESHE.* p 141.
- Levinsky, I., Araujo, M. B., Nogues-Bravo, D. *et al.* (2013). Climate envelope models suggest spatio-temporal co-occurrence of refugia of African birds and mammals. *Global Ecology and Biogeography* 22(3), pp. 351–363. doi: 10.1111/geb.12045
- Lewis, M. (2009). *Ethnologue: Languages of the World*. Sixteenth. Texas: SIL International
- Lewis, J. (2022). leastcostpath-1. CRAN: R Package. <https://cran.r-project.org/web/packages/leastcostpath/vignettes/leastcostpath-1.html>
- Linder, H. P., de Klerk, H. M., Born, J. *et al.* (2012). The partitioning of Africa: Statistically defined biogeographical regions in sub-Saharan Africa. *Journal of Biogeography* 39(7), pp. 1189–1205. doi: 10.1111/j.1365-2699.2012.02728.x.
- Lipson, M., Sawchuk, E.A., Thompson, J.C. *et al.* (2022). Ancient DNA and deep population structure in sub-Saharan African foragers. *Nature* 603, pp. 290–296. doi: 10.1038/s41586-022-04430-9
- Liu, Z., Ciais, P., Deng, Z. *et al.* (2020). Near-real-time monitoring of global CO<sub>2</sub> emissions reveals the effects of the COVID-19 pandemic. *Nature Communications* 11: 5172, doi: 10.1038/s41467-020-18922-7
- Lombard, M. (2007). Evidence for change in Middle Stone Age hunting behaviour at Blombos Cave: Results of a macrofracture analysis. *South African Archaeological Bulletin* 62(185), pp. 62–67.
- Loog, L., Mirazón Lahr, M., Kovacevic, M. *et al.* (2017). Estimating mobility using sparse data: Application to human genetic variation. *Proceedings of the National Academy of Sciences of the United States of America* 114(46), pp. 12213–12218, doi: 10.1073/pnas.1703642114
- Loy, A. and Slice, D. E. (2010). Image data banks and geometric morphometrics. In: Nimis, P. L. and Vignes Lebbe, R. (eds.) *Tools for Identifying Biodiversity: Progress and Problems*.
- Lupien, R. L., Russell, J. M., Subramanian, A. *et al.* (2021). Eastern African environmental variation and its role in the evolution and cultural change of Homo over the last 1 million years. *Journal of Human Evolution* 157, 103028, doi: 10.1016/j.jhevol.2021.103028
- Lycett, S. J. (2009). Quantifying transitions: Morphometric approaches to Palaeolithic variability and technological change. In: Camps M, Chauhan P (eds) *Sourcebook of Paleolithic Transitions: Methods, Theories, and Interpretations*, Springer New York, pp 9–92, doi: 10.1007/978-0-387-76487-0\_5.
- Lycett, S. J. and von Cramon-Taubadel, N. (2015) Toward a “Quantitative Genetic” Approach to Lithic Variation, *Journal of Archaeological Theory and Method* 22, pp. 646–675, doi: 10.1007/s10816-013-9200-9
- Lyman, L. L. and VanPool, T. L. (2009). Metric Data in Archaeology: A Study of Intra-Analyst and Inter-Analyst Variation, *American Antiquity* 74(3), pp. 485–504, doi: 10.1017/S0002731600048721
- Lyons, R. P., Scholz, C. A., Cohen, A. S. *et al.* (2015). Continuous 1.3-million-year record of East African hydroclimate, and implications for patterns of evolution and biodiversity. *Proceedings of the National Academy of Sciences of the United States of America* 112(51), pp. 15568–15573, doi: 10.1073/pnas.1512864112
- MacDonald, D. A., Royal, K. and Buchanan, B. (2020). Evaluating the effects of parallax in archaeological geometric morphometric analyses. *Archaeological and Anthropological Science* 12, 149, doi: 10.1007/s12520-020-01111-4
- Mackay, A., Stewart, B. A. and Chase, B. M. (2014). Coalescence and fragmentation in the late Pleistocene archaeology of southernmost Africa. *Journal of Human Evolution* 72, pp. 26–51. doi: 10.1016/j.jhevol.2014.03.003.



- Magnani, M., Douglass, M., Schroder, W. *et al.* (2020). The Digital Revolution to Come: Photogrammetry in Archaeological Practice. *American Antiquity* 85(4), pp. 737-760, doi: 10.1017/aaq.2020.59
- Maier, A., John, R., Linsel, F. *et al.* (2023). Analyzing Trends in Material Culture Evolution—a Case Study of Gravettian Points from Lower Austria and Moravia. *Journal of Paleolithic Archaeology* 6, 15 doi: 10.1007/s41982-023-00145-z
- Mallick, S., Li, H., Lipson, M. *et al.* (2016). The Simons Genome Diversity Project: 300 genomes from 142 diverse populations, *Nature*, 538(7624), pp. 201–206. doi: 10.1038/nature18964.
- Manica, A., Amos, W., Balloux, F. and Hanihara, T. (2007). The effect of ancient population bottlenecks on human phenotypic variation. *Nature* 448(7151):346-8. doi: 10.1038/nature05951.
- Manninen, M. and Knutsson, K. (2014). Lithic raw material diversification as an adaptive strategy technology, mobility, and site structure in Late Mesolithic northernmost Europe. *Journal of Anthropological Archaeology* 33, pp. 84-98.
- Marean, C. W. (1992a). Implications of late Quaternary mammalian fauna from Lukenya Hill (south-central Kenya) for paleoenvironmental change and faunal extinctions. *Quaternary Research* 37(2), pp. 239–255. doi: 10.1016/0033-5894(92)90085-W.
- Marean, C. W. (1992b). Hunter to herder: large mammal remains from the hunter-gatherer occupation at Enkapune Ya Muto rock-shelter, Central Rift, Kenya. *African Archaeological Review* 10, pp. 65-127, doi: 10.1007/BF01117697
- Marean, C. W., Bar-Matthews, M., Bernatchez, J. *et al.* (2007). Early human use of marine resources and pigment in South Africa during the Middle Pleistocene. *Nature* 449(7164), pp. 905–908. doi: 10.1038/nature06204.
- Marks, A. E. and Conard, N. J. (2008). Technology vs. Typology: the Case for and Against a Transition From the Msa To the Lsa at Mumba Cave, Tanzania. *BAR International Series* 1831, pp. 123–132.
- Marlowe, F. (2010). *The Hadza: Hunter-gatherers of Tanzania*, University of California Press.
- Marth, G. T., Czabarka, E., Murvai, J. & Sherry, S. T. (2004). The allele frequency spectrum in genome-wide human variation data reveals signals of differential demographic history in three large world populations. *Genetics* 166, pp. 351–372
- Martinón-Torres, M., d’Errico, F., Santos, E. *et al.* (2021). Earliest known human burial in Africa. *Nature* 593(7857), pp. 95–100, doi: 10.1038/s41586-021-03457-8
- Maraun, D. and Widmann, M. (2018). *Statistical downscaling and bias correction for climate research*, Cambridge University Press, Cambridge, UK.
- Marwick, B., Johnson, A., White, D. and Eff, A. (2016). binford: Binford’s Hunter-gatherer data. CRAN R Package. <https://cran.r-project.org/web/packages/binford/index.html>
- Marwick, B., Guedes, J. A., Barton, C. M. *et al.* (2017). Open Science in Archaeology. *The SAA Archaeological Record* doi: 10.17605/OSF.IO/3D6XX
- Maslin, M. A., Brierley, C. M., Milner, A. M. *et al.* (2014). East African climate pulses and early human evolution. *Quaternary Science Reviews* 101, pp. 1-17, doi: 10.1016/j.quascirev.2014.06.012
- Matzig, D. N. (2021). outlineR: An R package to derive outline shapes from (multiple) artefacts on JPEG images. *Zenodo*. <https://doi.org/10.5281/ZENODO.4527469>.
- Matzig, D.N., Hussain, S.T. and Riede, F. (2021). Design Space Constraints and the Cultural Taxonomy of European Final Palaeolithic Large Tanged Points: A Comparison of Typological, Landmark-Based and Whole-Outline Geometric Morphometric Approaches. *Journal of Palaeolithic Archaeology* 4, 27, doi: 10.1007/s41982-021-00097-2
- Mayr, E. (1942). *Systemics and the Origins of Species*. New York: Columbia University Press.
- Mayr, E. (2001) *What Evolution Is*. New York: Basic Books.
- McBrearty, S. and Brooks, A. S. (2000). The revolution that wasn’t: A new interpretation of the origin of modern human behavior. *Journal of Human Evolution* 39(5), pp. 453–563. doi: 10.1006/jhev.2000.0435.
- McBrearty, S. and Tryon, C. (2006). From Acheulean to Middle Stone Age in the Kapthurin Formation, Kenya. In: Hovers, E. and Kuhn, S. L. (eds) *Transitions Before the Transition: Evolution and Stability in the Middle Paleolithic and Middle Stone Age*. Boston, MA: Springer US, pp. 257–277. doi: 10.1007/0-387-24661-4\_14.
- McCall, G. S. and Thomas, J. T. (2012). Still Bay and Howiesons Poort Foraging Strategies: Recent Research and Models of Culture Change. *African Archaeological Review* 29, pp. 7–50.
- McCoy, M. D. (2020). The Site Problem: A Critical Review of the Site Concept in Archaeology in the Digital

- Age, *Journal of Field Archaeology* 45:sup1, pp. S18-S26, doi: 10.1080/00934690.2020.1713283
- McDermott, F., Grün, R., Stringer, C. and Hawesworth, C. J. (1993). Mass-spectrometric U-series Dates for Israeli Neanderthal/Early Modern Hominid Sites. *Nature* 363(6426), pp. 252–255. doi: 10.1038/363252a0.
- McDermott, F., Stringer, C., Grün, R. *et al.* (1996). New Late-Pleistocene uranium–thorium and ESR dates for the Singa hominid (Sudan). *Journal of Human Evolution* 31, pp. 507-516, doi: 10.1006/jhev.1996.0076
- McDougall, I., Brown, F. H. and Fleagle, J. G. (2005). Stratigraphic placement and age of modern humans from Kibish, Ethiopia. *Nature* 433(7027), pp. 733–736. doi: 10.1038/nature03258.
- McInerney, G. I. and Etienne, R.S. (2012). Ditch the niche – is the niche a useful concept in ecology or species distribution modelling? *Journal of Biogeography* 39, pp. 2096-2102 doi:10.1111/jbi.12033\
- McNabb, J. (2017). Journeys in space and time. Assessing the link between Acheulean Handaxes and genetic explanations, *Journal of Archaeological Science: Reports* (13), 403.
- McNabb, J., Sinclair, A., Wadley, L. *et al.* (2009) *The Cave of Hearths: Makapan Middle Pleistocene Research Project: Field Research by Antony Sinclair and Patrick Quinney 1996-2001*. Oxford: Archaeopress.
- Mehlman, M. J. (1989). *Late Quaternary archaeological sequences in Northern Tanzania*. Urbana: University of Illinois.
- Mendez, F. L., Krahn, T., Schrack, B. *et al.* (2013). An African American paternal lineage adds an extremely ancient root to the human y chromosome phylogenetic tree. *American Journal of Human Genetics* 92(3), pp. 454–459. doi: 10.1016/j.ajhg.2013.02.002.
- Meneganzin, A. and Bernardi, M. (2023, preprint). Were Neanderthals and Homo sapiens ‘good species’? *Quaternary Science Reviews*.
- Menendez, L. (2017). Comparing Methods to Assess Intraobserver Measurement Error of 3D Craniofacial Landmarks Using Geometric Morphometrics Through a Digitizer Arm. *Journal of Forensic Sciences* 62(3), doi: 10.1111/1556-4029.13301.
- Mercader, J. (2002). Forest People: The Role of African Rainforests in Human Evolution and Dispersal. *Evolutionary Anthropology Issues, News and Reviews* 11(3):117-124. doi: 10.1002/evan.10022
- Merrick, H. V. (1975). *Change in Later Pleistocene lithic industries in eastern Africa*. PhD dissertation, University of California.
- Merrick, H. V., Brown, F. H. and Nash, W. P. (1994). Use and movement of obsidian in the Early and Middle Stone Ages of Kenya and northern Tanzania. In: Childs, S. T. (ed.) *Society, Culture and Technology in Africa (MASCA Research Papers in Science and Archaeology, Supplement to Volume 11)*. Philadelphia: University of Pennsylvania Museum of Archaeology and Anthropology, pp. 29–44.
- Mesfin, I., Leplongeon, A., Pleurdeau, D. and Borel, A. (2020). Using morphometrics to reappraise old collections: The study case of the Congo Basin Middle Stone Age bifacial industry. *Journal of Lithic Studies* 7(1), doi: 10.2218/jls.4329.
- Miles, J., Pitts, M., Pagi, H., and Earl, G. (2014). New applications of photogrammetry and reflectance transformation imaging to an Easter Island statue. *Antiquity* 88(340), pp. 596-605, doi: 10.1017/S0003598X00101206
- Miller, C. S. and Gosling, W. D. (2014). Quaternary forest associations in lowland tropical West Africa. *Quaternary Science Reviews*, pp. 7–25. doi: 10.1016/j.quascirev.2013.10.027.
- Miller, J. M. and Wang, Y. V. (2022). Ostrich eggshell beads reveal 50,000-year-old social network in Africa. *Nature* 601, pp. 234–239, doi:10.1038/s41586-021-04227-2
- Minetti, A. E., Moia, C., Roi, G. S. *et al.* (2002). Energy cost of walking and running at extreme uphill and downhill slopes. *Journal of Applied Physiology* 93(3), pp. 1039-46. doi: 10.1152/jappphysiol.01177.2001.
- Mirazón Lahr, M. (1996). *The Evolution of Modern Human Diversity: A Study of Cranial Variation*. Cambridge: Cambridge University Press.
- Mirazón Lahr, M. and Foley, R. A. (1994). Multiple Dispersals and Modern Human Origins. *Evolutionary Anthropology*, 3(2), pp. 48–60. doi: 10.1002/evan.1360030206.
- Mirazón Lahr, M. and Foley, R. A. (1998). Towards a theory of modern human origins: geography, demography, and diversity in recent human evolution. *American Journal of Physical Anthropology* 107(S27), pp. 137–176. doi: 10.1002/(SICI)1096-8644(1998)107:27+%3c137::AID-AJPA6%3e3.0.CO;2-Q

- Mitteroecker, P. (2021). Morphometrics in Evolutionary Developmental Biology. In: de la Rosa, L. N. and Muller, G. B. (eds) *Evolutionary Development Biology*. Springer, Cham, pp 941-951, doi: 10.1007/978-3-319-32979-6\_119.
- Mitteroecker, P. and Bookstein, F. (2011). Linear Discrimination, Ordination, and the Visualization of Selection Gradients in Modern Morphometrics, *Evolutionary Biology* 38(1), pp. 100-144, doi: 10.1007/s11692-011-9109-8
- Moernaut, J., Verschuren, D., Charlet, F. *et al.* (2010). The seismic-stratigraphic record of lake-level fluctuations in Lake Challa: Hydrological stability and change in equatorial East Africa over the last 140 kyr. *Earth and Planetary Science Letters* 290(1-2), pp. 214-223. doi: 10.1016/j.epsl.2009.12.023
- Moodley, Y. and Harley, E. H. (2005). Population structuring in mountain zebras (*Equus zebra*): The molecular consequences of divergent demographic histories. *Conservation Genetics* 6(6), pp. 953–968. doi: 10.1007/s10592-005-9083-8.
- Moss, J. and Tveten, M. (2020). Kernel Density Estimation with Parametric Starts and Asymmetric Kernels. CRAN R Package. <https://cran.r-project.org/web/packages/kdensity/kdensity.pdf>
- Mounier, A. and Mirazón Lahr, M. (2019). Deciphering African late middle Pleistocene hominin diversity and the origin of our species. *Nature Communications* 10(1). doi: 10.1038/s41467-019-11213-w.
- Muirui, V. M., Owen, R. B., Lowenstein, T. K. *et al.* (2021). A million year vegetation history and palaeoenvironmental record from the Lake Magadi Basin, Kenya Rift Valley. *Palaeogeography, Paleoclimatology, Palaeoecology* 567(110247). doi: 10.1016/j.palaeo.2021.110247
- Müller, U. C., Pross, J., Tzedakis, P. C. *et al.* (2011). The role of climate in the spread of modern humans into Europe, *Quaternary Science Reviews* 30(3–4), pp. 273–279. doi: 10.1016/j.quascirev.2010.11.016.
- Mullin, S. K. and Taylor, P. J. (2002). The effects of parallax on geometric morphometric data. *Computers in Biology and Medicine* 32(6), pp. 455-464, doi: 10.1016/S0010-4825(02)00037-9
- Musson, C., Rog P. and Stefano C. (2013). *Flights into the Past. Aerial photography, photo interpretation and mapping for archaeology*, doi: 10.11588/propylaeumdok.00002009
- Natural Earth (2020). Natural Earth Data. Accessed at <https://www.naturalearthdata.com/downloads/50m-physical-vectors/50m-rivers-lake-centerlines/>
- Neiman, F. D. (1995). Stylistic variation in evolutionary perspective: inferences from decorative diversity and interassemblage distance in Illinois Woodland ceramic assemblages. *American Antiquity* 60(1), pp. 7-36.
- Nersting, L. G. and Arctander, P. (2001). Phylogeography and conservation of impala and greater kudu. *Molecular Ecology*, 10(3), pp. 711–719. doi: 10.1046/j.1365-294X.2001.01205.x.
- Neubauer, S., Gunz, P. and Hublin, J.-J. (2009). The pattern of endocranial ontogenetic shape changes in humans. *Journal of Anatomy* 215(3), pp. 240–255. doi: 10.1111/j.1469-7580.2009.01106.x.
- Neubauer, S., Hublin, J. J. and Gunz, P. (2018). The evolution of modern human brain shape. *Science Advances* 4(1), p. eaao5961. doi: 10.1126/sciadv.aao5961.
- Nettle, D. (1998). Explaining Global Patterns of Language Diversity. *Journal of Anthropological Archaeology* 17, pp. 354-374.
- Newman, S. E. (2015). Applications of Reflectance Transformation Imaging (RTI) to the study of bone surface modifications. *Journal of Archaeological Science* 53, pp. 536-549, doi: 10.1016/j.jas.2014.11.019
- Niang, K., Blinkhorn, J. and Ndiaye, M. (2018). The oldest Stone Age occupation of coastal West Africa and its implications for modern human dispersals: New insight from Tiémassas. *Quaternary Science Reviews* 188, pp. 167-173.
- Niang, K., Blinkhorn, J., Ndiaye, M. *et al.* (2020). The Middle Stone Age occupations of Tiémassas, coastal West Africa, between 62 and 25 thousand years ago. *Journal of Archaeological Science: Reports* 34, p. 102658.
- Nicholas, D. and Kramer, C. (2001). *Ethnoarchaeology in action*. Cambridge: Cambridge University Press.
- Nicholas, G. (2007). The past and future of Indigenous archaeology: Global challenges, North American perspectives, Australian prospects. *Australian Archaeology* 52, pp. 129–139, doi: 10.1080/03122417.2001.11681703
- Nix, H. A. (1986). Biogeographic Analysis of Australian Elapid Snakes. In: Longmore, R. (ed). *Atlas of Elapid Snakes of Australia. Australian Flora and Fauna Series No. 7*, Australian Government Publishing Service, Canberra, pp. 4-15.
- Nordling, L. (2021). Raising Up African Paleoanthropologists. *SAPIENS Anthropology Magazine*. Accessed

- online: <https://www.sapiens.org/biology/african-paleoanthropologists/>
- Odling-Smee, F. J., Laland, K.N. and Feldman, M. W. (2003). *Niche construction: The neglected process in evolution*, Princeton, NJ: Princeton University Press.
- Ogundiran, A. (2020). The COVID-19 Pandemic: Perspectives for Reimaging and Reimagining Archaeological Practice. *African Archaeological Review* 37, pp. 471–473, doi: 10.1007/s10437-020-09408-4
- Okumura M and Araujo, A. G. M. (2018). Archaeology, biology, and borrowing: A critical examination of geometric morphometrics in archaeology, *Journal of Archaeological Science* 101, pp. 149-158, doi: 10.1016/j.jas.2017.09.015
- Okasen, J., Simpson, G. L., Blanchet, F. G. *et al.* (2020). vegan: Community Ecology Package. CRAN R Package. <https://cran.r-project.org/web/packages/vegan/vegan.pdf>
- O’Leary, M. A. and Kaufman, S. (2011). MorphoBank: phylophenomics in the ‘cloud’, *Cladistics* 27(5), pp. 529-537, doi: 10.1111/j.1096-0031.2011.00355.x
- Oppenheimer, C. (2002). Limited global change due to the largest known Quaternary eruption, Toba  $\approx$ 74 kyr BP?. *Quaternary Science Reviews* 21(14–15), pp. 1593–1609. doi: 10.1016/S0277-3791(01)00154-8.
- Oppenheimer, S. (2003). *Out of Eden: the Peopling of the World*. London: Robinson.
- Osborne, A. H., Vance, D., Rohling, E. J. *et al.* (2008). A Humid Corridor Across the Sahara for the Migration of Early Modern Humans Out of Africa 120,000 years ago. *Proceedings of the National Academy of Sciences of the United States of America*. 105(43), pp. 16444–7. doi: 10.1073/pnas.0804472105.
- Osis, S., Hettinga, B., Macdonald, S. and Ferber, R. (2015). A novel method to evaluate error in anatomical marker placement using a modified generalized Procrustes analysis. *Computational Methods Biomechanics and Biomedical Engineering* 18, pp. 1108–1116, doi: 10.1080/10255842.2013.873034
- Ossendorf, G., Groos, A. R., Bromm, T. *et al.* (2019). Middle Stone Age foragers resided in high elevations of the glaciated Bale Mountains, Ethiopia. *Science* 365, pp. 583–587, doi: 10.1126/science.aaw8942
- Owen, R. B., Muirui, V. M., Lowenstein, T. K. *et al.* (2018). Progressive aridification in East Africa over the last half million years and implications for human evolution. *Proceedings of the National Academy of Sciences of the United States of America* 115(44), pp. 11174–11179, doi: 10.1073/pnas.1801357115
- Padilla-Iglesias, C., Atmore, L., Olivero, J. *et al.* (2022). Population interconnectivity over the past 120,000 years explains distribution and diversity of Central African hunter-gatherers. *Proceedings of the National Academy of Sciences of the United States of America* 119(21) e2113936119, doi: 10.1073/pnas.2113936119
- Pagani, L., Kivisild, T., Tarekegn, A. *et al.* (2012). Ethiopian genetic diversity reveals linguistic stratification and complex influences on the Ethiopian gene pool. *American Journal of Human Genetics* 91(1), pp. 83–96. doi: 10.1016/j.ajhg.2012.05.015.
- Pagani, L., Schiffels, S., Gurdasani, D. *et al.* (2015). Tracing the Route of Modern Humans out of Africa by Using 225 Human Genome Sequences from Ethiopians and Egyptians. *American Journal of Human Genetics* 96(6), pp. 986–991. doi: 10.1016/j.ajhg.2015.04.019.
- Page, J. W. (1976). A note on interobserver error in multivariate analyses of populations. *American Journal of Physical Anthropology* 44(3), pp. 521-525, doi: 10.1002/ajpa.1330440315
- Parkington, J. E. (1993). The neglected alternative: Historical narrative rather than cultural labelling. *South African Archaeological Bulletin* 48(158), pp. 94–97.
- Parry, W. and Kelly, R. (1987). Expedient core technology and sedentism. In: Johnson, J. and Morrow, C. (eds). *The Organisation of Core Technology*. Westview Press, Boulder, , pp.285-309
- Patalano, R., Hamilton, R., Finestone, E. *et al.* (2021). Microhabitat Variability in Human Evolution. *Frontiers in Earth Science* 9, 1208, doi: 10.3389/feart.2021.787669
- Patin, E., Lopez, M., Grollemund, R. *et al.* (2017). Dispersals and genetic adaptation of Bantu-speaking populations in Africa and North America. *Science* 356(6337), pp. 543–546. doi: 10.1126/science.aal1988.
- Pazan, K. R., Dewar, G. and Stewart, B. A. (2022). The MIS 5a (~80 ka) Middle Stone Age lithic assemblages from Melikane Rockshelter, Lesotho: Highland adaptation and social fragmentation. *Quaternary International* 611-512, pp. 115-133, doi: 10.1016/j.quaint.2020.11.046
- Perini, T. A., de Oliveira, G. L, Ornellas, J. D. S. and de Oliveira, F. P. (2005). Technical error of measurement in anthropometry. *Revista Brasileira de Medicina do Esporte* 11(1), pp. 86-90, doi: 10.1590/S1517-86922005000100009

- Petrík, J., Sosna, D., Prokeš, L., Štefanisko, D., and Galeta, P. (2018). Shape matters: Assessing regional variation of Bell Beaker projectile points in Central Europe using geometric morphometrics. *Journal of Archaeological and Anthropological Sciences* 10(4), pp. 893–904, doi: 10.1007/s12520-016-0423-z
- Phillips, S. J. and Dudík, M. (2008). Modeling of species distributions with Maxent: New extensions and a comprehensive evaluation. *Ecography* 31 (2), pp. 161-175, doi: 10.1111/j.0906-7590.2008.5203.
- Phillips, S. J., Dudík, M., Elith, J. *et al.* (2009). Sample selection bias and presence-only distribution models: Implications for background and pseudo-absence data. *Ecological Applications* 19(1), pp. 181-197, doi: 10.1890/07-2153.1
- Phillipson, D. W. (2005) *African Archaeology*. Third. Cambridge: Cambridge University Press.
- Pickrell, J. K., Patterson, N., Loh, P. R- *et al.* (2014). Ancient west Eurasian ancestry in southern and eastern Africa. *Proceedings of the National Academy of Sciences of the United States of America* 111(7), pp. 2632–2637. doi: 10.1073/pnas.1313787111.
- Piccolo, M., Cucci, C., Casini, A. and Stefani, L. (2020). Hyper-Spectral Imaging Technique in the Cultural Heritage Field: New Possible Scenarios. *Sensors* 20(10): 2843, doi: 10.3390/s20102843
- Pitra, C., Hansen, A. K., Lieckfeldt, D. and Arctander, P. (2002). An exceptional case of historical outbreeding in African sable antelope. *Molecular ecology*, 11, pp. 1197–1208. doi: 10.1046/j.1365-294X.2002.01516.x
- Plagnol, V. and Wall, J. D. (2006). Possible ancestral structure in human populations. *PLoS Genetics* 2, e105
- Pleurdeau, D. (2005). Human Technical Behavior in the African Middle Stone Age: The Lithic Assemblage of Porc-Epic Cave (Dire Dawa, Ethiopia). *African Archaeological Review* 22, pp. 177–197, doi: 10.1007/s10437-006-9000-7
- Pleurdeau, D., Hovers, E., Assefa, Z. *et al.* (2014). Cultural change or continuity in the late MSA/Early LSA of southeastern Ethiopia? The site of Goda Buticha, Dire Dawa area. *Quaternary International* 343, pp. 117-135, doi: 10.1016/j.quaint.2014.02.001
- Pope, K. O. and Terrell, J. E. (2008). Environmental setting of human migrations in the circum-Pacific region. *Journal of Biogeography* 35, pp. 1-11. doi: 10.1111/j.1365-2699.2007.01797.x.
- Porat, N., Chazan, M., Grün, R. *et al.* (2010). New radiometric ages for the Fauresmith industry from Kathu Pan, southern Africa: Implications for the Earlier to Middle Stone Age transition. *Journal of Archaeological Science* 37(2), pp. 269–283, doi: 10.1016/j.jas.2009.09.038
- Porraz, G., Val, A., Tribolo, C. *et al.* (2018). The MIS5 Pietersburg at '28' Bushman Rock Shelter, Limpopo Province, South Africa. *PLoS One* 13(10):e0202853. doi: 10.1371/journal.pone.0202853.
- Potts, R. (1998). Variability selection in hominid evolution. *Evolutionary Anthropology* 7(3), pp. 81–96. doi: 10.1002/(SICI)1520-6505(1998)7:3<81::AID-EVAN3>3.0.CO;2-A.
- Potts, R. (2012). Environmental and behavioral evidence pertaining to the evolution of Early Homo. *Current Anthropology* 53, S299–S317.
- Potts, R. and Faith, J. T. (2015). Alternating high and low climate variability: The context of natural selection and speciation in Plio-Pleistocene hominin evolution. *Journal of Human Evolution* 87, pp. 5–20. doi: 10.1016/j.jhevol.2015.06.014.
- Potts, R., Behrensmeier, A. K., Faith, J. T. *et al.* (2018). Environmental dynamics during the onset of the Middle Stone Age in eastern Africa. *Science* 360(6384), pp. 86–90. doi: 10.1126/science.aao2200.
- Potts, R., Dommain, R., Moerman, J. W. *et al.* (2020). Increased ecological resource variability during a critical transition in hominin evolution. *Nature* 6(43), doi: 10.1126/sciadv.abc8975
- Powell, A., Shennan, S. and Thomas, M. G. (2009). Late Pleistocene demography and the appearance of modern human behavior. *Science* (80-.). 324, pp. 1298–1301.
- Prugnolle, F., Manica, A. and Balloux, F. (2005). Geography Predicts Neutral Genetic Diversity of Human Populations. *Current Biology* 15(5), pp. 159–60. doi: 10.1016/j.cub.2005.02.038.
- Quick, L. J., Meadows, M., Bateman, M. *et al.* (2016). Vegetation and climate dynamics during the last glacial period in the fynbos-afrotemperate forest ecotone, southern Cape, South Africa. *Quaternary International*. 404, pp. 136–149. doi: 10.1016/j.quaint.2015.08.027.
- Quintana-Murci, L., Semino, O., Badelt, H. J. *et al.* (1999). Genetic evidence of an early exit of Homo sapiens from Africa through eastern Africa. *Nature Genetics* 23(4), pp. 437-41. doi: 10.1038/70550.
- R Core Team (2020) R: A language and environment for statistical computing. R Foundation for Statistical Computing, Vienna, Austria. URL: <https://www.R-project.org/>.
- Ramachandran, S., Deshpande, O., Roseman, C. C. *et al.* (2005). Support From the Relationship of Genetic

- and Geographic Distance in Human Populations for a Serial Founder Effect Originating in Africa. *Proceedings of the National Academy of Sciences* 102(44), pp. 15942–15947. doi: 10.1073/pnas.0507611102.
- Rasmussen, M., Guo, X., Wang, Y. *et al.* (2011). An Aboriginal Australian Genome Reveals Separate Human Dispersals into Asia. *Science* 334(6052), pp. 94–98. doi: 10.1126/science.1209202.
- Rayner, R. J., Moon, B. P. and Masters, J. C. (1993). The Makapansgat Australopithecine environment. *Journal of Human Evolution* 24, pp. 219–231
- Reich, D. E. *et al.* (2001). Linkage disequilibrium in the human genome. *Nature* 411, pp. 199–204
- Revell, L. (2012). phytools: Phylogenetic Tools for Comparative Biology (and Other Things). CRAN R Package. <https://cran.r-project.org/web/packages/phytools/phytools.pdf>
- Revelle, W. (2022). psych: Procedures for Psychological, Psychometric and Personality Research. CRAN R Package. <https://cran.r-project.org/web/packages/psych/index.html>
- Reyes-Centeno, H., Ghirotto, S., Déroit, F. *et al.* (2014). Genomic and Cranial Phenotype Data Support Multiple Modern Human Dispersals from Africa and a Southern Route into Asia. *Proceedings of the National Academy of Sciences of the United States of America* 111(20), pp. 7248–53. doi: 10.1073/pnas.1323666111.
- Reyes-Centeno, H., Hubbe, M., Hanihara, T. *et al.* (2015). Testing Modern Human Out-of-Africa Dispersal Models and Implications For Modern Human Origins. *Journal of Human Evolution* 87, pp. 95–106. doi: 10.1016/J.JHEVOL.2015.06.008.
- Reynolds, N. (2018). Decarbonising archaeology. *Nature Ecology and Evolution: News and Opinion*. Accessed online: <https://natureecoevocommunity.nature.com/posts/40589-cognitive-dissonance-and-archaeological-practice-the-challenge-of-decarbonising-a-discipline>
- Riaño, H. C., Jaramillo, N., Dujardi, J.-P. (2009). Growth changes in *Rhodnius pallescens* under simulated domestic and sylvatic conditions, *Infection, Genetics and Evolution* 9, pp. 162–168, doi: 10.1016/j.meegid.2008.10.009
- Ribot, I. Ghalem, Y. and Crevecoeur, I. (2023). The Position of the Hofmeyr Skull within Late Pleistocene African Regional Diversity: 2D and 3D Regional Morphometric Analyses. In: Grine, F.E. (eds) *Hofmeyr. Vertebrate Paleobiology and Paleoanthropology*. Springer, Cham. doi: 10.1007/978-3-031-07426-4\_7
- Richter, D., Grün, R., Joannes-Boyau, R. *et al.* (2017). The age of the hominin fossils from Jebel Irhoud, Morocco, and the origins of the Middle Stone Age. *Nature* 546(7657), pp. 293–296. doi: 10.1038/nature22335.
- Rifkin, R. F. (2011). Assessing the Efficacy of Red Ochre as a Prehistoric Hide Tanning Ingredient, *Journal of African Archaeology*, 9(2), pp. 131-158. doi: 10.3213/2191-5784-10199
- Rifkin, R. F. (2015). Ethnographic And Experimental Perspectives On The Efficacy Of Ochre As A Mosquito Repellent. *The South African Archaeological Bulletin*, vol. 70, no. 201, pp. 64–75
- Rifkin, R. F., Dayet, L., Queffelec, A. *et al.* (2015) Evaluating the Photoprotective Effects of Ochre on Human Skin by In Vivo SPF Assessment: Implications for Human Evolution, Adaptation and Dispersal. *PLoS ONE* 10(9): e0136090, doi: 10.1371/journal.pone.0136090
- Rizal, Y., Westaway, K. E., Zaim, Y. *et al.* (2020). Last appearance of *Homo erectus* at Ngandong, Java, 117,000–108,000 years ago. *Nature* 577, pp. 381–385. doi: 10.1038/s41586-019-1863-2
- Roberts, R. G., Jones, R. and Smith, M. A. (1990). Thermoluminescence dating of 50,000-year-old human occupation site in northern Australia. *Nature* 345, pp. 153–6. doi: 10.1016/0277-3791(92)90034-6.
- Roberts, P., Prendergast, M. E., Janzen, A. (2020). Late Pleistocene to Holocene human palaeoecology in the tropical environments of coastal eastern Africa. *Palaeogeography, Palaeoclimatology, Palaeoecology* 537, 109438. doi: 10.1016/j.palaeo.2019.109438
- Robinson, C. and Terhune, C. E. (2017) Error in geometric morphometric data collection: Combining data from multiple sources, *American Journal of Physical Anthropology* 164(1): pp. 62-75, doi: 10.1002/ajpa.23257
- Roe, D. A. (1964). *The British Lower and Middle Paleolithic: Some Problems, Methods of Study and Preliminary Results*. Proceedings of the Prehistoric Society.
- Rogers, A. R. and Jorde, L. B. (1995). Genetic evidence on modern human origins. *Human Biology* 67(1), pp. 1–36.
- Rose, J. I., Usik, V. I., Marks, A. E. *et al.* (2011). The Nubian Complex of Dhofar, Oman: An African Middle Stone Age Industry in Southern Arabia. *PLoS ONE* 6(11), p. e28239. doi:

- 10.1371/journal.pone.0028239.
- Rosso, D. E., d'Errico, F. and Zilhão, J. (2014). Stratigraphic and spatial distribution of ochre and ochre processing tools at Porc-Epic Cave, Dire Dawa, Ethiopia. *Quaternary International* 343, pp. 85–99, doi: 10.1016/j.quaint.2013.10.019
- Rosso, D. E., Martí, A. P. and d'Errico, F. (2016). Middle stone age ochre processing and behavioural complexity in the horn of Africa: Evidence from porc-épïc cave, dire dawa, Ethiopia. *PLoS ONE* 11(11), p. 164793. doi: 10.1371/journal.pone.0164793.
- Rots, V. (2016). Projectiles and Hafting Technology. In: Iovita, R., Sano, K. (eds) *Multidisciplinary Approaches to the Study of Stone Age Weaponry. Vertebrate Paleobiology and Paleoanthropology*. Springer, Dordrecht. Doi: 10.1007/978-94-017-7602-8\_12
- Rots, V. and Plisson, H. (2014). Projectiles and the abuse of the use-wear method in a search for impact, *Journal of Archaeological Science* 48(1), pp. 154–165. doi: 10.1016/j.jas.2013.10.027.
- Rots, V., van Peer, P. and Vermeersch, P. M. (2011). Aspects of tool production, use, and hafting in Palaeolithic assemblages from Northeast Africa', *Journal of Human Evolution* 60(5), pp. 637–664. doi: 10.1016/j.jhevol.2011.01.001.
- Sackett, J. R. (1982). Approaches to style in lithic archaeology. *Journal of Anthropological Archaeology* 1(1), pp. 59–112, doi: 10.1016/0278-4165(82)90008-3
- Sahle, Y. (2021). Fossil men: The quest for the oldest skeleton and the origins of humankind, *American Journal of Physical Anthropology* 176(2), pp. 340–341, doi: 10.1002/ajpa.24359
- Sahle, Y. and Brooks, A. S. (2019). Assessment of complex projectiles in the early Late Pleistocene at Aduma, Ethiopia. *PLoS ONE* 14(5). doi: 10.1371/journal.pone.0216716.
- Sahle, Y., Hutchings, W. K., Braun, D. R. *et al.* (2013) Earliest stone-tipped projectiles from the Ethiopian Rift date to >279,000 years ago, *PLoS ONE* 8(11), e78092, doi: 10.1371/journal.pone.0078092
- Sahle, Y., Morgan, L.E., Braun, D. R. *et al.* (2014). Chronological and behavioral contexts of the earliest middle stone age in the gademotta formation, main ethiopian rift. *Quaternary International* 331, pp. 6–19. doi: 10.1016/j.quaint.2013.03.010.
- Sankararaman, S., Mallick, S., Dannemann, M. *et al.* (2014). The genomic landscape of Neanderthal ancestry in present-day humans. *Nature* 507, pp. 354–357. doi: 10.1038/nature12961
- Scerri, E. M. L. (2013a). The Aterian and its place in the North African Middle Stone Age, *Quaternary International* 300, pp. 111–130. doi: 10.1016/j.quaint.2012.09.008.
- Scerri, E. M. L. (2013b). On the spatial and technological organisation of hafting modifications in the North African Middle Stone Age. *Journal of Archaeological Science* 40(12), pp. 4234–4248. doi: 10.1016/j.jas.2013.06.011.
- Scerri, E. M. L. (2017a). The North African Middle Stone Age and its place in recent human evolution. *Evolutionary Anthropology* 26(3), pp. 119–135. doi: 10.1002/evan.21527.
- Scerri, E. M. L. (2017b). The Stone Age Archaeology of West Africa. *Oxford Research Encyclopedia, African History*.
- Scerri, E. M. L., Drake, N. A., Jennings, R. and Groucutt, H. S. (2014). Earliest evidence for the structure of Homo sapiens populations in Africa. *Quaternary Science Reviews* 101, pp. 207–216. doi: 10.1016/j.quascirev.2014.07.019.
- Scerri, E. M. L., Gravina, B., Blinkhorn, J. and Delagnes, A. (2016). Can lithic attribute analyses identify discrete reduction trajectories? A quantitative study using refitted lithic sets. *Journal of Archaeological Method and Theory* 23(2), pp. 669–691.
- Scerri, E. M. L., Blinkhorn J., Niang, K. *et al.* (2017). Persistence of Middle Stone Age technology to the Pleistocene/Holocene transition supports a complex hominin evolutionary scenario in West Africa. *Journal of Archaeological Science: Reports* 11, pp. 639–646. doi: 10.1016/j.jasrep.2017.01.003.
- Scerri, E. M. L., Thomas, M. G., Manica, A. *et al.* (2018). Did Our Species Evolve in Subdivided Populations across Africa, and Why Does It Matter?. *Trends in Ecology and Evolution* 33(8), pp. 582–594. doi: 10.1016/j.tree.2018.05.005.
- Scerri, E. M. L., Chikhi, L. and Thomas, M. G. (2019). Beyond multiregional and simple out-of-Africa models of human evolution. *Nature: Ecology and Evolution* 3, pp. 1370–1372. doi: 10.1038/s41559-019-0992-1
- Scerri, E. M. L., Kühnert, D., Blinkhorn, J. *et al.* (2020). Field-based sciences must transform in response to COVID-19, *Nature Ecology and Evolution* 4, pp. 1571–1574, doi: 10.1038/s41559-020-01317-8
- Scerri, E. M. L., Niang, K., Candy, I. *et al.* (2021). Continuity of the Middle Stone Age into the Holocene.

- Scientific Reports* 11(70).
- Scerri, E. M. L. and Will M. (2023). The revolution that still isn't: The origins of behavioral complexity in *Homo sapiens*. *Journal of Human Evolution* 179, 103358, doi: 10.1016/j.jhevol.2023.103358
- Schaebitz, F., Asrat, A., Lamb, H. F. *et al.* (2021). Hydroclimate changes in eastern Africa over the past 200,000 years may have influenced early human dispersal. *Communications Earth and Environment*. 2, 123, doi: 10.1038/s43247-021-00195-7
- Schillinger, K., Mesoudi, A. and Lycett, S. (2014) Copying Error and the Cultural Evolution of “Additive” vs. “Reductive” Material Traditions: An Experimental Assessment, *American Antiquity* 79(1), pp. 128-143, doi: 10.7183/0002-7316.79.1.128
- Schlebusch, C. M., Skoglund, P., Sjödin, P. *et al.* (2012). Genomic variation in seven Khoe-San groups reveals adaptation and complex African history. *Science* 338(6105), pp. 374–379. doi: 10.1126/science.1227721.
- Schlebusch, C. M., Loog, L., Groucutt, H. S. *et al.* (2021). Human origins in Southern African palaeowetlands? Strong claims from weak evidence. *Journal of Archaeological Science* 130, 105374. doi: 10.1016/j.jas.2021.105374.
- Schlüter, T. (1997). *Geology of East Africa*. Stuttgart: Schweizerbart Science Publishers.
- Schwartz, J. H. and Tattersall, I. (2003). *The Human Fossil Record. Vol 2: Craniodental morphology of genus Homo (Africa and Asia)*. NJ: Wiley-Liss.
- Seielstad, M., Bekele, E., Ibrahim, M. *et al.* (1999). A View of Modern Human Origins from Y Chromosome Microsatellite Variation. *Genome Research* 9(6), pp. 558–67.
- Serwatka, K. and Riede, F. (2016). 2D geometric morphometric analysis casts doubt on the validity of large tanged points as cultural markers in the European Final Palaeolithic, *Journal of Archaeological Science: Reports* 9, pp. 150–159, doi: 10.1016/j.jasrep.2016.07.018
- Shea, J. J. (2008). The Middle Stone Age Archaeology of the Lower Omo Kibish Formation: Excavations, Assemblages and Inferred Patterns of early *Homo sapiens* behaviour. *Journal of Human Evolution* 55, pp. 448-485
- Shea, J. J. (2014). Sink the Mousterian? Named stone tool industries (NASTIES) as obstacles to investigating hominin evolutionary relationships in the Later Middle Paleolithic Levant. *Quaternary International* 350, pp. 169-179. doi: 10.1016/j.quaint.2014.01.024
- Shea, J. J. (2020). *Prehistoric Stone Tools of Eastern Africa: A Guide*. Cambridge University Press.
- Shea, J. J. and Hildebrand, E. A. (2010). The Middle Stone Age of West Turkana, Kenya. *Journal of Field Archaeology* 35(4), pp. 355-364.
- Shennan, S. (2020). Style, Function and Cultural Transmission. In: Groucutt, H. (eds) *Culture History and Convergent Evolution*. Vertebrate Paleobiology and Paleoanthropology. Springer, Cham. doi: 10.1007/978-3-030-46126-3\_15
- Shennan, S. and Wilkinson, J. R. (2001). Ceramic Style Change and Neutral Evolution: A Case Study from Neolithic Europe, *American Antiquity* 66(4), pp. 577-593, doi: 10.2307/2694174
- Shipton, C. Roberts, P., Archer, W. *et al.* (2018). 78,000-year-old record of Middle and Later stone age innovation in an East African tropical forest. *Nature Communications* 9(1), p. 28. doi: 10.1038/s41467-018-04057-3.
- Shott, M. J. (1997). Stones and Shaft Redux: The Metric Discrimination of Chipped-Stone Dart and Arrow Points. *American Antiquity* 62, pp. 86-102.
- Shott, M. J. (2020). Toward a Theory of the Point. In: Groucutt, H. S. (ed). *Culture History and Convergent Evolution*. Vertebrate Paleobiology and Paleoanthropology. Springer, Cham, doi: 10.1007/978-3-030-46126-3\_12
- Shott, M. J. and Trail, B. W. (2010). Exploring new approaches to lithic analysis: Laser scanning and geometric morphometrics. *Lithic Technology* 35(2), pp. 195–220, doi: 10.1080/01977261.2010.11721090
- Shrout, P. E. and Fleiss, J. L. (1979). Intraclass Correlation: Uses in Assessing Rater Reliability, *Psychological Bulletin* 86, pp. 420–28, doi: 10.1037//0033-2909.86.2.420
- Silverman, B. W. (1986). Density Estimation For Statistics And Data Analysis. In: *Monographs on Statistics and Applied Probability*, London: Chapman and Hall.
- Simpson, G. G., Roe, A. and Lewontin, R. C. (1960). *Quantitative Zoology*, revised edition. Harcourt, Brace, New York.
- Sisk, M. L. and Shea, J. J. (2009). Experimental use and quantitative performance analysis of triangular flakes



- (Levallois points) used as arrowheads, *Journal of Archaeological Science* 36(9), pp. 2039–2047.
- Sisk, M. L. and Shea, J. J. (2011). The African Origin of Complex Projectile Technology: An Analysis Using Tip Cross-Sectional Area and Perimeter, *International Journal of Evolutionary Biology*, 2011, 968012, doi: 10.4061/2011/968012
- Skoglund, P., Thompson, J. C., Prendergast, M. E. *et al.* (2017). Reconstructing Prehistoric African Population Structure. *Cell* 171(1), pp. 59–71.e21. doi: 10.1016/j.cell.2017.08.049.
- Skov, L., Macia, M. C., Sveinbjornsson, G. *et al.* (2020). The nature of Neanderthal introgression revealed by 27,566 Icelandic genomes. *Nature* 582, pp. 78–83. doi: 10.1038/s41586-020-2225-9
- Slater, P.A. (2016). Change in lithic technological organization strategies during the Middle and Later Stone Ages in East Africa. Ph.D. Thesis. University of Illinois.
- Smith, E. I., Jacobs, Z., Johnsen, R. *et al.* (2018). Humans thrived in South Africa through the Toba eruption about 74,000 years ago. *Nature* 555(7697), pp. 511–515. doi: 10.1038/nature25967.
- Soares, P., Alshamali, F., Pereira, J. B. *et al.* (2012). The Expansion of mtDNA Haplogroup L3 Within and Out of Africa. *Molecular Biology and Evolution* 29(3). pp. 915–927. doi: 10.1093/molbev/msr245.
- Soberon, J. (2007). Grinnellian and Eltonian niches and geographic distributions of species. *Ecology Letters* 10, pp. 115–1123, doi: 10.1111/j.1461-0248.2007.01107.x
- Spoor, F. (1998). Rare Temporal Bone Pathology of the Singa Calvaria From Sudan. *American Journal of Physical Anthropology* 107, pp. 41–50, doi: 10.1002/(SICI)1096-8644(199809)107:1%3C41::AID-AJPA4%3E3.0.CO;2-G
- Spratt, R. M. and Lisiecki, L. E. (2016). A Late Pleistocene sea level stack. *Climate Past* 12, pp. 1079–1092, doi: 10.5194/cp-12-1079-2016
- Stewart, J. R. (2009). The evolutionary consequence of the individualistic response to climate change, *Journal of Evolutionary Biology* 22(12), pp. 2363–2375. doi: 10.1111/j.1420-9101.2009.01859.x.
- Stewart, J. R. and Stringer, C. B. (2012). Human evolution out of Africa: The role of refugia and climate change. *Science* 335(6074), pp. 1317–1321. doi: 10.1126/science.1215627.
- Stewart, J. R., Lister, A. M., Barnes, I. and Dalen, L. (2010). Refugia revisited: Individualistic responses of species in space and time, *Proceedings of the Royal Society B: Biological Sciences* 277(1682), pp. 661–671. doi: 10.1098/rspb.2009.1272.
- Stewart, M., Louys, J., Price, G. J. *et al.* (2019). Middle and Late Pleistocene mammal fossils of Arabia and surrounding regions: Implications for biogeography and hominin dispersal., *Quaternary International* 515, pp. 12–29. doi: 10.1016/j.quaint.2017.11.052.
- Stoneking, M. and Cann, R. L. (1989). African origin of human mitochondrial DNA. In: Mellars, P. (ed.) *The Human Revolution: Behavioural and Biological Perspectives on the Origins of Modern Human*. Edinburgh: Edinburgh University Press.
- Stoye, E. (2020). How research funders are tackling coronavirus disruption. *Nature News*, doi:10.1038/d41586-020-01120-2
- Strait, D. S. and Wood, B. A. (1999). Early hominid biogeography. *Proceedings of the National Academy of Sciences of the United States of America* 96, pp. 9196–9200.
- Stringer, C. (2002). Modern Human Origins: Progress and Prospects. *Philosophical Transactions of the Royal Society B: Biological Sciences* 357(1420), pp. 563–579. doi: 10.1098/rstb.2001.1057.
- Stringer, C. (2014). Why We Are Not All Multiregionalists Now. *Trends in Ecology & Evolution* 29(5), pp. 248–51. doi: 10.1016/j.tree.2014.03.001.
- Stringer, C. (2016). The origin and evolution of Homo sapiens. *Philosophical Transactions of the Royal Society B: Biological Sciences* 371(1698). doi: 10.1098/rstb.2015.0237.
- Stringer, C. and Andrews, P. (1988). Genetic and fossil evidence for the origin of modern humans. *Science* 239(4845), pp. 1263–1268. doi: 10.1126/science.3125610.
- Stringer, C. B. and Buck, L. T. (2014). Diagnosing Homo sapiens in the fossil record. *Annals of Human Biology*, 41(4) pp. 312–322. doi: 10.3109/03014460.2014.922616.
- Stringer, C B, Hublin, J.-J. and Vandermeersch, B. (1984). The Origin of Anatomically Modern Humans in Western Europe. In: Stringer, C. (ed.) *The Origins of Modern Humans: A World Survey of the Fossil Evidence*. New York: Alan R. Liss, Inc., pp. 51–135.
- Stringer, C. B., Grün, R., Schwarcz, H. P. and Goldberg, P. (1989). ESR Dates for the Hominid Burial Site of Es Skhul in Israel. *Nature* 338(6218), pp. 756–758. doi: 10.1038/338756a0.
- Taylor, N. (2016). Across Rainforests and Woodlands: A systematic reappraisal of the Lupemban middle stone age in central Africa. In: *Vertebrate Paleobiology and Paleoanthropology*. Springer, pp. 273–

299. doi: 10.1007/978-94-017-7520-5\_15.
- Taylor, N. (2022). Riddles wrapped inside an enigma. Lupemban MSA technology as a rainforest adaptation: revisiting the lanceolate point. *Philosophical Transactions of the Royal Society B*. doi: 10.1098/rstb.2020.0484
- Teilhard de Chardin, P. (1930). Le paléolithique en Somalie française et en Abyssinie. *L'Anthropologie* 40, pp. 331–34.
- The General Bathymetric Chart of the Oceans (GEBCO). Gridded Bathymetry Data. Available online at: [https://www.gebco.net/data\\_and\\_products/gridded\\_bathymetry\\_data/](https://www.gebco.net/data_and_products/gridded_bathymetry_data/) (2020).
- Thompson, J. C., Mackay, A., Nightingale, S. *et al.* (2018). Ecological risk, demography and technological complexity in the Late Pleistocene of northern Malawi: implications for geographical patterning in the Middle Stone Age. *Journal of Quaternary Science*, 33(3), pp. 261–284. doi: 10.1002/jqs.3002.
- Thorne, A. G. (1984). Australia Human Origins - How Many Sources? *American Journal of Physical Anthropology* 63(2).
- Thorne, A. G. and Wolpoff, M. H. (1992). The Multiregional Evolution of Humans. *Scientific American* 266(4), pp. 76–83. doi: 10.1038/scientificamerican0492-76.
- Timbrell, L. (2020a). How to read stone tools: A new mode system for describing variation in the Eastern African lithic record? *Evolutionary Anthropology*;29(5):280–2. doi: 10.1002/evan.21866.
- Timbrell, L. (2020b). Strength in numbers: combining old datasets to answer new questions. In: Kaercher, K., Arntz, M., Bomentre, N., Hermoso Buxán, X. L., Day, K., Ki, S., Macleod, R., Muñoz Mojado, H., Timbrell, L., Wisner, I. (eds) *New Frontiers in Archaeology: Proceedings of the Cambridge Annual Student Archaeology Conference 2019*, Archaeopress: Access Archaeology. ISBN 978-1-78969-794-0
- Timbrell, L. (2022). A collaborative model for lithic shape digitization in museum settings. *Lithic Technology*. doi: 10.1080/01977261.2022.2092299
- Timbrell, L. and Plomp, K. (2019). Using the shape of the basicranial portion of the temporal bone to distinguish between relatively closely-related human populations. *Journal of Archaeological Science: Reports* 26 (101885), doi: 10.1016/j.jasrep.2019.101885.
- Timbrell, L., Grove, M., Manica, A., Rucina, S. and Blinkhorn, J. (2022a). A spatiotemporally explicit palaeoenvironmental framework for the Middle Stone Age of eastern Africa. *Scientific Reports* 12, 3689. doi: 10.1038/s41598-022-07742-y
- Timbrell, L., Scott, C., Habte, B., Tefera, Y., Monod, H., Qazzih, M., Marais, B., Black, W., Maroma, C., Ndiema, E., Henderson, S., Elmes, K., Plomp, K and Grove, M. (2022b). Testing inter-observer error under a collaborative research framework for studying lithic shape variability. *Archaeological and Anthropological Sciences*. 14(209). doi: 10.1007/s12520-022-01676-2
- Timbrell, L., de la Peña, P., Way, A., Hoggard, C. S., Backwell, L., d’Errico, F., Wadley, L. and Grove, M. (2022c). Technological and geometric morphometric analysis of ‘post-Howiesons Poort’ points at Border Cave, KwaZulu-Natal, South Africa. *Quaternary Science Reviews* 297(107813). doi: 10.1016/j.quascirev.2022.107813
- Tishkoff, S. A., Reed, F. A., Friedlaender, F. R. *et al.* (2009). The genetic structure and history of Africans and African Americans. *Science*, 324(5930), pp. 1035–1044. doi: 10.1126/science.1172257.
- Tobler, W. (1993). Three Presentations On Geographical Analysis And Modeling. *National Center for Geographic Information and Analysis: Technical Report* 93-1.
- Tomasso, S. and Rots, V. (2018). What is the use of shaping a tang? Tool use and hafting of tanged tools in the Aterian of Northern Africa. *Archaeological and Anthropological Science* 10, pp.1389–1417. doi:10.1007/s12520-016-0448-3
- Tostevin, G. (2012). *Seeing lithics: a middle-range theory for testing for a middle-range theory for testing for cultural transmission in the Pleistocene*. American School of Prehistoric Research Monograph Series, Peabody Museum, Harvard University, and Oxbow Books. ISBN: 978-1-84217-527-9
- Trauth, M. H., Maslin, M. A., Deino, A. L. *et al.* (2007). High- and low-latitude forcing of Plio-Pleistocene East African climate and human evolution. *Journal of Human Evolution* 53(5), pp. 475–486. doi: 10.1016/j.jhevol.2006.12.009.
- Trauth, M. H., Larrasoana, J. C. and Mudelsee, M. (2009). Trends, rhythms and events in Plio-Pleistocene African climate. *Quaternary Science Reviews* 28(5–6), pp. 399–411. doi: 10.1016/j.quascirev.2008.11.003.
- Trauth, M. H., Maslin, M. A., Deino, A. L. *et al.* (2010). Human evolution in a variable environment: The

- amplifier lakes of Eastern Africa. *Quaternary Science Reviews* 29(23–24), pp. 2981–2988. doi: 10.1016/j.quascirev.2010.07.007.
- Trauth, M. H., Asrat, A., Berner, N. *et al.* (2021). Northern Hemisphere Glaciation, African climate and human evolution, *Quaternary Science Reviews* 268(107095), doi: 10.1016/j.quascirev.2021.107095
- Tribolo, C., Mercier, N., Douville, E. *et al.* (2013). OSL and TL dating of the Middle Stone Age sequence at Diepkloof Rock Shelter (South Africa): A clarification. *Journal of Archaeological Science* 40, 3401–3411. doi: 10.1016/j.jas.2012.12.001
- Tribolo, C., Asrat, A., Bahain, J. J- *et al.* (2017). Across the Gap: Geochronological and Sedimentological Analyses from the Late Pleistocene-Holocene Sequence of Goda Buticha, Southeastern Ethiopia. *PLoS ONE*. 12(1): e0169418. doi: 10.1371/journal.pone.0169418
- Trigger, B. (1989). *The history of archaeological thought*. Cambridge: Cambridge University Press.
- Tryon, C. A. (2003). *The Acheulean to Middle Stone Age Transition: Tephrostratigraphic Context for Archaeological Change in the Kapthurin Formation, Kenya*. Ph.D. Thesis, University of Connecticut.
- Tryon, C. A. (2019). The Middle/Later Stone Age transition and cultural dynamics of late Pleistocene East Africa. *Evolutionary Anthropology: Issues, News, and Reviews* 28(5), pp. 267–282. doi: 10.1002/evan.21802.
- Tryon, C. A. and Faith, J. T. (2013). Variability in the Middle Stone Age of Eastern Africa. *Current Anthropology* 54(S8), doi: 10.1086/673752.
- Tryon, C. A. and Faith, J. T. (2016). A demographic perspective on the middle to later stone age transition from nasera rockshelter, Tanzania.. *Philosophical Transactions of the Royal Society B: Biological Sciences* 1698. doi: 10.1098/rstb.2015.0238.
- Tryon, C. A. and McBrearty, S. (2002). Tephrostratigraphy and the Acheulian to Middle Stone Age transition in the Kapthurin Formation, Kenya. *Journal of Human Evolution* 42(1–2), pp. 211–235. doi: 10.1006/jhev.2001.0513.
- Tryon, C. A., Faith, J. T., Peppe, D. J. *et al.* (2010). The Pleistocene archaeology and environments of the Wasiriya Beds, Rusinga Island, Kenya. *Journal of Human Evolution* 59(6), pp. 657–671. doi: 10.1016/j.jhevol.2010.07.020.
- Tryon, C. A., Crevecoeur, I., Faith, J. T. *et al.* (2015). Late Pleistocene age and archaeological context for the hominin calvaria from GvJm-22 (Lukenya Hill, Kenya). *Proceedings of the National Academy of Sciences USA* 112(9), pp. 2682–7. doi: 10.1073/pnas.1417909112.
- Tryon, C. A., Faith, J. T., Peppe, D. J. *et al.* (2016). The Pleistocene prehistory of the Lake Victoria basin, *Quaternary International* 404, pp. 100–114. doi: 10.1016/j.quaint.2015.11.073.
- Tryon, C. A., Lewis, J. E., Ranhorn, K. *et al.* (2018). Middle and later stone age chronology of kisese II rockshelter (UNESCO World Heritage Kondoa Rock-Art Sites), Tanzania. *PLoS ONE* 13(2), p. e0192029. doi: 10.1371/journal.pone.0192029.
- Tsosie, K. S., Yracheta, J. M., Kolopenuk, J. and Smith, R.A. (2020). Letter to the Editor: Indigenous data sovereignties and data sharing in biological anthropology. *American Journal of Physical Anthropology* doi: 10.1002/ajpa.24184.
- Ulijaszek, S. J. and Kerr, D. A. (1999). Anthropometric measurement error and the assessment of nutritional status. *British Journal of Nutrition* 82, pp. 165–177, doi: 10.1017/s0007114599001348
- Uren, C., Kim, M., Martin, A. R. *et al.* (2016). Fine-Scale Human Population Structure in Southern Africa Reflects Ecogeographic Boundaries. *Genetics* 204(1):303–14. doi: 10.1534/genetics.116.187369.
- van Baelen, A., Wilshaw, A., Griffith, P. *et al.* (2019). Prospect Farm and the Middle and Later Stone Age Occupation of Mt. Eburru (Central Rift, Kenya) in an East African Context. *African Archaeological Review* 36, pp. 397–417, doi: 10.1007/s10437-019-09342-0
- van de Loosdrecht, M., Bouzouggar, A., Humphrey, L. *et al.* (2018). Pleistocene north african genomes link near eastern and sub-saharan african human populations. *Science* 360(6388), pp. 548–552. doi: 10.1126/science.aar8380.
- van Etten, J. (2019). gdistance: Distances and Routes on Geographical Grids. CRAN R Package. <https://cran.microsoft.com/snapshot/2014-12-09/web/packages/gdistance/vignettes/gdistance.pdf>
- van Peer, P., Rots, V. and Vroomans, J. M- (2014). A story of colourful diggers and grinders: the Sangoan and Lupemban at site 8-B-11, Sai Island, Sudan. *Before Farming* 3, pp. 1–28. doi: 10.3828/bfarm.2004.3.1
- Vermeersch, P. M. (2002). *Palaeolithic Quarrying Sites in Upper and Middle Egypt*. Leuven: Leuven University Press.
- Vidal, C. M., Lane, C. S., Asrat, A. *et al.* (2022). Age of the oldest Homo sapiens from eastern Africa. *Nature*

- 601, pp. 579-583. doi: 10.1038/s41586-021-04275-8
- Villa, P., Soressi, M., Henshilwood, C. S. and Mourre, V. (2009). The Still Bay points of Blombos Cave (South Africa). *Journal of Archaeological Science* 36(2), pp. 441–460. doi: 10.1016/j.jas.2008.09.028.
- Vincent, A. S. (1985). Plant foods in savanna environments: a preliminary report of tubers eaten by the Hadza of Northern Tanzania. *World Archaeology* 17, pp. 131–148
- Vita-Finzi, C. and Higgs, E.S. (1970). Prehistoric economy in the Mount Carmel area of Palestine: site catchment analysis. *Proceedings of the Prehistoric Society* 36, pp. 1-37.
- Vogelsang, R., Richter, J., Jacobs, Z. *et al.* (2010). New Excavations of Middle Stone Age Deposits at Apollo 11 Rockshelter, Namibia: Stratigraphy, Archaeology, Chronology and Past Environments. *Journal of African Archaeology* 8 (2), pp. 185-218.
- von Cramon-Taubadel, N., Frazier, B. C. and Mirazón Lahr, M. (2007). The problem of assessing landmark error in geometric morphometrics: Theory, methods, and modifications, *American Journal of Physical Anthropology* 134, pp. 24–35, doi: 10.1002/ajpa.20616
- von Cramon-Taubadel, N. and Lycett, S. J. (2008). Brief Communication: Human Cranial Variation Fits Iterative Founder Effect Model With African Origin. *American Journal of Physical Anthropology* 136, pp. 108–113. doi: 10.1002/ajpa.20775.
- von der Meden, J., Pickering, R., Schoville, B. J. *et al.* (2022). Tufas indicate prolonged periods of water availability linked to human occupation in the southern Kalahari. *PLoS ONE* 7(7): e0270104, doi: 10.1371/journal.pone.0270104
- Vrba, E. S. (1992). Mammals as a Key to Evolutionary Theory. *Journal of Mammalogy* 73(1), pp. 1–28. doi: 10.2307/1381862.
- Vrba, E. S. (1993). Turnover-pulses, the Red Queen, and related topics. *American Journal of Science* pp. 418–452. doi: 10.2475/ajs.293.A.418.
- Wadley, L. (2005). Putting ochre to the test: replication studies of adhesives that may have been used for hafting tools in the Middle Stone Age. *Journal of Human Evolution* 49(5), pp. 587-601
- Wadley, L. (2015) Those marvellous millennia: the Middle Stone Age of Southern Africa, *Azania: Archaeological Research in Africa* 50(2), pp. 155-226, doi: 10.1080/0067270X.2015.1039236
- Waguespack, N. M., Surovell, T. A., Denver, A. *et al.* (2009). Making a point: wood-versus stone-tipped projectiles, *Antiquity* 83(321), pp. 786–800
- Wall, J. D., Lohmueller, K. E. and Plagnol, V. (2009). Detecting Ancient Admixture and Estimating Demographic Parameters in Multiple Human Populations. *Molecular Biology and Evolution* 26(8), pp. 1823–1827. doi: 10.1093/molbev/msp096.
- Walter, R. C., Buffer, R. T., Bruggemann, J. H- *et al.* (2000). Early human occupation of the Red Sea coast of Eritrea during the last interglacial. *Nature* 405(6782), pp. 65–69. doi: 10.1038/35011048.
- Walter, M., Lovett, R., Maher, B. *et al.* (2020). Indigenous Data Sovereignty in the era of Big Data and Open Data. *Australian Social Policy Issues. Special Issue: Big Data and Social Policy in Australia* 56(2), pp. 143-156, doi: 10.1002/ajs4.141
- Wang, L.-Y. and Marwick, B. (2020). Standardization of ceramic shape: A case study of Iron Age pottery from northeastern Taiwan. *Journal of Archaeological Science: Reports* 33: 102554, doi: 10.1016/j.jasrep.2020.102554
- Washburn, S. L. (1960). Tools and human evolution. *Scientific American* 203, pp. 63–75, doi: 10.1038/scientificamerican0960-62(1960).
- Watts, I., Chazan, M. and Wilkins, J. (2016). Early evidence for brilliant ritualized display: Specularite use in the northern cape (South Africa) between ~500 and ~300 Ka. *Current Anthropology* 57(3), pp. 287–310. doi: 10.1086/686484.
- Way, A. M. and Hiscock, P. (2021). The evolution of Still Bay points at Sibudu. *Archaeological and Anthropological Sciences* 13, 122., doi: 10.1007/s12520-021-01359-4
- Way, A. M., de la Pena, P., de la Pena, E. and Wadley, L. (2022). Howiesons Poort backed artifacts provide evidence for social connectivity across southern Africa during the Final Pleistocene. *Scientific Reports* 12, 9227. doi: 10.1038/s41598-022-12677-5
- Wayland, E. (1929). African pluvial periods. *Nature*, 123(607).
- Weaver, T. D. and Roseman, C. C. (2008). New Developments in the Genetic Evidence for Modern Human Origins. *Evolutionary Anthropology* 17(1), pp. 69–80. doi: 10.1002/evan.20161.
- Weidenreich, F. (1938). The Discovery of the Femur of *Sinanthropus pekinensis*. *Science* 87(2258), pp. 322–

323. doi: 10.1126/science.87.2258.322.
- Weidenreich, F. (1946). Report on the latest discoveries of early man in the far east. *Experientia* 2, pp. 265–272. doi: 10.1007/BF02157044
- Werdelin, L. and Sanders, W. J. (2010). *Cenozoic Mammals of Africa*. Berkeley, California: University of California Press.
- Whallon, R. (2006). Social networks and information: Non-“utilitarian” mobility among hunter-gatherers. *Journal of Anthropological Archaeology* 25(2), pp. 259-270, doi: 10.1016/j.jaa.2005.11.004
- White, A. A. (2013). Functional and Stylistic Variability in Paleoindian and Early Archaic Projectile Points from Midcontinental North America. *North American Archaeologist* 34(1), pp. 71-108, doi: 10.2190/NA.34.1.c
- White, F. (1983). *The Vegetation of Africa: A descriptive memoir to accompany the Unesco/AETFAT/UNSO vegetation map of Africa*. Paris.
- White, T. D. (1986). Cut marks on the Bodo cranium: A case of prehistoric defleshing. *American Journal of Physical Anthropology* 69(4), pp. 503–509. doi: 10.1002/ajpa.1330690410.
- White, T. D., Asfaw, B., DeGusta, D. *et al.* (2003). Pleistocene Homo sapiens from Middle Awash, Ethiopia. *Nature* 423(6941), pp. 742–747. doi: 10.1038/nature01669.
- Whittaker, R. H. (1975). *Communities and Ecosystems*. 2nd edition. New York: MacMillan Publishing Co., Inc.
- Wiessner, P. (1977). *Hxaro: A regional system of reciprocity for reducing risk among the !Kung San*. Ph.D. thesis, University of Michigan
- Wiessner, P. (1982). Risk, reciprocity and social influences on! Kung San economics. In: Leacock, E. and Lee, R. B. (eds). *Politics and history in band societies*, pp. 61-84. Cambridge: Cambridge University Press.
- Wiessner, P. (1983). Style and Social Information in Kalahari San Projectile Points. *Society for American Archaeology* 48(2), pp. 253–276. doi: 10.2307/280450
- Wiessner, P. (1985). Style or Isochrestic Variation? A Reply to Sackett. *American Antiquity* 50(1), pp. 160–166. doi: 10.2307/280643.
- Wilkins, J. (2010). Style, Symboling, and Interaction in Middle Stone Age Societies. *vis-à-vis: Explorations in Anthropology* 10(1), pp. 102–125.
- Wilkins, J. (2020). Is it Time to Retire NASTIES in Southern Africa? Moving Beyond the Culture-Historical Framework for Middle Stone Age Lithic Assemblage Variability. *Lithic Technology* 45(4), pp. 295–307. doi: 10.1080/01977261.2020.1802848.
- Will, M. and Mackay, A. (2020). A Matter of Space and Time: How Frequent Is Convergence in Lithic Technology in the African Archaeological Record over the Last 300 kyr?. In: Groucutt, H. (eds) *Culture History and Convergent Evolution*. Vertebrate Paleobiology and Paleoanthropology. Springer, Cham, doi: 10.1007/978-3-030-46126-3\_6
- Will, M., Kandel, A. W., Kyriacou, K. and Conard, N. K. (2016). An evolutionary perspective on coastal adaptations by modern humans during the Middle Stone Age of Africa. *Quaternary International* 404B, pp. 68-86. doi: 10.1016/j.quaint.2015.10.021
- Will, M., Tryon, C., Shaw, M. *et al.* (2019). Comparative analysis of Middle Stone Age artifacts in Africa (CoMSAfrica). *Evolutionary Anthropology: Issues, News and Reviews* 28(2), pp. 57-59. doi: 10.1002/evan.21772.
- Will, M., Krapp, M., Stock, J. T. and Manica, A. (2021). Different environmental variables predict body and brain size evolution in Homo. *Nature Communications* 12, 4116, doi: 10.1038/s41467-021-24290-7
- Williams, M. (2019). *The Nile Basin: Quaternary geology, geomorphology and prehistoric environments*. Cambridge: Cambridge University Press.
- Wolpoff, M. H. (1986). Describing Anatomically Modern Homo sapiens: A Distinction Without a Definable Difference. In: *Fossil man - New Facts, New Ideas. Papers in honour of Jan Jelinek's life anniversary*. Brno: Anthropos, pp. 41–53.
- Wolpoff, M. H. (1989). Multiregional Evolution: The Fossil Alternative to Eden. In: Mellars, P. and Stringer, C. B. (eds) *The Human Revolution: Behavioural and Biological Perspectives on the Origins of Modern Humans*. Edinburgh. pp. 62–108.
- Wolpoff, M. H., Wu, X. and Thorne, A. G. (1984). Modern Homo sapiens Origins: A General Theory of Hominid Evolution Involving The Fossil Evidence From East Asia. In: Smith, F. and Spender, F. (eds) *The Origins of Modern Humans: A World Survey of the Fossil Evidence*. Alan R. Li. New York,

pp. 411–483.

- Wolpoff, M. H., Thorne, A. G., Jelinek, J. and Yinyun, Z. (1994). The Case for Sinking *Homo erectus*. 100 years of *Pithecanthropus* is Enough!. *Courier Forschungs-Institut Senckenberg*, 171(1), pp. 341–361.
- Wren, C. D. and Burke, A. (2019). Habitat suitability and the genetic structure of human populations during the Last Glacial Maximum (LGM) in Western Europe. *PLoS ONE* 14(6): e0217996, doi: 10.1371/journal.pone.0217996
- Wright, S. (1943). Isolation by distance. *Genetics* 28, pp. 114–138
- Wright, S. (1982). The shifting balance theory and macroevolution. *Annual Review Genetics* 16:001-19
- Wu, X.-J., Pei, S. -W., Cai, Y, -J. *et al.* (2019). Archaic human remains from Hualongdong, China, and Middle Pleistocene human continuity and variation. *Proceedings of the National Academy of Sciences of the United States of America*. 116 (20) 9820-9824. doi: 10.1073/pnas.1902396116.
- Wurz, S. (2002). Variability in the Middle Stone Age lithic sequence, 115,000-60,000 years ago at Klasies River, South Africa. *Journal of Archaeological Science* 29(9), pp. 1001–1015. doi: 10.1006/jasc.2001.0799.
- Wurz, S. (2013). Technological trends in the middle stone age of South Africa between MIS 7 and MIS 3. *Current Anthropology* 54(S8), pp. S305-19. doi: 10.1086/673283.
- Wurz, S, Bentsen, S. E., Reynard, J. *et al.* (2018). Connections, culture and environments around 100 000 years ago at Klasies River main site. *Quaternary International* 495, pp. 102–115. doi: 10.1016/j.quaint.2018.03.039.
- Xu, D., Pavlidiz, P., Taskent, R. O. *et al.* (2017). Archaic Hominin Introgression in Africa Contributes to Functional Salivary MUC7 Genetic Variation. *Molecular Biology and Evolution*, 34(10), pp. 2704–2715. doi: 10.1093/molbev/msx206.
- Yellen, J. E. (1977) *Archaeological Approaches to the Present*. New York: Academic Press.
- Yellen, J. and Harpending, H. (1972). Hunter-gatherer populations and archaeological inference. *World Archaeology* 4(2), pp. 244–253. doi: 10.1080/00438243.1972.9979535.
- Yellen, J. E., Brooks, A., Helgren, D. *et al.* (2005). The archaeology of Aduma Middle Stone Age sites in the Awash Valley, Ethiopia. *PaleoAnthropology* 2005(10), pp. 25–100.
- Yezerinac, S. M., Loughheed, S. C. and Handford, P. (1992). Measurement Error and Morphometric Studies: Statistical Power and Observer Experience, *Systematic Biology* 41(4), pp. 471–482, doi: 10.1093/sysbio/41.4.471
- Zelditch, M. L., Swiderski, D. L., Sheets, D. H. and Fink, W. L. (2004). *Geometric Morphometrics for Biologists: A Primer*, Academic Press.
- Zeng, L. and Zou, X. (2019). Error Analysis and Experimental Research on 3D Printing, *IOP Conference Series on Material Science and Engineering* 592, 012150.
- Zhang, G., Zhu, A, X.-., Windels, S. K. and Qin, C, Z-. (2018). Modelling species habitat suitability from presence-only data using kernel density estimation. *Ecological Indicators* 93, pp. 387–396. doi: 10.1016/j.ecolind.2018.04.002.
- Ziegler, M., Simon, M. H., Hall, I. R. *et al.* (2013). Development of Middle Stone Age innovation linked to rapid climate change. *Nature Communications* 4(1), pp. 1–9. doi: 10.1038/ncomms2897.

## Appendices

Appendix 1. Supplementary Online Materials for ‘A spatiotemporally explicit paleoenvironmental framework for the Middle Stone Age of eastern Africa’ (Timbrell et al., 2022; Sci Rep).

**Supplementary Table S1.** Summary of the Middle Stone Age occupations studied. Mean and standard deviation of mean annual temperature, total annual precipitation, and altitude are calculated across 50km for each occupation. Minimum, maximum, and mid-point age is derived from Blinkhorn and Grove [1], where radiometric dates for each assemblage collected from original references. Biome classification was extracted at the site coordinates and ecotones expressed as the percentage of cells per biome within 50km at each occupation.

|                                      | Temp<br>(°C) | Prec<br>(mm) | Alt<br>(masl) | Min<br>age<br>(kya) | Max<br>age<br>(kya) | Mid<br>age<br>(kya) | Biome                               | Ecotones  |
|--------------------------------------|--------------|--------------|---------------|---------------------|---------------------|---------------------|-------------------------------------|---|
| Goda<br>Buticha_<br>Complex<br>2_DEF | 19 (2)       | 742<br>(90)  | 1478<br>(564) | 22                  | 70                  | 46                  | Temperate<br>conifer forest         | Temperate conifer<br>forest (65%),<br>Tropical<br>xerophytic<br>shrubland (35%) |
| Mumba_<br>L_III_38                   | 16 (0)       | 800<br>(25)  | 1514<br>(353) | 33                  | 40                  | 37                  | Tropical<br>xerophytic<br>shrubland | Temperate conifer<br>forest (36%),<br>Tropical<br>xerophytic<br>shrubland (64%) |
| Mumba_<br>L_V_81                     | 16 (0)       | 797<br>(28)  | 1514<br>(353) | 52                  | 61                  | 57                  | Tropical<br>xerophytic<br>shrubland | Temperate conifer<br>forest (36%),<br>Tropical<br>xerophytic<br>shrubland (64%) |
| Mumba_<br>L_VI_38                    | 16 (0)       | 797<br>(28)  | 1514<br>(353) | 52                  | 61                  | 57                  | Tropical<br>xerophytic<br>shrubland | Temperate conifer<br>forest (36%),<br>Tropical<br>xerophytic<br>shrubland (64%) |
| Mumba_<br>L_VI_A                     | 18 (0)       | 782<br>(33)  | 1514<br>(353) | 86                  | 115                 | 101                 | Tropical<br>xerophytic<br>shrubland | Tropical<br>xerophytic<br>shrubland (100%)                                      |
| Mumba_<br>MU_V_8<br>1                | 16 (0)       | 917<br>(33)  | 1514<br>(353) | 47                  | 55                  | 51                  | Tropical<br>xerophytic<br>shrubland | Temperate conifer<br>forest (38%),<br>Tropical<br>xerophytic<br>shrubland (62%) |
| Mumba_<br>U_V_38                     | 15 (0)       | 949<br>(28)  | 1514<br>(353) | 44                  | 53                  | 49                  | Tropical<br>xerophytic<br>shrubland | Temperate conifer<br>forest (38%),<br>Tropical<br>xerophytic<br>shrubland (62%) |

|                               |           |           |            |    |     |     |                               |  |
|-------------------------------|-----------|-----------|------------|----|-----|-----|-------------------------------|--|
| Mumba_<br>U_VI_A              |           |           |            |    |     |     |                               | Temperate conifer forest (38%),<br>Tropical xerophytic shrubland (62%)   |
|                               | 15 (0)    | 804 (24)  | 1514 (353) | 57 | 69  | 63  | Tropical xerophytic shrubland |  |
| Mumba_<br>VI_B                |           |           |            |    |     |     |                               | Tropical xerophytic shrubland (100%)   |
|                               | 19 (0)    | 864 (34)  | 1514 (353) | 86 | 153 | 120 | Tropical xerophytic shrubland |  |
| Panga_ya<br>_Saidi_17         |           |           |            |    |     |     |                               | Tropical deciduous forest/woodland (28%), Tropical savanna (48%), Tropical xerophytic shrubland (24%)            |
|                               | 24 (0)    | 1152 (45) | 143 (84)   | 65 | 80  | 73  | Tropical savanna              |  |
| Panga_ya<br>_Saidi_18         |           |           |            |    |     |     |                               | Tropical xerophytic shrubland (100%)   |
|                               | 24 (0)    | 996 (42)  | 143 (84)   | 67 | 86  | 77  | Tropical xerophytic shrubland |  |
| Panga_ya<br>_Saidi_19         |           |           |            |    |     |     |                               | Tropical xerophytic shrubland (100%)   |
|                               | 24 (0)    | 996 (42)  | 143 (84)   | 67 | 86  | 77  | Tropical xerophytic shrubland |  |
| Enkapune<br>_ya_Muto<br>_RBL4 |           |           |            |    |     |     |                               | Temperate conifer forest (37%), Warm mixed forest (63%)  |
|                               | 13 (1)    | 1118 (69) | 1960 (386) | 43 | 45  | 45  | Warm mixed forest             |  |
| Fincha<br>Habera<br>8_10      |           |           |            |    |     |     |                               | Steppe tundra (204), Temperate conifer forest (31), Temperate sclerophyll woodland (15), Warm mixed forest (120) |
|                               | 9 (1)     | 1150 (21) | 2712 (613) | 27 | 34  | 31  | Steppe tundra                 |  |
| Fincha<br>Habera<br>8_11      |           |           |            |    |     |     |                               | Steppe tundra (55%), Temperate conifer forest (9%), Temperate sclerophyll woodland (4%), Warm mixed forest (32%) |
|                               | 9.0 (1)   | 1150 (21) | 2712 (613) | 27 | 34  | 31  | Steppe tundra                 |  |
| Fincha<br>Habera<br>8_8       |           |           |            |    |     |     |                               | Steppe tundra (55%), Temperate conifer forest (9%), Temperate sclerophyll woodland (4%), Warm mixed forest (32%) |
|                               | 9.0 (0.8) | 1150 (21) | 2712 (613) | 27 | 34  | 31  | Steppe tundra                 |  |
| Fincha<br>Habera<br>8_9       |           |           |            |    |     |     |                               | Steppe tundra (55%), Temperate conifer forest (9%), Temperate  |
|                               | 9.0 (0.8) | 1150 (21) | 2712 (613) | 27 | 34  | 31  | Steppe tundra                 |  |



|  |        |              |               |    |    |    |                                     |   |
|--|--------|--------------|---------------|----|----|----|-------------------------------------|---|
|  |        |              |               |    |    |    |                                     | sclerophyll<br>woodland (4%),<br>Warm mixed<br>forest (32%)   |
| Fincha<br>Habera 9                     |        |              |               |    |    |    |                                     | Steppe tundra<br>(55%), Temperate<br>conifer forest<br>(9%), Temperate<br>sclerophyll<br>woodland (4%),<br>Warm mixed<br>forest (32%) |
|  | 10 (1) | 1144<br>(21) | 2712<br>(613) | 33 | 42 | 38 | Steppe<br>tundra                    |   |
| Kiese<br>II_18                         |        |              |               |    |    |    |                                     | Temperate conifer<br>forest (2%),<br>Tropical<br>xerophytic<br>shrubland  |
|  | 16 (0) | 865<br>(22)  | 1397<br>(232) | 38 | 39 | 39 | Tropical<br>xerophytic<br>shrubland | Tropical<br>xerophytic<br>shrubland (98%)   |
| Kiese<br>II_19                         |        |              |               |    |    |    |                                     | Temperate conifer<br>forest (2%),<br>Tropical<br>xerophytic<br>shrubland  |
|  | 16 (0) | 865<br>(22)  | 1397<br>(232) | 31 | 46 | 39 | Tropical<br>xerophytic<br>shrubland | Tropical<br>xerophytic<br>shrubland (98%)   |
| Kiese<br>II_20                         |        |              |               |    |    |    |                                     | Temperate conifer<br>forest (2%),<br>Tropical<br>xerophytic<br>shrubland  |
|  | 16 (0) | 928<br>(21)  | 1397<br>(232) | 42 | 45 | 44 | Tropical<br>xerophytic<br>shrubland | Tropical<br>xerophytic<br>shrubland (98%)   |
| Kiese<br>II_21                         |        |              |               |    |    |    |                                     | Temperate conifer<br>forest (2%),<br>Tropical<br>xerophytic<br>shrubland  |
|  | 16 (0) | 911<br>(20)  | 1397<br>(232) | 43 | 46 | 45 | Tropical<br>xerophytic<br>shrubland | Tropical<br>xerophytic<br>shrubland (98%)   |
| LaasGeel<br>_SU_711                    |        |              |               |    |    |    |                                     | Open conifer<br>woodland (15%),<br>Tropical<br>xerophytic<br>shrubland  |
|  | 18 (1) | 396<br>(56)  | 1113<br>(189) | 40 | 42 | 42 | Tropical<br>xerophytic<br>shrubland | Tropical<br>xerophytic<br>shrubland (85%)   |
| Lukenya<br>HillGvJm<br>22_F170_<br>205 |        |              |               |    |    |    |                                     | Temperate conifer<br>forest (332),<br>Tropical<br>xerophytic<br>shrubland (34)  |
|  | 14 (1) | 934<br>(67)  | 1547<br>(149) | 25 | 32 | 29 | Temperate<br>conifer forest         |   |
| Magubike<br>_MSA                       |        |              |               |    |    |    |                                     | Temperate conifer<br>forest (88%),<br>Tropical<br>xerophytic<br>shrubland (12%)   |
|  | 16 (1) | 955<br>(86)  | 1365<br>(394) | 35 | 48 | 42 | Temperate<br>conifer forest         |   |
| Mochena<br>Borago_L<br>owerT           |        |              |               |    |    |    |                                     | Temperate conifer<br>forest (100%)  |
|  | 15 (0) | 1282<br>(19) | 1638<br>(345) | 49 | 50 | 50 | Temperate<br>conifer forest         |   |
| Mochena<br>Borago_R<br>Group           |        |              |               |    |    |    |                                     | Temperate conifer<br>forest (98%),<br>Warm mixed<br>forest (2%)   |
|  | 14 (0) | 1297<br>(19) | 1638<br>(345) | 36 | 43 | 40 | Temperate<br>conifer forest         |   |

|                              |        |               |               |     |     |     |                                     |  |
|------------------------------|--------|---------------|---------------|-----|-----|-----|-------------------------------------|--|
| Mochena<br>Borago_S<br>Group | 15 (0) | 1270<br>(19)  | 1638<br>(345) | 43  | 46  | 45  | Temperate<br>conifer forest         | Temperate conifer<br>forest (100%)   |
| Mochena<br>Borago_<br>UpperT | 15 (0) | 1274<br>(19)  | 1638<br>(345) | 45  | 49  | 48  | Temperate<br>conifer forest         | Temperate conifer<br>forest (100%)   |
| Nasera_1<br>2_17             | 16 (0) | 778<br>(41)   | 1710<br>(289) | 53  | 58  | 56  | Temperate<br>conifer forest         | Temperate conifer<br>forest (71%),<br>Tropical<br>xerophytic<br>shrubland (29%)                        |
| Nasera_6<br>_7               | 16 (0) | 770<br>(41)   | 1710<br>(289) | 50  | 58  | 54  | Tropical<br>xerophytic<br>shrubland | Temperate conifer<br>forest (16%),<br>Tropical<br>xerophytic<br>shrubland (86%)                        |
| Nasera_8/<br>9_11            | 16 (0) | 770<br>(41)   | 1710<br>(289) | 50  | 58  | 54  | Tropical<br>xerophytic<br>shrubland | Temperate conifer<br>forest (16%),<br>Tropical<br>xerophytic<br>shrubland (86%)                        |
| Shurmai_<br>MSA              | 15 (2) | 1165<br>(109) | 1443<br>(374) | 39  | 50  | 45  | Temperate<br>conifer forest         | Steppe tundra<br>(2%), Temperate<br>conifer forest<br>(55%), Tropical<br>xerophytic<br>shrubland (43%) |
| Abdur_N<br>_C_S              | 25 (2) | 658<br>(99)   | 773<br>(798)  | 118 | 132 | 125 | Tropical<br>xerophytic<br>shrubland | Open conifer<br>woodland (18%),<br>Tropical<br>xerophytic<br>shrubland (82%)                           |
| AdumaA<br>1                  | 23 (1) | 620<br>(75)   | 723<br>(166)  | 80  | 100 | 90  | Tropical<br>xerophytic<br>shrubland | Tropical<br>xerophytic<br>shrubland (100%)   |
| AdumaA<br>4C                 | 23 (1) | 620<br>(75)   | 723<br>(166)  | 80  | 100 | 90  | Tropical<br>xerophytic<br>shrubland | Tropical<br>xerophytic<br>shrubland (100%)   |
| AdumaA<br>5Ex                | 23 (1) | 620<br>(75)   | 723<br>(166)  | 80  | 100 | 90  | Tropical<br>xerophytic<br>shrubland | Tropical<br>xerophytic<br>shrubland (100%)   |
| AdumaA<br>5ExSurf            | 23 (1) | 620<br>(75)   | 723<br>(166)  | 80  | 100 | 90  | Tropical<br>xerophytic<br>shrubland | Tropical<br>xerophytic<br>shrubland (100%)   |
| AdumaA<br>8                  | 23 (1) | 620<br>(75)   | 723<br>(166)  | 80  | 100 | 90  | Tropical<br>xerophytic<br>shrubland | Tropical<br>xerophytic<br>shrubland (100%)   |
| AdumaA<br>8AC                | 23 (1) | 620<br>(75)   | 723<br>(166)  | 80  | 100 | 90  | Tropical<br>xerophytic<br>shrubland | Tropical<br>xerophytic<br>shrubland (100%)   |
| AdumaA<br>8AG                | 23 (1) | 620<br>(75)   | 723<br>(166)  | 80  | 100 | 90  | Tropical<br>xerophytic<br>shrubland | Tropical<br>xerophytic<br>shrubland (100%)   |

|                                  |        |               |               |     |     |     |                                      |  |
|----------------------------------|--------|---------------|---------------|-----|-----|-----|--------------------------------------|--|
| AdumaA<br>8ASurf                 | 23 (1) | 620<br>(75)   | 723<br>(166)  | 80  | 100 | 90  | Tropical<br>xerophytic<br>shrubland  | Tropical<br>xerophytic<br>shrubland (100%)   |
| AdumaA<br>8B                     | 23 (1) | 620<br>(75)   | 723<br>(166)  | 80  | 100 | 90  | Tropical<br>xerophytic<br>shrubland  | Tropical<br>xerophytic<br>shrubland (100%)   |
| EyasiShor<br>e_77_81             | 19 (0) | 713<br>(19)   | 1508<br>(356) | 91  | 132 | 112 | Tropical<br>xerophytic<br>shrubland  | Tropical<br>xerophytic<br>shrubland (100%)   |
| EyasiShor<br>e_W_insit<br>u      | 19 (0) | 713<br>(19)   | 1508<br>(356) | 91  | 132 | 112 | Tropical<br>xerophytic<br>shrubland  | Tropical<br>xerophytic<br>shrubland (100%)   |
| Gademott<br>a_ETH72<br>_1        | 13 (1) | 1368<br>(48)  | 1898<br>(316) | 172 | 274 | 223 | Warm mixed<br>forest                 | Temperate conifer<br>forest (46%),<br>Warm mixed<br>forest (54%)   |
| Gademott<br>a_ETH72<br>_6        | 13 (1) | 1368<br>(48)  | 1898<br>(316) | 172 | 274 | 223 | Warm mixed<br>forest                 | Temperate conifer<br>forest (46%),<br>Warm mixed<br>forest (54%)   |
| KapForm<br>_Koimilot<br>GnJh74_1 | 18 (1) | 977<br>(86)   | 1428<br>(369) | 198 | 237 | 218 | Temperate<br>conifer forest          | Temperate conifer<br>forest (61%),<br>Warm mixed<br>forest (39%)   |
| KapForm<br>_Koimilot<br>GnJh74_2 | 18 (1) | 977<br>(86)   | 1428<br>(369) | 198 | 237 | 218 | Temperate<br>conifer forest          | Temperate conifer<br>forest (61%),<br>Warm mixed<br>forest (39%)   |
| KapForm<br>_SSRS                 | 19 (1) | 947<br>(83)   | 1319<br>(335) | 198 | 237 | 218 | Tropical<br>xerophytic<br>shrubland  | Temperate conifer<br>forest (42%),<br>Tropical<br>xerophytic<br>shrubland (58%)  |
| Karungu_<br>A3Ex                 | 18 (1) | 1385<br>(108) | 1254<br>(125) | 42  | 115 | 79  | Tropical<br>xerophytic<br>shrubland  | Temperate conifer<br>forest (17%),<br>Tropical<br>xerophytic<br>shrubland (83%)  |
| Lukenya<br>Hill_GvJ<br>m46       | 13 (1) | 1064<br>(63)  | 1547<br>(149) | 21  | 27  | 24  | Temperate<br>conifer forest          | Temperate conifer<br>forest (17%),<br>Tropical<br>xerophytic<br>shrubland (83%)  |
| Marmone<br>t<br>Drift_H2         | 10 (1) | 1103<br>(110) | 2215<br>(341) | 89  | 205 | 147 | Temperate<br>sclerophyll<br>woodland | Steppe tundra<br>(28%), Temperate<br>conifer forest<br>(20%), Temperate<br>sclerophyll<br>woodland (43%),<br>Warm mixed<br>forest (9%) |
| Marmone<br>t<br>Drift_H4         | 14 (1) | 937<br>(114)  | 2215<br>(341) | 90  | 130 | 110 | Temperate<br>conifer forest          | Temperate conifer<br>forest (64%),<br>Tropical   |

|                                    |        |               |               |     |     |     |                                     |  |
|------------------------------------|--------|---------------|---------------|-----|-----|-----|-------------------------------------|--|
|                                    |        |               |               |     |     |     |                                     | xerophytic<br>shrubland (18%),<br>Warm mixed<br>forest (18%)   |
| Marmone<br>t<br>Drift_H5           | 13 (1) | 1173<br>(113) | 2215<br>(341) | 90  | 98  | 94  | Temperate<br>conifer forest         | Temperate conifer<br>forest (68%),<br>Tropical<br>xerophytic<br>shrubland (20%),<br>Warm mixed<br>forest (17%) |
| Marmone<br>t<br>Drift_I_b<br>ottom | 12 (1) | 1368<br>(113) | 2215<br>(341) | 205 | 257 | 231 | Warm mixed<br>forest                | Temperate conifer<br>forest (40%),<br>Warm mixed<br>forest (60%)   |
| Ologesai<br>lie_BOK1<br>E          | 17 (2) | 770<br>(108)  | 1360<br>(381) | 295 | 320 | 308 | Tropical<br>xerophytic<br>shrubland | Temperate conifer<br>forest (16%),<br>Tropical<br>xerophytic<br>shrubland (84%)                                |
| Ologesai<br>lie_BOK2               | 17 (2) | 770<br>(108)  | 1360<br>(381) | 295 | 320 | 308 | Tropical<br>xerophytic<br>shrubland | Temperate conifer<br>forest (16%),<br>Tropical<br>xerophytic<br>shrubland (84%)                                |
| Ologesai<br>lie_BOK3               | 17 (2) | 770<br>(108)  | 1360<br>(381) | 295 | 320 | 308 | Tropical<br>xerophytic<br>shrubland | Temperate conifer<br>forest (16%),<br>Tropical<br>xerophytic<br>shrubland (84%)                                |
| Ologesai<br>lie_BOK4               | 17 (2) | 675<br>(112)  | 1360<br>(381) | 288 | 301 | 295 | Tropical<br>xerophytic<br>shrubland | Temperate conifer<br>forest (64%),<br>Tropical<br>xerophytic<br>shrubland (36%)                                |
| Omo_AH<br>S1-5                     | 23 (0) | 582<br>(48)   | 450<br>(118)  | 193 | 201 | 197 | Tropical<br>xerophytic<br>shrubland | Tropical<br>xerophytic<br>shrubland (100%)   |
| Omo_AH<br>S6_8                     | 23 (0) | 582<br>(48)   | 450<br>(118)  | 193 | 201 | 197 | Tropical<br>xerophytic<br>shrubland | Tropical<br>xerophytic<br>shrubland (100%)   |
| Omo_BN<br>S_L3                     | 24 (0) | 534<br>(48)   | 450<br>(118)  | 96  | 111 | 104 | Tropical<br>xerophytic<br>shrubland | Desert (13%),<br>Tropical<br>xerophytic<br>shrubland (87%)   |
| Omo_KH<br>S2/3                     | 23 (0) | 582<br>(48)   | 450<br>(118)  | 193 | 201 | 197 | Tropical<br>xerophytic<br>shrubland | Tropical<br>xerophytic<br>shrubland (100%)   |
| VictoriaC<br>abera_2               | 17 (0) | 657<br>(25)   | 1765<br>(349) | 70  | 91  | 81  | Tropical<br>xerophytic<br>shrubland | Tropical<br>xerophytic<br>shrubland (100%)   |
| VictoriaC<br>abera_2a              | 17 (0) | 657<br>(25)   | 1765<br>(349) | 70  | 91  | 81  | Tropical<br>xerophytic<br>shrubland | Tropical<br>xerophytic<br>shrubland (100%)   |

|                              |        |              |               |     |     |     |                                     |   |
|------------------------------|--------|--------------|---------------|-----|-----|-----|-------------------------------------|---|
| VictoriaC<br>abera_3         | 17 (0) | 657<br>(25)  | 1765<br>(349) | 70  | 91  | 81  | Tropical<br>xerophytic<br>shrubland | Tropical<br>xerophytic<br>shrubland (100%)  |
| VictoriaC<br>abera_4         | 18 (0) | 613<br>(23)  | 1765<br>(349) | 79  | 91  | 86  | Tropical<br>xerophytic<br>shrubland | Tropical<br>xerophytic<br>shrubland (100%)  |
| AdumaV<br>P1/1               | 23 (1) | 620<br>(75)  | 723<br>(166)  | 80  | 100 | 90  | Tropical<br>xerophytic<br>shrubland | Tropical<br>xerophytic<br>shrubland (100%)  |
| AdumaV<br>P1/3               | 23 (1) | 620<br>(75)  | 723<br>(166)  | 80  | 100 | 90  | Tropical<br>xerophytic<br>shrubland | Tropical<br>xerophytic<br>shrubland (100%)  |
| EyasiShor<br>e_N_surf<br>ace | 19 (0) | 713<br>(19)  | 1508<br>(356) | 91  | 132 | 112 | Tropical<br>xerophytic<br>shrubland | Tropical<br>xerophytic<br>shrubland (100%)  |
| EyasiShor<br>e_W_surf        | 19 (0) | 713<br>(19)  | 1508<br>(356) | 91  | 132 | 112 | Tropical<br>xerophytic<br>shrubland | Tropical<br>xerophytic<br>shrubland (100%)  |
| KapedoT<br>uffs              | 23 (1) | 751<br>(91)  | 1106<br>(267) | 120 | 135 | 128 | Tropical<br>xerophytic<br>shrubland | Temperate conifer<br>forest (2%),<br>Tropical<br>deciduous<br>forest/woodland<br>(15%), Tropical<br>xerophytic<br>shrubland (83%) |
| Karungu_<br>Kisaaka_<br>Main | 16 (1) | 1499<br>(93) | 1231<br>(116) | 42  | 56  | 49  | Temperate<br>conifer forest         | Temperate conifer<br>forest (70%),<br>Tropical<br>xerophytic<br>shrubland (30%)   |
| Karungu_<br>Kisaaka_<br>ZTG  | 18 (1) | 1374<br>(97) | 1230<br>(116) | 42  | 115 | 79  | Tropical<br>xerophytic<br>shrubland | Temperate conifer<br>forest (12%),<br>Tropical<br>xerophytic<br>shrubland (88%)   |
| MalewaG<br>orge              | 15 (1) | 991<br>(182) | 2240<br>(388) | 240 | 240 | 240 | Temperate<br>conifer forest         | Temperate conifer<br>forest (74%),<br>Tropical<br>xerophytic<br>shrubland (26%)   |
| Ndutu_14                     | 17 (0) | 1089<br>(37) | 1527<br>(209) | 220 | 240 | 230 | Tropical<br>xerophytic<br>shrubland | Tropical<br>xerophytic<br>shrubland (100%)  |
| Ndutu_72                     | 17 (0) | 1089<br>(37) | 1527<br>(209) | 220 | 240 | 230 | Tropical<br>xerophytic<br>shrubland | Tropical<br>xerophytic<br>shrubland (100%)  |
| Omo_AH<br>Ssurface           | 23 (0) | 582<br>(48)  | 450<br>(118)  | 193 | 201 | 197 | Tropical<br>xerophytic<br>shrubland | Tropical<br>xerophytic<br>shrubland (100%)  |
| Omo_BN<br>S<50m              | 24 (0) | 534<br>(48)  | 450<br>(118)  | 96  | 111 | 104 | Tropical<br>xerophytic<br>shrubland | Desert (13%),<br>Tropical<br>xerophytic<br>shrubland (87%)  |

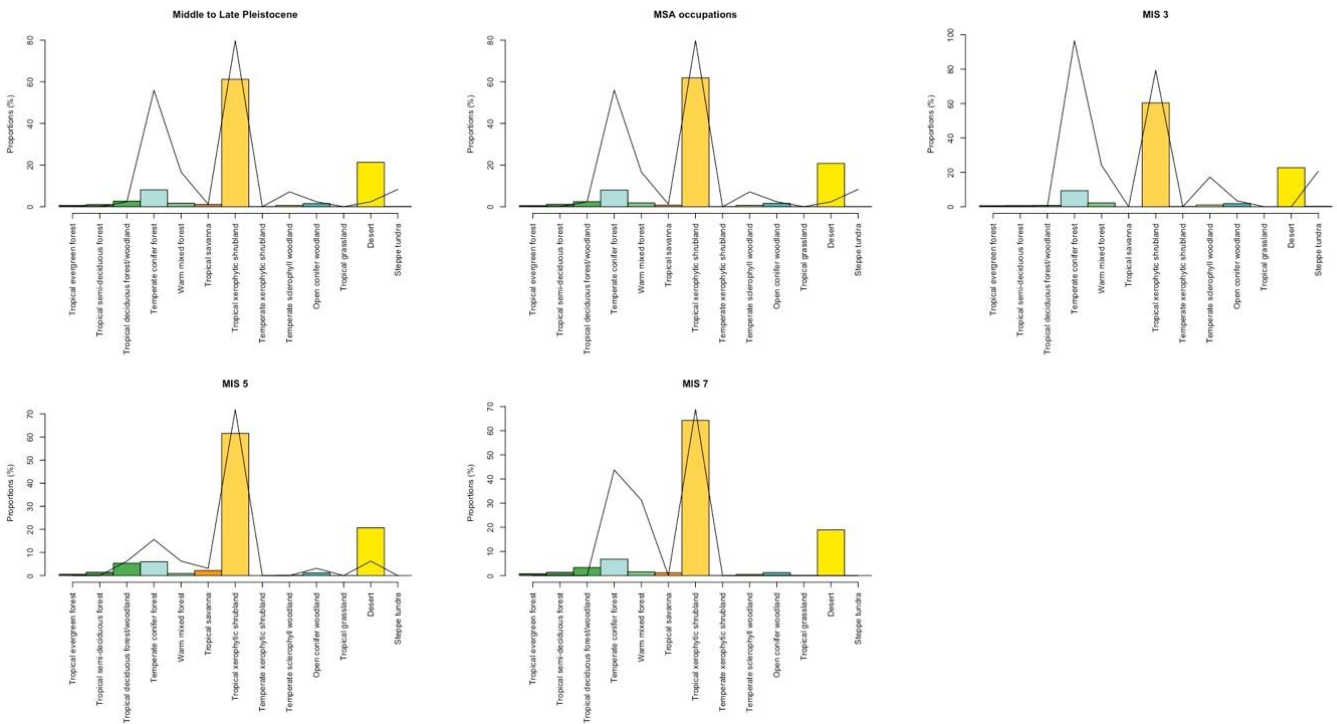
|                        |        |               |               |     |     |     |                                     |  |
|------------------------|--------|---------------|---------------|-----|-----|-----|-------------------------------------|--|
| Omo_KH<br>SNgully      | 23 (0) | 582<br>(48)   | 450<br>(118)  | 193 | 201 | 197 | Tropical<br>xerophytic<br>shrubland | Tropical<br>xerophytic<br>shrubland (100%) |
| Omo_KH<br>SNMKen<br>ya | 23 (0) | 582<br>(48)   | 450<br>(118)  | 193 | 201 | 197 | Tropical<br>xerophytic<br>shrubland | Tropical<br>xerophytic<br>shrubland (100%) |
| Omo_KH<br>SSgully      | 23 (0) | 582<br>(48)   | 450<br>(118)  | 193 | 201 | 197 | Tropical<br>xerophytic<br>shrubland | Tropical<br>xerophytic<br>shrubland (100%) |
| Rusinga_<br>Nyamita    | 16 (1) | 1593<br>(134) | 1226<br>(114) | 42  | 56  | 49  | Temperate<br>conifer forest         | Temperate conifer<br>forest (100%)         |

**Supplementary Table S2.** Proportions of biomes available across eastern Africa (P1) throughout the Middle to Late Pleistocene (full date range of the assemblages from 21-320 kya), MSA occupational phases, and Marine Isotope Stage (MIS) 3, MIS 5 and MIS 7, compared to the proportions of biomes available at MSA occupations (P2). Grey cells represent the biomes available in eastern Africa that were not inhabited by MSA populations during that period. Tropical evergreen forest = 1, Tropical semi-deciduous forest = 2, Tropical deciduous forest/woodland = 3, Temperate conifer forest = 4, Warm mixed forest = 5, Tropical savanna = 6, Tropical xerophytic shrubland = 7, Temperate xerophytic shrubland = 8, Temperate sclerophyll woodland = 9, Open conifer woodland = 10, Tropical grassland = 11, Desert = 12, Steppe tundra = 13.

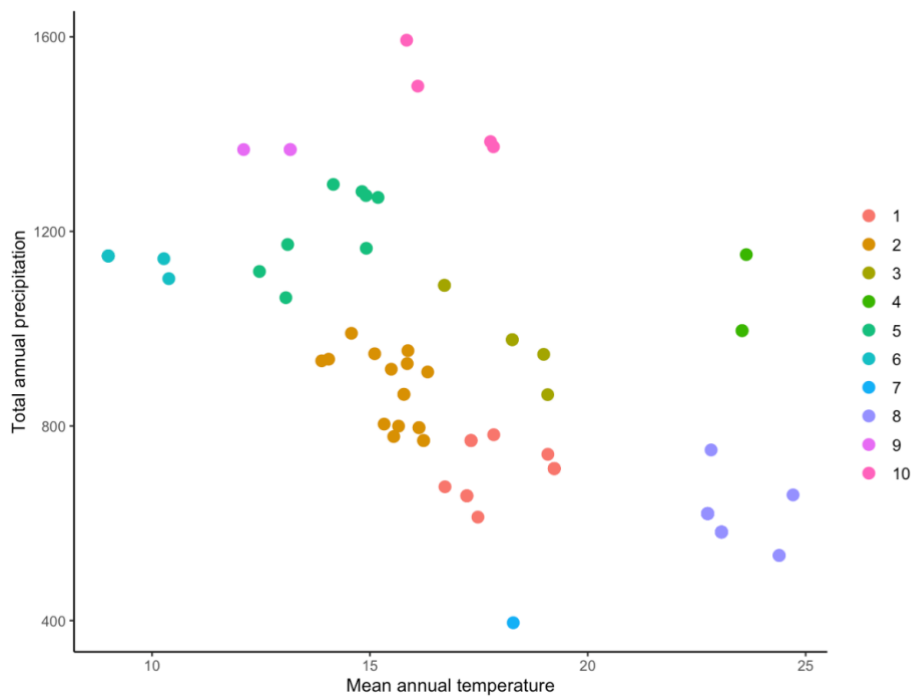
|    | Full date range |       | MSA occupations |       | MIS 3 |       | MIS 5 |       | MIS 7 |       |
|----|-----------------|-------|-----------------|-------|-------|-------|-------|-------|-------|-------|
|    | P1              | P2    | P1              | P2    | P1    | P2    | P1    | P2    | P1    | P2    |
| 1  | 0.006           |       | 0.005           |       | 0.60  |       | 0.58  |       | 0.74  |       |
| 2  | 0.010           |       | 0.011           |       | 0.68  |       | 1.45  |       | 1.36  |       |
| 3  | 0.027           | 0.024 | 0.025           | 0.024 | 0.78  |       | 0.053 | 0.063 | 3.31  |       |
| 4  | 0.081           | 0.560 | 0.080           | 0.560 | 0.094 | 0.966 | 0.060 | 0.156 | 0.068 | 0.438 |
| 5  | 0.017           | 0.167 | 0.019           | 0.167 | 0.022 | 0.241 | 0.009 | 0.063 | 0.015 | 0.313 |
| 6  | 0.012           | 0.012 | 0.008           | 0.012 | 0.02  |       | 0.022 | 0.031 | 1.16  |       |
| 7  | 0.612           | 0.798 | 0.619           | 0.798 | 0.603 | 0.793 | 0.616 | 1.000 | 0.643 | 0.688 |
| 8  | 0.001           |       | 0.001           |       | 0.15  |       | 0.01  |       | 0.05  |       |
| 9  | 0.006           | 0.071 | 0.006           | 0.071 | 0.010 | 0.172 | 0.16  |       | 0.51  |       |
| 10 | 0.015           | 0.024 | 0.016           | 0.024 | 0.019 | 0.034 | 0.012 | 0.031 | 1.22  |       |
| 11 | 0.001           |       | 0.001           |       | 0.02  |       | 0.05  |       | 0.11  |       |
| 12 | 0.213           | 0.024 | 0.208           | 0.024 | 0.227 |       | 0.207 | 0.063 | 18.92 |       |
| 13 | 0.001           | 0.083 | 0.001           | 0.083 | 0.002 | 0.207 | 0.00  |       | 0.00  |       |

**Supplementary Table S3.** Results from two sample proportion tests, comparing the proportions of biomes available across the region and the biomes occupied during that period (see Supplementary Table S2 and Figure S2). Z values and p-values are reported here to demonstrate the strength of effects and where there are significant differences at  $p < 0.05$  (\*) or  $p < 0.01$  (\*\*). Grey cells represent the biomes available in eastern Africa that were not inhabited by MSA hominins during that period. Tropical deciduous forest/woodland = 1, Temperate conifer forest = 2, Warm mixed forest = 3, Tropical savanna = 4, Tropical xerophytic shrubland = 5, Temperate sclerophyll woodland = 6, Open conifer woodland = 7, Desert = 8, Steppe tundra = 9.

|   | Full date range |         | MSA occupations |         | MIS 3  |         | MIS 5  |          | MIS 7 |         |
|---|-----------------|---------|-----------------|---------|--------|---------|--------|----------|-------|---------|
|   | Z               | p       | Z               | p       | Z      | p       | Z      | p        | Z     | p       |
| 1 | 0.000           | 1.000   | 0.000           | 1       |        |         | 0.000  | 1        |       |         |
| 2 | 15.882          | <0.01** | 15.974          | <0.01** | 15.764 | <0.01** | 1.918  | 0.055    | 5.368 | <0.01** |
| 3 | 10.186          | <0.01** | 9.631           | <0.01** | 7.336  | <0.01** | 2.294  | 0.022*   | 8.676 | <0.01** |
| 4 | 0.000           | 1.000   | 0.000           | 1       |        |         | 0.000  | 1        |       |         |
| 5 | 3.38            | <0.01** | 3.257           | <0.01** | 1.895  | 0.058   | 3.574  | <0.001** | 0.113 | 0.91    |
| 6 | 7.025           | <0.01** | 6.642           | <0.01** | 7.843  | <0.01** |        |          |       |         |
| 7 | 0.184           | 0.854   | 0.131           | 0.896   | 0.000  | 1       | 0.204  | 0.684    |       |         |
| 8 | -4.104          | <0.01** | -4.030          | <0.01** |        |         | -1.794 | 0.073    |       |         |
| 9 | 18.626          | <0.01** | 21.497          | <0.01** | 20.208 | <0.01** |        |          |       |         |



**Supplementary Figure S1.** Proportion (expressed as a percentage) of biomes available across eastern African during the Middle to Late Pleistocene, for full date range of the assemblages (21-320 kya), MSA occupational phases and Marine Isotope Stage (MIS) 3, MIS 5 and MIS 7 (bars) with the percentage of biomes available at eastern African MSA occupations through time (lines).



**Supplementary Figure S2.** The k-means ( $n = 10$ ) clusters plotted against mean annual temperature ( $^{\circ}\text{C}$ ) and total annual precipitation (mm). The average silhouette method identified that ten was the optimal division of the data, and this value was used to cut the resulting dendrogram of the site.



## Supplementary Methods:

### S1. Palaeoreconstructions of shorelines

We used a global bathymetry model [2] with sea-level reconstructions from Spratt and Lisiecki [3] to predict the coastline for each thousand years. First, we cropped the bathymetry model to the extent of eastern Africa. To predict the palaeocoastline  $h$  at any time  $t$ , expressed relative to the present coastline  $h(t_p)$ , the equation outlined by Lambeck *et al.* [4] was employed:

$$h(t) = h(t_p) - \Delta\zeta(t)$$

where  $\Delta\zeta(t)$  is the sea level difference at  $t$  compared with the present. We mapped the coastline for each time slice onto the bathymetry model to produce a series of digital elevation models, stored in raster format in a raster stack.

### S2. Calculation of distance matrices

Following Blinkhorn and Grove [1], we produced a series of distance matrices to explore effects of age, distance in space, and geographic and environmental characteristics of the landscapes surrounding them on toolkit composition and raw material use. Here, we provide a basic description of each variable include in the matrix correlations, however further description and the data can be found in Blinkhorn and Grove [1].

Toolkit composition is representative by the presence/absence of 16 artefact categories within the assemblage. These are backed pieces/microliths, bipolar technology, blade technology, borers, burins, centripetal technology, core tools, denticulates, Levallois blade technology, Levallois flake technology, Levallois point technology, notched pieces, platform cores, point technology, retouched bifacial tools and scrapers. Raw material use was recorded as the presence/absences of 8 categories: cherts, quartz, obsidians, basalts, metamorphics, crypto-crystalline silica (CCS), other igneous and other sedimentary. Site types involved the designation between open-air sites or rock shelters and caves. Method of site investigation was recorded as either excavation or survey. We used the mid-age of each assemblage as a simple estimation of the date of each assemblage. Maximum and minimum dates were ascertained from the literature based on the errors of the dating, and the median was taken to represent the mid-age.

### Cost path:

To represent the physical distance between sites, we calculated the cost path as this is a more representative measure than the Euclidean or geodesic distance. Cost of movement over

heterogeneous landscapes was determined to predict the fastest routes between the eastern African sites. Cost path analyses calculate which route across a rough topographic landscape joins two points (sites) with the lowest accumulated cost. In this sense, whilst the shortest distance between two sites is a straight line (the Euclidean distance), it may be much faster, and therefore less costly, to walk around a mountain even if the distance is further.

We applied Tobler's Hiking Function which is often used cost-analyses to estimate the maximum hiking speed ( $s$ ) given the slope of the terrain ( $m$ ) [5]. It is preferred over just the slope as it accounts for anisotropy (the direction of movement has an impact on the cost) and nonlinear cost estimation (the cost of travel can change far more rapidly than the linear change from one input to the next). The maximum speed of off-path hiking (in km/h) is calculated as:

$$s = 6e^{-3.5|m+0.05|}$$

Tobler's Hiking function is not symmetric around 0, and this is because humans tend to walk fastest on gently downward slopes ( $m = -0.05$ ), where they can walk faster than on flat terrain ( $m = 0$ ). To compute a transition layer using the Hiking Function, we calculated the slope  $m$  of the terrain from the altitude  $z$  and the distance between cell centres  $d$  of each DEM for each pair of cells  $i$  and  $j$ . This was performed using the `gdistance` package in R [6], with major water bodies masked from the analysis.

$$m_{ij} = (z_j - z_i)/d_{ij}$$

The slope ( $m$ ) was then used to calculate the travel time  $T$  in hours of moving between cells of the DEM using the reciprocal of Tobler Hiking Function:

$$T = 0.6e^{3.5|m+0.05|}$$

Finally, a correction procedure was employed to consider the distance between cell centres, as when travelling with the same speed, a diagonal connection between cells takes longer to cross than a straight connection.

#### Altitude and roughness at 50km:

We sampled from the slope ( $m$ ) rasters at a 50km radius around each site to ascertain the mean and standard deviation of altitude of the logistical landscape each assemblage was situated in. We then transformed the slope ( $m$ ) raster into values of energy expenditure (Joules per metre per second for an

average 60kg person) following Minetti *et al.* [7]. This formula accounts for the fact that there are different energetic costs ( $cw$ ) associated with moving on flat ground vs 10° slopes compared to 10° and 20° slopes, despite the difference in slope being the same.

$$cw = 60 \cdot \left( (280.5m^5) - (58.7m^4) - (76.8m^3) + (51.9m^2) + (19.6m) + 2.5 \right)$$

We sampled from the resulting roughness rasters at a 50km radius around each occupation and took the mean and standard deviation.

### S3. Downscaling approaches

To capture climatic variation across the logistical landscape of each occupation, we decided to increase the climate model beyond its native 0.5° resolution. We tested two methods of downscaling – delta downscaling [8], the bias-correction method found by Beyer *et al.* [9] to perform best at minimising the difference between empirical data and the temperature and precipitation simulations [10], and simple bilinear interpolation. Delta downscaling calculates the differences between models present and past climates and applies them to modern observed datasets to correct biases in the simulated data [10]. In this way, the delta method assumes that present day local variation remains constant through time. Using the delta-method, we downscaled the data to 2.5' resolution (cells representing 4.625km) based on that of the modern data used, WorldClim version 2.1 (<https://www.worldclim.org/data/worldclim21.html>), and followed methods set out by Beyer *et al.* [9]. Alternatively, bilinear interpolation is a resampling method that disaggregates the climate model through distance weighted averaging of the four nearest cell values in order to estimate the value of a new cell. Whilst this method has been found to produce spatial artefacts [11], bilinear interpolation is commonly used in paleoclimate modelling to remap data due to its simplicity and lack of assumptions about the data. We disaggregated the model using bilinear interpolation at a factor of 12 to obtain cells representative of 4.625km resolution, matching that of the delta-downscaled data.

To test the effects of downscaling on our results, we ran the simple Mantel tests and the multiple matrix regressions on the bilinear interpolated and delta downscaled data, with sea-level estimates cropping both versions of the model according to the palaeocoastline, as well as the original climatic model at its raw resolution. As shown by Supplementary Methods S3 Tables S1-2, the simple Mantel tests return statistically significant results for the effects of both temperature and precipitation on toolkit composition and raw material use for all versions of the climate data, except for delta-downscaled precipitation on raw material.

We then performed multiple matrix regressions to understand the independent effects of the variables on toolkit composition and raw material use (Supplementary Methods S3 Tables S3-4). For toolkit composition, we found that all datasets returned significant correlations between raw material, site type, roughness and precipitation (bar delta-downscaled). For raw material, toolkit composition, simple age, cost path and roughness are consistently significant, and precipitation significant for the raw data and close to significant for the bilinear interpolated data. Overall, this suggests that the delta downscaling approach is the most conservative approach, whilst using the raw data is the least conservative. In light of these results, we have opted to employ the bilinear interpolation approach to downscaling that offers increased resolution than the raw dataset but requires fewer processing steps or assumptions about how representative modern day spatial variability in local climatic variation may be for the past.

**Supplementary Methods S3 Table S1.** Simple mantel tests of the effects of precipitation on toolkit composition, raw material use and the other variables. Statistical significance highlighted at  $p < 0.05$  (\*) or  $p < 0.01$  (\*\*). The Benjamini-Hochberg procedure was used to adjust p values.

|                     | Raw    |         |         | Bilinear |         |         | Delta       |         |         |
|---------------------|--------|---------|---------|----------|---------|---------|-------------|---------|---------|
|                     | coef   | p       | adj. p  | coef     | p       | adj. p  | coef        | p       | adj. p  |
| Toolkit composition | 0.1956 | 0.001** | 0.003** | 0.1972   | 0.001** | 0.003   | 0.155       | 0.001** | 0.004** |
| Raw material        | 0.1632 | 0.001** | 0.003** | 0.1587   | 0.001** | 0.003   | 0.0635      | 0.064   | 0.073   |
| Method              | 0.0742 | 0.059   | 0.067   | 0.0957   | 0.041*  | 0.047*  | 0.0887      | 0.051   | 0.068   |
| Site                | 0.113  | 0.002** | 0.004** | 0.0906   | 0.005** | 0.01**  | 0.0835      | 0.007** | 0.013*  |
| Simple age          | 0.0419 | 0.163   | 0.163   | 0.0311   | 0.207   | 0.207   | -<br>0.0342 | 0.717   | 0.717   |
| Cost path           | 0.121  | 0.003** | 0.005** | 0.1127   | 0.006** | 0.001** | 0.2491      | 0.001** | 0.004** |
| Altitude            | 0.2128 | 0.001** | 0.003** | 0.2071   | 0.001** | 0.003** | 0.1352      | 0.008** | 0.013*  |
| Energy              | 0.1138 | 0.009** | 0.012*  | 0.1087   | 0.027*  | 0.036*  | 0.1560      | 0.004** | 0.011*  |

**Supplementary Methods S3 Table S2.** Simple mantel tests of the effects of temperature on toolkit composition, raw material use and the other variables. Statistical significance highlighted at  $p < 0.05$  (\*) or  $p < 0.01$  (\*\*). The Benjamini-Hochberg procedure was used to adjust p values.

|                     | Raw     |         |         | Bilinear |         |         | Delta  |         |         |
|---------------------|---------|---------|---------|----------|---------|---------|--------|---------|---------|
|                     | coef    | p       | adj. p  | coef     | p       | adj. p  | coef   | p       | adj. p  |
| Toolkit composition | 0.2365  | 0.001** | 0.001** | 0.2144   | 0.001** | 0.001** | 0.1998 | 0.001** | 0.001** |
| Raw material        | 0.1452  | 0.001** | 0.001** | 0.1532   | 0.001** | 0.001** | 0.171  | 0.001** | 0.001** |
| Method              | -0.0089 | 0.532   | 0.532   | 0.0077   | 0.433   | 0.433   | 0.041  | 0.219   | 0.219   |
| Site                | 0.1757  | 0.001** | 0.001** | 0.1568   | 0.001** | 0.001** | 0.1376 | 0.001** | 0.001** |
| Simple age          | 0.0519  | 0.12    | 0.137   | 0.0465   | 0.152   | 0.174   | 0.0734 | 0.092   | 0.105   |

|           |        |         |         |        |         |         |        |         |         |
|-----------|--------|---------|---------|--------|---------|---------|--------|---------|---------|
| Cost path | 0.2658 | 0.001** | 0.001** | 0.2637 | 0.001** | 0.001** | 0.1932 | 0.001** | 0.001** |
| Altitude  | 0.8094 | 0.001** | 0.001** | 0.8041 | 0.001** | 0.001** | 0.839  | 0.001** | 0.001** |
| Energy    | 0.5037 | 0.001** | 0.001** | 0.4687 | 0.001** | 0.001** | 0.4633 | 0.001** | 0.001** |

**Supplementary Methods S3 Table S3.** Multiple matrix regression results for toolkit composition. Statistical significance highlighted at  $p < 0.05$  (\*) or  $p < 0.01$  (\*\*).

|               | Raw     |         | Bilinear interpolation |         | Delta-downscaling |         |
|---------------|---------|---------|------------------------|---------|-------------------|---------|
|               | coef    | p       | coef                   | p       | coef              | p       |
| Raw material  | 0.149   | 0.001** | 0.1483                 | 0.001** | 0.155             | 0.001** |
| Method        | 0.0114  | 0.629   | 0.009                  | 0.698   | 0.0083            | 0.716   |
| Site type     | 0.0296  | 0.016*  | 0.0328                 | 0.018*  | 0.034             | 0.014*  |
| Simple Age    | 0.0157  | 0.702   | 0.0184                 | 0.668   | 0.019             | 0.68    |
| Cost path     | 0.0068  | 0.88    | 0.0172                 | 0.669   | 0.0102            | 0.806   |
| Altitude      | -0.1476 | 0.219   | -0.0896                | 0.473   | -0.0886           | 0.48    |
| Roughness     | 0.2652  | 0.003** | 0.2645                 | 0.004** | 0.2543            | 0.004** |
| Temperature   | 0.1335  | 0.082   | 0.0672                 | 0.298   | 0.0862            | 0.276   |
| Precipitation | 0.0909  | 0.031*  | 0.111                  | 0.02*   | 0.0855            | 0.066   |

**Supplementary Methods S3 Table S4.** Multiple matrix regression results for raw material. Statistical significance highlighted at  $p < 0.05$  (\*) or  $p < 0.01$  (\*\*).

|                     | Raw     |         | Bilinear interpolation |         | Delta-downscaling |         |
|---------------------|---------|---------|------------------------|---------|-------------------|---------|
|                     | coef    | p       | coef                   | p       | coef              | p       |
| Toolkit composition | 0.3139  | 0.001** | 0.3119                 | 0.001** | 0.3242            | 0.001** |
| Method              | 0.0353  | 0.1722  | 0.0351                 | 0.192   | 0.0379            | 0.164   |
| Site type           | -0.0056 | 0.727   | -0.006                 | 0.7     | -0.0075           | 0.6426  |
| Simple Age          | 0.1495  | 0.005** | 0.149                  | 0.007** | 0.1404            | 0.01**  |
| Cost path           | 0.2055  | 0.002** | 0.1991                 | 0.001** | 0.19              | 0.001** |
| Altitude            | 0.2646  | 0.064   | 0.2206                 | 0.106   | 0.0439            | 0.767   |
| Roughness           | -0.2319 | 0.012*  | -0.2286                | 0.017*  | -0.2              | 0.027*  |
| Temperature         | -0.0575 | 0.533   | -0.0108                | 0.896   | 0.1605            | 0.091   |
| Precipitation       | 0.1211  | 0.015*  | 0.1124                 | 0.053   | -0.0192366        | 0.737   |

#### S4. Logistic regressions of individual technologies on significant predictors

Following the multiple matrix regressions, we conducted further analyses on significant predictors of differences in toolkit composition (site type, energy, precipitation, and raw material) to determine which individual technologies were significantly influenced by those predictors. We conducted 16 independent logistic binary regressions (one for each technology); each regression controlled for the effects of all other variables except cost path, which due its derivation was only available as a distance matrix. To control for the effects of raw material on toolkit composition, which was originally

represented as a single distance matrix in our initial correlation analysis, we included the presence or absence of each raw material in each assemblage as a set of 8 independent variables (one for each raw material). Cost-path was excluded from the analysis as this variable is only available as a distance matrix, which are unsuitable for logistic regression analysis. Traditional logistic regression failed to converge, due to perfect (or quasi-) separation of multiple independent variables and the relatively small size of the dataset. To ensure convergence, we employed penalized maximum likelihood using the Jeffreys invariant prior using the R package brglm [12]. All results are summarised in Supplementary Methods S4 Table S1.

**Supplementary Methods S4 Table S1.** Each column represents a binary logistic regression of one technology on the full set of independent variables shown as rows in the table across all 84 assemblages. The table shows positive (+) and negative (-) effects of independent variables significant at  $p < 0.05$  (\*) or  $p < 0.01$  (\*\*). Blanks indicate non-significant relationships. Min Sample Size is the smaller of the total number of assemblages in which the technology is present or the total number of assemblages in which the technology is absent.

|                   | Backed_Microlith | BipolarTech | BladeTech | Borer | Burin | CentripetalTech | CoreTool | Denticulate | LevalloisBladeTech | LevalloisFlakeTech | LevalloisPointTech | Notch | PlatformCore | PointTech | RTBifacial | Scraper |   |   |
|-------------------|------------------|-------------|-----------|-------|-------|-----------------|----------|-------------|--------------------|--------------------|--------------------|-------|--------------|-----------|------------|---------|---|---|
| (Intercept)       |                  |             |           |       |       | +               | *        |             |                    |                    |                    |       |              |           |            | +       | * |   |
| Method            |                  |             |           |       |       |                 |          |             |                    |                    |                    |       |              |           |            |         |   |   |
| Site Type         | +                | *           | +         | *     |       |                 |          |             |                    | +                  | *                  |       |              |           |            |         |   |   |
| Simple age        |                  |             |           |       |       |                 | +        | *           |                    | +                  | *                  |       |              |           |            |         |   |   |
| Basalts           |                  |             |           | -     | **    |                 |          |             |                    |                    |                    | -     | *            |           |            |         |   |   |
| Cherts            |                  |             |           |       |       |                 |          |             |                    |                    |                    |       |              |           |            |         |   |   |
| CCS               |                  |             |           | +     | *     |                 |          |             |                    |                    |                    |       |              |           |            |         |   |   |
| Obsidians         |                  |             | +         | **    | +     | **              | +        | *           |                    |                    | +                  | **    | +            | *         |            | +       | * |   |
| Metamorphics      |                  |             | +         | **    | +     | **              | +        | *           |                    |                    | +                  | *     |              |           | +          | *       |   |   |
| Quartzs           |                  |             |           |       |       |                 |          |             |                    |                    |                    |       | +            | *         |            |         |   |   |
| Other Igneous     |                  |             | +         | *     |       |                 |          |             |                    |                    |                    |       |              |           |            |         |   |   |
| Other Sedimentary |                  |             |           | +     | *     |                 |          |             |                    | -                  | **                 |       |              |           |            |         |   |   |
| Temperature       |                  |             |           |       |       |                 |          |             |                    |                    |                    |       |              |           |            |         |   |   |
| Precipitation     | -                | *           |           | -     | *     | -               | **       |             |                    |                    |                    |       | -            | *         |            |         | - | * |
| Altitude          |                  |             |           |       |       |                 |          |             |                    |                    |                    |       | -            | *         |            |         |   |   |
| Roughness         | -                | *           |           |       |       |                 |          |             | -                  | *                  | -                  | *     |              |           |            |         |   |   |
| Min Sample Size   | 32               | 35          | 26        | 32    | 14    | 29              | 37       | 15          | 10                 | 17                 | 19                 | 33    | 40           | 27        | 15         | 21      |   |   |

## References

- [1] Blinkhorn, J. & Grove, M. Explanations of variability in Middle Stone Age stone tool assemblage composition and raw material use in Eastern Africa. *J. Archaeol. Anthropol. Sci.* 13(14), (2021). [10.1007/s12520-020-01250-8](https://doi.org/10.1007/s12520-020-01250-8)

- [2] The General Bathymetric Chart of the Oceans (GEBCO). Gridded Bathymetry Data. Available online at: [https://www.gebco.net/data\\_and\\_products/gridded\\_bathymetry\\_data/](https://www.gebco.net/data_and_products/gridded_bathymetry_data/) (2020).
- [3] Spratt, R. M. & Lisiecki, L. E. A Late Pleistocene sea level stack. *Clim. Past*, **12**, 1079–1092, (2016). [10.5194/cp-12-1079-2016](https://doi.org/10.5194/cp-12-1079-2016)
- [4] Lambeck, K., Purcell, A., Flemming, N. C., Vita-Finzi C., Alsharekh, A. M. & Bailey, G. N. Sea level and shoreline reconstructions for the Red Sea: Isostatic and tectonic considerations and implications for hominin migration out of Africa, *Quat. Sci. Rev.*, **30** (25–26), 3542–3574, (2011). [10.1016/j.quascirev.2011.08.008](https://doi.org/10.1016/j.quascirev.2011.08.008)
- [5] Tobler, W. *Three presentations on geographical analysis and modeling*. University of California, Santa Barbara, California, (1993).
- [6] van Etten, J. R package gdistance: Distances and routes on geographical grids, *J. Stat. Softw.* **76**(13),1-21. (2017). [10.18637/jss.v076.i13](https://doi.org/10.18637/jss.v076.i13)
- [7] Minetti, A. E., Moia, C., Roi, G. S., Susta, D. & Ferretti, G. Energy cost of walking and running at extreme uphill and downhill slopes, **93**(3), 1039–1046; [10.1152/jappphysiol.01177.2001](https://doi.org/10.1152/jappphysiol.01177.2001) (2002).
- [8] Maraun D. & Widmann, M. *Statistical Downscaling and Bias Correction for Climate Research*. Cambridge: Cambridge University Press, (2018).
- [9] Beyer, B., Krapp, M & Manica, A. An empirical evaluation of bias correction methods for palaeoclimate simulations. *Clim. Past* **16**, 1493–1508, (2020). [10.5194/cp-16-1493-2020](https://doi.org/10.5194/cp-16-1493-2020)
- [10] Krapp, M., Beyer, R. M., Edmundson, S. L., Valdes, P. J. & Manica, A. A statistics-based reconstruction of high-resolution global terrestrial climate for the last 800,000 years. *Sci. Data* **8**, 228, (2021). [10.1038/s41597-021-01009-3](https://doi.org/10.1038/s41597-021-01009-3)
- [11] Latombe, G. *et al.*, Comparison of spatial downscaling methods of general circulation model results to study climate variability during the Last Glacial Maximum, *Geosci. Model Dev.* **11**, 2563–2579, (2018). [10.5194/gmd-11-2563-2018](https://doi.org/10.5194/gmd-11-2563-2018)
- [12] Kosmidis, I. ‘brglm’: Bias reduction in binary-response Generalized Linear Models. CRAN: R Packages: <https://cran.r-project.org/web/packages/brglm2/brglm2.pdf> (2007).

Appendix 2: Supplementary Online Materials for ‘Testing inter-observer error under a collaborative research framework for studying lithic shape variability’ (Timbrell et al., 2022; Anth. Archae. Sci.)

**Supplementary Table S1.** Triangle and vertices data for the obj. models that were created for 3D printing.

| Model     | 1        | 2        | 3        | 4        | 5        | 6        |
|-----------|----------|----------|----------|----------|----------|----------|
| Triangles | 4739974  | 6511000  | 3979922  | 9021498  | 3658156  | 8977254  |
| Vertices  | 14219922 | 19533000 | 11939766 | 27064494 | 10974468 | 26931762 |

**Supplementary Table S2.** Tukey HSD results comparing artefact group means of principal components (PC) 1-3. Statistical significance is marked as  $p < 0.05$  (\*) and  $< 0.001$  (\*\*).

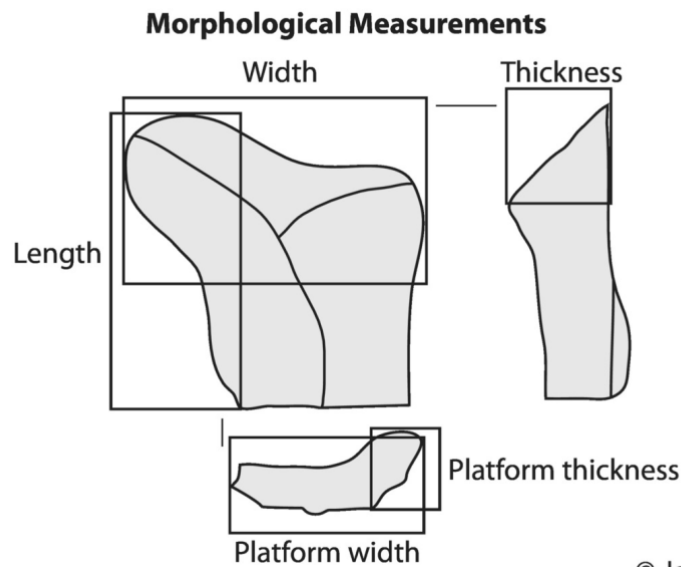
| Artefact number | PC1     | PC2     | PC3     |
|-----------------|---------|---------|---------|
| 2-1             | 0.000** | 0.292   | 0.000** |
| 3-1             | 0.000** | 0.000** | 0.017*  |
| 4-1             | 0.000** | 0.000** | 0.968   |
| 5-1             | 0.676   | 0.008*  | 0.999   |
| 6-1             | 0.000** | 0.000** | 0.980   |
| 3-2             | 0.000** | 0.000** | 0.000** |
| 4-2             | 0.000** | 0.000** | 0.000** |
| 5-2             | 0.000** | 0.000** | 0.000** |
| 6-2             | 0.000** | 0.000** | 0.000** |
| 4-3             | 0.000** | 0.000** | 0.000** |
| 5-3             | 0.000** | 0.000** | 0.101   |
| 6-3             | 0.000** | 0.000** | 0.007*  |
| 5-4             | 0.000** | 0.000** | 0.088   |
| 6-4             | 0.000** | 0.000** | 1       |
| 6-5             | 0.000** | 0.000** | 0.886   |

**Supplementary Table S3.** Coefficient of reliability (R) values for pair-wise combinations of assemblages using the first 3 PC scores, recorded by the single observer. For assemblage numbers and associated observer codes, see Table 1. All values have been rounded to 3 decimal places.

|              | Assemblage 1 | Assemblage 2 | Assemblage 3 | Assemblage 4 | Assemblage 5 |
|--------------|--------------|--------------|--------------|--------------|--------------|
| Assemblage 2 | 0.998        |              |              |              |              |
| Assemblage 3 | 0.998        | 0.998        |              |              |              |
| Assemblage 4 | 0.997        | 0.998        | 0.995        |              |              |

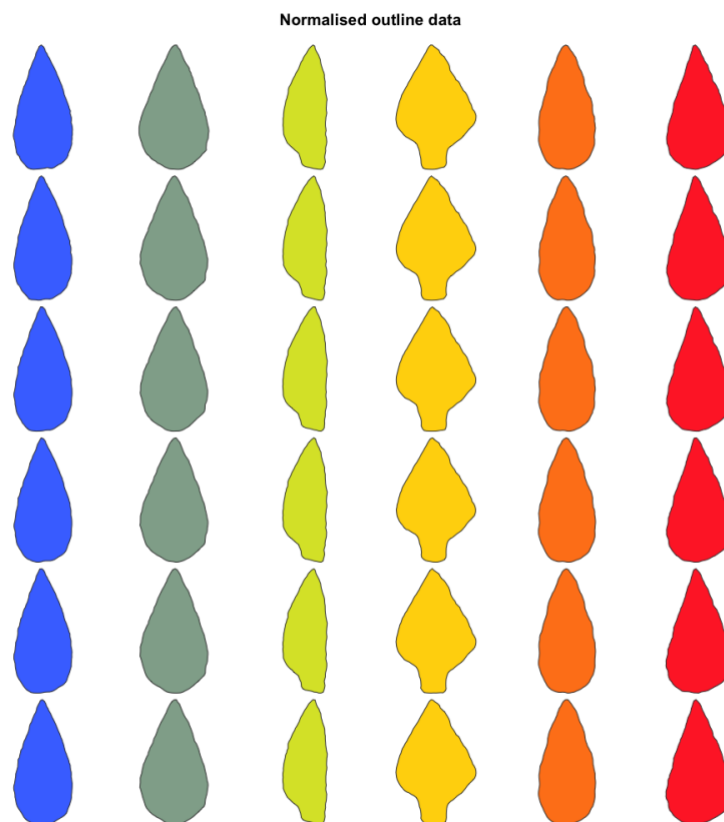


|              |       |       |       |       |       |
|--------------|-------|-------|-------|-------|-------|
| Assemblage 5 | 0.996 | 0.995 | 0.994 | 0.996 |       |
| Assemblage 6 | 0.998 | 0.997 | 0.999 | 0.995 | 0.995 |

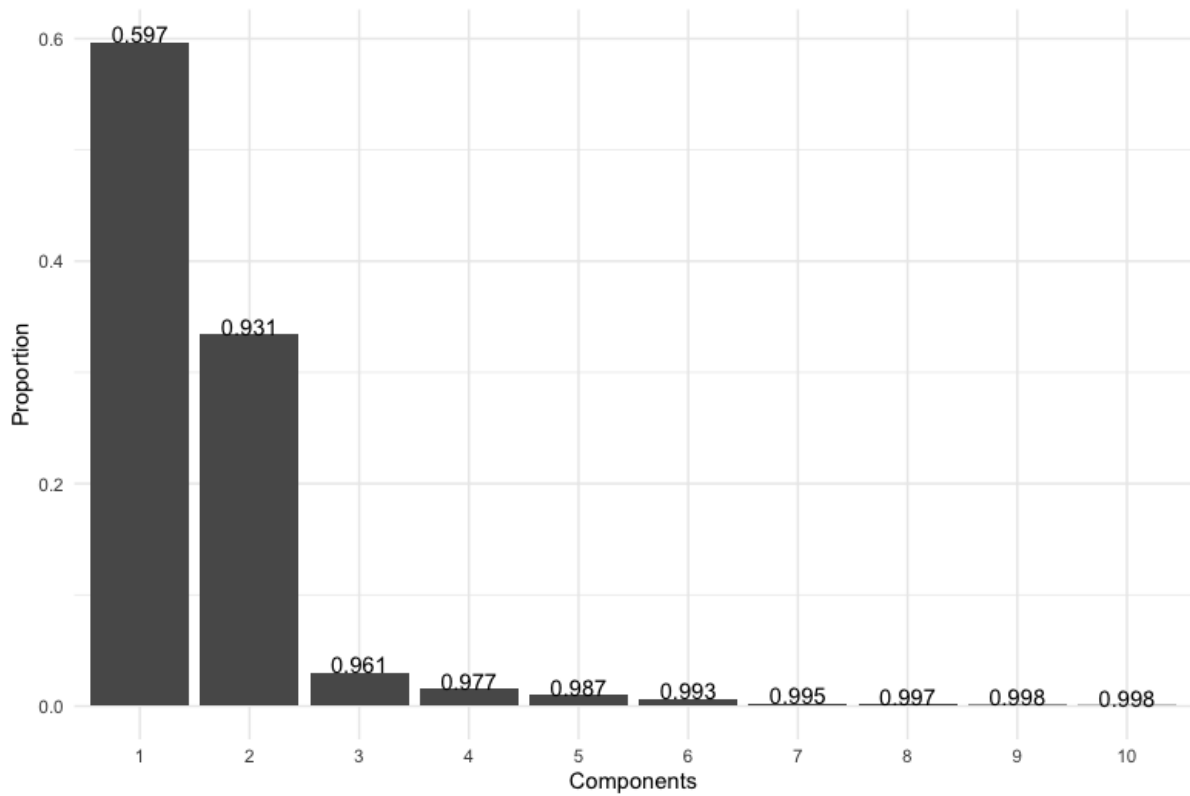


© John J. Shea

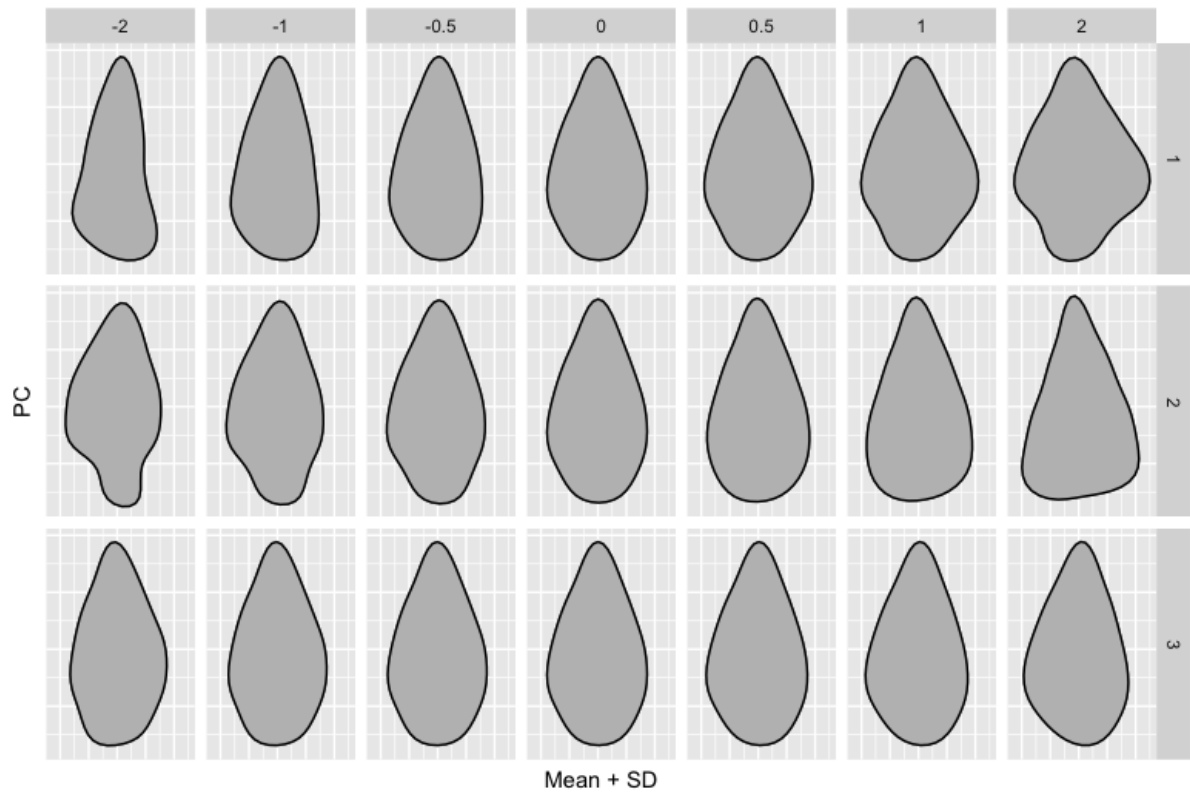
**Supplementary Figure S1.** A schematic reprinted from Shea (2020) demonstrating the morphological measurements recorded. Length is defined as the maximum dimension of the lithic, width as the maximum measurement in the perpendicular dimension to length, and thickness as the maximum measurement in the third dimension



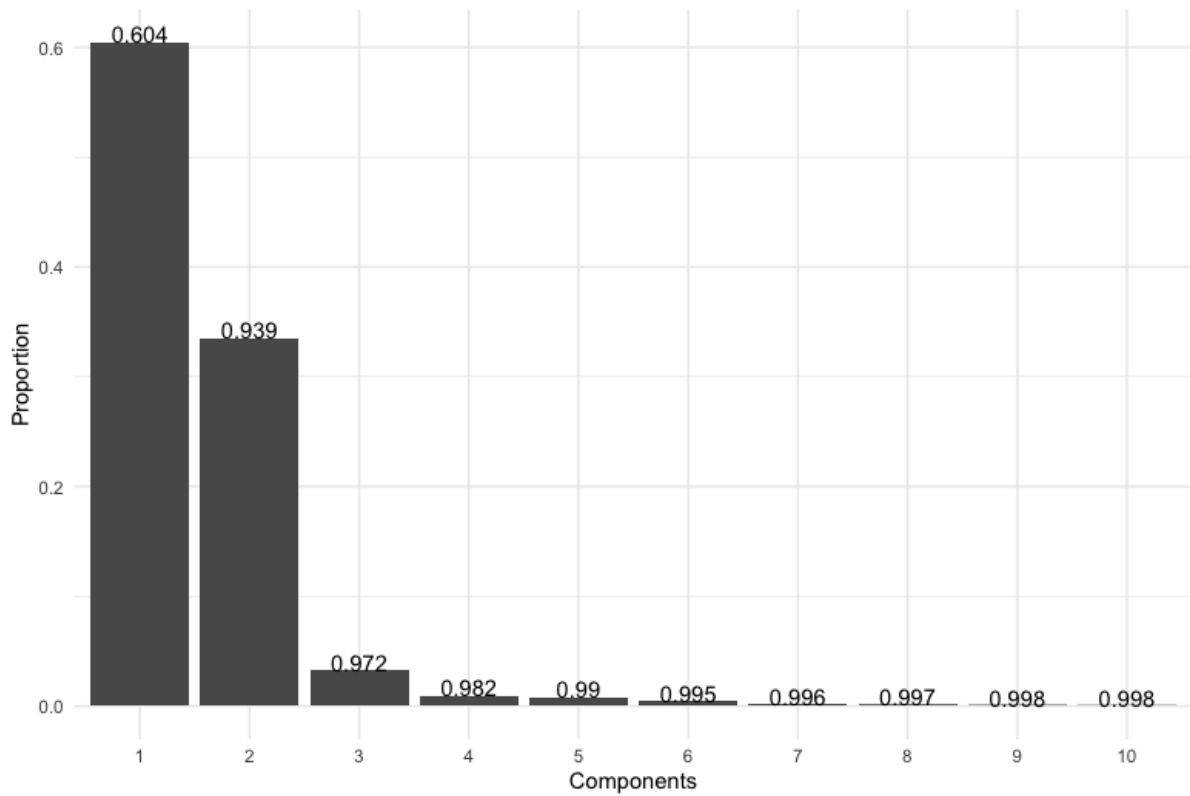
**Supplementary Figure S2.** Outline data of the tools captured by six observers. Replicas are coloured by tool type.



**Supplementary Figure S3.** Scree plot of the principal component (PC) loadings of the multiple observer data, with the cumulative variance reported above the bars.



**Supplementary Figure S4.** Principal component (PC) contributions along the first 3 axes for both the single and multiple observer data. Note this is very similar to Figure 20, as is to be expected.



**Supplementary Figure S5.** Scree plot of the principal component (PC) loadings of the single and multiple observer data together, with the cumulative variance reported above the bars.

## Appendix 3: Supplementary Materials for Chapter 8 – Eastern African Middle Stone Age Point Variability

### Supplementary Methods S1: Power analysis

I performed a power analysis, following recommendations by Cohen (1988), on raw materials, sites and assemblages, each time calculating the sample size needed in each group to obtain a power of 0.80, when the effect size is moderate (0.25) and a significance level of 0.05 is employed. For raw materials, it suggests that a sample size of 35 per group would be sufficient; in the case of the three main raw materials (obsidian, basalt and chert), the sample sizes well exceed this threshold, suggesting that the results in these cases are robust. I therefore limited my interpretation to these three materials. The sample sizes for sites ( $n = 35$ ) and assemblage ( $n = 21$ ) both were found to be insufficient by the power analysis, with only 2 of the sites yielding  $>35$  samples and 4 of the assemblages having  $>21$  samples. This suggests that the results require exploration with larger samples to confirm these trends.

**Supplementary Table S1.** Regression results demonstrating the relationship between PC1-6 and centroid size. Statistical significance is highlighted at  $p < 0.05$  (\*) and  $p < 0.001$  (\*\*).

|     | Correlation coefficient | Adjusted R <sup>2</sup> | P-value  |
|-----|-------------------------|-------------------------|----------|
| PC1 | 0.362                   | 0.127                   | <0.001** |
| PC2 | -0.160                  | 0.020                   | 0.020*   |
| PC3 | -0.170                  | 0.024                   | 0.012*   |
| PC4 | 0.217                   | 0.043                   | 0.001**  |
| PC5 | 0.198                   | 0.035                   | 0.003**  |
| PC6 | 0.014                   | -0.004                  | 0.835    |

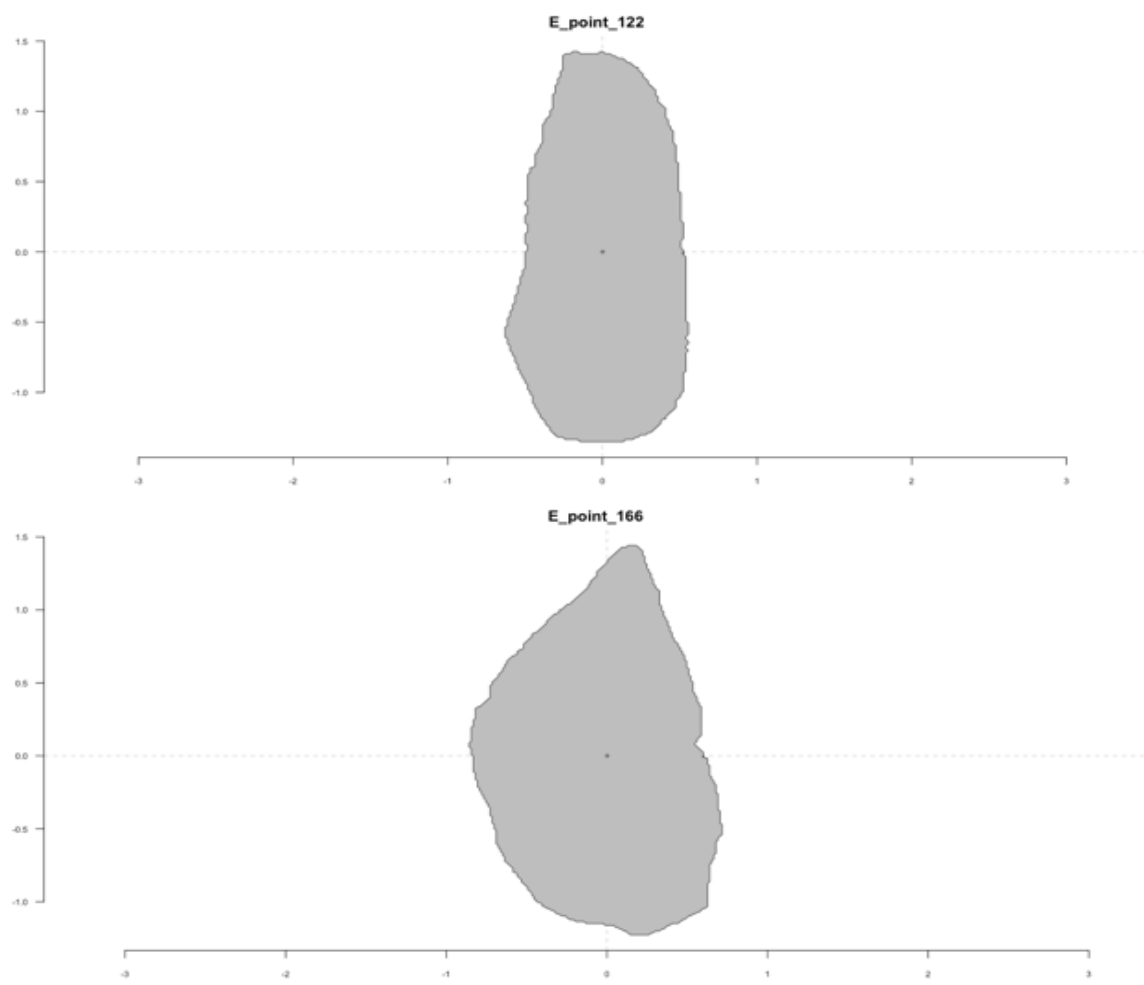
**Supplementary Table S2.** P-values from Tukey Honestly Significant Difference analyses for length and width, as well as principal component (PC)1 and 6 and centroid size for each pair of assemblages. Statistical significance is highlighted at  $p < 0.05$  (\*) and at  $p < 0.01$  (\*\*) and cells have been shaded grey to assist identification. All values have been rounded to 3 decimal places.

|                           | Length  | Width   | PC1     | PC3     | CS      |
|---------------------------|---------|---------|---------|---------|---------|
| Chert-Basalt              | 0.989   | 0.999   | 0.977   | 0.638   | 0.540   |
| Fossilised wood-Basalt    | 0.998   | 0.505   | 0.649   | 0.989   | 0.991   |
| Obsidian-Basalt           | 0.833   | 0.980   | 0.032*  | 0.210   | 0.563   |
| Quartzite-Basalt          | 0.061   | 1.000   | 0.422   | 1.000   | 0.998   |
| Rhyolite-Basalt           | 0.039*  | 0.018*  | 0.935   | 0.992   | 0.644   |
| Fossilised wood-Chert     | 1.000   | 0.451   | 0.552   | 0.938   | 1.000   |
| Obsidian-Chert            | 0.290   | 0.794   | 0.001** | 0.000** | 0.002** |
| Quartzite-Chert           | 0.082   | 1.000   | 0.510   | 1.000   | 1.000   |
| Rhyolite-Chert            | 0.064   | 0.011** | 0.840   | 0.882   | 0.922   |
| Obsidian-Fossilised wood  | 0.987   | 0.582   | 0.916   | 1.000   | 0.946   |
| Quartzite-Fossilised wood | 0.536   | 0.850   | 0.151   | 0.988   | 1.000   |
| Rhyolite-Fossilised wood  | 0.857   | 1.000   | 0.958   | 1.000   | 1.000   |
| Quartzite-Obsidian        | 0.032*  | 1.000   | 0.155   | 0.986   | 0.977   |
| Rhyolite-Obsidian         | 0.011** | 0.029*  | 1.000   | 1.000   | 0.313   |

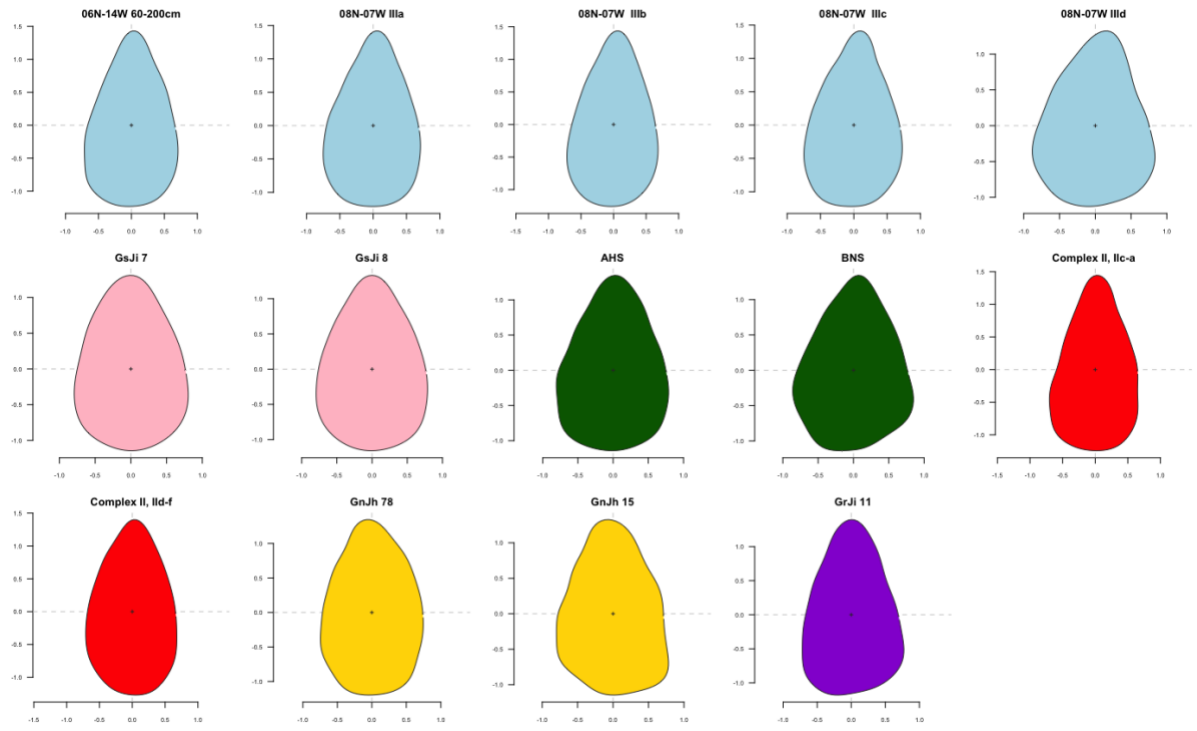
---

|                    |       |       |       |       |       |
|--------------------|-------|-------|-------|-------|-------|
| Rhyolite-Quartzite | 0.941 | 0.614 | 0.278 | 0.995 | 0.999 |
|--------------------|-------|-------|-------|-------|-------|

---



**Supplementary Figure S1.** Points that are outliers in terms of size. E\_point\_122 (top) comes from Kaputhurin Formation and E\_point\_166 (bottom) comes from Prospect Farm.

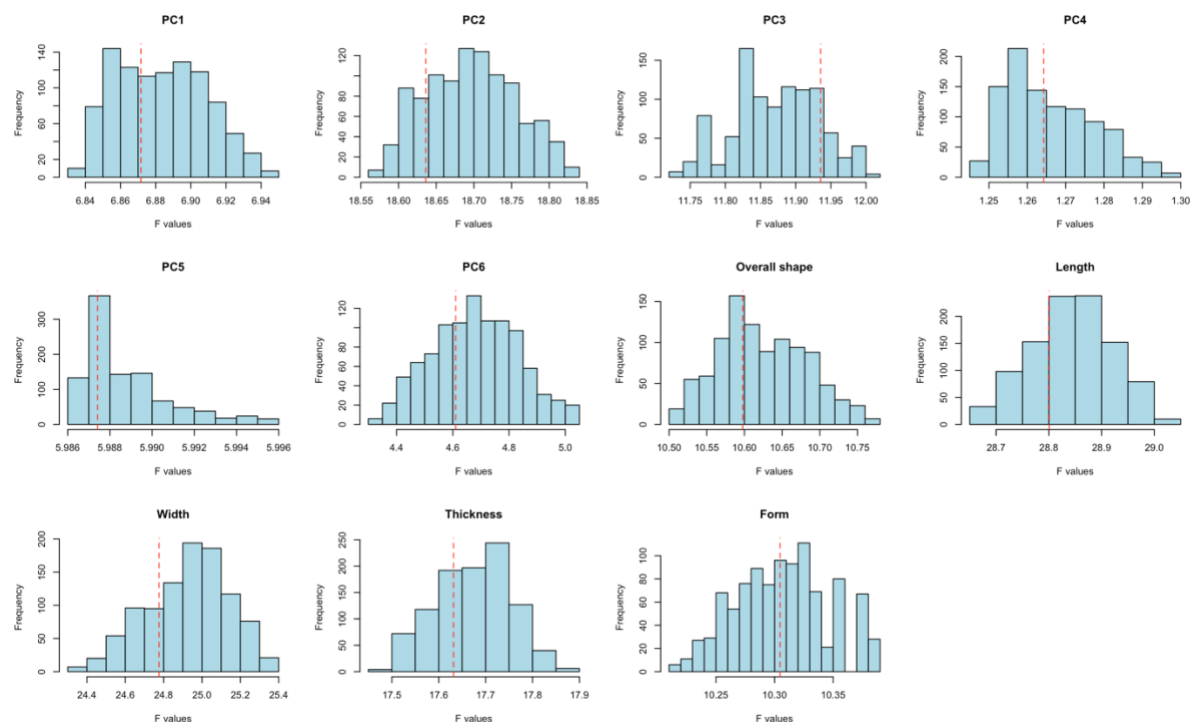


**Supplementary Figure S2.** Mean shapes of each assemblage coloured by site: blue = Porc-Epic, pink = Prospect Farm, green = Omo Kibish, red = Goda Buticha, yellow = Kaputhurin Formation, purple = Prolonged Drift.

## Appendix 4: Supplementary Materials for Chapter 9 – Integrating the habitability model with point shape variability

### Supplementary Methods S1: Permutation results.

I have iterated across the dating range of each assemblage, taking 1000 random samples each iteration and recording the overall model coefficient and p-value from multiple matrix regressions of each shape/size variable. Supplementary Figure S1 demonstrates that the coefficient distributions are mainly symmetrical and multimodal, with the vertical lines for the original coefficients generally near the middle. Supplementary Table S1 confirms that none of the coefficients generated using the ‘simple age’ fall into the tails of the permuted distributed (defined as below 5% or above 95%), with many falling around the middle of the distribution at 50%. This confirms that the initial analyses using the ‘simple age’ are robust to chronological uncertainty.



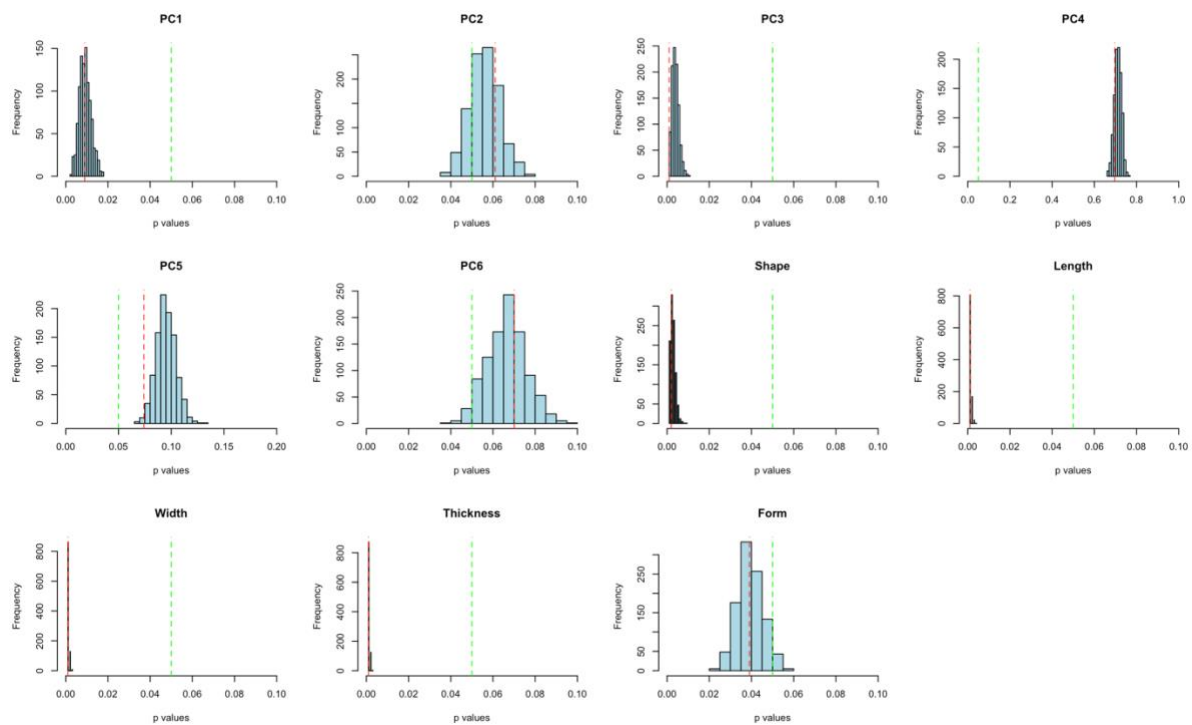
Supplementary Figure S1. Coefficient distributions from the multiple matrix regressions using the permuted samples, with the original coefficient value based on the ‘simple age’ highlighted in red.

Supplementary Table S1. Results from the permuted multiple matrix regressions

|     | Original coefficient based on ‘simple age’ | Median coefficient of permuted distribution | Percentile of distribution corresponding to the original coefficient |
|-----|--|---|--|
| PC1 | 6.87                                       | 6.88  | 35.5%  |
| PC2 | 18.64                                      | 18.70                                       | 20.4%  |
| PC3 | 11.94                                      | 11.87                                       | 87.4%  |
| PC4 | 1.26                                       | 1.26  | 38.9%  |

|               |       |       |       |
|---------------|-------|-------|-------|
| PC5           | 5.99  | 5.99  | 78.9% |
| PC6           | 4.61  | 4.68  | 34.3% |
| Overall shape | 10.60 | 10.62 | 39.4% |
| Length        | 28.80 | 28.84 | 28.4% |
| Width         | 24.78 | 24.94 | 24.1% |
| Thickness     | 17.63 | 17.68 | 31.1% |
| Overall form  | 10.30 | 10.30 | 43.4% |

Supplementary Figure S2 highlights that the p-values for PC1, PC3, PC4 PC5, overall shape (PC1-6 combined), length, width and thickness all remain either 100% or 0% over the threshold of 0.05 and therefore are considered robust as either all or none of the iterations return significant results. The iterations of PC6 and form (Length, Width and Thickness combined) return less than 5% of p-values falling the ‘wrong’ side of the threshold (PC6 – 3.4% were significant, Form – 4.8% were not significant), and therefore can also be considered robust. The only variable that appears significantly affected by dating errors is PC2 where 14.1% of the iterations return a significant p-value over 0.05, but this is because the significance of the model falls around the threshold level, rather than because dating error resulted in large differences in p-values.



Supplementary Figure S2. Distributions of the p-values returned from the multiple matrix regressions of the permuted samples, with the original coefficient value based on the ‘simple age’ highlighted in red, and the significance threshold of 0.05 highlighted in green.